



Antigen discovery in *Trypanosoma vivax*

Thesis submitted in accordance with the requirements of the University of
Liverpool for the degree of Doctor in Philosophy by

Alessandra Isabella Romero Ramirez

February 2020

Author's declaration

The expression of recombinant proteins was performed by Dr. Nicole Muller-Sienerth at the Cell Surface Signalling Laboratory from the Wellcome Trust Sanger Institute (Cambridge, UK).

The mice immunization and challenge was carried out by Dr. Delphine Autheman from the Cell Surface Signalling Laboratory at the animal facility from the Wellcome Trust Sanger Institute.

The immunization and challenge of goats as well as sample collection was performed by MSc. Kayo José Garcia de Almeida Castilho Neto at the Faculty of Agricultural and Veterinary Sciences from the Sao Paulo State University (UNESP) in Jaboticabal, Sao Paulo, Brazil.

Except from the advice acknowledged, I declare that this thesis is a presentation of my own original work.

Alessandra Isabella Romero Ramirez

20th February 2020

ACKNOWLEDGEMENTS

First of all, I would like to express my sincere gratitude to my PhD thesis supervisor, Dr. Andrew Jackson for his guidance throughout the project, patience and belief in me. I highly appreciate his motivation, immense knowledge and critical advice during these years. I am truly thankful for the guidance and opportunities given.

I gratefully acknowledge the funding body that made my PhD work possible. I was funded by FONDECYT-CONCYTEC, the National Council of Science, Technology and Innovation from Peru (grant contract number 001-2016-FONDECYT).

I would specially like to acknowledge members from the Cell Surface Signalling laboratory at the Wellcome Sanger Institute, to the group leader Gavin Wright, postdoctoral Delphine Autheman and the senior technician Nicole Muller-Sienerth for their enormous contribution on this doctoral project. In addition, I would also like to acknowledge members at the Faculty of Agricultural and Veterinary Sciences from the Sao Paulo State University in Sao Paulo, Brazil, to Kayo Neto and Rosangela Zacarias Machado for the help and making my time in Brazil a wonderful experience. A special thanks to Dr. Robin Flynn for his help on the immunological experimental designs and for reading part of my thesis. The recommendations were highly appreciated.

I would like to acknowledge the technicians from the Ic2 for their constant support and help during these years. Many thanks to my lovely friend Isabel, for not only our conversations about science but also for the amazing friendship during these years. To my flatmate and friend Jordana, for the patience, laughs, good moments and for being my guinea pig trying all the recipes I prepared at home.

Last but not least I would like to thank my family for their love and unconditional support. Thanks for the video calls, recipes, photos and invaluable moments that made me feel a little closer to home. Los amo mucho.

Abstract

Trypanosoma vivax is a major animal pathogen causing African Animal Trypanosomiasis (AAT) in livestock across Africa and South America. No vaccine is available for AAT due to antigenic variation of the Variant Surface Glycoprotein (VSG) coating the parasite surface, which leads to effective immune evasion. However, the *T. vivax* genome contains diverse species-specific genes that encode cell-surface proteins (TvCSP) expressed during the bloodstream stage. This indicates that the surface coat includes invariant proteins besides the VSG, which might be vaccination targets. Using a reverse vaccinology approach, this thesis examines these TvCSP and their utility as vaccines against the parasite. In silico sequence analysis of TvCSP (Chapter 2) indicates that most TvCSP are transmembrane proteins, present in diverse clinical isolates and containing minimal polymorphism. The identification of immunogenic linear B-cell epitopes based on a customized peptide microarray (Chapter 3) reveals one protein family (FamX) to be the most immunogenic in natural infections (besides VSG), and four FamX proteins were successfully expressed in recombinant form. FamX proteins are used to immunize BALB/c mice with multiple adjuvants prior to parasite challenge (Chapter 4) to explore the resultant immune response and the protective properties of vaccination. Immunization stimulated high levels of pro-inflammatory cytokines indicating that FamX proteins stimulated a mixed Th1/Th2-type immune response, and one antigen (AJ6), co-administrated with a Quil-A adjuvant, induced partial protection with 60% efficacy in mice. AJ6 was also localized to the cell-surface based on immuno-fluorescence microscopy. Challenge experiments in goats were conducted using IFX antigen, another FamX protein, in order to analyze its possible protective immunity in a natural host (Chapter 5) but IFX failed to protect despite effective seroconversion. This thesis describes the discovery of a novel protein component of the *T. vivax* surface coat that is invariant and immunogenic, which offers promise of an effective vaccine for animal African trypanosomiasis.

Table of contents

Author's declaration	I
Acknowledgements	II
Abstract	III
Table of contents	IV
List of figures	VIII
List of tables	XIII
List of abbreviations	XV
Chapter 1. General introduction	1
1.1. Animal African Trypanosomiasis.....	1
1.1.1. Organism and taxonomy.....	1
1.1.2. Geographic distribution.....	5
1.1.3. Impact.....	6
1.1.4. Vector.....	7
1.1.5. Development of <i>T. vivax</i>	9
1.1.6. Course of infection and pathogenesis.....	11
1.1.7. Diagnosis.....	13
1.1.8. Treatment and control strategies.....	15
1.2. Antigenic variation.....	17
1.3. Immune response to African trypanosomes.....	18
1.3.1. Innate immune response.....	19
1.3.2. Adaptive immune response.....	20
1.3.3. Humoral immune response.....	24
1.3.4. Immuno-suppression.....	26
1.4. Vaccination against African trypanosomes.....	27
1.5. Profile of an effective vaccine.....	32
1.6. Potential vaccine targets on trypanosomes cell-surfaces.....	34
1.7. Reverse vaccinology.....	35
1.8. Aims of the thesis.....	37
Chapter 2: in silico sequence analysis of <i>Trypanosoma vivax</i>-specific cell-surface gene families	39

2.1. Introduction	39
2.2. Materials and methods	44
2.2.1. Data sources.....	44
2.2.2. In silico structural characterization.....	44
2.2.3. Gene family phylogenetic analysis.....	44
2.2.4. Population genetic analysis.....	45
2.2.5. Mapping sequence data to reference genome.....	46
2.2.6. Population genetic variation.....	48
2.2.7. T-cell epitope prediction.....	48
2.2.8. Linear B-cell epitope prediction.....	49
2.3. Results	51
2.3.1. Secondary protein structure prediction.....	51
2.3.2. Prediction of glycosylation sites.....	51
2.3.3. Prediction of tertiary structures.....	54
2.3.4. Phylogenetic analysis.....	55
2.3.5. Population genetic analysis.....	70
2.3.6. Levels of nucleotide diversity and neutrality among TvCSP gene families.....	72
2.3.7. In silico T-cell epitope prediction	74
2.3.8. In silico B-cell epitope prediction	78
2.4. Discussion	81
2.5. Conclusion	87
Chapter 3: Identification of linear B-cell epitopes in TvCSP families using immunogenicity assays on natural infections	88
3.1. Introduction	88
3.2. Materials and methods	92
3.2.1. Sera screening.....	92
3.2.2. Design and production of TVCSP peptide microarray.....	95
3.2.3. Immunoprofiling	97
3.2.4 Data analysis.....	99
3.2.4.1. First approach – (Loeffler <i>et at</i> , 2016)	99
3.2.4.2. Second approach – (Sundaresh <i>et al</i> , 2006)	100
3.2.4.3. Third approach – limma package.....	100

3.2.5. Expression of recombinant proteins.....	103
3.2.5.1. Selection of <i>T. vivax</i> proteins and AVEXIS expression technique.....	103
3.2.5.2. Design and construction of vector expressions.....	103
3.2.5.3. Plasmid purification.....	104
3.2.5.4. HEK293-6E cell culture and transfections.....	104
3.2.5.5. Protein normalization.....	105
3.2.5.6. Confirmation of recombinant proteins.....	105
3.3. Results.....	107
3.3.1. Serum screening.....	107
3.3.2. Peptide microarray analysis.....	110
3.3.2.1. Raw data.....	110
3.3.2.2. Between-array value normalization	121
3.3.2.3. Identification of significant immunogenic peptides.....	124
3.3.3. Expression of recombinant proteins.....	129
3.4. Discussion.....	131
3.5. Conclusion.....	135
Chapter 4: Evaluation of the immunogenicity and protective properties of FamX recombinant antigens in a murine model.....	136
4.1. Introduction.....	136
4.2. Materials and methods.....	141
4.2.1. Immunization.....	141
4.2.1.1. Animals.....	141
4.2.1.2. Vaccine preparation.....	141
4.2.1.3. Murine immunization.....	141
4.2.2. Challenge and data acquisition.....	142
4.2.2.1. Challenge.....	142
4.2.2.2. In vivo imaging.....	142
4.2.2.3. Sample collection.....	144
4.2.3. In vitro antigen stimulation and cytokine measurement.....	145
4.2.3.1. Culture of splenocytes.....	145
4.2.3.2. Cytokine measurement	145
4.2.4. IgG-specific antibody response in mice.....	146

4.2.5. IgG-specific antibody response in cattle.....	146
4.2.6. Cellular localization of AJ antigens in BSF parasites.....	147
4.2.7. Statistical analysis.....	149
4.3. Results.....	150
4.3.1. Humoral immune response against recombinant proteins in cattle.....	150
4.3.2. Comparative humoral immune response against AJ antigens in mice.....	153
4.3.3. Antigen specific cellular immune response.....	157
4.3.4. Protection of vaccinated mice from <i>T. vivax</i> infection.....	159
4.3.5. Cellular localization of recombinant proteins.....	175
4.4. Discussion.....	180
4.5. Conclusion.....	185
Chapter 5: Evaluation of a FamX experimental vaccine in a caprine model.....	187
5.1. Introduction.....	187
5.2. Materials and methods.....	191
5.2.1. Study ethics.....	191
5.2.2. Animals.....	191
5.2.3 IFX vaccination against <i>T. vivax</i>	191
5.2.4. Collection of serum.....	193
5.2.5. Parasites.....	194
5.2.6. Challenge.....	194
5.2.7. Antibody titration.....	194
5.2.8. Statistical analysis.....	195
5.3. Results.....	196
5.3.1. Vaccine safety.....	196
5.3.2. Humoral immune response to an IFX + Freund's vaccine.....	198
5.3.3. Evaluation against homologous challenge with <i>T. vivax</i>	199
5.4. Discussion.....	205
5.5. Conclusion.....	211
Chapter 6: General discussion.....	212
6.1. Final conclusion.....	218
References.....	220

List of figures

Figure 1.1. Geographical distribution of African animal trypanosomiasis in Africa and South America caused by <i>T. evansi</i> , <i>T. brucei</i> , <i>T. vivax</i> and <i>T. congolense</i>	6
Figure 1.2. Distribution of <i>Morsitans</i> , <i>Fusca</i> and <i>Palpalis</i> group of tsetse flies across Africa.....	8
Figure 1.3. A suggested model for the <i>Trypanosoma vivax</i> life cycle.....	10
Figure 1.4. Examples of common clinical symptoms during <i>T. vivax</i> infection.....	13
Figure 1.5. Waves of parasitaemia characteristic of African trypanosome bloodstream infections, and reflective of VSG switching.....	18
Figure 1.6. A model of the role of macrophages during an African trypanosome infection.....	23
Figure 1.7. A model of B-cell development and humoral immune response against African trypanosomes within the mammalian host.....	25
Figure 1.8. Requirements for an effective vaccine against African trypanosomes.....	33
Figure 1.9. Comparative pipelines for the conventional and reverse vaccinology approaches.	36
Figure 2.1. A schematic representation of the secondary structure of each BSF TvCSP family.....	53
Figure 2.2. Tertiary structure predictions based on the amino acid sequence for A) TvY486_0043530 and B) TvY486_0019430.....	55
Figure 2.3. Comparison of Maximum likelihood phylogenetic trees based on the Tamura-Nei model of CDS and 3' and 5'UTR sequences for Fam27.....	57
Figure 2.4 (overleaf). Comparison of Maximum likelihood phylogenetic trees based on the Tamura-Nei model of CDS and 3' and 5'UTR sequences for Fam35.....	58
Figure 2.5 (overleaf). Comparison of Maximum likelihood phylogenetic trees based on the Tamura-Nei model of CDS and 3' and 5'UTR sequences for Fam43.....	58
Figure 2.6 (overleaf). Comparison of Maximum likelihood phylogenetic trees based on the Tamura-Nei model of CDS and 3' and 5'UTR sequences for Fam28 (A) and Fam29 (B)	61

Figure 2.7. Comparison of Maximum likelihood phylogenetic trees based on the Tamura-Nei model of CDS and 3' and 5'UTR sequences for Fam30.....	62
Figure 2.8. Comparison of Maximum likelihood phylogenetic trees based on the Tamura-Nei model of CDS and 3' and 5'UTR sequences for Fam31.....	63
Figure 2.9. Comparison of Maximum likelihood phylogenetic trees based on the Tamura-Nei model of CDS and 3' and 5'UTR sequences for Fam32.....	64
Figure 2.10 (overleaf). Comparison of Maximum likelihood phylogenetic trees based on the Tamura-Nei model of CDS and 3' and 5'UTR sequences for Fam34.....	65
Figure 2.11. Comparison of Maximum likelihood phylogenetic trees based on the Tamura-Nei model of CDS and 3' and 5'UTR sequences for Fam36 (A) and Fam37 (B)	66
Figure 2.12 (overleaf). Comparison of Maximum likelihood phylogenetic trees based on the Tamura-Nei model of CDS and 3' and 5'UTR sequences for Fam38 (A) and Fam42 (B)	67
Figure 2.13. Comparison of Maximum likelihood phylogenetic trees based on the Tamura-Nei model of CDS and 3' and 5'UTR sequences for Fam44.....	68
Figure 2.14. Comparison of Maximum likelihood phylogenetic trees based on the Tamura-Nei model of CDS and 3' and 5'UTR sequences for FamX.....	69
Figure 2.15. Scatter plot of the pairwise nucleotide diversity values (π) using PopGenome and SNPgenie servers and Tajima's <i>D</i> estimation according to the families based on the 244 TvCSG.....	73
Figure 2.16. Number of similar T-cell epitopes for MHC-I (A) and MHC-II (B) after their evaluation of antigenicity.	75
Figure 2.17. Similar predicted MHC-I epitopes for FamX proteins according to their position in the amino acid sequence.....	77
Figure 3.1. Map of a peptide microarray chip showing TvCSP families included in the design and production of the second generation based on their position.....	97
Figure 3.2. Examples of serum screening using Very-Diag tests.....	109
Figure 3.3. Spot intensities obtained from PEPperPRINT peptide arrays using naturally infected Cameroonian sera.....	112
Figure 3.4. Spot intensities obtained from PEPperPRINT peptide arrays using naturally infected Malawian sera.....	113

Figure 3.5. Spot intensities obtained from PEPperPRINT peptide arrays using naturally infected Kenyan sera.....	114
Figure 3.6. Spot intensities obtained from PEPperPRINT peptide arrays using experimentally infected samples from Brazil.....	115
Figure 3.7. Spot intensities obtained from PEPperPRINT peptide arrays using seronegative era from United Kingdom.....	116
Figure 3.8. Spot intensities obtained from PEPperPRINT peptide arrays using seronegative era from Malawi.....	117
Figure 3.9. Spot intensities obtained from PEPperPRINT peptide arrays using seropositive sera for <i>T. congolense</i> from Cameroon.....	118
Figure 3.10 (from previous page). Scatter plot displaying the raw signal intensity (AU) of (A) all median values (first and second approach) and (B) raw mean values (third approach) for each group of samples.....	120
Figure 3.11 (from previous page). Scatter plot displaying normalized intensity values for all samples by location, based on the second (Acton) and third normalization approach (B.)	123
Figure 3.12. Volcano plot of limma results comparing positive samples versus controls.....	127
Figure 3.13. A) Location of the significant epitopes identified in the peptide microarray analysis on the protein linear structure. B) Comparison of best peptides from the peptide microarray versus the in silico predicted epitopes.....	128
Figure 3.14. A) Normalization of AJ1 protein using two-fold serial dilutions. B) Normalization of AJ2, AJ3 and AJ6 proteins. C) Western blot analysis confirming protein expression.....	130
Figure 4.1. Scheme of mouse immunization protocol.....	144
Figure 4.2. List of different fixation methods, blocking solutions, temperatures and conjugates tested for the optimization of the IFA protocol with <i>T. vivax</i> BSF.....	148
Figure 4.3. Indirect ELISA for the detection of specific antibodies against each recombinant protein in naturally infected cattle.....	152
Figure 4.4. Indirect ELISA for the detection of specific antibodies against each recombinant protein in experimentally infected calves (n = 3; A1-3).....	153

Figure 4.5 (overleaf). Titration of <i>T. vivax</i> antigens-specific IgG1 and IgG2a antibody response in BALB/c mice before and after immunization	155
Figure 4.6. Cytokine responses in <i>in vitro</i> stimulated splenocytes from BALB/c mice vaccinated with the different panel of antigens.....	159
Figure 4.7. In vivo imaging of BALB/c mice immunized with each antigen co-administrated with Quil-A prior challenge with <i>T. vivax</i>	162
Figure 4.8. Luminescent values during the course of infection of luciferase-expressing <i>T. vivax</i> in challenged mice.....	163
Figure 4.9. Change (Δ Total flux) in luminescence between the control group and each antigen-vaccinated group.....	164
Figure 4.10 (overleaf). Cellular and humoral response before and after challenge with <i>T. vivax</i> in Quil-A vaccinated mice (n=8)....	166
Figure 4.11. In vivo imaging of BALB/c mice immunized with AJ6+ Quil-A prior challenge with <i>T. vivax</i> (n=15/group)....	171
Figure 4.12. Luminescent values and survival rate during the course of infection of luciferase-expressing <i>T. vivax</i> in challenged mice vaccinated with AJ6 (n=15/group).....	172
Figure 4.13. Cytokine responses in <i>in vitro</i> stimulated splenocytes after challenge with <i>T. vivax</i> in AJ6+Quil-A vaccinated mice and control group (n=15/group).....	174
Figure 4.14. Cellular localization of AJ antigens in <i>T. vivax</i> bloodstream-forms.....	177
Figure 4.15 (previous page). Cellular localization of AJ6 in <i>T. vivax</i> bloodstream-forms using purified polyclonal antibodies.....	179
Figure 5.1. A. Antibody titration of IgG isotypes against IFX in vaccinated mice (n=15) co-administrated with alum (intraperitoneally). B. Long-lasting immunity against <i>T. vivax</i> infection in IFX+ alum mice (n=15) compared to the control group.....	188
Figure 5.2. Experimental design for the immunization and challenge in goats.....	193
Figure 5.3. Local skin reactions at injection sites following immunization with IFX antigen in combination with Freund's (A) or Quil-A adjuvants (B)	197
Figure 5.4. Antibody titration of <i>T. vivax</i> IFX antigen-specific antibodies produced in goats before challenge.....	199
Figure 5.5. Parasitaemia levels of infected goats previously immunized with A) Freund's or B) Quil-A adjuvant during the course of infection (40 days).....	203

Figure 5.6. Rectal temperature and PCV values during the course of infection of goats vaccinated with IFX +Freund **(A)**, Freund only **(B)**, IFX +Quil-A **(C)** and Quil-A only **(D)**...
..... 204

List of tables

Table 1.1. Classification of trypanosomes.....	4
Table 1.2. Chronological list of examples of previous attempts for the identification of vaccine candidates against African trypanosomes.....	31
Table 2.1. List of TvCSP families with potential cell-surface location, their respective number of paralogs and the life cycle stage in which they are preferentially expressed.....	41
Table 2.2. List of clinical isolates used to generate DNA sequence data for the population genetic analysis, according to location, host, passage species and genome completeness.....	46
Table 2.3. List of BoLA and HLA alleles used for the in silico prediction of MHC-I and MHC-II epitopes respectively in TvCSP protein sequences.....	49
Table 2.4. In silico structural predictions for TvCSP families.....	52
Table 2.5. Comparison of phylogenetic relationships among TvCSP gene members based on sequence domain.....	70
Table 2.6. List of <i>T. vivax</i> isolates from the five populations studied showing the summary of mapping statistics against the TvY486 reference <i>T. vivax</i> genome.....	71
Table 2.7. In silico prediction of B-cell linear epitopes in TvCSP sequences according to their family.....	80
Table 3.1. A. Relation of samples used for the peptide microarray immunoassay. B. Descriptive summary of samples from Brazilian experimentally infected animals applied to the peptide microarray.....	94
Table 3.2. List of samples used for the detection of immunogenic B-cell epitopes with the peptide array immunoassay.....	98
Table 3.3. Pipeline for the identification of significant immunogenic peptides from <i>T. vivax</i> protein microarrays using Loeffler <i>et al</i> methodology (first approach), Sundaresh <i>et al</i> methodology (second approach) and limma package from Bioconductor (third approach).....	102
Table 3.4. List of selected proteins to be recombinantly expressed by the AVEXIS technique.....	103

Table 3.5. Comparison of results obtained from samples from naturally and experimentally infected livestock using Very-Diag test.....	108
Table 3.6. List of significant peptides identified from the peptide microarray analysis using at least two approaches.....	126
Table 4.1. Vaccine preparation according to the different experimental groups of mice.....	143
Table 4.2. List of 15 samples used for the identification of IgG1 and IgG2 levels by ELISA against AJ's recombinant proteins.....	147
Table 4.3. Log50% and endpoint titres of bovine IgG1 against each recombinant antigen in naturally and experimentally infected cattle.....	152
Table 5.1. Vaccine formulation for antigen-vaccinated and control goats.....	191

List of Abbreviations

aaMØs	Alternative activated macrophages
AAT	African Animal Trypanosomiasis
ANOVA	Analysis of variance
AP	Alkaline phosphatase
APC	Antigen presenting cells
AU	Arbitrary units
AVEXIS	Avidity-Extracellular Interaction Screen
BAM	Binary format of SAM file
BCR	B-cell receptor
BH	Benjamini and Hochberg's method
BirA	Protein-biotin ligase plasmid
BoLA	Bovine leucocyte antigen
BRF1	<i>T. brucei</i> RNA polymerase subunit transcription factor
BSA	Bovine serum albumin
BSF	Bloodstream form
BWA-MEM	The Burrows-Wheeler Alignment tool
caMØs	Classical activation of macrophages
CDS	Coding Sequence
CFA	Complete Freund's adjuvant
ConA	Concanavalin A
CSP	Cell Surface Phylome
CTL	Cytotoxic T lymphocytes
CTLs	CD8 ⁺ cytotoxic T cells
DAB	3,3' diaminobenzidine
DAMPs	Damage-associated molecular patterns
DAPI	4',6-diamidino-2-phenylindole
DC	Dendritic cells
DPI	Days post infection
ELISA	Enzyme-linked immunosorbent assay

ER	Endoplasmic reticulum
FACS	Fluorescence-activated cell sorting
FC	Fold change
FCS	Foetal calf serum
FP	Flagellar pocket
GATK	Genome Analysis Toolkit
GIP-sVSG	Soluble glycosylinositolphosphate VSG
GPI	Glycophosphatidylinositol
GPI-PLC	Endogenous GPI-phospholipase C
HAT	Human African Trypanosomiasis
HDL	High density lipoproteins
Hf	Heart frequency
HLA	Human leucocyte antigen
HRP	Enzyme horseradish peroxidase
HTS	High-Throughput Sequencing
IEDB	Immune Epitope Database
IFA	Immunofluorescence assay
IFA	Incomplete Freund's adjuvant
IFN- γ	Interferon gamma
IFX	Invariant flagellum antigen
IgG	Immunoglobulin G
IgM	Immunoglobulin M
IL-10	Interleukin 10
IL-12	Interleukin 12
IL-2R	IL-2 receptor
IL-4	Interleukin 4
ILRI	International Livestock Research Institute
Indel	Insertions and deletions
ISCOM	Immunostimulatory complex
ISG	Invariant surface glycoproteins
LAMP	Loop-Mediated Isothermal Amplification
LDL	Low density lipoproteins

LS	Long slender form
MET	Metacyclic form
mfVSG	Membrane form of VSG molecules
MHC-I	Major Histocompatibility complex I
MHC-II	Major Histocompatibility complex II
M ϕ s	Macrophages
MSP	Merozoite surface protein family
MyD88	Myeloid differentiation factor 88
MZB	Marginal zone B-cells
NF- κ B	Nuclear factor kappa-light-chain-enhancer of activated B cells
NMR	Nuclear magnetic resonance
NO	Nitric oxide
OPG	Oocyst per gram of faeces
PAMPs	Pathogen-associated molecular patterns
PBS	Phosphate Buffered Saline
PCR	Polymerase chain reaction
PCV	Packed cell volume
PCV	Packed cell volume
PEG	Polyethylene glycol
PEI	Polyethylenimine
PFA	Paraformaldehyde
PHI	Pairwise Homoplasmy Index
PRRs	Pattern recognition receptors
PSI-BLAST	Position-specific iterated blast basic local alignment search tool
PSSM	Position specific scoring matrix
Rf	Respiratory frequency
ROS	Reactive oxygen species
RT	Room temperature
RV	Reverse vaccinology
SAM	Sequence Alignment/Map format
SDS-PAGE	Sodium dodecyl sulfate–polyacrylamide gel electrophoresis
SEM	Standard error of the mean

SNPs	Single nucleotide polymorphisms
SP	Signal peptide
SR-A	Type A scavenger receptor
SRP	Signal recognition peptide
SS	Short stumpy form
T1	Transitional B-cell
TCR	T-cell receptor
Tf-R	Transferrin receptor
TGF- β	Transforming growing factor beta
Th1	T helper type 1
TLR	Toll-like receptor
TLR9	Toll like receptor 9
TMB	3,3',5,5'-tetramethylbenzidine
TMD	Transmembrane domain
TNF- α	Tumour necrosis factor alpha
T _{reg} cells	Regulatory T-cells
TvCSG	<i>T. vivax</i> cell-specific surface proteins
TvMi	<i>T. vivax</i> strain 'Miranda'
UNESP	Universidade Estadual Paulista
UTR	Untranslated region
VAT	Variant antigenic types
VCF	Variant call format
VSG	Variant surface glycoprotein
VSSA	Variant-specific surface antigen
WTSI	Wellcome Trust Sanger Institute
π	Nucleotide diversity

Chapter 1

General Introduction

1.1. Animal African trypanosomiasis

African trypanosomiasis is a parasitic disease in vertebrates with a global distribution caused by flagellate protozoa from the genus *Trypanosoma*. Trypanosomiasis is vector-borne, transmitted by the bite of a tsetse fly (*Glossina* spp.) or other biting fly and the disease is classified according to the trypanosome species, host and the geographic distribution (Bruce, 1915; Yaro *et al*, 2016). In sub-Saharan African countries, *Trypanosoma brucei* is the causative agent of Human African Trypanosomiasis (HAT), also known as “sleeping sickness”. Specifically, 95% of HAT cases are caused by *T. brucei gambiense* in Western and Central Africa, producing a more chronic form of the disease (Stijlemans *et al*, 2016). In contrast, *T. brucei rhodesiense* causes the acute form of HAT in Eastern and Southern Africa accounting only 5% of cases (Black and Seed, 2001; Barrett *et al*, 2003). These sub-species are morphologically indistinguishable and both can cause fatal syndromes affecting the central nervous system (Baral, 2010). Trypanosomes are also the causative agent of Animal African Trypanosomiasis (AAT) or Nagana, a livestock disease caused by three African trypanosome species: *T. brucei brucei*, *T. congolense* and *T. vivax* (Black and Seed, 2001). AAT affects wild and domestic animals causing chronic anemia, weight loss, severe effects on reproduction and cardiac lesions, and in some severe cases could develop neurological dysfunctions, resulting in death if untreated.

1.1.1. Organism and taxonomy

Trypanosomes are unicellular, flagellated haemoparasites belonging to the phylum *Euglenozoa*, class *Kinetoplastida* (See Table 1.1). They are transmitted by blood-sucking arthropods and can be classified in two groups depending on their transmission mode: Stercoraria (Subgenus *Megatrypanum*, *Herpetosoma* and

Schizotrypanum) and Salivaria (Subgenus *Dutonella*, *Nannomonas*, *Trypanozoon* and *Pycnomonas*) (Botero *et al*, 2003). In the Stercoraria group, mammalian trypanosomes infect through feces by contaminative transmission after they develop and multiply in the digestive tract. In contrast, Salivarian parasites develop in the mouthparts of anterior gut and are transmitted via the flies' saliva by inoculative transmission (Osório *et al*, 2008). This group includes all the African trypanosomes able to infect mammals. The Salivarian group comprises the subgenus *Dutonella* including *T. vivax* and *T. uniforme*, *Trypanozoon* including *T. equiperdum*, *T. evansi* and *T. brucei* and the subgenus *Nannomonas* including *T. congolense*, *T. simiae* and *T. godfreyi* (Desquesnes, 2004).

Nagana is mainly caused by three types of trypanosomes; *T. brucei*, which can infect both humans and animals and *T. congolense* and *T. vivax*, both exclusively animal pathogens and are the main causative agents in livestock (Bruce, 1915). Nagana can be caused by one of these species or several in combination, causing single and mixed infections respectively. *T. vivax* is able to infect non-tsetse vector species and transmit mechanically, and has thereby spread to areas in northern Africa and South America (Finelle, 1974).

African trypanosomes may be differentiated by their morphological features and developmental life cycles. *T. vivax* has three morphological forms: bloodstream-form trypomastigote (BSF), epimastigote and metacyclic-form trypomastigote (MET) (Hoare, 1972). *T. vivax* trypomastigotes have an elongated cell-body, within which the nucleus is characteristically the largest organelle. The cytoplasm is limited by the pellicle or outer membrane that enables body movement (Uilenberg and Boyt, 1998). The flagellum emerges from a small membrane invagination called the flagellar pocket (FP), a place for endocytosis and exocytosis (Field and Carrington, 2009). The free flagellum can extend (7 μm) helping the parasite to swim effectively.

The kinetoplast of *T. vivax* BSF can be distinguished from other African trypanosomes by its size of 1.1 μm compared to 0.7 μm and 0.6 μm for *T. congolense* and *T. brucei*, respectively. The kinetoplast, which plays a fundamental role in energy metabolism

and reproduction, is always rounded in *T. vivax* and located at a terminal or subterminal position. In *T. congolense*, the kinetoplastid is rounded and in a subterminal position, whereas in *T. brucei* it is rod-shaped located at subterminal position (Hoare, 1938). *T. vivax* has a mean body length of 21-26 μm and a width of 1.5-3 μm , although this can differ significantly depending on the isolate (Hoare, 1972).

In *T. brucei*, the species that accounts for most research on trypanosome development, the BSF displays pleomorphy and can also be divided in slender and stumpy forms (Matthews and Gull, 1994). In the mammalian host, *T. brucei* parasites undergo an irreversible developmental transition from long slender (LS) to short stumpy (SS) forms. LS cells are characterized by a rounded posterior end and rapid cell division, but are not infective to tsetse flies. During infection, LS cells are the predominate form at peaks of parasitemia, while non-replicative SS predominate when parasitemia declines (Seed and Black, 1997). If a bloodmeal is taken, stumpy cells are infective to the vector and will differentiate in the tsetse midgut, otherwise, these parasites will die. The LS to SS transition, therefore, represents a developmental commitment to transmission. Pleomorphic bloodstream forms have not been observed in *T. vivax* infections and it is not clear if the parasite undergoes a comparable developmental transition.

Phylum	Euglenozoa					
Order	Kinetoplastida					
Suborder	Trypanosomatina					
Family	Trypanosomatidae					
Genus	Trypanosoma					
Subgenus	Herpetosoma	Megatrypanum	Schizotrypanum	Dutonella	Nannomomas	Pycnomomas
Species	<i>T. theileri</i>	<i>T. rangeli</i> <i>T. lewisi</i> <i>T. muscui</i>	<i>T. cruzi</i>	<i>T. vivax</i> <i>T. uniforme</i>	<i>T. congolense</i> <i>T. simiae</i> <i>T. godfreyi</i>	<i>T. equiperdum</i> <i>T. evansi</i> <i>T. brucei</i>
Subspecies					<i>T.b. brucei</i> <i>T.b. rhodesiense</i> <i>T.b. gambiense</i>	
Transmission mode	Stercoraria			Salivaria		

Table 1.1. Classification of trypanosomes.

1.1.2. Geographic distribution

In contrast to HAT, which is distributed specifically within 20 sub-Saharan African countries, AAT has a wider geographic distribution (Namangala and Odongo, 2014) (Figure 1.1). In Africa, AAT is found where tsetse fly vectors live (Eshetu and Begejo, 2015), and distributed throughout this 'tsetse belt' (Pollock, 1982). However, AAT caused by *T. vivax* is also found in tsetse-free areas of Ethiopia (Roeder *et al*, 1984) and Chad (Delafosse *et al*, 2006), due to mechanical transmission by other biting insects (Desquesnes and Dia, 2003).

The tsetse-infested area is approximately between latitude 14° North and 29° South of the Equator (Steverding, 2008), specifically from the southern Sahara Desert to Angola, Zimbabwe and Mozambique (Finelle, 1974). This covers an area of 10 million km² (more than a third of the African land area) and comprises 37 countries (Yaro *et al*, 2016). Although trypanosomes transmitted by tsetse flies are restricted to sub-Saharan countries, the incidence of infection can vary according to region. *T. congolense* infection occurs in regions of East, West and Central Africa more frequently than in Southern Africa (Mamabolo *et al*, 2009). In contrast, *T. vivax* infections are predominant in West African regions (Adam *et al*, 2012; Sow *et al*, 2012).

AAT can extend beyond the tsetse belt due to mechanical transmission by other blood-sucking flies, most notably in south Asia and in Latin America (Silva *et al*, 1996). In fact, it was demonstrated that *T. vivax* has lost its capacity to develop in *Glossina* (*Glossina palpalis*) by Roubaud *et al* (Roubaud and Provost, 1939) suggesting that other vectors were implicated for the transmission. A plausible explanation for the dispersal of *T. vivax* to South America is the introduction of infected zebus (*Bos indicus*) from Senegal to Guyana and the French West Indies as a consequence of European colonization (Jones and Dávila, 2001; Dávila *et al*, 2003; Osório *et al*, 2008). It is well established that the first report of the introduction of *T. vivax* in the American continent was in French Guiana and the French West Indies, named then as *T. guyanense* (Leger and Vienne, 1919). In the New World, *T. vivax* has been

identified in naturally infected cattle in French Guyana, Colombia, Venezuela, Brazil, Peru, Bolivia, Costa Rica and Panama (Johnson, 1941; Clarkson, 1976; Silva *et al*, 1998; Tafur *et al*, 2002; Dávila *et al*, 2003; Quispe *et al*, 2003; Garcia *et al*, 2005; Osório *et al*, 2008; Oliveira *et al*, 2009; Cadioli *et al*, 2012). Here, AAT is known by different names according to the country like “Huequera”, “Cacho Hueco” or “Secadera” (Desquesnes, 2004).

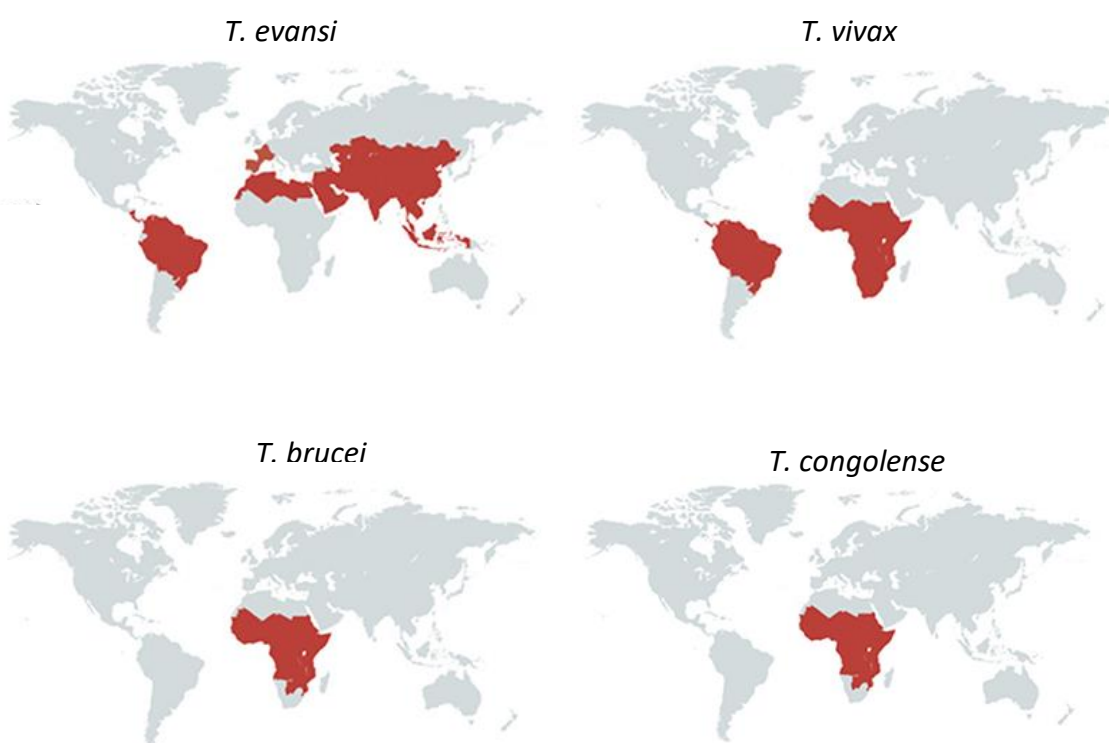


Figure 1.1. Geographical distribution of African animal trypanosomiasis in Africa and South America caused by *T. evansi*, *T. brucei*, *T. vivax* and *T. congolense*. In Africa, the distribution of AAT is in Sub-Saharan countries while in South America can be spread in almost the whole continent caused only by *T. vivax*. Picture taken from (Radwanska *et al*, 2018).

1.1.3. Impact

AAT has a direct impact on agriculture productivity and as a consequence, is an obstacle to the economy in Sub-Saharan African regions. In Africa, It has been

estimated that calf mortality goes up to 20% in infected regions (Shaw, 2009), and AAT can reduce cattle density by 37-70% and productivity by 50% (Gardiner, 1989). Losses in milk and beef production as well as secondary products like leather can be estimated in millions of dollars per year (Perry, 2015). Moreover, AAT not only has an impact in animal production but also in crop yields (Connor, 1994) since cattle draught is used as part of farming systems in many sub-Saharan countries. As a consequence, family income as well as human nutrition is affected. The economic impact of control strategies have also affect African farmers with an investment of US\$35 million per year in trypanocidal drugs (Dagnachew and Bezie, 2015).

In South America, AAT is spread throughout the whole continent with more than 11 million head of cattle at risk of acquiring the disease, representing losses up to US\$160 million per year (Seidl *et al*, 1999). However, in some countries it is hard to establish the economic importance of AAT due to the fact that the prevalence of *T. vivax* can be variable in time and space.

1.1.4. Vector

African trypanosomes are transmitted by the bite of tsetse flies from the genus *Glossina* in sub-Saharan African countries (Figure 1.2). This genus comprises 31 species and subspecies of flies, all are potential vectors for trypanosomes. The distribution of *Glossina* species depends on their different ecological requirements and geographical conditions such as temperature, vegetation and food.

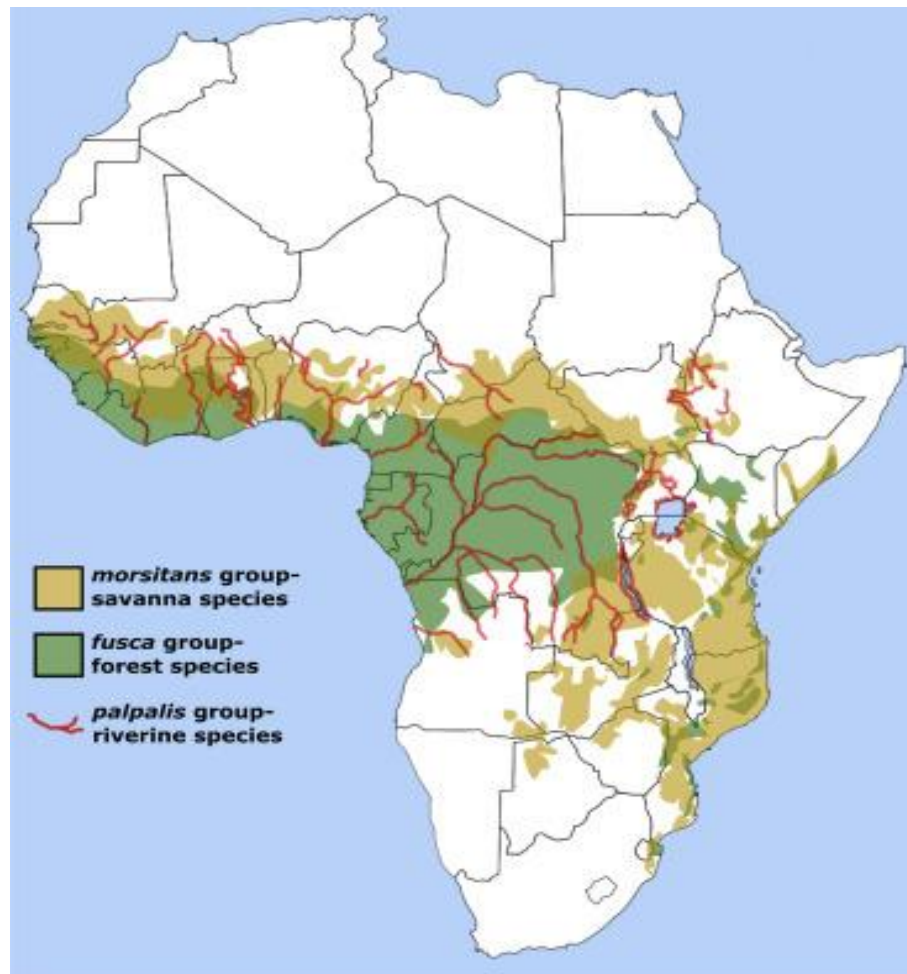


Figure 1.2. Distribution of *Morsitans*, *Fusca* and *Palpalis* group of tsetse flies across Africa. Figure taken from Tsetse flies (*Glossinidae*) (Krinsky, 2019).

There are three groups or subgenera of *Glossina* species: *Morsitans* (savanna species), *Palpalis* (riverine group) and *Fusca* (forest group) (Jordan, 1993). The subgenus *Glossina sensu stricto* or *morsitans* group correspond to species that are distributed in the grassy woodland of the African Savannah (Pollock, 1982) and are limited by climatic conditions, avoiding the wettest areas. The genus *Nemorhina*, or *palpalis* group, correspond to flies living in humid and wet areas like the rainforest and mangrove swamps of central and west Africa. They can live in periurban and urban areas due to their adaptation to environmental changes (Krafsur, 2009). Flies from the subgenus called *Austenina* or *fusca* group have a more limited distribution depending of the subgroup. However, the majority of the species live predominantly in forest belts. Some of the factors affecting the transmission rate of *T. vivax* include

seasonal variations; the infection rate of *G. palpalis* is higher during heavy rainfall (July-October) (Squire, 1951), while the rate of *G. morsitans* is higher during hot seasons (Jordan, 1964). In addition, there is also evidence that vector species affects the virulence of the *T. vivax* isolate; Hoare (1972) comments that isolates transmitted by *G. fuscipes* cause chronic infections followed by death, whereas those transmitted by *G. pallipides* cause predominantly acute infections (Hoare, 1972).

1.1.5. Development of *T. vivax*

T. vivax is an heteroxenous parasite in Africa. Its development begins in the bloodstream of the mammalian host where the trypomastigotes proliferate (Figure 1.3). When a tsetse fly ingests the parasite during a blood meal (day 0), a reduced population of elongated trypomastigotes stay in the foregut and proventriculus, while the majority degenerates in the midgut after a few days. *T. vivax* migrates (day 1-3) to the cibarium and proboscis where they transform into epimastigotes. It is still unclear if there is an intermediate stage during this transition. Epimastigotes attach to the proboscis using their flagellum and multiply forming rosettes, colonizing the region in a process called metacyclogenesis. During their multiplication, epimastigotes can either undergo symmetric division generating two epimastigotes daughters or go under asymmetric division generating one epimastigote and one trypomastigote (day 3-7). The pre-metacyclic trypomastigote produced by the asymmetric division then becomes detached and migrates to the hypopharynx, where they mature into metacyclic trypomastigote forms (Ooi *et al*, 2016). Metacyclogenesis is one of the most important life cycle phases since the metacyclic-forms are the only stage able to infect the mammalian host. The cycle is completed when the mammalian host is inoculated by the tsetse fly when it feeds.

The development of *T. vivax* appears to be simpler when compared to the *T. brucei* or *T. congolense* life cycles. For example, in the *T. brucei* life cycle, once the BSF parasite is ingested, the procyclic form is the first stage of the cycle that develops in the mid-gut, which then migrates to the salivary glands to later differentiate into

epimastigotes (Matthews, 2005). *T. vivax* lacks the procyclic stage, and comparative genomics has shown that procyclin, the major surface glycoprotein of the procyclic form, is absent from the *T. vivax* genome (Jackson *et al*, 2013).

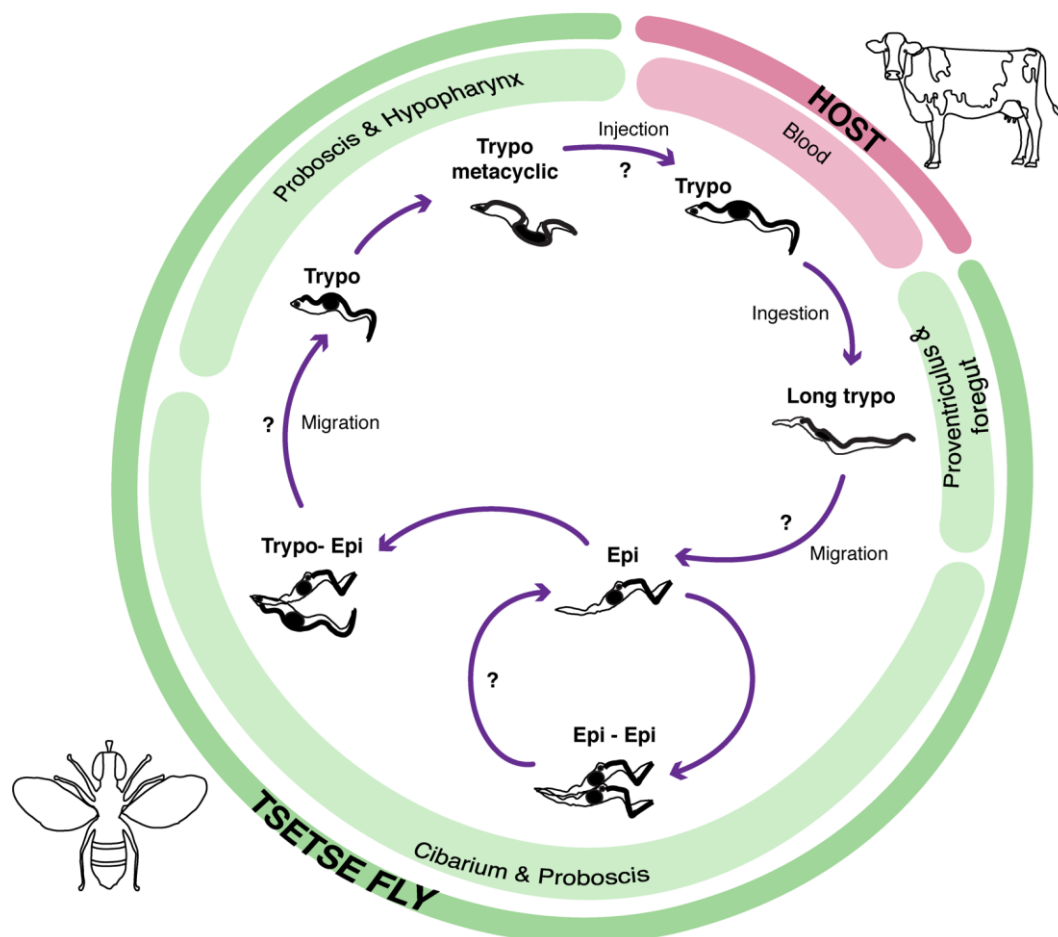


Figure 1.3. A suggested model for the *Trypanosoma vivax* life cycle. Question marks indicate transitions in the cycle that are not fully understood. Trypo: trypomastigote, Epi: epimastigote. Life cycle model based on (Ooi *et al*, 2016).

1.1.6. Course of infection and pathogenesis

African trypanosomes can infect a wide variety of animals; cattle, goats and sheep are the most important hosts with regard to economic impact in sub-Saharan African countries. AAT infect domestic and wild animals living alongside cattle, such as water-buffalo, horses, donkeys and others (Spickler, 2010). In cattle infected with *T. vivax*, the incubation period is between 9-59 days, while in sheep and goats it is between 4-12 days (Hoare, 1972; Stephen, 1986).

The course of *T. vivax* infection can be divided into acute and chronic phases. During the acute phase, anaemia is the most common clinical symptom due to erythrocyte lysis and a consequent reduction in the Packed Cell Volume (PCV) and haemoglobin concentration. This form of inflammatory anaemia has been suggested to be the major contributor to deaths (Figure 1.4). Other typical signs of the acute phase are fever, lethargy, weight loss, decrease in milk production, diarrhoea, lacrimation and severe effects in reproduction leading to abortions and changes in sperm morphology (Murray *et al*, 1979).

During the chronic, parasitemic stage, *T. vivax* can be found in extravascular regions like lymph nodes and aqueous humour in eyes (Whitelaw *et al*, 1988). Clinical manifestations during chronic infections with African trypanosomes are characterized by cachexia, leucocytosis and leukopenia being the two latter one of the most important events during infections in cattle, sheep and goats. However, a decrease in white blood cell levels can be also seen during the acute phase (Fidelis Junior *et al*, 2016). During the chronic phase, the adaptive immune response plays a crucial role to controlling the infection. In some severe cases, the host develops neurological dysfunctions resulting in death if untreated; nonetheless animals can die whether or not they present clinical symptoms.

Pathological manifestations, as well as the severity of the disease, depend on the parasite isolate and the host environment. In Africa, cattle are the principal host for *T. vivax* presenting severe disease with a 70% mortality rate. Sheep and goats present

a moderate disease severity, although mortality rate can reach 70% and 12% respectively (Hoof *et al*, 1948). It is usual to observe mixed infections with *T. congolense*. Moreover, it is clear that animals infected with trypanosomes are more susceptible to other pathogens (Taylor and Authié, 2004). Interestingly, there are some African livestock breeds that live in tsetse fly areas and are able to survive to trypanosome infections naturally, without the need for treatment. This phenomenon is called trypanotolerance and refers to N'Dama cattle, Djallonke sheep and West African Dwarf goats (Yaro *et al*, 2016). The mechanisms of trypanotolerance are still unknown; nevertheless they might have developed their reduced susceptibility due to cross breeding with an old indigenous bovine population (Naessens, 2006). Due to the fact that trypanotolerant animals have lower parasite levels, less anaemia and greater productivity, their cultivation is considered an economically sustainable way to control AAT (Murray, 1983).

The pathogenicity of AAT depends on the parasite strain, particularly if it is isolated from different geographical locations (Taylor and Authié, 2004). There are differences in virulence between West and East African isolates of *T. vivax*. East African strains are associated with a moderate infection and lower mortality compared to West African strains, which are more virulent and cause a more severe disease in cattle (Hornby, 1952; Black and Seed, 2001). This general trend notwithstanding, it has been shown that some East African strains can cause severe symptoms like haemorrhagic syndromes. In 1981, Mwongela *et al* monitored naturally infected cattle from two farms during an AAT outbreak in Kenya in an attempt to identify the etiological agent (Mwongela *et al*, 1981). The animals presented a haemorrhagic disease, became markedly anorexic, and showed both decreased rumenal motility and milk yield. All such animals were positive for *T. vivax* only, confirming that *T. vivax* caused this syndrome in cattle.

In the case of South American strains, genetic analysis has indicated a close phylogenetic relationship with West African strains (Cortez *et al*, 2006). *T. vivax* can be found in diverse ruminants as well as horses causing severe disease and death (Da Silva *et al*, 2011). AAT in South America is highly pathogenic and has a high mortality

rate linked to newly infected animals (Desquesnes, 2004). The haemorrhagic syndrome described in East African strains has been also described in a Brazilian isolate (Strain 'Lins') (Cadioli *et al*, 2012).

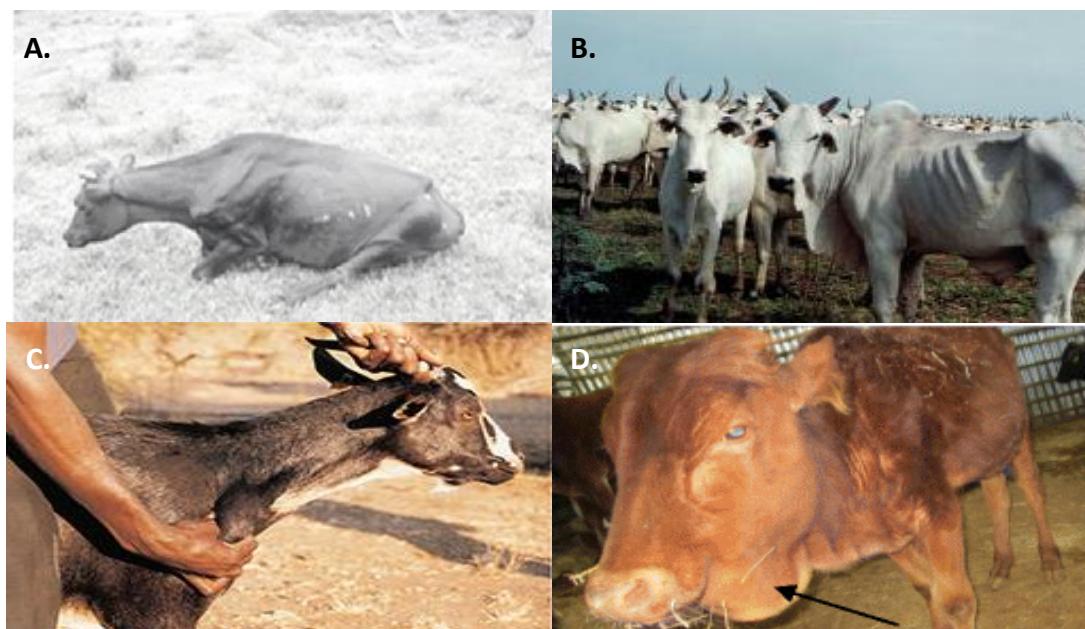


Figure 1.4. Examples of common clinical symptoms during *T. vivax* infection. **A.** Acute phase of a cow positive for *T. vivax*, displaying difficulties in walking in Rio Grande do Sul, Brazil (da Silva *et al*, 2009). **B.** Cattle displaying weight loss due to an AAT outbreak in Pantanal, Mato Grosso do Sul, Brazil (Osório *et al*, 2008). **C.** A goat naturally infected with *T. vivax* presenting enlargement of lymph nodes (Afrivip.org). **D.** A Zebu cow experimentally infected with *T. vivax* presenting oedema (indicated by black arrow) at 19 dpi (Dagnachew *et al*, 2015).

1.1.7. Diagnosis

An accurate diagnosis of AAT is needed to develop control strategies for tsetse flies and for epidemiological studies (Eshetu and Begejo, 2015). Signs presented during acute and chronic infection must be taken into consideration for clinical diagnosis, especially in endemic areas. However, they are unreliable since it can be confused

with other infections affecting the host. AAT diagnosis is particularly challenging due to the lack of specific clinical manifestations, and not applied effectively to improve treatment at village level (Luckins *et al*, 2004).

The presence of actively motile *T. vivax* in blood samples diagnosed by parasitological tests provides a reliable measurement of the infection status (Luckins, 1992). The Woo technique (Woo, 1969) is the most common parasitological method of diagnosis but no parasitological method for diagnosis is entirely effective in the identification of infected animals, and the Woo technique has low sensitivity in chronic infections due to low parasitemia (Osório *et al*, 2008). The examination of lymph can also lead to the correct diagnosis of *T. vivax* when collected from lymph nodes (Taylor, 2016).

Serological tests are another diagnostic technique developed to detect specific circulating antibodies produced by the mammalian host against trypanosomes. There are two main immunological tests: Indirect immunofluorescence assay (IFA) and the Enzyme-linked immunosorbent assay (Berriman *et al*) (Eshetu and Begejo, 2015). The sensitivity and specificity of detecting *T. vivax* with ELISA in naturally and experimentally infected livestock depends on the nature of the antigen and is variable within experiments (Eisler *et al*, 1998; Madruga *et al*, 2006). Typically, a crude antigen is produced by each laboratory for diagnosis, and there is no validated ELISA to diagnose AAT (Black and Seed, 2001). Using ELISA with recombinant proteins has been demonstrated in previous reports for AAT to have good sensitivity but not high specificity (Nguyen *et al*, 2015).

Serological tests by antibody detection is not necessarily indicative of active infection; antibodies can still be detected in sera even after the infection is cleared. Yet, several *T. vivax* antigens are now used as candidates for diagnosis in cattle with high sensitivity (Pillay *et al*, 2013). However, they may show false negatives for recently infected animals and can cross-react with other trypanosomes like *T. theileri* and until now, there is no ELISA assay able to detect circulating antigens.

The diagnosis by molecular tests like Polymerase Chain Reaction (PCR) assay establishes the presence of trypanosome DNA using species specific primers. There have been several studies using different primer sets that have detected African trypanosomes in whole blood or sera (Masiga *et al*, 1992; Desquesnes, 1997; Desquesnes *et al*, 2001; Desquesnes and Davila, 2002; Cox *et al*, 2005; Hamilton *et al*, 2008; Fikru *et al*, 2014; Tran *et al*, 2014). PCR positive results are indicative of active infection due to the short period of time DNA remains in the host (Eshetu and Begejo, 2015). The specificity of diagnosis is highly improved compared to parasitological and serological tests but it is still uncertain if the primers can recognize all strains of species (Geysen *et al*, 2003). Low levels of parasitemia, a characteristic of chronic infections can lead to false negatives.

Rapid diagnostic tests for AAT based on an immune-chromatography has been recently developed. The Very Diag test (Ceva, Africa) is a novel rapid test that can be used in the field being able to detect *T. vivax* and *T. congolense* simultaneously in the same sample (Boulangé *et al*, 2017). Likewise, another rapid test specifically for the detection of *T. vivax* using a recombinant species-specific antigen (TvY486_0045500 and TvY486_0019690) was reported (Fleming *et al*, 2016). Despite having a high sensitivity and specificity with no cross-reaction with *T. congolense*, it is yet to be commercialized.

1.1.8. Treatment and control strategies

Control strategies are based on two approaches: vector control and treatment of the infected host. In endemic areas of sub-Saharan Africa, controlling tsetse using traps and insecticides by spraying is crucial to prevent control infections (Connor, 1992). These control strategies are commonly used locally due to their low cost and time required, but, while they can be very effective, they are expensive and require considerable logistical support on a country-wide scale. In this regard, vector control is not always sustainable and other measures are needed for an effective control (Holmes, 2013).

The current treatment for AAT is focused on endemic areas and relies on chemotherapy and chemoprophylaxis. Drugs like diminazene aceturate and isometamidium chloride have been widely used in chemotherapy (Kuzoe and Schofield, 2004). A successful treatment is usually combined with quarantines, movement controls and euthanasia of infected animals (Spickler, 2010). Despite this, other factors like a good nutrition plan and monitoring clinical signs are crucial for the animals' recovery. The antitrypanosomal activity of certain drugs like isometamidium is very high for *T. vivax* and *T. congolense* in cattle and in *T. brucei* and *T. evansi* in infections in horses and donkeys. Transition of infected animals to the chronic phase usually occurs after failed drug treatment, and even successful drug treatment may not clear the pathogen, leaving treated animals with residual signs like anaemia and weight loss (Kinabo, 1993).

Drug resistance among African trypanosomes is well documented. There are 17 sub-Saharan African countries, with drug resistance reports in which 8 of them present multiple resistance. However, this number might be underestimated due to the lack of reports in several countries (Delespaux *et al*, 2008). A plausible explanation for drug resistance is the long-term usage and lack of choice among drugs available in the market (Geerts *et al*, 2001). This leads to treatment failure and ineffective disease control. Therefore, it remains the case that alternative trypanocidal drugs are needed.

Vaccination of the host against AAT has been an elusive prospect and persistent challenge over the years. There is no commercially available vaccine for AAT, and it has often been thought that such a vaccine is implausible due to antigenic variation (Van Meirvenne *et al*, 1975; Van Meirvenne *et al*, 1975; La Greca and Magez, 2011; Black and Mansfield, 2016). Potential immunological targets have been identified in pursuit of a vaccine (see 1.4) without success. In the absence of an effective vaccine, trypanocidal drugs are still the key to control trypanosomiasis.

1.2. Antigenic variation

Antigenic variation describes the ability of a pathogen to escape from the host immune response by changing their surface molecules (Clements *et al*, 1988). Besides African trypanosomes, variation of surface glycoproteins as to avoid the antibody response is the principal mechanism of immune evasion in diverse pathogens such as *Plasmodium* spp., viruses such as *Influenza* spp., and *Mycobacterium* spp. (Clements *et al*, 1988).

During an infection with African trypanosomes, specific antibodies against the surface of the parasites are produced by the host. Antigenic variation refers to the ability of Salivarian trypanosomes to express distinctive antigens on their surface facilitating the evasion of such antibodies. The principal target of host antibodies, and the phenotypic basis to antigenic variation, in African trypanosomes are the Variable Surface Glycoproteins (VSG). VSG are the major constituent of the BSF cell surface glycocalyx; the coat contains approximately 10^7 VSGs displayed as homodimers (50-60 kDa subunits), and attached via glycosylphosphatidylinositol (GPI) anchors, producing a thick monolayer over the entire parasite's surface, and representing about 20% of the total cell protein (Horn, 2014). The surface organization of the VSG coat consists of molecules firmly packed with an orientation of the C-terminal domain close to the membrane (Borst and Cross, 1982). The arrangement of the coat serves as a physical barrier with two main purposes: (1) to protect the parasites from the immune system and lysis by the complement system and (2) to shield from the immune system invariant proteins that might also have a surface location (Stijlemans *et al*, 2016).

VSG are highly immunogenic but serial replacement of the VSG renders the prevalent antibody response redundant and leads to chronic infections (Gardiner *et al*, 1996) (Figure 1.5). During an infection the host immune system recognizes VSGs, the antibody titre increases and as a consequence, most of the parasites expressing that same VSG are destroyed. Nevertheless, a few parasites remain alive since they have switched their active VSG (Horn, 2014). The serial replacement of the dominant

parasite clone by another expressing a distinct VSG gives parasitaemia a particular pattern. During the early stage of the infection, peaks or “waves” of parasitaemia are seen; the ascending phase corresponds to a high level of parasites occurring before the antibody response, while the descending phase reflects a successful, but temporary, protective effect (Osório *et al*, 2008).

African trypanosome genomes contain a library of over a thousand alternative VSG providing ample material for repeated antigenic switches (Berriman *et al*, 2005; Jackson *et al*, 2012), but VSG genes display monoallelic expression (Pinger *et al*, 2017).

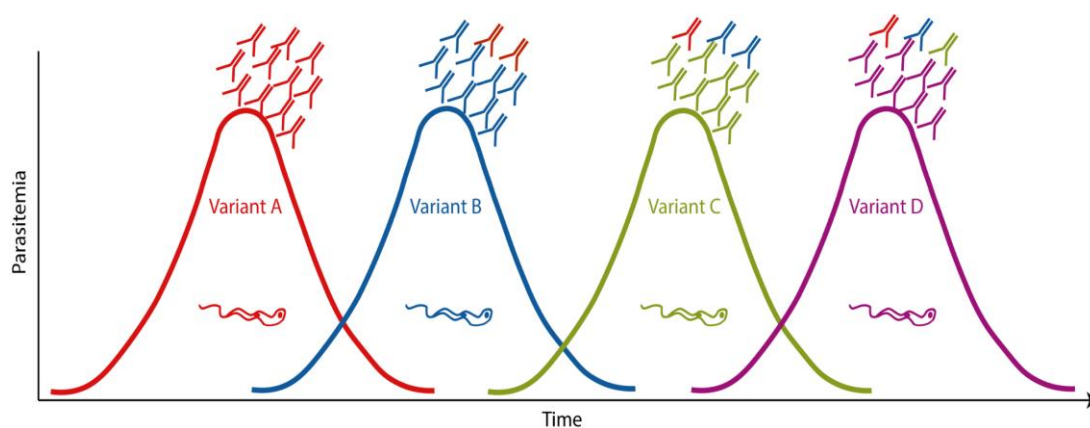


Figure 1.5. Waves of parasitaemia characteristic of African trypanosome bloodstream infections, and reflective of VSG switching. Antigenic variation of VSG produces waves of parasitaemia (different colors). Highly immunogenic VSG trigger the production of specific antibodies, however low frequency parasite clones express an alternative VSG and evade the antibody response, resulting in chronic infection.

1.3. Immune response to African trypanosomes

The interaction between African trypanosomes and their mammalian host begins when the tsetse fly injects metacyclic trypomastigotes intradermally. The parasite

must fight against the two types of immune response: (1) the non-specific innate immune response and (2) the antigen-specific adaptive immune response.

The immunology and the mechanisms of immune evasion have been widely studied in *T. brucei* since its relevance as human pathogen. The immunology of livestock trypanosomes has focused on *T. congolense* infections in cattle. By contrast, the immune response to *T. vivax* is poorly understood. Therefore, it is important to note that most of the immunobiology described in the following sections are based on studies of *T. brucei*.

1.3.1. Innate immune response

After a blood-meal, the saliva of tsetse flies plays a crucial role in the parasite transmission. The saliva proteins are highly immunogenic, and have two broad effects on the injection site micro-environment (Telleria *et al*, 2014). First, they allow blood-feeding by inhibiting coagulation, vasoconstriction and platelet aggregation (Ribeiro and Francischetti, 2003). Second, they inhibit innate immunity effectors (Bai *et al*, 2015).

One crucial event during the infection is the activation of myeloid lineage cells like macrophages (MØs), monocytes, dendritic cells (Cuglovici *et al*) and some granulocytes, which contribute the first line of defense against trypanosomes (Namangala, 2012). The classical activation of macrophages (caMØs) is established during early stages of infection (Figure 1.6). Activation occurs in a type-I cytokine environment (interferon gamma (IFN- γ), interleukin 12 (IL-12) and tumour necrosis factor alpha (TNF- α)) and is inhibited by type-II cytokines (interleukin 4 (IL-4), interleukin 10 (IL-10)). caMØs release reactive oxygen species (ROS) as part of a pro-inflammatory process, performing an anti-proliferative role (Namangala *et al*, 2001). Activation of these cells occurs when damage-associated molecular patterns (DAMPs) and pathogen-associated molecular patterns (PAMPs) like lipoproteins and flagellin from the parasite are bound by host membrane pattern recognition

receptors (PRRs) (Namangala, 2012). Receptor-mediated MØs secrete pro-inflammatory cytokines, chemokines and IFN- γ generating an inflammatory response (Stijlemans *et al*, 2016), contributing to control the first peak of parasitemia (Baral, 2010).

The activation of macrophages is due to their interaction with different parasite-derived molecules. The parasite-derived GPI-anchor of the VSG is a macrophage-activating agent activating TNF- α , a cytokine involved in immunosuppression in cattle (Stijlemans *et al*, 2010). The endogenous GPI-phospholipase C (GPI-PLC) is activated and cleaves the GPI anchor of the membrane form of VSG molecules (mfVSG) releasing the soluble glycosylinositolphosphate VSG (GIP-sVSG) from the membrane into tissues and blood (Stijlemans *et al*, 2016). The GIP residues of sVSG molecules activate MØs by binding to their Type A scavenger receptor (SR-A) (Leppert *et al*, 2007); this results in the induction of the nuclear factor kappa-light-chain-enhancer of activated B cells (NF- κ B) and MAPK pathways, triggering a pro-inflammatory immune response (Mansfield *et al*, 2014). The GIP-sVSG/SR-A interaction also leads the activation of toll-like receptors (TLR) and myeloid differentiation factor 88 (MyD88) (Mansfield *et al*, 2014).

At this point of the infection, a large number of trypanosomes are destroyed by innate immune cells, releasing internal components into circulation which are also detected. The unmethylated CpG DNA released by damaged or dead trypanosomes is another PAMP recognized by the immune system. CpG DNA activates toll like receptor 9 (TLR9) resulting in caMØs, triggering the expression of pro-inflammatory genes and cytokine production (Stijlemans *et al*, 2016).

1.3.2. Adaptive immune response

The immune response caused by pro-inflammatory cytokines produced during early infection can cause pathology if prolonged. caMØs, as well as pro-inflammatory cytokines, are down-regulated by switching from a type I to a type II immune

response (Figure 1.4). Anti-inflammatory cytokines (transforming growing factor beta (TGF- β), IL-4, IL-10) are secreted by the alternative-activated macrophages (aaM ϕ s) once the infection is established and in a type-II cytokine environment (Namangala *et al*, 2001). As a result, a shift from type I to type II immune response benefits the host leading to a longer survival (Baral, 2010).

T-cells are essential for African trypanosome control and in preventing further pathology like anaemia (Stijlemans *et al*, 2010). The presence of pro-inflammatory IL-12 is required for T-cell polarization to T helper type 1 (Th1) cells producing a Th1 cytokine pattern (Swain, 1995; Mansfield *et al*, 2014). Th1 cells potentially recognize peptides located in the N-terminal domain of the VSG molecule (Mansfield *et al*, 2014). However, the parasite evades the immune system by inducing non-essential responses during early infection and by suppressing T-cells (Namangala, 2011). This suppressive phenotype is due to a down-regulation of IL-2 secretion and the IL-2 receptor (IL-2R) (Stijlemans *et al*, 2016). Another means of immuno-suppression is IL-10 production (Taylor and Mertens, 1999). As described above, IL-10 triggers the aaM ϕ s and plays a key role in regulating both trypanotolerance and pathogenicity. Regulatory T-cells (T_{reg} cells) produce IL-10, inhibiting caM ϕ s activation and IFN- γ production by T-cells (Namangala, 2012). As a result, this T_{reg} cell-mediated suppression reduces immunopathology, allowing chronic infection and extended parasite survival (Guilliams *et al*, 2008). Furthermore, there is a lack of immunological memory by T-cell populations associated with a defects in the function of antigen presenting cells (APC), which allowing trypanosomes to maintain chronic infections (Mansfield *et al*, 2014).

Figure 1.6. A model of the role of macrophages during an African trypanosome infection. During early stages of infection, the parasite releases TLTF activating CD8⁺ and NKT cells to secrete IFN- γ . PAMPs, in concert with IFN- γ , will activate caM \emptyset releasing pro-inflammatory cytokines such as TNF- α and NO, controlling the parasite load during the first peak of parasitemia. During later stages, there is a switch from caM \emptyset to aaM \emptyset secreting anti-inflammatory cytokines like IL-10 to reduce inflammation enabling survival of the host. TLTF: trypanosome-derived lymphocyte-triggering factor, PAMPs: pathogen-associated molecular patterns, PRRs: pattern recognition receptors, caM \emptyset : classically activated macrophages, aaM \emptyset : alternatively activated macrophages, NO: nitric oxide, Tip-DC: TNF- α and inducible NO synthase producing dendritic cell, Source: (Baral, 2010; Stijlemans *et al*, 2010; Namangala, 2012).

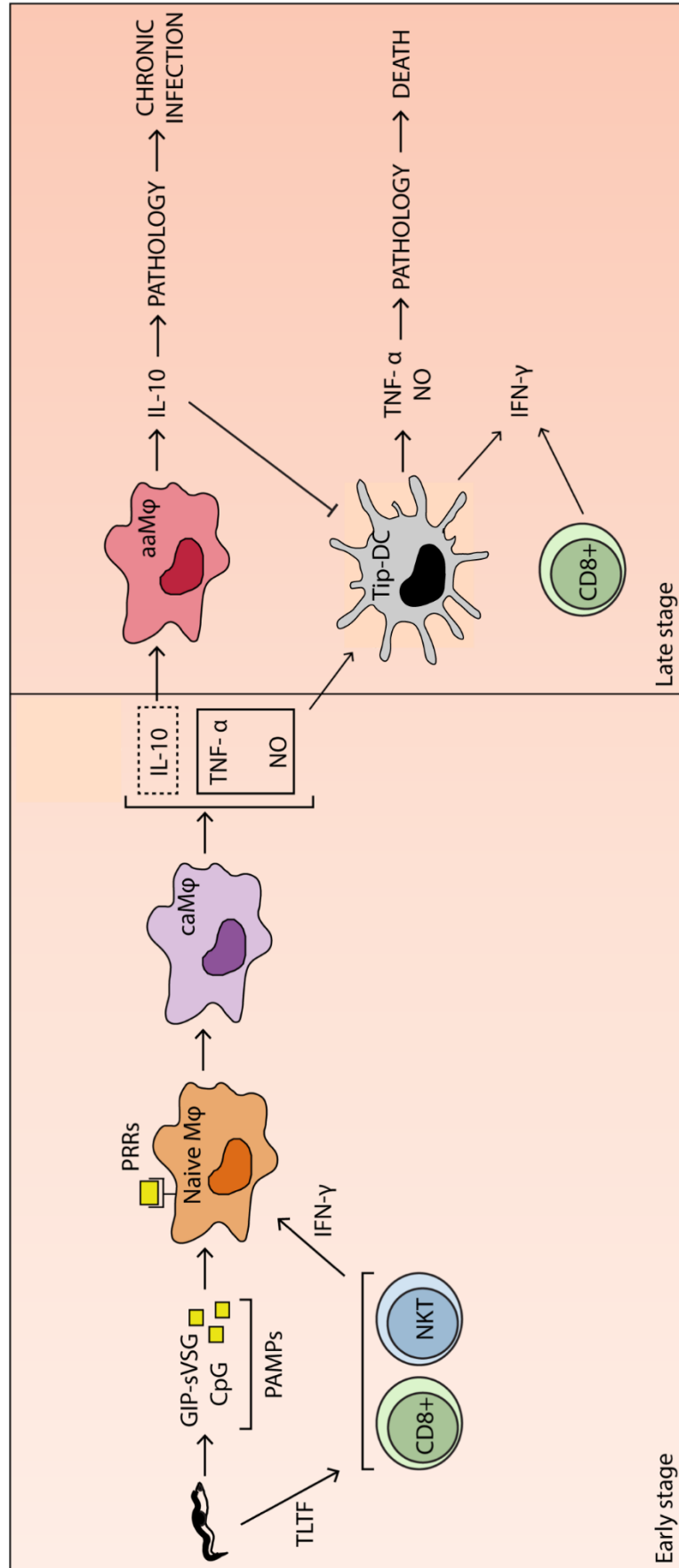


Figure 1.6

1.3.3. Humoral immune response

The humoral immune response starts with polyclonal B-cell activation by trypanosome-derived factors (Figure 1.7). Immature B-cells, which express large amounts of immunoglobulin M antibody, migrate from the bone marrow to the spleen as transitional B cells (T1) to complete their development. In the spleen, immature B-cells differentiate into mature naïve cells called marginal zone B cells (MZB) (Stijlemans *et al*, 2017). This activation is fast, T-cell independent and leads to the production of low-affinity IgM antibodies. These antibodies have a short life and attain their maximum level between 3-4 days after the peak of parasitemia; they are crucial for parasitaemia control (Magez and Radwanska, 2014).

The host mounts a humoral immune response after VSG-specific B-cell activation by producing VSG-specific IgM antibodies that results in parasite destruction and control of the first peak of parasitemia. However, polyclonal B-cell activation is suppressed, making it difficult to control the infection during late stages of infection (Baral, 2010). Linear VSG epitopes of dead or damaged trypanosomes are exposed in a way they can be recognized by IgMs (Taylor, 1998). Buried epitopes are not accessible to these antibodies due to the density of the VSG coat (Schwede *et al*, 2015). As described above, antibodies against specific epitopes are not able to kill trypanosomes with new VSG antigens on their surface, producing a new peak of parasitemia. Although these antibodies are polyspecific and do not confer memory against other VSGs (Magez and Radwanska, 2014), the massive production of IgM antibodies due to non-specific B-cell activation can, nonetheless, lead to hyperplasia in lymph nodes and spleen causing pathology (Donelson *et al*, 1998).

It is important to note that the peak in parasitaemia is independent of the production of IgM VSG-antibodies. Some researchers suggest that there is an immunoglobulin G (IgG) production with normal amounts comparable to IgMs levels (Sendashonga and Black, 1982). Still, it is now known that cattle and mice infected with African trypanosomes are able to produce long-lived IgG antibodies helping the clearance of circulating parasites (Stijlemans *et al*, 2007). Moreover, a long term IgG1 and a

temporal IgG2 isotypes response against buried VSG epitopes are detected in bovine trypanosomiasis (Williams *et al*, 1996). In general, trypanosusceptible bovines present an unsatisfactory humoral immune response with defects in the switch mechanism from IgM to IgG antibodies, lower levels of VSG-specific IgG1 and an IgG response that occurs later and weaker when compared with trypanotolerant cattle (Taylor *et al*, 1996).

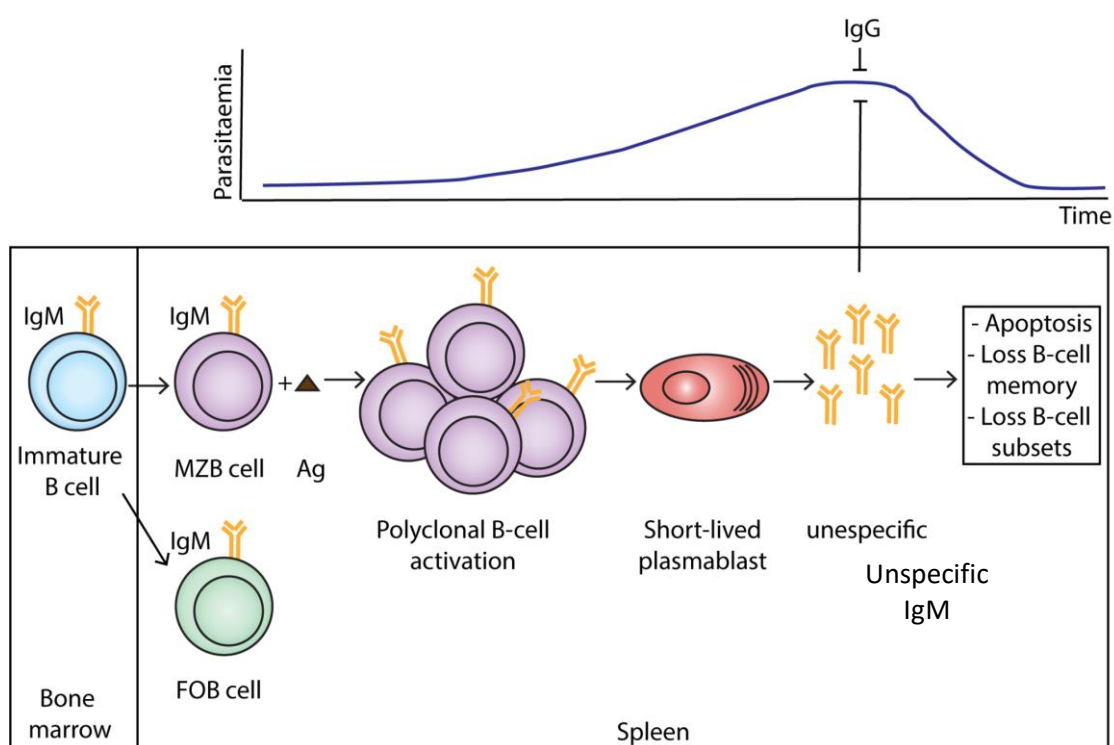


Figure 1.7. A model of B-cell development and humoral immune response against African trypanosomes within the mammalian host. Polyclonal B-cell activation leads to short-lived non-specific IgM antibodies able to control the first peak of parasitemia. B-cells differentiate into short-lived plasmablast producing unspecific IgMs for immediate protection and IgGs for long-term response. Figure based on (Stijlemans *et al*, 2016; Stijlemans *et al*, 2017).

1.3.4. Immuno-suppression

One of the hallmarks of an African trypanosome infection is immuno-suppression. It has been shown that the immuno-suppression in African trypanosomiasis varies according to the species of parasite and strain. Chronic infections of cattle with *T. congolense* and *T. brucei* seem to suppress the antibody response to a greater extent compared to *T. vivax* (Rurangirwa *et al*, 1983).

Immuno-suppression seems to be a universal feature of an infection with African trypanosomes characterized by a generalized suppression that affects humoral and cellular immune functions leading to immuno-pathology (Baral, 2010). Suppression is marked by a decrease in T-cell proliferation and subsequent cytokine production (Taylor, 1998). In *T. brucei*, immuno-suppression is closely related to a decrease in IL-2 production and its receptor (IL-2R) (Sileghem *et al*, 1986). The mechanisms to control T-cell suppression are not fully understood but there are clear differences between phases of *T. brucei* infections. During early stages, activated macrophages secrete NO and prostaglandins in the lymph node that inhibit IL-2 production. A reduction of IL-2R can be reversed by anti-IFN- γ specific antibodies (Darji *et al*, 1993). During late stages of the infection, the inhibition of T-cell proliferation is independent of NO and prostaglandins, instead anti-inflammatory cytokines like IL-10 might play a crucial role (Baral, 2010).

It has been suggested that IL-10 might contribute to the failure of macrophages to produce inflammatory products in infected cattle. Indeed, it is suggested that this cytokine might be related to the de-activation of macrophages during *T. congolense* infections (Taylor and Mertens, 1999). Downregulation of macrophages and Th1 cytokines by IL-10 have been demonstrated to protect against different pathogens but can also be ineffective for parasite clearance (Heinzel *et al*, 1991).

1.4. Vaccination against African trypanosomes

Anti-trypanosomiasis vaccines should be a crucial component in the fight against AAT and are the best strategy to protect animals from re-infection. However, after many attempts and approaches using different antigens from distinct life cycle stages, not a single vaccine trial has showed to be effective with full protection. As previously stated, antigenic variation is the major obstacle to vaccination. Anti-VSG specific antibodies are able to control the first peak of parasitaemia but immuno-suppression and the destruction of B-cell memory leads to chronic infection and in unsuccessful vaccine development. Before this was fully appreciated, various studies over the last 50 years tried to apply conventional vaccinology approaches (Table 2).

One of the first attempts to vaccinate used irradiated parasites as antigen in different animals experimentally infected with *T. congolense* (Duxbury *et al*, 1972). In this study, *T. congolense* parasites were first exposed to radiation in a gammacell with cobalt and then used to immunize mice, dogs and cattle. All animals were challenged observing differences between animal models but only partial protection was observed in mice.

In 1982, 10^7 irradiated *T. brucei* parasites and purified VSG were used to immunized cattle prior infection with 10^4 trypanosomes (Morrison *et al*, 1982). They demonstrated a high antibody response against both antigens with complete protection but the effect was not reproducible when the inoculum was lower (partial protection only).

Vaccines against other pathogens have also been tested for their ability to protect against trypanosomes. Rurangirwa *et al* (Rurangirwa *et al*, 1980) examined the effect of the live rinderpest virus vaccine on Boran cattle experimentally infected with *T. vivax* and *T. congolense*. Animals from vaccinated and control groups showed no significant differences in parasitaemia against either trypanosome. In addition, the same vaccine was tested against both parasites in Orman Boran and Galana Boran cattle producing the same negative results (Stevenson *et al*, 1999). Vaccination with

the *Brucella abortus* S19 vaccine against *T. congolense* and *T. vivax* in experimental bovine infections (Rurangirwa *et al*, 1983) demonstrated only partial protection with a reduction in specific IgG subclasses against *T. congolense* but not for *T. vivax* (Rurangirwa *et al*, 1983).

With vaccination using the entire parasite or with vaccines against other pathogens unsuccessful in cattle, other approaches then focused on specific parasite antigens. In 1982, Wells and collaborators immunized cattle with soluble variant-specific antigen of *T. brucei* (VSSA) from the ILTat 1.3 clone with a panel of different adjuvants including incomplete (IFA) and complete Freund's adjuvant (CFA), saponin and aluminum hydroxide (AH) (Wells *et al*, 1982). The experiment showed a complete protection against an homologous challenge in cattle immunized against *T. brucei* infection with VSSA, but only in combination with certain adjuvants. However, the majority induced high antibody titres after immunization. Membrane proteins were also used as vaccine antigens in experimentally infected cattle. In 1984, a purified membrane protein of 83kDa from *T. brucei*, apparently present in other African trypanosomes, was used to vaccinate goats using IFA and rabbits prior to challenge with tsetse-transmitted *T. vivax* and *T. brucei* (Rovis *et al*, 1984). Despite supposedly being conserved among species, the vaccine did not elicit antibody production and was therefore unprotective. Other purified membrane proteins like the flagellar protein antigen against *T. brucei rhodesiense* in a cattle model showed partial protection with a mean prevalence of infection of 12% (Mkunza *et al*, 1995), the flagellar fraction against *T. brucei* in a murine model (Radwanska *et al*, 2000) and tubulin from *T. brucei* against the same parasite, *T. brucei rhodesiense* and *T. congolense* have conferred partial protection of 60% and 33%, respectively.

Immunization against African trypanosomes using specific recombinant proteins has been widely used in recent years. In 2001, recombinant cysteine proteases from *T. congolense*, which have been demonstrated to elicit high levels of IgG in trypanotolerant cattle and low levels in susceptible cattle, were used to vaccinate cattle in combination with a saponin adjuvant (Authié *et al*, 2001). Cattle were challenged one month later from the last immunization with *T. congolense* IL 12-E3

parasites and both vaccinated and control groups exhibited similar prepatent periods. Vaccination showed no protection, with both groups displaying similar parasite load. In other experiments, recombinant beta-tubulin and actin both from *T. evansi* were used to vaccinate BALB/c mice against *T. evansi*, *T. equiperdum* and *T. b. brucei* (Li *et al*, 2007; Li *et al*, 2009). In both cases, the antibody response of vaccinated mice recognized the specific antigens with high levels of IgG. The immunoprotection in mice showed a partial protection against each trypanosome with parasitaemia emerging later in the vaccinated groups compared with control groups. More recently a recombinant trans-sialidase was used to vaccinate BALB/c mice against *T. congolense* infection but again partial protection was observed after challenge (Coustou *et al*, 2012).

DNA vaccines using plasmids that encode specific antigens have also been applied to African trypanosomes. Silva *et al* (2009) produced a plasmid encoding *T. brucei* trans-sialidase to vaccinate mice prior to challenge with *T. brucei* GVR 35/1.5 (Silva *et al*, 2009). This produced high IgG antibody titre and sterilely protected 60% of challenged mice, perhaps demonstrating an application in a potential control strategy against African trypanosomiasis. Two years later in 2011 another vaccine against *T. brucei* was tested using plasmid DNA encoding one invariant surface glycoprotein (ISG) in a murine model (Lança *et al*, 2011). ISGs are immunogenic antigens conserved among all African trypanosomes and expressed in the BSF but at low level (Black and Mansfield, 2016). A plasmid DNA encoding a single ISG gene from *T. brucei* showed it was able to elicit a humoral response of Th1-like IgG2a antibodies and partial protection with 40% survival rate against infection in BALB/c mice (Lança *et al*, 2011).

ISGs are immunogenic, able to induce a Th2 cell-dependent antibody response during *T. congolense* infection (Fleming *et al*, 2014). Since they can induce a T-dependent B-cell immune response, it has been suggested that it would be possible to use them for vaccination. To date, they are considered the most abundant cell-surface proteins after VSGs. Studies in *T. brucei* invariant proteins demonstrated that VSGs present a copy number between 50,000 -70,000 molecules per cell and a ratio of 1 ISG per 100

VSGs (Overath *et al*, 1994). Their structure consists of N-terminal signal sequences with a short intracellular domain and are possibly attached to the lipid bilayer by α -helix between VSG molecules. In live cells, ISGs are expressed on the surface but not detected by antibodies from the host since they are hidden by the VSGs and so having poor accessibility.

The majority of vaccine candidates and challenge experiments so far have used BSF rather than MET. Thus, another approach to vaccination against AAT could be to use MET targets characterized with a lower number of variant antigenic types (VAT) (Magez *et al*, 2010). In addition, motility proteins beneath the surface membrane like microtubules and actin have also been used as vaccine targets due to their non-variable constitution. Nevertheless, most studies have only reported promising results but no experimental vaccine against African trypanosomes has been reported to deliver complete and reproducible protection against heterologous challenge in a natural host.

Table 1.2. Chronological list of examples of previous attempts for the identification of vaccine candidates against African trypanosomes. Vaccines against different trypanosomes were used predominantly in either a murine or a bovine model giving partial or no protection against infection.

Year	Species	Host	Host strain	Antigen	Adjuvant	Protection	Reference
1972	<i>T. congolense</i>	Mice, dogs, cattle	(ICR) mice, beagle dogs and Hereford cattle	Irradiated parasites	-	Partial	Duxbury <i>et al</i> , 1972
1980	<i>T. congolense</i> , <i>T. vivax</i>	Cattle	Boran	Rinderpest virus vaccine	-	No protection	Rurangirwa <i>et al</i> , 1980
1982	<i>T. brucei</i>	Cattle	Boran	Soluble variant-specific antigen (VSSA)	Panel of different adjuvants	Protection	Well <i>et al</i> , 1982
1982	<i>T. brucei</i>	Cattle	Hereford	Irradiated parasites and purified VSG	IFA for purified VSG only	Protection	Morrison <i>et al</i> , 1982
1983	<i>T. congolense</i> , <i>T. vivax</i>	Cattle	Boran	Brucella abortus S19 vaccine	-	Partial	Rurangirwa <i>et al</i> , 1983
1984	<i>T. vivax</i> , <i>T. brucei</i>	Goat, rabbit	Galla goat, New Zealand rabbit	Purified 83kDa membrane protein	IFA	No protection	Rovis <i>et al</i> , 1984
1995	<i>T. brucei rhodesiense</i>	Cattle		Purified flagellar pocket antigen	Alum	Partial	Mkunza <i>et al</i> , 1995
1999	<i>T. congolense</i> , <i>T. vivax</i>	Cattle	Orma Boran and Galana Boran	Rinderpest virus vaccine	-	No protection	Stevenson <i>et al</i> , 1999
2000	<i>T. brucei</i>	Mice	BALB/c	Purified flagellar pocket fraction	IFA+CFA	Partial	Radwanska <i>et al</i> , 2000
2001	<i>T. congolense</i>	Cattle	Boran	Recombinant cysteine protease	RWL (saponin)	No protection	Authié <i>et al</i> , 2001
2002	<i>T. brucei</i> , <i>T. rhodesiense</i> , <i>T. congolense</i>	Mice	Swiss	Purified tubulin from <i>T. brucei</i>	IFA+CFA	Partial	Lubega <i>et al</i> , 2002
2007	<i>T. evansi</i> , <i>T. equipedum</i> <i>T. b. brucei</i>	Mice	BALB/c	Recombinant beta-tubulin from <i>T. evansi</i>	IFA+CFA	Partial	Li <i>et al</i> , 2007
2009	<i>T. brucei</i>	Mice	BALB/c	Plasmid encoding trans-sialidase		Partial	Silva <i>et al</i> , 2009
2009	<i>T. evansi</i> , <i>T. equipedum</i> <i>T. b. brucei</i>	Mice	BALB/c	Recombinant actin from <i>T. evansi</i>	IFA+CFA	Partial	Li <i>et al</i> , 2009
2011	<i>T. brucei</i>	Mice	BALB/c	Plasmid DNA encoding ISG	-	Partial	Lanca <i>et al</i> , 2011
2012	<i>T. congolense</i>	Mice	BALB/c	Recombinant trans-sialidase	IFA+CFA	Partial	Coustou <i>et al</i> , 2012

Table 1.2

1.5. Profile of an effective vaccine

An effective AAT vaccine has several requirements (Figure 1.8). It is well established that B-cell compartments in the host are constantly suppressed during infection (Radwanska *et al*, 2008). Based on this and other immunological events occurring during infection, an important criterion for an effective vaccine is the availability to eliminate circulating trypanosomes before the suppression and destruction of B-cell memory. While most research is done, by necessity, in murine models, it is also necessary that positive results are reproduced in natural hosts.

Destruction of B-cell memory in *T. vivax* infection is associated with B-cell depletion as confirmed in a murine model (Blom-Potar *et al*, 2010). The experiment was performed in male outbred CD-1 mice experimentally infected with *T. vivax* ILRAD 1392 strain and lymphocyte populations were examined by flow cytometry using different organs. The results demonstrated an increase of immature B-cells in the spleen while MZB decreases and a severe depletion of follicular B-cells. Moreover, pro-B cells maturation into pre-B-cells was also compromised indicating a deficiency in B-cell precursors. This impacts directly on B-cell maturation and therefore a reduction in their number in the periphery preventing a suitable control of the infection.

To date, the majority of experimental vaccines against African trypanosomiasis have been achieved with intracellular and extracellular proteins. Extracellular proteins are of great importance since their epitopes are accessible and recognized by antibodies. However, in order to have a successful immune response, proteins must be abundant and invariant. Proteins expressed on the surface of trypanosomes like ISG and VSG have been used demonstrating partial or no protection at all. A reasonable approach for vaccine design is then identifying invariant and abundant antigens located at the cell-surface that can eliminate circulating trypanosomes.

The profile of an effective vaccine should also be focused on its mechanism of action leading to high titres of protective anti-trypanosome antibodies, even in the absence

of circulating antigens (Magez and Radwanska, 2014). This humoral immune response stimulation could therefore prevent a bloodstream-stage infection from becoming established. Moreover, the protective stimulation has to be maintained throughout the infection even under limited immuno-pathology and must confer protection in all populations.

Another major pitfall of vaccine candidates is their immunogenicity or their capacity to provoke a robust immune response against the parasite. This requirement makes the vaccine dose-dependent; the more immunogenic the antigen is, the lower the amount needed to elicit a good immune response (Mahanty *et al*, 2015). Moreover, the greater the immunogenicity of an antigen, the more it leads to a strong peripheral memory and higher affinity in the epitope-target interaction.

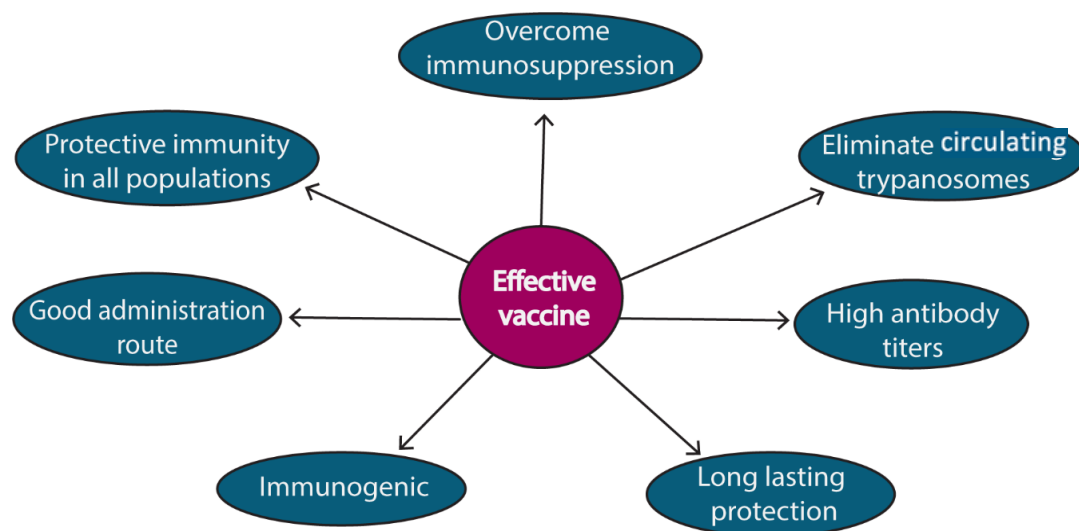


Figure 1.8. Requirements for an effective vaccine against African trypanosomes. The vaccine strategy must overcome different difficulties to prevent animals for re-infection.

1.6. Potential vaccine targets on trypanosomes cell-surfaces

Although VSG dominate the cell-surface of all BSF and MET African trypanosomes, characterization of the parasites' genomes, and latterly, cell surface revealed that there are invariant proteins distributed beside the VSG or in the FP. As stated before, the FP is an invagination of the plasma membrane that serves as the main site of membrane exchange for all African trypanosomes. In general, the FP membrane contains invariant receptors for host-derived nutrients (Field and Carrington, 2009). These include surface receptors of vital importance for the parasite survival, even though the majority have not been characterized. For example in *T. brucei*, the transferrin receptor (Tf-R) is required for iron uptake (Steverding *et al*, 1995), while high density lipoproteins (HDL) is taken up by haptoglobin-haemoglobin (HpHb) receptor (Vanhollebeke *et al*, 2008). As an invagination, the FP membrane is concealed and in the past it was established that host antibodies are thought to be unable to access invariant antigens restricted to this compartment (Black and Seed, 2001). Nonetheless, this assumption was later rejected demonstrating antibody clearance of the cell surface; IgG antibodies can enter the FP by endocytosis when they form an immunocomplex with VSG molecules (Engstler *et al*, 2007). There have been several attempts to develop vaccines using FP membrane antigens like the purified FP portion derived from *T. brucei rhodesiense* or the FP fraction from *T. brucei* AnTat 1.1E clone with little success (Mkunza *et al*, 1995; Radwanska *et al*, 2000).

During the past decade, efforts for an effective vaccine have been focused on invariant proteins able to overcome immuno-suppression and antigenic variation (Authié, 1994). It is now well established that the genome of the different African trypanosomes that cause AAT contains species-specific cell surface gene families (Jackson *et al*, 2013). These genes are very important particularly in *T. vivax* as they encode developmentally regulated proteins that could be vaccine targets (Jackson *et al*, 2015). This thesis concerns those diverse *T. vivax*-specific cell surface gene families and the extent to which they fulfil the profile of ideal vaccine antigens.

1.7. Reverse vaccinology

This thesis will take a reverse vaccinology (RV) approach to the identification of potential vaccine antigens among *T. vivax* genes. The conventional vaccinology approach has been applied for decades in antigen discovery (Figure 9). This approach can be divided into two main steps: (1) obtaining live-attenuated pathogens by serial passage *in vitro* or *in vivo* (Rappuoli, 2000). In other words, it is a requirement to grow the pathogen in laboratory conditions, which in many cases is not feasible; and (2) identification of possible protective antigens useful for subunit vaccines. Antigens are identified and separated one at the time by serological, biochemical and genetic methods. Although this approach has successfully identified vaccine candidates, the major disadvantages of this last step are that it is time-consuming and only identifies purified proteins with high levels of expression.

The term reverse vaccinology was first used by Rino Rappuoli in 2000 and describe the identification of candidate antigens using the pathogen genome sequence, selecting from among the many different proteins the pathogen can plausibly express and using various rational criteria or assays to select only the potential antigen candidates (Rappuoli, 2000). The advantage of RV compared with the classical vaccinology is that, by applying genomic technologies, many proteins that were not previously considered become scrutable, providing a much wider variety of candidates (Donati and Rappuoli, 2013). In fact, the entire protein repertoire of the pathogen is considered by the RV approach, leading to the discovery of many novel and unique antigens (Sette and Rappuoli, 2010). Another difference between conventional and reverse vaccinology is the immunology of the antigens. The traditional approach selects highly immunogenic antigens mostly with high diversity in protein sequence due to immune selective pressure. Instead, RV identifies and selects conserved antigens with potential protection despite their immunogenicity. Moreover, RV can consider *in silico* screening of immune epitopes available including overlapping peptides that can identify every possible T-cell epitope, while the traditional approach only identifies limited and known epitopes (Sette and Rappuoli, 2010)

RV has successfully been used for the development of veterinary vaccines against bacterias and viruses (Donati and Rappuoli, 2013). However, the number of veterinary parasite vaccines is still small and mostly based on live-attenuated organisms (Lew-Tabor and Valle, 2016). Several approaches to vaccine design now apply not only RV but also structural biology. In this way, RV pipelines are enhanced with crystallography and NMR spectroscopy techniques identifying the protein structure and epitopes. In addition, the use of different omic tools has helped the creation of immuno-informatics leading to the identification of B and T cell epitopes, antigenic regions and pathway interactions (Hegde *et al*, 2018).

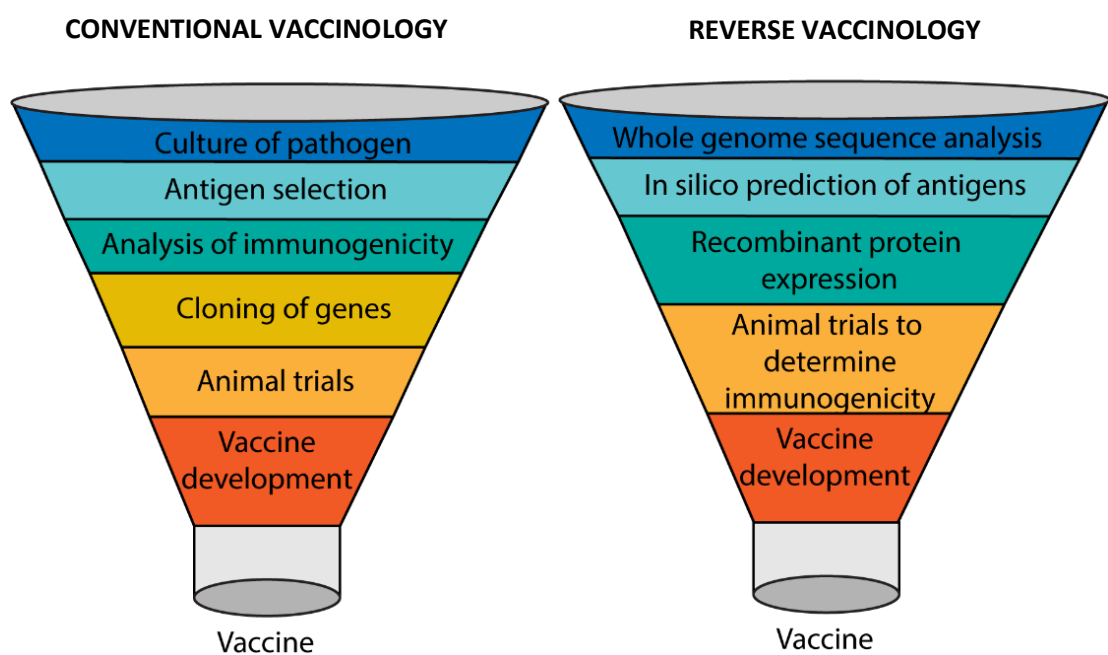


Figure 1.9. Comparative pipelines for the conventional and reverse vaccinology approaches. The application of bioinformatic tools in the reverse vaccinology brings advantages for antigen discovery compared to the classical vaccinology.

1.8. Aims of the thesis

The identification of antigens for experimental vaccines against African trypanosomes has been a major challenge over the past decades. The failure of the different vaccine strategies to provide sterile immunity to AAT has been caused mainly due to the antigenic variation and immuno-suppression (Black and Mansfield, 2016). Moreover, the individual surface proteins used as vaccine antigens so far, like VSG or ISG, are known to confer no immunity to heterologous challenge (Wells *et al*, 1982) or to be concealed beneath the VSG coat, respectively. The recent description of the cell surface phylome in African trypanosomes has demonstrated that *T. vivax* in particular presents a great diversity of species-specific gene families indicating that, besides the VSG, the surface presents other abundant proteins that might be exposed to host antibodies (Jackson *et al*, 2013). Moreover, these proteins are mainly expressed in the bloodstream form of the parasite suggesting that they might be exploited (Jackson *et al*, 2015). Hence, the aim of this thesis was the identification of invariant novel antigens in *T. vivax* and their analysis as candidates for a vaccine against animal African trypanosomiasis, using a reverse vaccinology approach. Specifically, it investigates whether I) the candidate antigens are surface expressed, II) are expressed throughout the population, III) are immunogenic, IV) they have the ability to stimulate an immune response and confer protection against infection in a murine model and V) they confer protection when used to immunize goats against experimental infections.

These objectives are reflected in the structure of the thesis:

- CHAPTER 2: In silico sequence analysis of families of *T. vivax*-specific cell-surface protein (TvCSP) genes.
- CHAPTER 3: Identification of immunogenic linear B-cell epitopes among TvCSP and expression of recombinant proteins.
- CHAPTER 4: Evaluation of the immune response and protection against heterologous challenge of TvCSP in BALB/c mice and immunofluorescent cellular localization of TvCSP.

- CHAPTER 5: A vaccination-challenge trials in goats to evaluate the protective efficacy of the V23 recombinant antigen.

CHAPTER 2

In silico sequence analysis of *Trypanosoma vivax*-specific cell-surface gene families

2.1. INTRODUCTION

Cell surface proteins play an essential role in host-parasite interactions, and those of African trypanosomes are vital in the establishment and maintenance of bloodstream infections (Shimogawa *et al*, 2015). Trypanosome cell surface proteins have diverse roles in evasion of the immune system, as well as nutrient acquisition and energy metabolism pathways (Borst and Fairlamb, 1998).

There is no vaccine available for *T. vivax* due largely to antigenic variation of its Variant Surface Glycoprotein (VSG). Although VSGs represent about 20% of the total cell-surface protein content (Horn, 2014), and cover a great proportion of the cell surface, there are other surface proteins located beneath the VSG surface coat in the FP (Overath *et al*, 1994). Having established that there was no way to vaccinate against VSG, research efforts have become focused on identifying and exploiting invariant surface proteins as vaccine candidates (Morrison *et al*, 2016). In the case of *T. vivax*, recent studies have identified diverse genes with possible cell-surface expression. The Cell Surface Phylome (CSP) described in Jackson *et al*. (2013) described the species-specific gene families from *T. brucei*, *T. congolense* and *T. vivax* with putative cell-surface location (Jackson *et al*, 2013). Numerous differences between *T. vivax* and other African trypanosomes in terms of specific gene families and gene expression were discovered, which may have importance in pathogenesis, but otherwise point to substantial inter-species differences in the composition of cell surface coat (Greif *et al*, 2013; Jackson *et al*, 2013; Jackson *et al*, 2015).

In a three-way genomic comparison, *T. vivax* has a greater number of species-specific gene families with predicted cell-surface expression (19) than either *T. congolense* (5) or *T. brucei* (9) (Jackson *et al*, 2013). This certainly reflects the more recent

common ancestor of *T. brucei* and *T. congolense*, (and therefore, a higher degree of orthology between gene families in those species), but it may also reflect compositional differences in the *T. vivax* surface coat, which is considered to be less dense compared to *T. brucei* (Gardiner, 1989). Jackson et al. (2013) grouped these *T. vivax* cell-specific surface proteins (TvCSP) into multi-copy gene families ('Fam27-Fam45' inclusive) that vary in the number of gene copies (paralogs) derived by duplication, but are each descended from a single common ancestor and are absent from other species (Jackson *et al*, 2013). Evidence for gene expression from proteomic and transcriptomic data revealed most of the TvCSP families to be developmentally regulated (Jackson *et al*, 2015). Fam27, Fam35 and Fam43 are preferentially expressed in metacyclic-forms while Fam28-32, Fam34, Fam36-39, Fam42 and FamX are preferentially expressed in bloodstream-forms. Four sequence families (Fam33, Fam40, Fam41 and Fam45) did not show any evidence of expression and were excluded from further analysis (Jackson *et al*, 2015). The 15 remaining TvCSP families are listed in Table 2.1; in addition, 'FamX' is listed as a family of 44 uncharacterized genes in the *T. vivax* genome, not included in the CSP but observed subsequently in bloodstream-forms displaying the greatest differential expression of all *T. vivax* genes besides VSG (Jackson *et al*, 2015). TvCSP genes do not have any known predicted protein structure nor any evidence regarding their cellular function.

Family	No. paralogs	Stage
Fam27	5	MET
Fam28	6	BSF
Fam29	21	BSF
Fam30	51	BSF
Fam31	38	BSF
Fam32	8	BSF
Fam34	34	BSF
Fam35	17	MET
Fam36	5	BSF
Fam37	5	BSF
Fam38	5	BSF
Fam39	5	BSF
Fam42	15	BSF

Fam43	9	MET
Fam44	13	BSF
FamX	44	BSF

Table 2.1. List of TvCSP families with potential cell-surface location, their respective number of paralogs and the life cycle stage in which they are preferentially expressed (MET: metacyclic-forms; BSF: bloodstream-forms).

The discovery of these TvCSP families, and their abundant expression during bloodstream infections (Greif *et al*, 2013; Jackson *et al*, 2015) indicates that the *T. vivax* surface coat could have very different composition compared to *T. brucei*, and perhaps immunological properties. Setting aside the fact that the functions of TvCSP families are entirely unknown, and much remains to be done to resolve this, we may say a priori that secreted and surface-exposed antigens play a key role in vaccine formulations since they can be easily recognized by the immune system and, therefore, TvCSP families are plausible candidates for vaccine development against *T. vivax*. However, considering the current level of understanding, there are various basic aspects that must be addressed before pursuing them in this regard. Hence, this chapter develops our understanding of TvCSP families through analysis of protein domain organisation, polymorphism and antigenic properties.

The immune response of African trypanosomes in the mammalian host has been widely studied using *T. brucei* as a model organism (Stijlemans *et al*, 2016). However, gene expression in *T. vivax* has indicated that its surface architecture differs from the other African trypanosomes, suggesting that the model used so far to understand immunological events might be inappropriate for *T. vivax*. In this sense, the immunology of *T. vivax* infections and wider host-parasite interactions requires attention when antigens are tested as potential vaccine candidates. The immune response elicited by TvCSP in the host remain obscure but will be addressed in this chapter *in silico*. To examine the potential of antigens to be recognised by the immune system, bioinformatic algorithms have been developed (Sette and Rappuoli, 2010). Computer algorithms for identifying antigenic peptides have been applied

previously to Kinetoplastids. For example, the identification of epitopes in *T. cruzi*, the etiologic agent of Chagas disease, has been widely used for vaccine development (Nakayasu *et al*, 2011; Eickhoff *et al*, 2015) as well in *Leishmania* spp (Guerfali *et al*, 2009; Seyed *et al*, 2011; e Silva *et al*, 2016).

The humoral and cellular adaptive immune system is driven by T and B-cells that present specific receptors at their surface, which are able to recognize foreign antigens. In the case of B-cells, they differentiate and release specific antibodies that then bind to epitopes on the antigen. T-cells also recognize specific epitopes presented by APCs bound to major histocompatibility complex I and II (MHC-I and II respectively) (Sanchez-Trincado *et al*, 2017). Thus, *in silico* prediction tools identifying T and B-cell epitopes are available to understand the potential immunogenicity of antigens and the possible interaction between the parasite and the host.

The purpose of predicting T-cell epitopes is to identify sequences that can stimulate CD4 and CD8 T-cells, which bind to MHC-II and MHC-I molecules respectively (Desai and Kulkarni-Kale, 2014). Epitope production begins when potentially antigenic proteins are cleaved by proteolytic enzymes in the APC producing several different protein fragments. However, only around 2% of these fragments will later become epitopes since they have the correct amino acid sequence to bind the MHC molecule at the APC surface (Weber *et al*, 2009). The prediction of T-cell epitopes can be achieved using bioinformatics tools available online, and are classified in two main groups: direct and indirect methods. Direct methods rely on protein sequence and structure analysis of the epitopes but the predictions often have high false positives and low accuracy (Desai and Kulkarni-Kale, 2014). On the other hand, indirect methods like artificial neural networks (ANN), the stabilized matrix method (SMM), or support vector machines (SVM) are based on quantitative matrices and have the advantage of avoiding high rates of false positives.

The aim of predicting B-cell epitopes is to identify peptides that can replace an antigen for antibody detection and production (Ponomarenko and Van Regenmortel, 2009). These epitopes are more difficult to predict since the software uses sequence-

based propensity scales and machine learning algorithms to discriminate experimental from non B-cell epitopes (Potocnakova *et al*, 2016). Nevertheless, B-cell predictions are used to identify vaccine candidates on a panel of antigens and for the improvement of diagnostic methods. Previous studies have demonstrated the characterization of in silico B-cell epitopes in *T. vivax* to identify potential epitopes for diagnosis purposes (Guedes *et al*, 2018). The epitopes were identified based on transcriptome data and considered diverse intracellular proteins besides TvCSP. The findings based on in silico and bioinformatics predictions are of great interest as they facilitate the identification of potential epitopes with time and cost savings. However, they must be validated experimentally to corroborate their accuracy.

This chapter aims to:

1. Predict the secondary protein structures and glycosylation sites of 12 *T. vivax*-specific gene families preferentially expressed in bloodstream-forms using in silico approaches.
2. Quantify the polymorphism of each TvCSP family (i.e. number of isoforms) among various clinical strain genome sequences, relative to the reference strain by phylogenetic and population genetic analyses.
3. Predict T-cell and B-cell epitopes from TvCSP sequences in silico and evaluate their antigenicity properties.

2.2. MATERIALS AND METHODS

2.2.1. Data sources

The African trypanosome Cell Surface Phylome (Jackson *et al*, 2013) was used as the basis for TvCSP families. Gene sequences belonging to 12 bloodstream-form families (Fam28-32, Fam34, Fam36-38, Fam42, Fam44 and FamX) and three metacyclic-forms families (Fam27, Fam35 and Fam43) were extracted from the *T. vivax* Y486 reference genome sequence (Release 44) through the TriTrypDB portal (www.TriTrypDB.org). 'FamX' is a gene family consisting of uncharacterized genes unique to *T. vivax* that was not included in the original CSP but was subsequently observed to be among the most abundant transcripts preferentially expressed in bloodstream-forms (Jackson *et al*, 2015).

2.2.2. In silico structural characterization

TvCSP gene sequences were used to perform *in silico* predictions of protein secondary structure. For all family members, the InterProScan (Quevillon *et al*, 2005) and Predictprotein servers (Rost *et al*, 2004) were used to identify protein domains. GPI anchor prediction was made using PredGPI (Pierleoni *et al*, 2008) and Big-Pi predictor (Eisenhaber *et al*, 1999) webservers. Predictions of post-translational modification sites in all predicted proteins were made using the ModPred server (Pejaver *et al*, 2014) and compared with N, C and O-glycosylation sites identified by NetNGlyc 1.0, NetCGlyc 1.0 and NetOGlyc 4.0, servers respectively. Tertiary structure prediction was carried out on predicted amino acid sequences with Phyre2 V2.0 (Kelley *et al*, 2015).

2.2.3. Gene family phylogenetic analysis

To understand antigenic variability within a protein family, it is necessary to know if gene paralogs are capable of recombination, potentially producing new sequence variants. While not variant antigens, it is possible that recombination diversifies

TvCSP genes. I approached this issue first by comparing phylogenies for protein coding sequences (CDS) and untranslated regions (UTRs) of each gene family. Paralogs from each gene family were aligned and phylogenies were generated for CDS, 5' UTR and 3' UTR, and then compared to identify possible recombination events. In addition, the CDS phylogeny for each gene family was analysed to identify the number of isoforms within each family. 5' and 3' UTRs were equated with the 500bp regions upstream and downstream of each CDS. For the phylogenetic analysis, nucleotide sequences of the CDS, 5'UTR and 3'UTR respectively of specific genes within a family were aligned using ClustalW and manually edited using BioEdit 7.1.13. Maximum likelihood phylogenies were estimated using Tamura-Nei model (Tamura and Nei, 1993) as it takes into account variable base frequencies and transition rates but equal transversion rates. The trees were generated in Mega7 (Kumar *et al*, 2016) with 100 non-parametric bootstrap replicates and were mid-point rooted due to the lack of an obvious outgroup.

To complement the phylogenetic comparison, CDS alignments were also analysed for incompatible sites (a signature of historical recombination) using the Pairwise Homoplasy Index statistical test (PHI) in SplitsTree v.4 (Huson, 1998) with a p-value <0.05 set as the threshold for significant evidence for recombination.

2.2.4. Population genetic analysis

Highly polymorphic antigens are not suitable for vaccines given that the precise composition of the antigen in the disease setting cannot be predicted securely. Population genetic analysis was carried out on TvCSP gene sequences to identify possible antigen genes that are found universally throughout the population with low polymorphism. Twenty isolates from countries across Africa and South America (Table 2.2) previously described were used for the analysis (Pereira *et al*, 2019). Briefly, DNA sequence data were generated from blood stabilates derived from natural *T. vivax* infections of cattle in Ivory Coast (n=3), Nigeria (n=11), Uganda (n=4) and The Gambia (n=1). Parasite isolates were selected from the International Livestock Research Institute (ILRI) Azizi repository. In addition, one sample from Brazil

(n=1) was selected, originating from an experimental infection of goats using the *T. vivax* Lins strain (Cadioli *et al*, 2012). DNA sequence data were generated on the Illumina Hiseq platform (Pereira *et al*, 2019).

2.2.5. Mapping sequence data to reference genome

The Burrows-Wheeler Alignment tool (BWA-MEM) (Li and Durbin, 2010) applying default parameters was used to map the raw reads from the 20 isolates to the *T. vivax* Y486 reference genome. The resulting mapping reads were saved in a Sequence Alignment/Map format (SAM) file and converted into BAM files (binary format of SAM file) to further perform the data analysis.

ID	Date	Location	Host	Passage species	Genome Completeness
IL11	1973	Zaria, Nigeria	Bovine	Mice	0.79
IL1392	1981	Yakawada, Nigeria	Bovine	Goat	0.77
IL2005	1969	Lugala, Uganda	Tsetse Fly	Goat	0.61
IL2323	1969	Luuka, Uganda	Tsetse Fly	Rat	0.71
IL2714	1969	Lugala, Uganda	Tsetse Fly	Rat	0.70
IL306	1973	Zaria, Nigeria	Bovine	Mice	0.79
IL3171	unknown	The Gambia	Bovine	Bovine	0.55
IL319	1973	Zaria, Nigeria	Bovine	Mice	0.70
IL338	1973	Yakwada, Nigeria	Bovine	Mice	0.80
IL340	1962	Zaria, Nigeria	Bovine	Mice	0.78
IL3638	1990	Ivory Coast	Bovine	unknown	0.72
IL3651	1990	Ivory Coast	Bovine	Rat	0.71
IL3658	1990	Ivory Coast	Bovine	unknown	0.72
IL462	1973	Yakwada, Nigeria	Bovine	Mice	0.79
IL465	1973	Yakwada, Nigeria	Bovine	Mice	0.79
IL493	1973	Yakwada, Nigeria	Bovine	Mice	0.79
IL596	1973	Yakawada, Nigeria	Bovine	Mice	0.80
IL684	1973	Yakawada, Nigeria	Bovine	Mice	0.80
ILV-21	1972	Antapar Teso, Uganda	Bovine	Goat	0.51
Lins	2012	Lins, Brazil	Bovine	Goat	67.2

Table 2.2. List of clinical isolates used to generate DNA sequence data for the population genetic analysis, according to location, host, passage species and genome completeness (Pereira *et al*, 2019).

The program for High-Throughput Sequencing data (HTS) SAMtools was used to view, sort and index the genomic reads (Li *et al*, 2009) using the sort and index options respectively under default parameters. In addition, specific tools from Picard 1.97 were applied in order to process the data. The read groups were added with the Picard argument `AddOrReplaceReadGroups` and afterwards each BAM file was cleaned with `CleanSam`. To ensure that all read information retained mate-pairs, the option `FixMateInformation` was used and duplicates within a file were identified with `MarkDuplicates`. The `BuildBamIndex` option was then used to create an index file for each BAM file respectively.

The genome Analysis Toolkit (GATK) (McKenna *et al*, 2010) was used to avoid mismatches due to the presence of insertions and deletions (indels) in the sample genomes. The `RealignerTargetCreator` GATK tool was applied creating intervals to use in the local realignment around indels using the BAM file from the last step with Picard analysis as input. Other tools like `IndelRealigner` and tool `CallableLoci` were applied to perform the realignment of all reads and to analyse the number of callable bases respectively. Finally, `HaplotypeCaller` was applied to call all single nucleotide polymorphisms (SNPs) and indels simultaneously. The intermediate genomic gVCF and the option “discovery” for genotyping mode parameters were set up to generate a variant call format file (VCF) as output. All VCF files were joined with `GenotypeGVCFs` tool.

Selection and extraction of SNPs and indels were performed under the `SelectVariants` tool creating new VCF files. Both SNPs and indels variant calls were filtered with `VariantFiltration` using the hard filtering method suggested for GATK. The parameters were as follows: variance confidence with `QualByDepth (QD) < 2.0`, Fisher Strand (Krafsur, 2009) `> 60.0`, mapping quality ranksum test (`MQRankSum < -12.5` and rank sum test (`ReadPosRankSum < -8.0`). All filtered SNPs and indels of each sample were joined into a single file. The number of mapped reads and the number of reads mapped to the reference genome was calculated with `SAMTOOLS flagstat`.

2.2.6. Population genetic variation

The R package PopGenome 2.2.4 (Pfeifer *et al*, 2014) and the program SNPgenie (Nelson *et al*, 2015) were used to analyse genetic polymorphisms based on neutrality tests as well as nucleotide diversity statistics. For each population, the number of segregating sites was calculated.

For all TvCSP genes expressed in bloodstream-forms, statistical tests for neutrality were carried out using Tajima's *D* (Tajima, 1989). This was calculated to ask if the genes were evolving neutrally or under selection. In addition, the genes were also used to analyse the nucleotide diversity within populations (Nei, 1987). Tajima's *D* could not be computed for the Brazilian and Gambian sequences (since $N = 1$) and were not considered in the analysis for this reason. Tajima's *D* neutrality test is based on the number of segregating sites and pairwise diversity. The number of samples for this and other neutrality tests are crucial since they are all sensitive to the structure of the population. Taking this into account, Tajima's *D* test requires a sample size large enough to calculate values with small error (Weedall and Conway, 2010). A low sample size number used for neutrality tests can directly affect the calculation creating bias (Subramanian, 2016).

2.2.7. T-cell epitope prediction

To identify peptides that could be recognised as epitopes located on the surface of APC's, an *in silico* prediction for MHC-I and MHC-II T-cell epitopes was made. The predicted protein sequences from all TvCSP genes were used as input to predict MHC-I epitopes using the Immune Epitope Database (IEDB) (Vita *et al*, 2014) available online (<http://tools.iedb.org>). This database was used as it is one of only two prediction programs available for MHC molecules that considers non-human organisms (the second being NetMHC 4.0 Server, which uses the ANN method).

The IEDB recommended prediction method was selected using six bovine leucocyte antigen (BoLA) alleles (Table 2.3) with a percentile rank of 0.3 and epitope length of

11 aa. The MHC alleles were selected on the basis of the common BoLA molecules between both NetMHC and IEDB servers.

In the case of MHC-II predictions, BoLA alleles were not used for the analysis because there is no software able to make predictions for other MHC-II molecules besides human or mouse. Instead, the human leucocyte antigen (HLA) on seven human HLA-DR alleles were used as previously done (Farrell *et al*, 2016). Predictions were carried out by the TEPITOPEpan server (Zhang *et al*, 2012), based on the position specific scoring matrix (PSSM), and the IEDB server. Seven HLA selected alleles (Table 2.3) were assumed in both cases, with a 3% of percentile rank cut-off and a peptide length of 15-mer. In addition, all the predicted epitopes were evaluated for antigenicity capacity with VaxiJen v2.0 (Doytchinova and Flower, 2007) selecting parasite as target organism and using 0.05 as threshold.

No.	BoLA allele	HLA allele
1	D18.4 (BoLA-1*02301)	DRB1*0401
2	HD6 (BoLA-6*01301)	DRB1*0301
3	JSP.1 (BoLA-3*00201)	DRB1*1401
4	T2A (BoLA-2*01201)	DRB1*1101
5	T2B (BoLA-6*04101)	DRB3*0201
6	T2C (BoLA-3*00101)	DRB1*0801
7	-	DRB3*0101

Table 2.3. List of BoLA and HLA alleles used for the in silico prediction of MHC-I and MHC-II epitopes respectively in TvCSP protein sequences.

2.2.8. Linear B-cell epitope prediction

The identification of B-cell linear epitopes was performed with three tools. First, BCPred (EL-Manzalawy *et al*, 2008) using the ANN prediction method. Second, ABCPred (Saha and Raghava, 2006) using string kernels method. And third, the IEDB server and Bepipred Linear Epitope Prediction (Jespersen *et al*, 2017) using a random

forest algorithm. The threshold was set to 0.8 and 20aa for peptide length in BCPred and ABCPred predictions.

2.3. RESULTS

2.3.1. Secondary protein structure prediction

To evaluate and make predictions from sequence data for *T. vivax* cell-specific surface families, a secondary structure prediction was performed with InterProScan, Predictprotein, PredGPI, Big-Pi, NetNGlyc 1.0, NetCGlyc 1.0 and NetOGlyc, 4.0 and Phyre2 V2.0 servers. The analysis showed that most predicted proteins, regardless of the family or the parasite stage in which they are mainly expressed, included probable signal peptides (SP); 83% (BSF) and 74% (MET) (Table 2.4). The secondary structure of many TvCSP were also highly hydrophobic at the C-terminal region where transmembrane domains (TMD) were predicted to be present in 36% of proteins expressed in bloodstream-forms. TMD were located between positions 7-29 of the protein sequences. None of the sequences preferentially expressed in metacyclic-forms included a probable TMD.

2.3.2. Prediction of glycosylation sites

In addition to the predictions performed by InterProScan, glycosylation sites were analysed in silico. The average number of glycosylation sites per TvCSP family was estimated (Table 2.4), showing that each sequence had multiple O- and N-glycosylation sites. Fam28, Fam31 and Fam27 have the greatest number of N-glycosylation sites with 16, 16 and 19 sites respectively. This scenario was different when compared with the average number of O-glycosylation predictions in which all families except Fam29 and Fam37 presented at least 12 sites. This indicates that O-glycosylation sites were present in all TvCSP families with a higher average number than N-glycosylation sites. C-glycosylation sites were found in few proteins only from Fam29-30, Fam34, Fam38 and Fam42.

The position of the glycosylation sites predicted for bloodstream-form protein families showed no specific distribution pattern within the protein sequence, being

distributed along the protein structure. In the case of metacyclic-form proteins, sites were present between amino acid 68-287 for N- glycosylation and 22-305 for O-glycosylation.

Family	N	SP+	TM	GPI+	Glycosylation sites per family					
					N		O		C	
					AN	AP	AN	AP	AN	AP
Fam28	6	6	3	0	16	61-647	21	68-616	0	-
Fam29	21	15	0	0	6	43-275	3	152-274	3	267-334
Fam30	51	38	4	3	12	38-559	23	104-616	5	27-317
Fam31	37	28	4	2	16	66-621	20	88-620	0	-
Fam32	8	7	1	5	2	225-273	12	174-314	0	-
Fam34	34	33	27	1	6	97-372	13	80-465	2	2-397
Fam36	5	5	0	0	6	79-496	14	88-587	0	-
Fam37	5	4	1	0	6	59-249	6	43-230	0	-
Fam38	5	2	0	1	6	113-250	15	120-241	1	13
Fam42	15	13	7	5	10	58-511	32	102-646	2	99-292
Fam44	13	11	5	0	8	70-640	24	93-679	0	-
FamX	44	32	36	2	2	138-290	15	84-305	0	-
Fam27	5	1	0	2	19	83-287	21	22-315	0	-
Fam35	17	15	0	11	3	82-283	44	35-305	0	-
Fam43	9	7	0	6	5	68-222	20	145-305	0	-
Total	275	218	88	38						

Table 2.4. In silico structural predictions for TvCSP families. N describes the number of genes in each family in the Y486 reference genome sequence. SP+, TM and GPI+ denote the number of family members with predicted signal peptides, transmembrane helices and a glycosylphosphatidylinositol (GPI) anchor. The number of N-, O- and C-linked glycosylation sites are shown. AN denotes the average number of glycosylation sites. AP denotes the average position of a glycosylation site in the protein sequence.

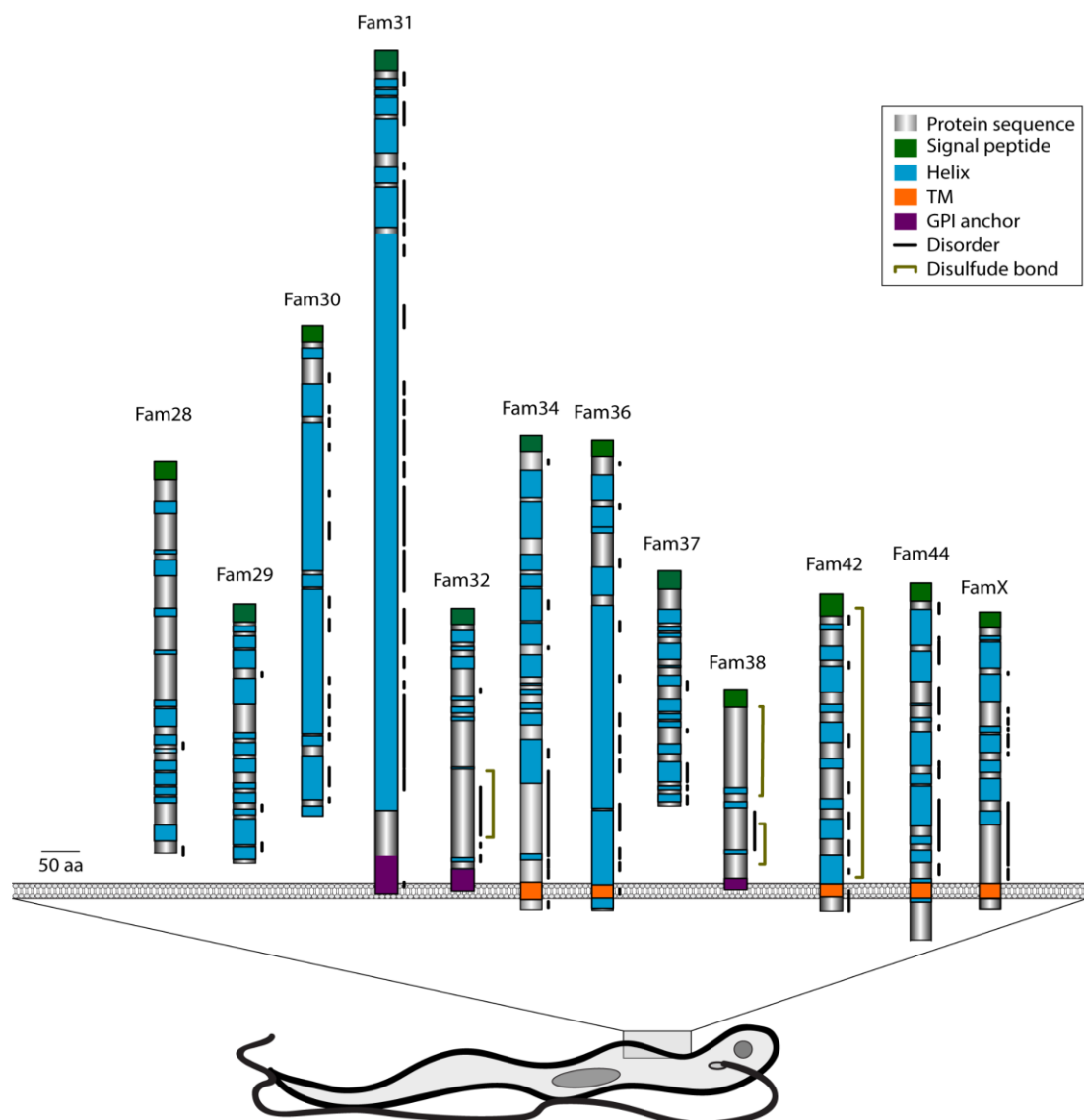


Figure 2.1. A schematic representation of the secondary structure of each BSF TvCSP family. Only one protein per family was selected to show the different motifs and its possible cell-surface location. Fam 31, 32 and 38 are predicted to be membrane-tethered via a C-terminal GPI anchor molecule. Fam 34, 36, 42, 44 and FamX are predicted to be type 1 transmembrane proteins, attached to the membrane by a single C-terminal transmembrane domain. Fam28, 29, 30 and 37 are predicted to be secreted.

2.3.3. Prediction of tertiary structures

Tertiary structure predictions based on each amino acid sequence was predicted through comparison with homologous proteins. Most predictions for bloodstream-stage proteins showed low confidence and model coverage percentages respectively (< 50% in both cases). In some proteins, the coverage was less than 10% indicating that approximately 40 residues were modelled based on the highest scoring template. Metacyclic-stage proteins showed a higher confidence model (more than 95%) with a moderate coverage level. For example, the Fam27 protein TvY486_0043530 showed a tertiary structure prediction (Figure 2.2A) modelled with 99.2% confidence and with 94% sequence coverage (311 residues) being homologous to collagen alpha 1 (template code: c1ygvA). Moreover, the protein TvY486_0019430 also from the same family showed a 3D prediction (Figure 2.2B) of 99.6% confidence and 84% coverage (245 residues) modelled on to the same template.

The predictions for these sequences had contained up to 95% disordered regions in their secondary structure. Disordered regions are often difficult to predict even though they can perform important functions within the structure. These results are validated based on the criteria of Phyre server only if there is a high number of different sequences homologous on the position-specific iterated blast basic local alignment search tool (PSI-BLAST) results (Kelley *et al*, 2015). Taking this into account, the accuracy of the prediction of these regions was on average 80% (moderate confidence) as all the proteins displayed a high number of different sequence homologues. Overall, the prediction of tertiary structures for both BSF and MET proteins indicated they do not match with any template and their protein modelling does not seem to be represented by any protein from the database.

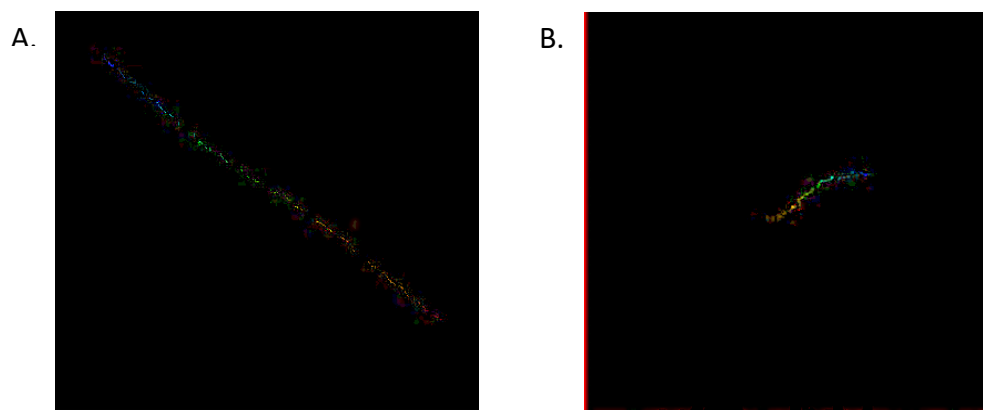


Figure 2.2. Tertiary structure predictions based on the amino acid sequence for **A)** TvY486_0043530 and **B)** TvY486_0019430.

2.3.4. Phylogenetic analysis

Phylogenetic trees were constructed with the maximum likelihood method for 12 gene families preferentially expressed in bloodstream-forms and three preferentially expressed in metacyclic-form *T. vivax*. Recombination between paralogous genes can lead to unique sequence types and protein polymorphism that would undermine the universality of any vaccine based on that protein. In order to explore and understand recombination events, a comparison between the CDS, 3'UTR and 5'UTR was analysed. In addition, the CDS sequences were also used to identify the number of isoforms within a family.

The multiple sequence alignment from Fam27 showed that all members possess a repetitive domain of 9 residues (ESDQDAKGN) from position 80 to the end of the sequences. This repetitive domain was absent in the other TvCSP families. Instead, all gene members from Fam35 and Fam43 displayed conserved cysteine residues at the C-terminal and hydrophobic amino acids at N-terminal positions. The phylogenies for metacyclic-form families were constructed and gene clusters (clades) were identified where CDS sequences exceeded a threshold of 70% identity in a reciprocal BLAST. Figure 2.3 shows that Fam27 showed four robust clades in the CDS tree, three of which contain only one gene member, indicating that only two sequences from the family shared >90% nucleotide identities. Likewise, the CDS trees from Fam35

(Figure 2.4; 9 clades) and Fam43 (Figure 2.5; 7 clades) contained 4 and 5 clades with one gene member only.

The comparison of phylogenies for CDS and both UTRs relating to metacyclic-form gene families revealed a lack of topological conservation. Clades with more than one paralog often showed a different relative position within the phylogeny (robustly supported by bootstrap values) when CDS trees were compared to 3' and 5' UTR trees, indicating possible historical recombination events between genes from the same family. For example, CDS trees from Fam35 (Figure 2.4.) showed 7 robust clades which are conserved in the 5'UTR phylogeny. However, clade 1 and 3 from CDS tree are split in the 3'UTR tree. Likewise, when considered the CDS from Fam43 (Figure 2.5), clade 1 is divided in two small clades with one paralog each in both 3'UTR and 5'UTR trees, respectively.

To extend this result, an analysis of recombination breakpoints in the CDS alignments of each gene family was carried out using PHI test. Table 2.5 shows that this detected significant incompatibility between sites, and therefore evidence for historical recombination, in all metacyclic-form gene family sequence alignments ($p < 0.05$).

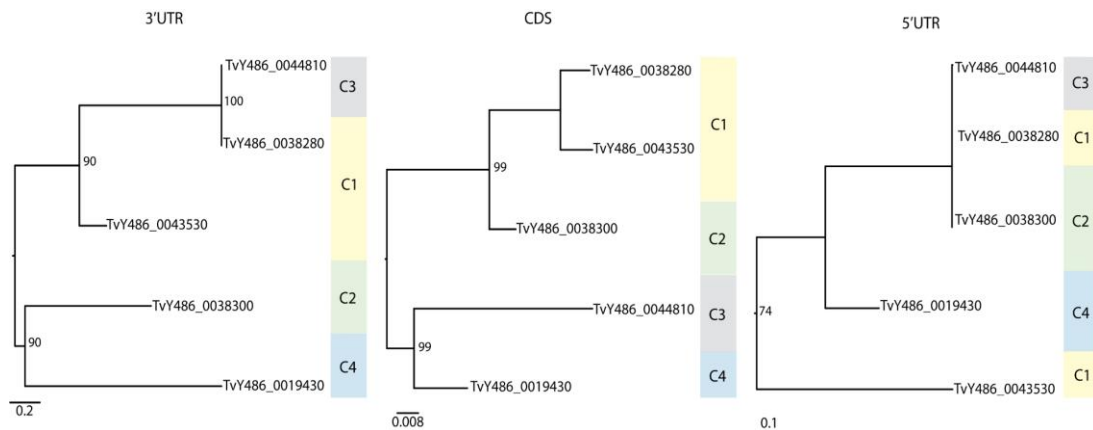


Figure 2.3. Comparison of Maximum likelihood phylogenetic trees based on the Tamura-Nei model of CDS and 3' and 5'UTR sequences for Fam27. Clusters were defined based on the CDS sequences that shared an identity >90%. The different clusters are represented by a colour and number at the right side of each tree (C: clade). A distance scale is shown for each tree. The trees are mid-point rooted.

Figure 2.4 (overleaf). Comparison of Maximum likelihood phylogenetic trees based on the Tamura-Nei model of CDS and 3' and 5'UTR sequences for Fam35. Clusters were defined based on the CDS sequences that shared an identity >90%. The different clusters are represented by a colour and number at the right side of each tree (C: clade). A distance scale is shown for each tree. The trees are mid-point rooted.

Figure 2.5 (overleaf). Comparison of Maximum likelihood phylogenetic trees based on the Tamura-Nei model of CDS and 3' and 5'UTR sequences for Fam43. Clusters were defined based on the CDS sequences that shared an identity >90%. The different clusters are represented by a colour and number at the right side of each tree (C: clade). A distance scale is shown for each tree. The trees are mid-point rooted.

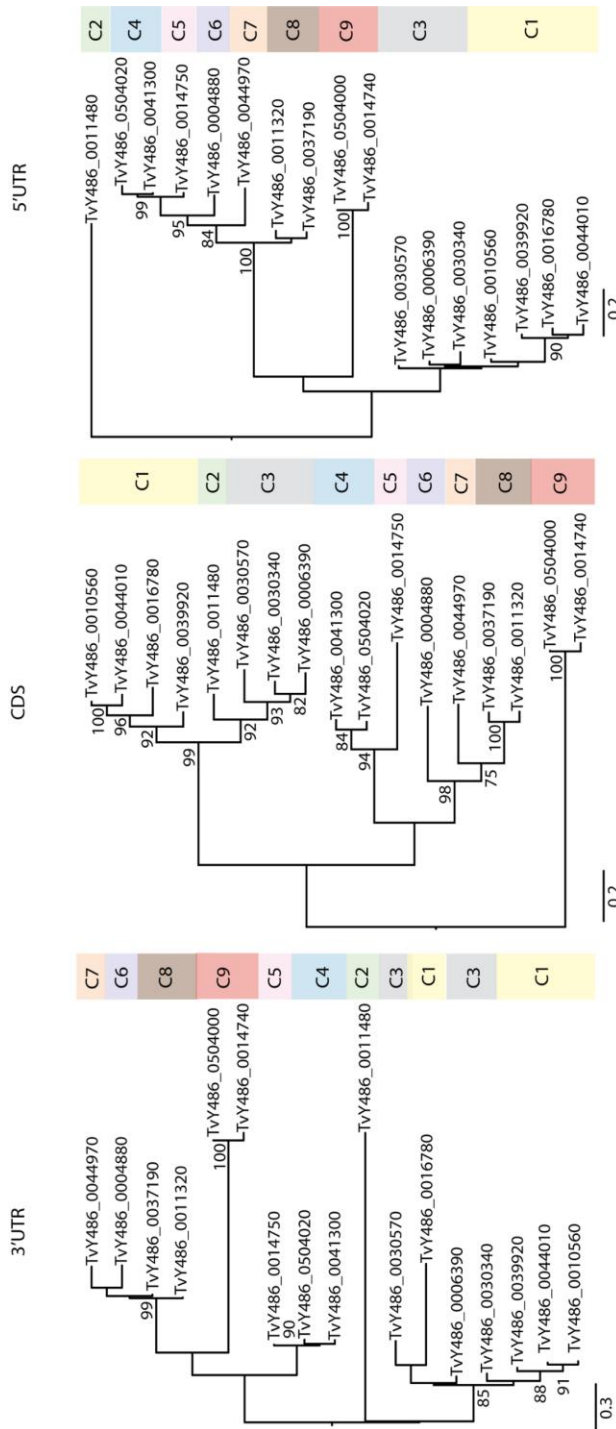


Figure 2.4

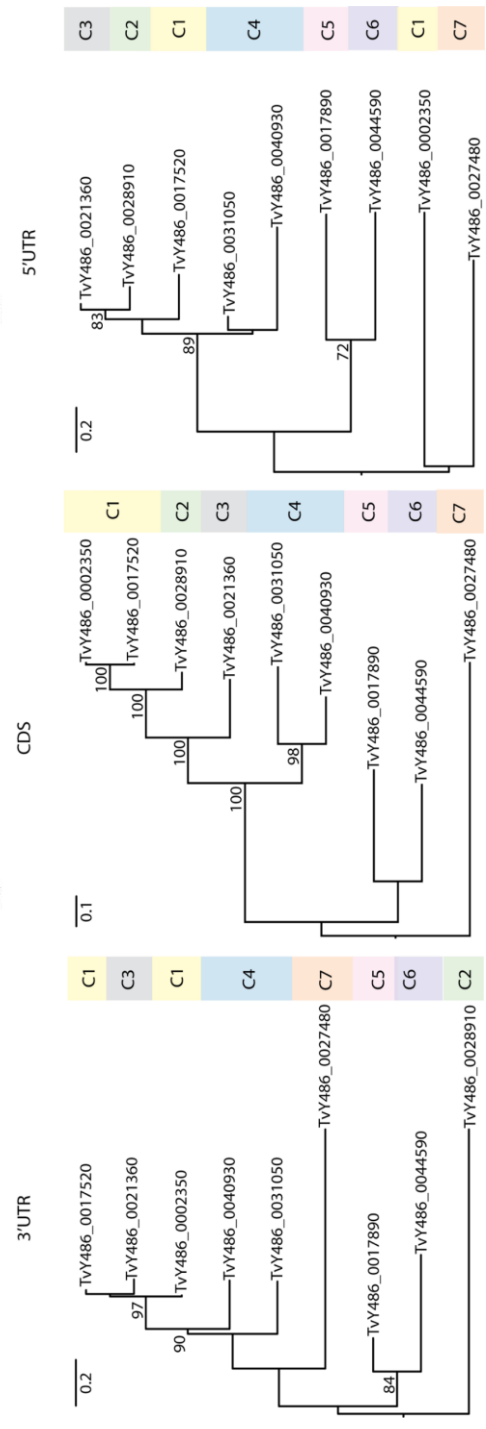


Figure 2.5

The 5' and 3'UTR trees showed changes in the topology when compared to the CDS tree of each family but with the conservation of the cladistics structure. For example, 3'UTR and CDS trees from Fam27 showed topological congruence in which the structure of the 7 clades are well conserved but there is a disagreement when compared with the CDS topology (Figure 2.3). This scenario was consistent for all BSF families except for Fam38 that presented the same phylogenetic structure for CDS and 3'UTR trees (Figure 2.12A). In addition, the comparison between CDS and 5'UTR trees showed distinct topologies for all families with only some conserved clades within CDS and the 5'UTR region. Clear examples of incongruence between 5'UTR regions and CDS trees are showed in Fam35 (Figure 2.4), Fam32 (Figure 2.9) and Fam34 (Figure 2.10) in which the majority of the clades displayed an agreement with the CDS tree but others showed a different topology.

When applied to bloodstream-form families, the PHI test showed variable levels of evidence for recombination among paralogs. Fam28-31, Fam34 and Fam38-44 showed no statistically significant evidence for within-family recombination (Table 2.5). However, results for Fam32, Fam36 and Fam37 did indicate statistically significant evidence for recombination. Interestingly, these families have the smallest number of genes of all bloodstream-form families ($n = 5$ for Fam36 and Fam37 and $n=8$ for Fam32). Moreover, the phylogenies from these families displayed very short branches indicating a short genetic distance between members compared to the other families, consistent with frequent genetic exchange (Bell and McCulloch, 2003).

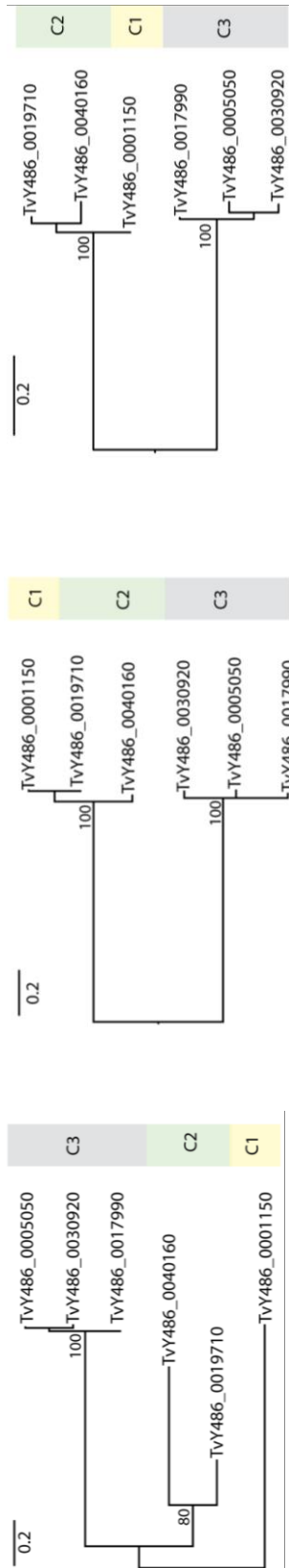
FamX is the second biggest family expressed in the bloodstream-form, and described formally for the first time here. FamX consists of 44 hypothetical genes that can vary in length from 245 to 433 amino acids. The multiple sequence alignment from the translated nucleotide sequences showed that there are five highly conserved cysteine residues in all proteins positioned towards the N-terminal and central region. The similarity between FamX genes was determined in order to subgroup the family and identify the number of possible isoforms. This was performed by a basic local alignment search with BLASTp using each FamX gene against the rest of the family.

The differentiation criteria into clades was set based on sequence similarities with a cut-off > 70%. The maximum likelihood phylogeny showed that this novel family is divided into 14 different robust clades (Figure 2.14). Four genes occupy long branches and are not closely related to any other paralog: clade 2 (TvY486_0027210), clade 3 (TvY486_0900440), clade 9 (TvY486_0008690) and clade 13 (TvY486_00003390). All FamX genes occupy loci in the genome 'bin' of unassembled sequence (primarily sub-telomeric regions), except for one. TvY486_0900440 (clade 3) is the only FamX gene to be located at a chromosome-internal locus (on chromosome 9). FamX also presents 8 clades containing between two and five members (clade 4, 5, 6, 7, 8, 10, 11, 12) and only two clades with more than 5 members (clade 1 and 14). The FamX alignment was also examined for recombination events using PHI test. The results indicated that there is no statistically significant evidence for incompatibility among sites that would indicate a history of recombination ($p=1$).

In summary, among TvCSP gene families, those preferentially expressed in metacyclic-forms contain a lower number of genes compared with those expressed in bloodstream-forms. The latter are variable in size, some of them more abundant (e.g. Fam30, FamX) than others (e.g. Fam36-38). TvCSP phylogenies show that all metacyclic-form families and three bloodstream-form families (Fam32, Fam36-37) show signs of recombination among gene copies.

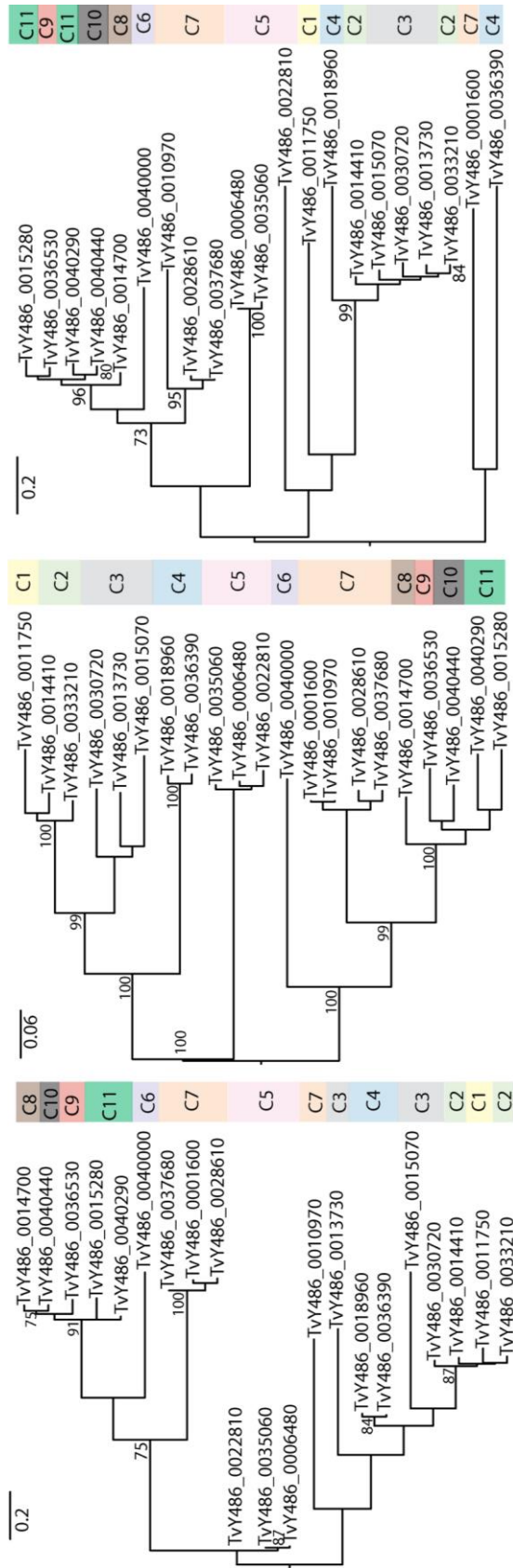
Figure 2.6 (overleaf). Comparison of Maximum likelihood phylogenetic trees based on the Tamura-Nei model of CDS and 3' and 5'UTR sequences for Fam28 **(A)** and Fam29 **(B)**. Clusters were defined based on the CDS sequences that shared an identity >90%. The different clusters are represented by a colour and number at the right side of each tree (C: clade). A distance scale is shown for each tree. The trees are mid-point rooted.

A.



Fam28

B.



Fam29

5'UTR

CDS

3'UTR

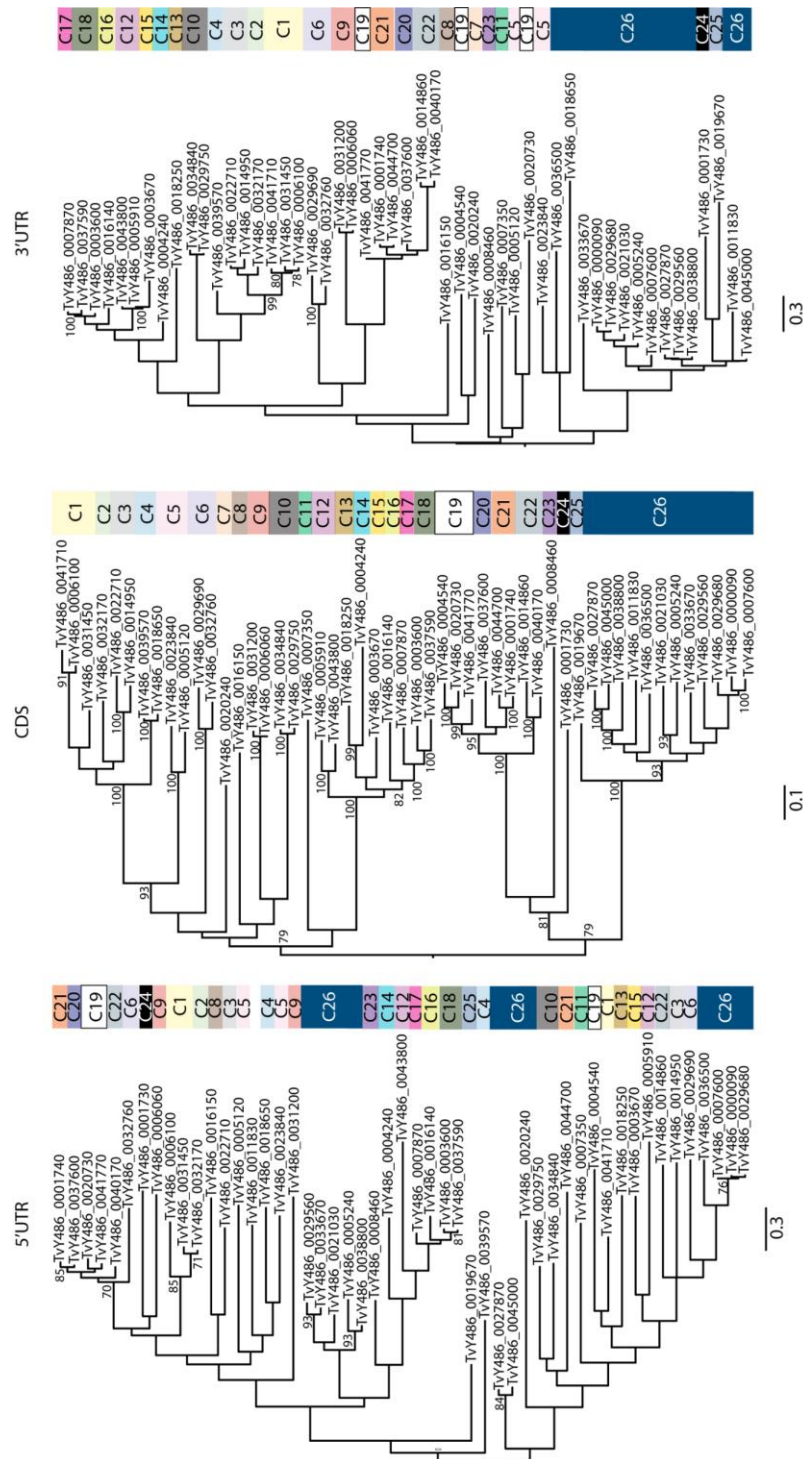


Figure 2.7. Comparison of Maximum likelihood phylogenetic trees based on the Tamura-Nei model of CDS and 3' and 5'UTR sequences for Fam30. Clusters were defined based on the CDS sequences that shared an identity >80%. The different clusters are represented by a colour and number at the right side of each tree (C: clade). A distance scale is shown for each tree. The trees are mid-point rooted.

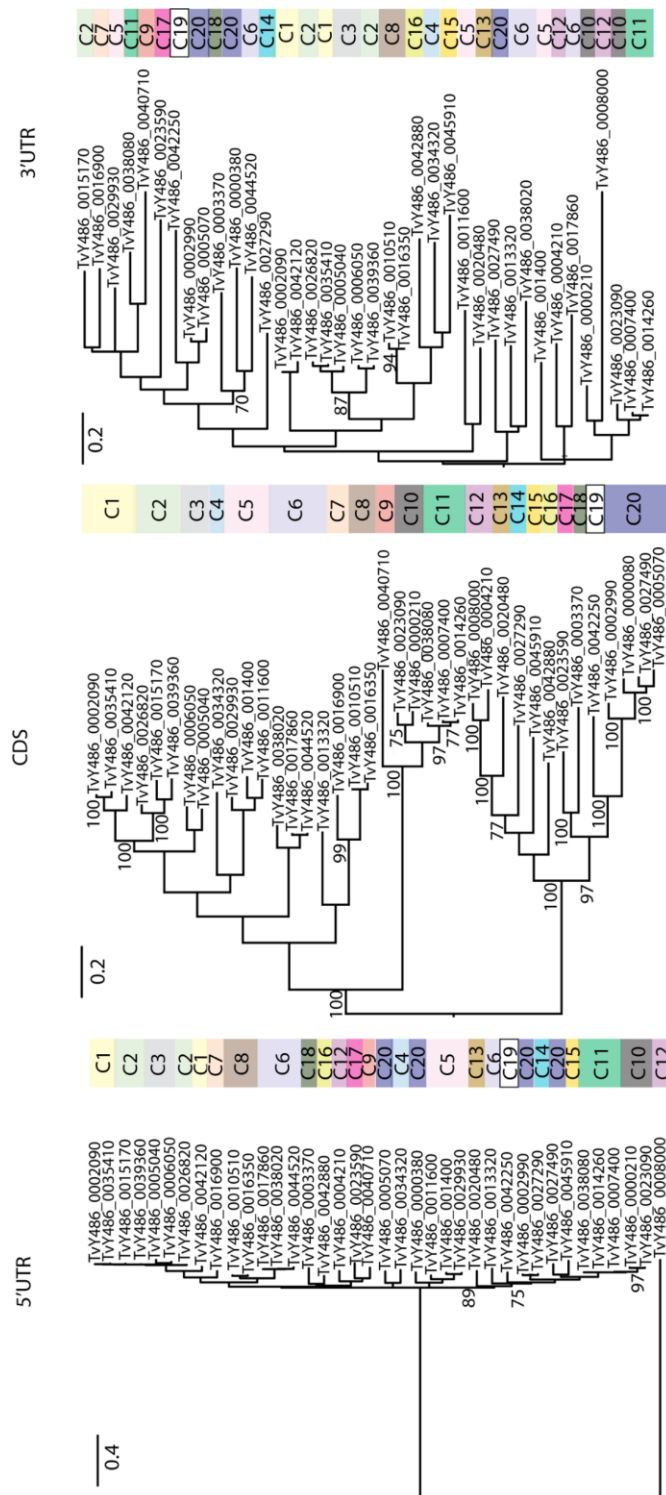


Figure 2.8. Comparison of Maximum likelihood phylogenetic trees based on the Tamura-Nei model of CDS and 3' and 5'UTR sequences for Fam31. Clusters were defined based on the CDS sequences that shared an identity >70%. The different clusters are represented by a colour and number at the right side of each tree (C: clade). A distance scale is shown for each tree. The trees are mid-point rooted.

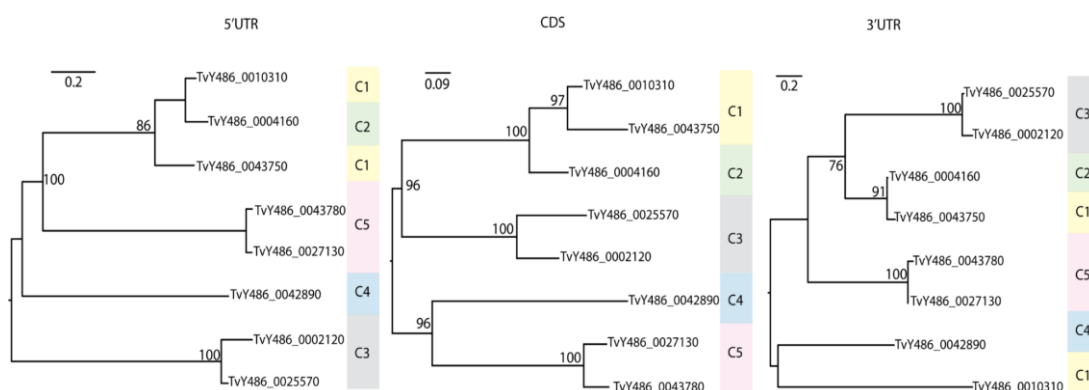
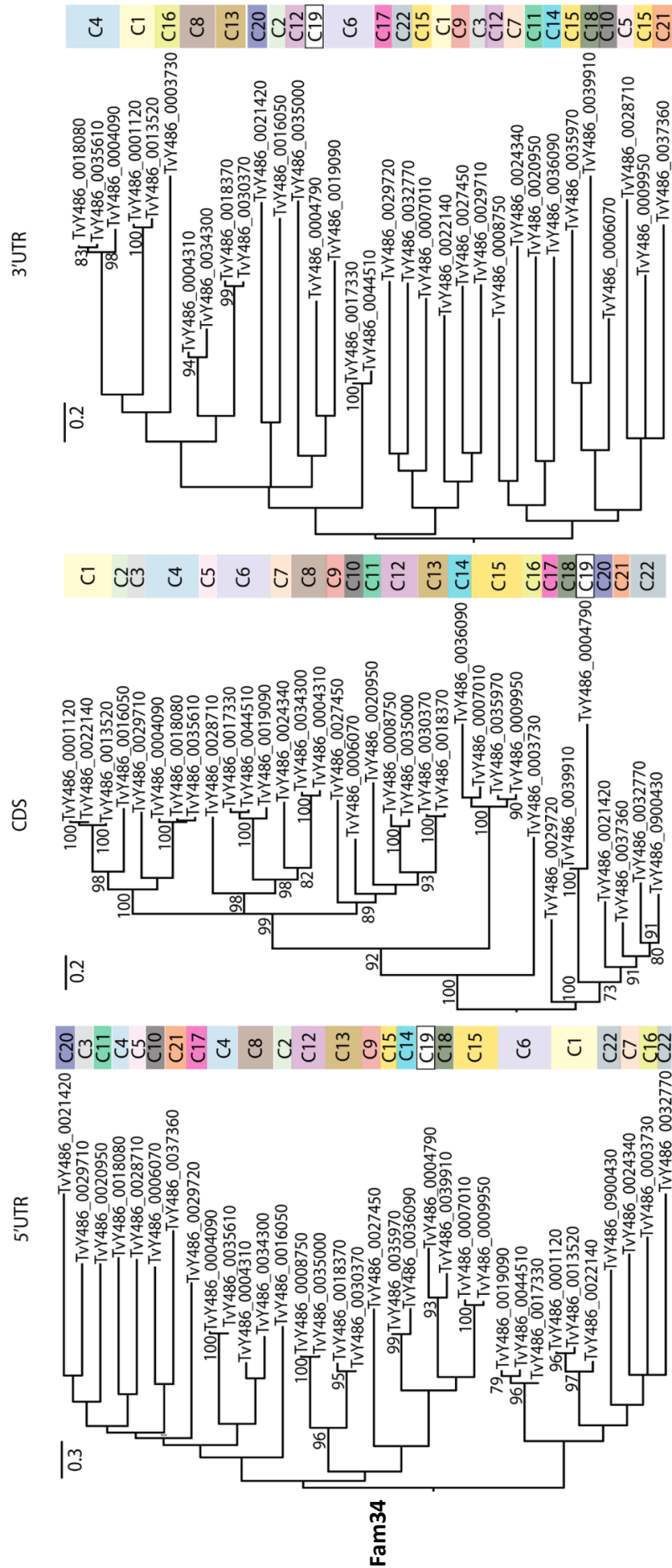


Figure 2.9. Comparison of Maximum likelihood phylogenetic trees based on the Tamura-Nei model of CDS and 3' and 5'UTR sequences for Fam32. Clusters were defined based on the CDS sequences that shared an identity >90%. The different clusters are represented by a colour and number at the right side of each tree (C: clade). A distance scale is shown for each tree. The trees are mid-point rooted.

Figure 2.10 (overleaf). Comparison of Maximum likelihood phylogenetic trees based on the Tamura-Nei model of CDS and 3' and 5'UTR sequences for Fam34. Clusters were defined based on the CDS sequences that shared an identity >70%. The different clusters are represented by a colour and number at the right side of each tree (C: clade). A distance scale is shown for each tree. The trees are mid-point rooted.



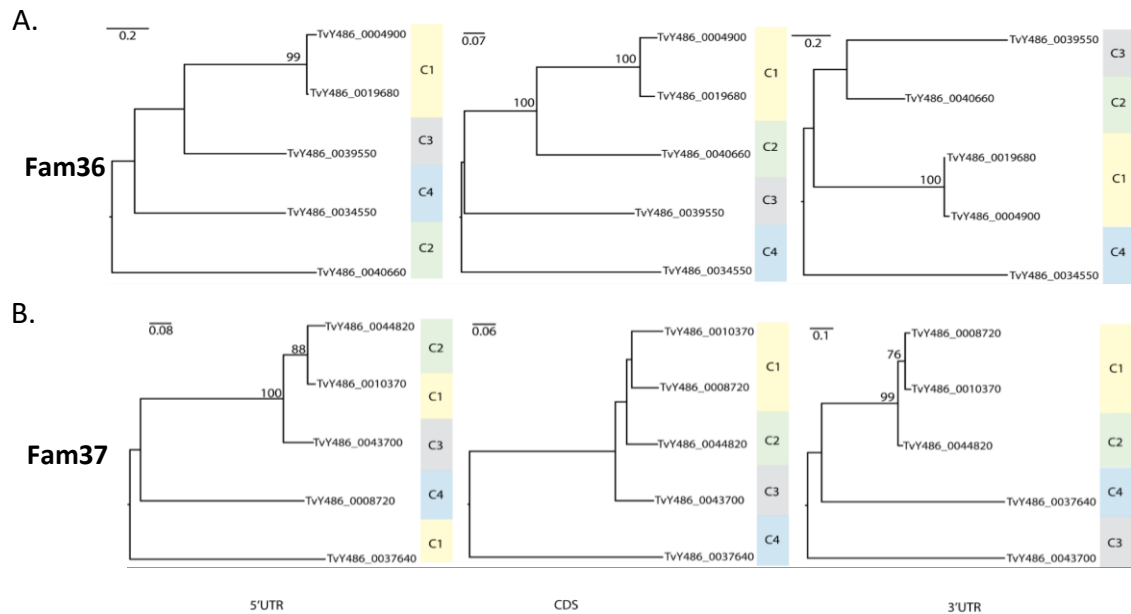
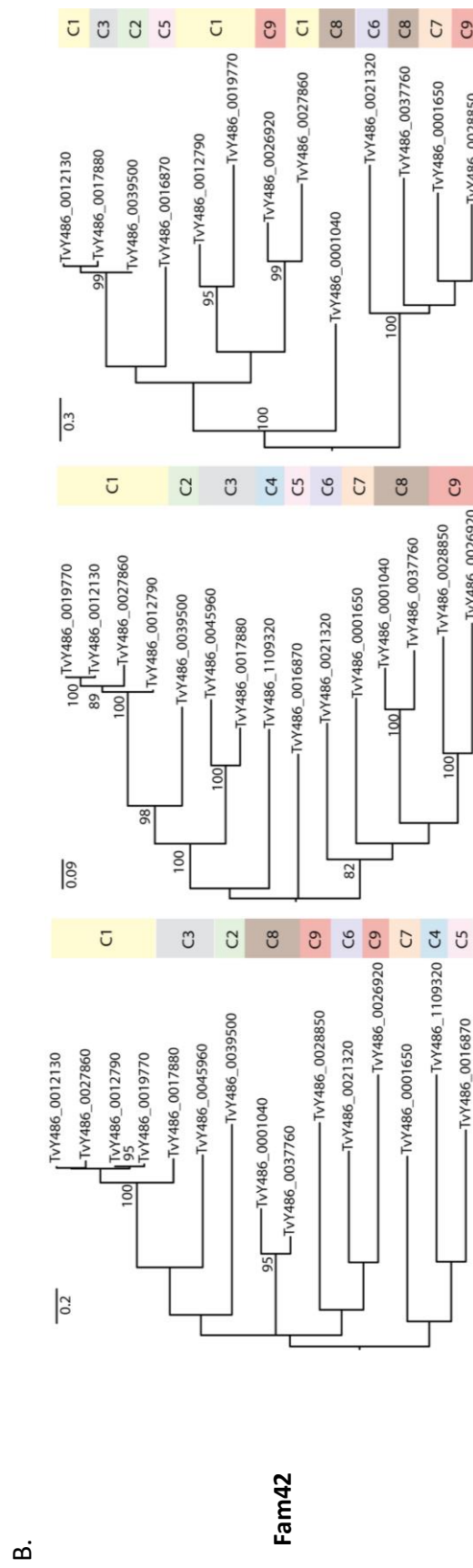
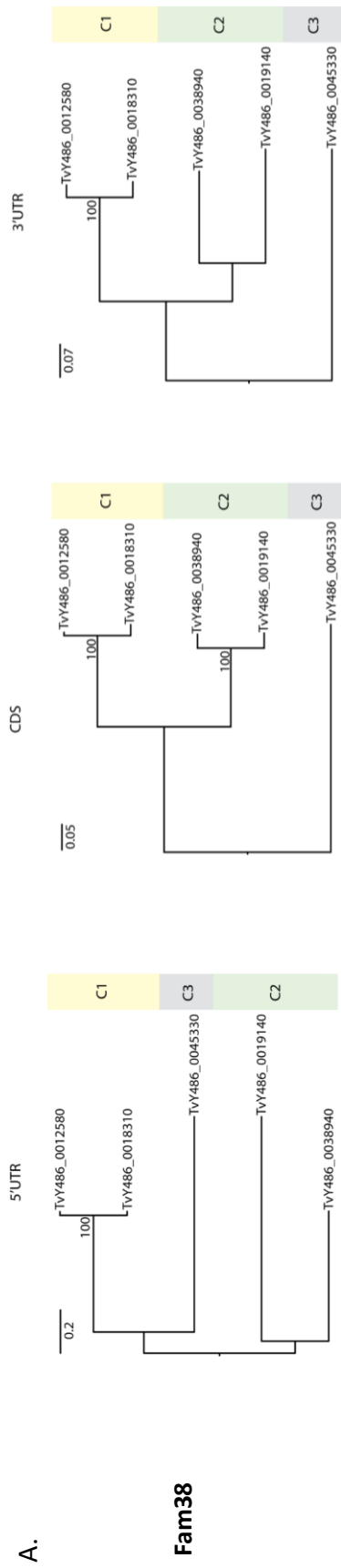


Figure 2.11. Comparison of Maximum likelihood phylogenetic trees based on the Tamura-Nei model of CDS and 3' and 5'UTR sequences for Fam36 (**A**) and Fam37 (**B**). Clusters were defined based on the CDS sequences that shared an identity >90%. The different clusters are represented by a colour and number at the right side of each tree (C: clade). A distance scale is shown for each tree. The trees are mid-point rooted.

Figure 2.12 (overleaf). Comparison of Maximum likelihood phylogenetic trees based on the Tamura-Nei model of CDS and 3' and 5'UTR sequences for Fam38 (**A**) and Fam42 (**B**). Clusters were defined based on the CDS sequences that shared an identity >90%. The different clusters are represented by a colour and number at the right side of each tree (C: clade). A distance scale is shown for each tree. Trees are mid-point rooted.



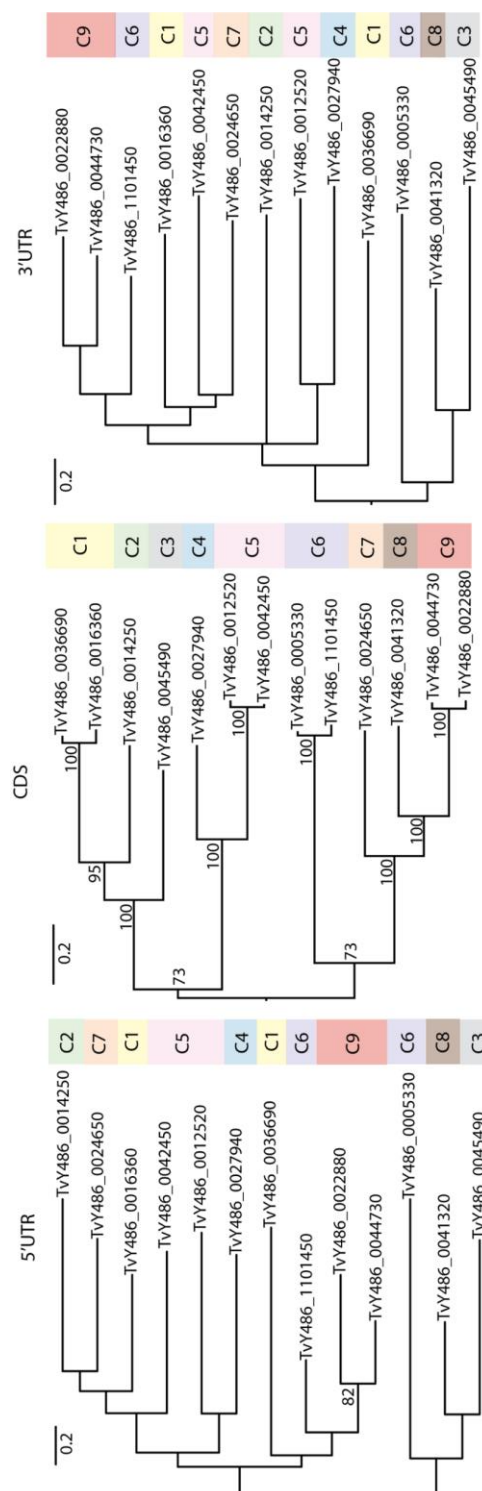


Figure 2.13. Comparison of Maximum likelihood phylogenetic trees based on the Tamura-Nei model of CDS and 3' and 5'UTR sequences for Fam44. Clusters were defined based on the CDS sequences that shared an identity >80%. The different clusters are represented by a colour and number at the right side of each tree (C: clade). A distance scale is shown for each tree. Trees are mid-point rooted.

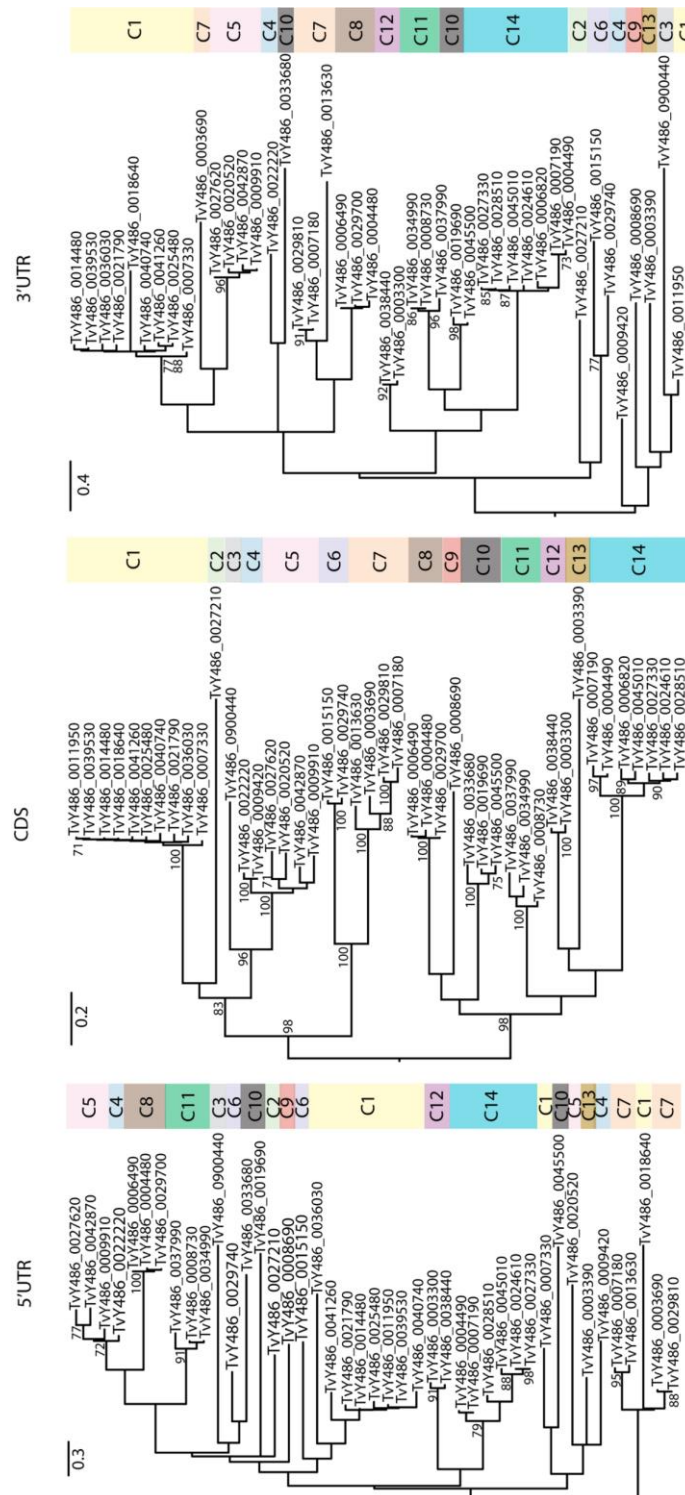


Figure 2.14. Comparison of Maximum likelihood phylogenetic trees based on the Tamura-Nei model of CDS and 3' and 5' UTR sequences for FamX. Clusters were defined based on the CDS sequences that shared an identity >70%. The different clusters are represented by a colour and number at the right side of each tree (C: clade). A distance scale is shown for each tree. Trees are mid-point rooted.

Stage	Fam	Putative role	N _g	N _c	CDS = 3'UTR	CDS = 5'UTR	Length (bp)	<i>p</i>
MET	27	membrane protein	5	4	3	3	2016	9.184x10⁻⁴
MET	35	MASP-like protein	17	9	7	8	1074	0.003
MET	43	secreted protein	9	7	6	6	2313	1.418x10⁻⁴
BSF	28	membrane protein	6	3	3	3	1224	0.118
BSF	29	secreted protein	21	11	18	18	963	0.845
BSF	30	secreted protein	51	26	23	15	2013	1
BSF	31	secreted protein	38	20	12	15	1839	1
BSF	32	membrane protein	8	5	4	4	630	2.662x10⁻⁷
BSF	34	secreted protein	34	22	19	20	888	1
BSF	36	secreted protein	5	4	4	4	2442	0.005
BSF	37	membrane protein	5	4	4	3	2820	8.058x10⁻⁶
BSF	38	secreted protein	5	3	3	3	1353	0.0567
BSF	42	secreted protein	15	9	6	8	1374	1
BSF	44	secreted protein	13	9	6	7	1206	1
BSF	X	membrane protein	44	14	33	27	1074	1

Table 2.5. Comparison of phylogenetic relationships among TvCSP gene members based on sequence domain. N_g and N_c denote the number of genes and clades in each family respectively. The number of genes retaining the same sister taxon in comparisons of trees based on CDS and 3'UTR or 5'UTR respectively are indicated. The length of the sequence alignment used in estimation of recombination frequency using PHI is shown. The *p* value of the PHI test is shown; TvCSP families showing significant evidence for recombination in their sequence alignments are shown in bold.

2.3.5. Population genetic analysis

Single nucleotide polymorphisms (SNPs) among 20 different *T. vivax* clinical isolates from across four countries in Africa and one from South America were analysed to evaluate genetic variation among TvCSP genes. A total number of 1,082,148 SNPs were identified across the genome, representing 1 SNP every 44bp. From the total number of SNPs, 35,671 of them were present in all isolates with only one allele in one site (also called monomorphic or monoallelic) were excluded from the analysis, leaving 1,046,477 SNPs polymorphic SNPs in the analysis.

The average number of mapped reads for all isolates was 65.31×10^5 having Tv1392 and TvLins isolates the highest number of reads with 131.60×10^5 and 108.90×10^5 reads respectively (Table 2.6). On average, 48.12% of the reads mapped to the TvY486 reference genome (mean= 3,575,784). The Nigerian samples achieved a coverage between 33.11% - 84.39%, a higher range if compared with the Ugandan samples with a coverage between 7.66%-71.69%. TvLins was the isolate with the highest number of reads mapped to the reference genome with 10323735 reads (94.81%).

Isolate ID	Location	No. of mapped reads ($\times 10^5$)
IL11	Nigeria	67.70
IL1392	Nigeria	131.60
IL306	Nigeria	79.90
IL319	Nigeria	43.75
IL338	Nigeria	46.03
IL340	Nigeria	66.01
IL462	Nigeria	57.28
IL465	Nigeria	51.67
IL493	Nigeria	35.18
IL596	Nigeria	43.59
IL684	Nigeria	51.88
IL2005	Uganda	39.28
IL2323	Uganda	83.79
IL2714	Uganda	97.12
ILV-21	Uganda	48.70
IL3171	Gambia	43.89
IL3638	Ivory Coast	49.64
IL3651	Ivory Coast	65.03
IL3658	Ivory Coast	95.21
TvLins	Brazil	108.90
Average		65.31

Table 2.6. List of *T. vivax* isolates from the five populations studied showing the summary of mapping statistics against the TvY486 reference *T. vivax* genome.

2.3.6. Levels of nucleotide diversity and neutrality among TvCSP gene families

Analysis of neutrality and nucleotide diversity among clinical isolates using the filtered SNPs showed that the frequency distribution of the nucleotide diversity (π) across TvCSP genes was very similar within populations (Figure 2.15). From the 244 TvCSP studied, 112 of them showed a $\pi=0$ using the PopGenome software. In contrast, only 14 genes corresponding to Fam29-31, Fam34, Fam42-44 and FamX showed zero values based on the SNPgenie analysis. This low nucleotide diversity value suggests that the level of polymorphisms of these genes across all populations are null showing no divergence.

According to the analysis, each gene displayed very low π values when compared to a threshold of the average nucleotide diversity of 20 VSG genes (Figure 2.15). Results showed that between gene members from the same family, no difference of diversity values was observed. In addition, π values for a specific family compared to the rest of TvCSP families showed no significant difference. The gene TvY486_0011750 from Fam29 showed the highest value for nucleotide diversity with $\pi =0.0204$ and $\pi =0.0182$ from PopGenome and SNPgenie respectively. In the same way, the gene with the lowest nucleotide diversity using PopGenome was TvY486_0001040 from Fam42 with $\pi =2.04248E-05$ and $\pi =0$ for SNPgenie analysis. Using SNPgenie, there were 12 genes with $\pi=0$, the lowest nucleotide diversity values. In addition, there were 2 genes with $\pi =0$ using both software indicating that the degree of polymorphisms within the population is minimum.

The levels of neutrality for each TvCSP according to each population was also analysed based on the frequency-based Tajima's D statistic. This test was computed to identify if the allelic variation was caused by a recent positive or balancing selection. From the 244 genes analysed, 112 genes (45.9%) did not produce a value for D (Figure 2.15). If we only consider those genes that returned a value, 76 genes (31.15% $D<0$) showed negative values, while 56 genes returned a positive value (22.95% $D>0$).

No TvCSP family displayed only positives or negatives D values across all gene copies. Fam38 (n=5) did show positive values for three genes and no-value for two genes. Most families gave mixed results; FamX displayed the highest number of genes with negative D values (n=16) compared with $D>0$ (n=4).

In general, positive Tajima's D values suggest balancing selection of a recent bottleneck within the population, whereas negative values indicate a recent selective sweep with a high number of low frequency polymorphisms (Tajima, 1989). The fact that the majority of genes returned D values <0 suggests the presence of rare alleles with low frequencies in all the isolates analysed.

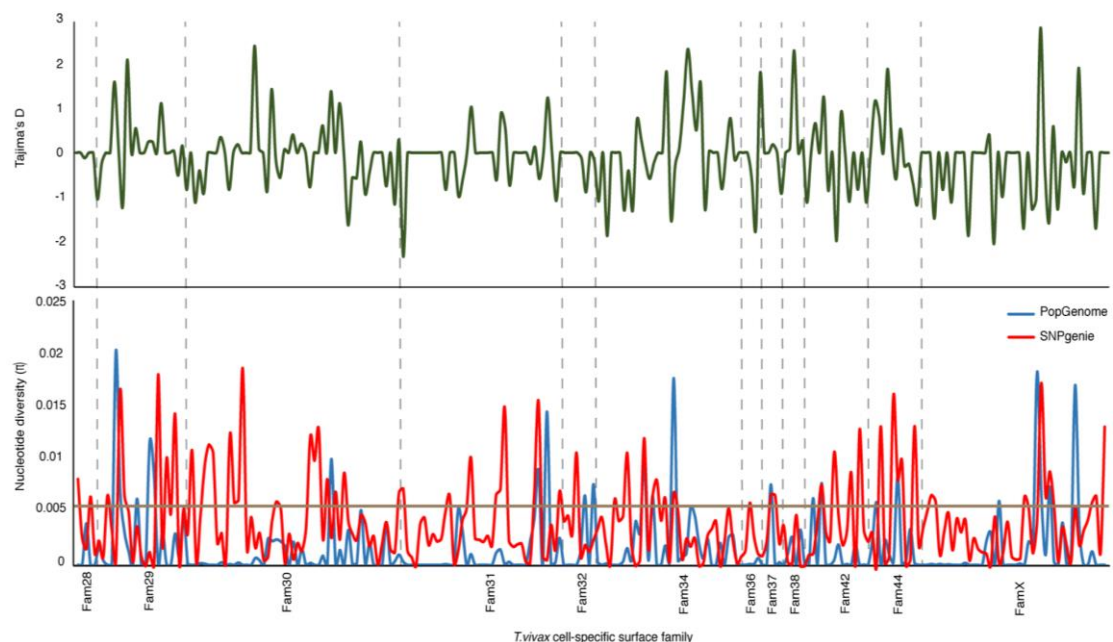


Figure 2.15. Scatter plot of the pairwise nucleotide diversity values (π) using PopGenome and SNPgenie servers and Tajima's D estimation according to the families based on the 244 TvCSP. The threshold of the nucleotide diversity graph correspond to the average π values of 20 VSG genes (brown line).

2.3.7. In silico T-cell epitope prediction

T-cell epitopes were predicted for all bloodstream-form TvCSP amino acid sequences to identify proteins with MHC binding properties. The results are presented in Figure 2.16, and take into account the number of similar MHC-I and MHC-II epitopes with antigenic and non-antigenic properties. Epitopes from different members of the same TvCSP family were considered similar if they differed by three amino acids or fewer. Based on this criterion, the results show clear differences in the number of the predicted epitopes between families. Indeed, some families like Fam32 and Fam37 did not display any predicted MHC-I or MHC-II epitopes that were similar across their members (Figure 2.16). Other families like Fam29 did not display any predictions for similar MHC-I epitopes, while Fam36 and Fam42 displayed no similar MHC-II epitopes.

Overall, the number of MHC-I and MHC-II epitopes predicted for each family was <80 and <50 respectively, except for FamX. Moreover, all the families presented a higher number of predicted MHC-I than MHC-II epitopes. The number of promiscuous MHC-I epitopes was on average of 3 epitopes per family. However, there were no predicted promiscuous MHC-II epitopes for any family except for Fam30 and Fam31 that displayed 7 and 1 promiscuous peptides respectively.

The prediction of binding ligands for FamX members showed 308 and 103 unique MHC-I and MHC-II epitopes respectively. The results displayed 147 potentially antigenic MHC-I epitopes compared to 161 non-antigenic epitopes. FamX proteins were divided according to phylogenetic clades to examine variation in epitope number. Interestingly, the highest number of antigenic epitopes were present in clade 10 (37 epitopes) while clade 1 displayed the highest number of non-antigenic epitopes (45). Clade 11 was the only isoform with no potential antigenic epitopes predicted.

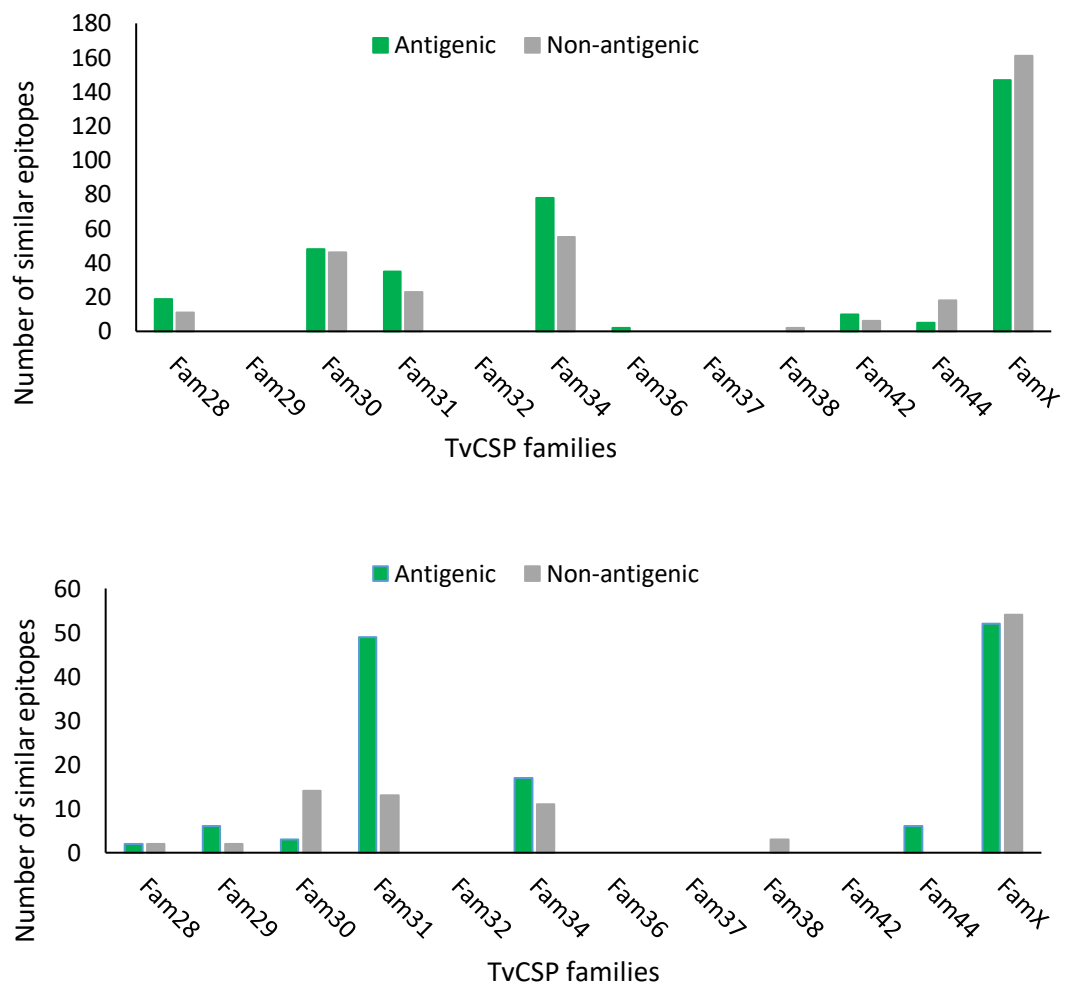


Figure 2.16. Number of similar T-cell epitopes for MHC-I (A) and MHC-II (B) after their evaluation of antigenicity.

The identification of similar epitopes within FamX clades showed that 137/147 antigenic epitopes were found in at least two proteins while 10/147 unique to one protein. In fact, 54/137 'similar' epitopes displayed no sequence variation at all but were conserved across all FamX copies in which they were found. Most epitopes were found in the central region and near the C-terminal domain (Figure 2.17). In addition, the analysis showed 39 promiscuous peptides being 23 of them possibly antigenic while 16 possibly non-antigenic. The majority of the promiscuous epitopes were predicted to bind D18.4 allele in addition to one or four more alleles.

T-helper epitopes were also predicted using HLA instead of BoLA alleles since no online tools are available to perform these predictions. MHC-II consensus results showed 54 and 52 possibly antigenic and non-antigenic epitopes respectively predicted using TEPITOPEpan and IEDB online servers. The results showed that the number of MHC-I epitopes were greater than for MHC-II. In the identification of promiscuous epitopes also using HLA alleles, 31 peptides were predicted as promiscuous from which 17 were possibly antigenic while 14 were non-antigenic. The allele HLA DRB3*08:01 was able to bind almost all the promiscuous epitopes with few exceptions only. Moreover, most promiscuous epitopes were predicted to bind two different alleles presenting inclusively a small group that bind 5-7 alleles.

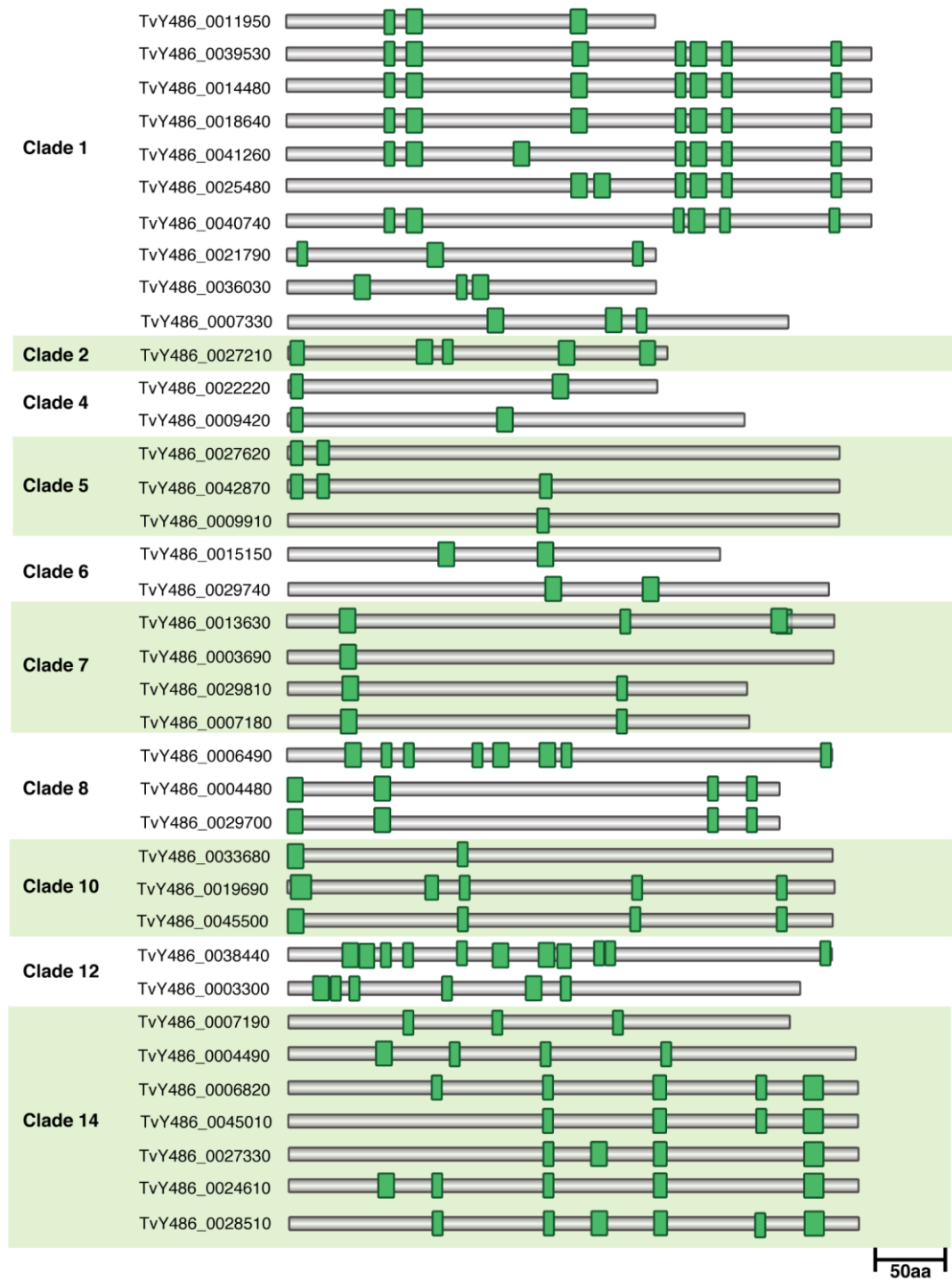


Figure 2.17. Similar predicted MHC-I epitopes for FamX proteins according to their position in the amino acid sequence.

2.3.8. In silico B-cell epitope prediction

The amino acid sequences of all TvCSP family members were used to predict B-cell epitopes using three different online resources. Predicted epitopes are a consensus of identical predictions by at least two of the methods. Based on this criterion, 69 linear 20-mer B-cell epitopes were predicted as shown in Table 2.7. The number of B-cell epitopes varies quite substantially among TvCSP families, and, within each family, epitopes were not predicted in every paralog. No epitopes were predicted for Fam32. Overall, FamX had the highest number of B-cell epitopes following by Fam30 and Fam29 (Table 2.7). Based on their position in the protein sequence, the majority of epitopes were non-overlapping and unique epitopes, while a minor proportion were overlapping. There was only one predicted linear B-cell epitope for most proteins and, in only few cases, was there multiple epitopes predicted for a single protein, e.g. TvY486_0001150 from Fam28 and TvY486_0001730 from Fam30 (both with two predicted peptides respectively).

FamX had the highest number of linear B-cell epitopes according to the consensus results. In some cases, the same epitope was predicted in different proteins, for example, ₃₂₆PTSPSTLSAPAPPPAISQQS₃₄₅ and ₃₃₆QTADKPSSANNSKLTPTNLA₃₅₅ were found in five proteins from clade 1 and in two proteins from clade 10 respectively. These results, in conjunction with the T-cell predictions, indicate that FamX proteins include binding sites for both MCH molecules and antibodies, and therefore, may have the greatest potential for mediating the immune response of all TvCSP families.

No.	Family	TvY486_ID	Peptide	Start	End	No. Epitopes
1	28	0001150	KAQKINTTSSQMSAVANETA	120	139	7
2	28	0001150	MRDKAQKINTTSSQMSAVAN	117	136	
3	28	0001150	TFAASATRERPYGQQRAVYE	23	42	
4	28	0019710	MRDKAQKINTTSSQMSAVAN	117	136	
5	28	0019710	ELARLNSTESSVVDGGRNVS	91	110	
6	28	0040160	MRDKAQKINTTSSQMSAIAN	117	136	
7	28	0040160	VERNSSIAGKSRDAVVKAFF	72	91	
8	29	0036390	DKFCWRQRNVSDNITNQLLG	269	288	8
9	29	0033210	IRNNTGELINYNTIGSIDR	249	268	
10	29	0011750	GSIDKFDERQPGASGNITKK	266	285	
11	29	0013730	AAKRKNEEERRHSCTDLWSQ	314	333	
12	29	0030720	AAKRKNEEERRHSCTDLWSQ	284	303	
13	29	0030720	ERARLENDGTFNNTSDAREV	55	74	
14	29	0015070	GSIDRFDEGQRNASSNTTNK	148	167	
15	29	0015070	IGSIDRFDEGQRNASSNTTN	147	166	
16	30	0041770	DSLKKANAVSDSAEAAVKEA	714	733	14
17	30	0020730	KGHLATAQGNIDSAAKAAKK	319	338	
18	30	0014860	MRESLKTNGISDNAAEAAVK	598	617	
19	30	0001730	SVTEWKEEMVSMVNKTYDTF	200	219	
20	30	0001730	SVKEATNATAAAKQSKESVI	120	139	
21	30	0003600	QGAEKNVANATNEVEAVNAT	269	288	
22	30	0007870	INVVSQELEITEESGAKTYD	617	636	
23	30	0005240	NLSGVIRQVQEAKSNAQNAS	483	502	
24	30	0005240	QTNESELKAKHAASEAEASE	119	138	
25	30	0011830	HKPKTCWPYDSPTKNQKCAA	21	40	
26	30	0011830	NEVELVAENAAKEASGSLYS	119	138	
27	30	0019670	CSSLNSAGNNRNEVENVDKA	29	48	
28	30	0032760	LQTIDEGVGAADKFNEAVQ	240	259	
29	30	0031450	NESERNATEAANTSINITGSF	124	143	
30	31	0038020	NATNGVRAEMGTSDEKQKEV	1000	1019	4
31	31	0035410	RAVAAEPHAAEATAQYQLTG	935	954	
32	31	0007400	AQRLGSDDVKRLQGSDSPL	467	486	
33	31	0045910	ATVEKAKNSLSDALKRQRRE	684	703	
34	34	0039910	TDTRDTQRMAEQAEREAAA	293	312	6
35	34	0900430	KAAAEAEKNSAEGPGSRTV	468	487	
36	34	0019090	WSVSDYDSSCSSTWQTSER	136	154	
37	34	0021420	AAEANAGSSERGANRGDGNV	457	476	
38	34	0029720	VSQATSSHVAPHTAERNEAL	22	41	
39	34	0035970	VQVTSEERAPTEAGSSRAEY	578	597	
40	36	0039550	VATAIKKSRDAMEKMKREKFP	457	476	1
41	37	0037640	NETYEEAVQARSDETLLNL	181	200	1
42	38	0012580	RCDHEGQSAHFTGCSADDPK	73	92	4
43	38	0018310	VARNISTESKTTNKSAREDP	125	144	
44	38	0018310	RCEHEGQSAHFTGCSADDPK	44	63	
45	38	0045330	WPSTGPPQRDISCRNAEAPMT	64	83	
46	42	1109320	IKNVTGEKDQEISSDCSGHD	397	416	3
47	42	0016870	VKSLSEKANENAQTGQYTK	310	329	
48	42	0021320	ASKLAEFARSAAEKVKEGVQ	363	382	
49	44	0014250	GLSKGQSERLKGESDQMKAS	672	691	4

50	44	0036690	RSAEELDLVRKGGKRIREGA	659	678	
51	44	0012520	SAEKAQKPDSEEHRNAARKV	24	43	
52	44	0042450	SAEKAQKPDSEEHRNAARKV	24	43	
53	X	0022220	EENSQNLHWRKEQEKLEE	178	197	17
54	X	0009420	DYKKYFYRDGDNGFKNMFDT	81	100	
55	X	0042870	VEASGQPSNMKSGGMTTTLNL	339	358	
56	X	0042870	EASGQHSNMQSGSMTTTLNLV	341	360	
57	X	0040740	PTSPSTLSAPAPPPAISQQS	326	345	
58	X	0025480	PTSPSTLSAPAPPPAISQQS	326	345	
59	X	0041260	PTSPSTLSAPAPPPAISQQS	326	345	
60	X	0014480	PTSPSTLSAPAPPPAISQQS	326	345	
61	X	0018640	PTSPSTLSAPAPPPAISQQS	326	345	
62	X	0007180	GLYPATEREITELVKTNRSS	144	163	
63	X	0015150	DAVAENPAGARSSGLAPGIL	254	273	
64	X	0028510	YDAESEVSSPGFATEKLRKD	89	108	
65	X	0024610	REKVYNAESEVSSPGFATEK	85	104	
66	X	0004490	REKIYDAESEVSSPELATKK	85	104	
67	X	0033680	QTADKPSSANNSKLTPTNLA	336	355	
68	X	0045500	QTADKPSAANNSKLSPTNLA	336	355	
69	X	0004480	FRRTDSSNEKLTSWKQFTE	235	254	

Table 2.7. In silico prediction of B-cell linear epitopes in TvCSP sequences according to their family. Epitopes were considered in the results if they were predicted in at least two of the three servers used for the analysis. The amino acid sequence of each peptide and its start and end position is displayed.

2.4. DISCUSSION

This chapter has examined the predicted protein structure of, and structural variability among, TvCSP gene families. It has confirmed their putative cell-surface position and quantified their natural polymorphism. Bloodstream-form TvCSP families have been shown to be universal among clinical isolates from across Africa and South America. Finally, the antigenic properties of TvCSP were evaluated through in silico analysis of linear B-cell and T-cell epitopes, which demonstrates that FamX has the highest number of predicted epitopes, and suggests that FamX proteins could stimulate CD4 and CD8 T-cells as well as bind to specific IgG antibodies. As the second largest TvCSP family after Fam30 and among the most abundant transcripts in bloodstream-form cells (Jackson *et al*, 2015), FamX is an important addition to the TvCSP suite.

The identification of proteins located at the cell surface that are easily accessible to the adaptive immune system are crucial for vaccine development. Of the 244 bloodstream-forms TvCSP examined, 79% possess a putative signal peptide indicating that they participate in the secretory pathway, since signal peptides cause proteins to be translocated from the intracellular domain to the endoplasmic reticulum (ER) after they are recognized by the signal recognition peptide (SRP) (Ahmed *et al*, 1998). Meanwhile, 88 (32%) of TvCSP possess a TMD, indicating that only a minority of TvCSP proteins are inserted into the parasite membrane, while the majority are either GPI anchored or (presumably) secreted. It was reported previously that TvCSP families were thought to be positioned on the cell surface (Jackson *et al*, 2013); however, this prediction was based on single representatives of each TvCSP family. This chapter has now analysed all members of each family and shown unequivocally that all TvCSP family members presented domains and motifs which are consistent with their localization on the surface of the parasite. We can infer then that these proteins are expressed and localized in the outer surface of *T. vivax*.

No previous analysis was made of post-translational modifications of TvCSP families. Glycosylation plays a fundamental roll in cellular adhesion, creating residues that can

be recognized by the immune system (Wiederschain, 2009). N-linked glycosylation, O-linked glycosylation and C-mannosylation were predicted for all TvCSP families. Proteins attached to the parasite surface membrane with GPI anchors can play crucial roles in the immune response such as interaction with the antigen-presenting cells (Paulick and Bertozzi, 2008; Savage *et al*, 2012). As such, GPI-anchored proteins members from Fam27, Fam35 and Fam43 might probably have the capacity to activate T-cells (Brown and Wanek, 1992). It has been shown that trypanosome cell surfaces at all stages of their life cycle are mostly covered by GPI-anchored proteins and have the ability to stimulate the host immune system (Ferguson *et al*, 1988; Nosjean *et al*, 1997; Ferguson, 1999; Ferguson *et al*, 2009). The presence of GPI anchors in several TvCSP families, and abundant glycosylation sites in all families suggests that they might probably have an immune-modulatory role in *T. vivax* infections.

The methodology used in this chapter has been widely used to perform *in silico* characterizations in related parasites as a way to determine functional characteristics. InterProScan was chosen as it employs a variety of online software tools developed using different approaches to find protein motifs based on amino acid sequences (Quevillon *et al*, 2005). The same bioinformatic tools used here have been applied in the identification of potential surface proteins like RNA polymerase subunit transcription factor (BRF1) in *T. brucei* (Yahya *et al*, 2012; Velez-Ramirez *et al*, 2015) and the recognition of protein domains and motifs in *L. major* and *T. cruzi* (Kramer *et al*, 2010). The prediction of secondary structures based on the topology of proteins have also been achieved for the screening of vaccine candidates in related species like other African trypanosomes (Coustou *et al*, 2012; Sharma *et al*, 2016), *Plasmodium falciparum* (Campbell *et al*, 2014; Kaushik *et al*, 2014; Gupta *et al*, 2015), *Plasmodium vivax* (Nanda Kumar *et al*, 2016), *L. major* (Opperdoes and Szikora, 2006) and *T. cruzi* (Bhatia *et al*, 2004; Lima *et al*, 2016). Despite the reliability of these methods, none of the TvCSP sequences identified any known protein motifs, indicating that these proteins are unique to *T. vivax*.

The tertiary protein structures produced by PHYRE based on homology modelling showed very low coverage and confidence values, unlike previous results concerning related parasites (Silva *et al*, 2010; Kaur *et al*, 2011; Khademvatan *et al*, 2013). This indicates that no authentic sequence homology exists between TvCSP and known proteins structure, reinforcing previous conclusions that these proteins evolved in the *T. vivax* lineage only (Jackson *et al*, 2013). Further experiments (i.e. crystallography) will be necessary to confirm its tertiary structure, which may still be homologous to known structures.

The CDS, 3' UTR and 5' UTR phylogenies for each gene family revealed differences in topology that suggest recombination occurs among paralogs of specific gene families. This observation was extended by the results of using PHI to examine phylogenetic incompatibility, which confirmed that all metacyclic-form families displayed signatures of past recombination events. It has been shown that the sequence identity is proportional to recombination frequency (Bell and McCulloch, 2003) and this might explain why metacyclic-form families display such evidence for recombination. In the case of bloodstream-form families, there were minor topological differences between CDS and UTR trees for all families, but only three families (Fam32, Fam36 and Fam37) showed significant phylogenetic incompatibility with PHI. Even where incompatibility is significant, the number of genes implicated in recombination events only represents 18% of all TvCSP (n = 49), suggesting that within the families, recombination is not ubiquitous, as it is among closely related VSG paralogs (Pereira *et al*, 2018; Pereira *et al*, 2019). Indeed, these results have demonstrated that certain TvCSP genes are devoid of recombination and widespread polymorphism, showing definitively that they are not variant antigens in the VSG sense.

Interestingly, the UTR phylogenies contain several robust clades suggesting that UTR subtypes exist within TvCSP families, which do not always correspond with, and might be decoupled from, CDS subtypes. UTRs are important since they maintain mRNA stability in trypanosomes (Mayr, 2016) and thereby mediate post-transcriptional regulation of gene expression (Mazumder *et al*, 2003; Resch *et al*, 2009), as well as

control interaction between proteins to regulate protein localization (Berkovits and Mayr, 2015). The cladistics structure among UTR sequences may reflect evolutionary pressure to conserve the specific regulation of TvCSP subtypes, perhaps according to subtle developmental changes during metacyclic and bloodstream stages.

Understanding the genetic diversity of TvCSP is crucial to design a vaccine against *T. vivax*. The genetic diversity of highly conserved *T. vivax* genes not expressed in these families were also analysed in order to compare their behaviour. Two genes expressing gGAPDH (TvY486_0603710 and TvY486_1006840) and TviCatL-like (TvY486_060500 and TvY486_0600530) showed a nucleotide diversity of $\pi = 0$ corroborating previous studies (Rodrigues *et al*, 2017). Moreover, their comparison with other surface proteins like VSG showed that TvCSP have lower diversity suggesting that TvCSP behave in the same way as any other gene in the genome but less diverse than VSGs.

Genes with low diversity are important in immunity since they can increase vaccine effectiveness due to epitopes present in conserved regions that could be targets for the immune system (Guy *et al*, 2018). Plausible vaccine antigens should have low polymorphism as they must confer the same vaccine efficacy in all populations (Takala *et al*, 2009) like for example the potential vaccine candidates using the malaria merozoite surface protein family (MSP) from *P. falciparum* (Pattaradilokrat *et al*, 2016; Patel *et al*, 2017). Previous studies have shown that MSP-1 42kDa fragment, a conserved fragment that can inhibit parasite invasion, possess low nucleotide diversity and positive natural selection (Pacheco *et al*, 2007), both characteristics showed for the majority of TvCSP. This chapter analysed the levels of diversity of TvCSP among *T. vivax* clinical isolates and shows that all TvCSP families display low nucleotide diversity and conservation of family sub-types across clinical isolates. This supports the idea that TvCSP may maintain their structural conformation, especially conserving their secondary structure thus allowing the protein to be recognized by the immune system (Chenet *et al*, 2012).

Calculation of Tajima's D statistic revealed that the majority of the TvCSP seemed not to be under positive selection pressure. This is not unexpected given the high degree of sequence conservation between isolates. However, although genes with positive D values were relatively rare, they were present in almost all family genes. Of all TvCSP families, Fam29 has the highest number of genes with positive D values indicating significant evidence of balancing selection. The gene TvY486_0027620 from FamX showed the highest D value (2.82). This might suggest that the TvY486_0027620 protein is a focus for immune selection, which should be taken into account as a possible candidate target of immunity (Ochola *et al*, 2010). However, it is important to consider that grouping samples from highly divergent populations can artificially increase Tajima's D value (Tajima, 1989).

T-cell epitopes in the cell-surface are able to bind BoLA molecules with high affinity playing a crucial role in the immunogenicity. This allows then the recognition of epitopes with TCR (Weber *et al*, 2009). In humans, HLA molecules are expressed in the host cells and their main function is to present intracellular peptides to the CD8⁺ cytotoxic T cells (CTLs). In cattle, BoLA molecules can act in a similar way to HLA and to other MHC-I molecules present in other mammals (De Groot *et al*, 2003). The scarcity of databases for non-human MHC molecules when compared to the large number available for HLA (Soria-Guerra *et al*, 2015), which can be attributed to the lack of information on alleles and MHC haplotypes for animal vaccine development (De Groot *et al*, 2003), means that T-cell epitope predictions in this chapter were made using only one bioinformatic program. T-cells stimulated by peptides can usually bind to several BoLA alleles or promiscuous epitopes (Acton, 2013), which is of enormous interest for vaccine development. Most of the promiscuous epitopes identified here were predicted to potentially bind the D18.4 allele. This promiscuity along with a potential high binding affinity could make these epitopes able to induce an immune response in populations with different BoLA genotypes (Farrell *et al*, 2016).

Epitope production starts when potentially antigenic proteins are cleaved by proteolytic enzymes in the APC, producing different protein fragments. However,

approximately only 2% of them will later become an epitope, presented on the APC's surface, since they must have the correct amino acid sequence to bind the MHC (Weber *et al*, 2009). All epitopes predicted here were linear T-cell peptides overlapping each other for a specific protein. The results showed that epitopes were predicted in all families but not in all their members. The number of antigenic and non-antigenic MHC-I peptides represented 55% and 45% respectively of all the epitopes predicted for all the families except FamX. Likewise, antigenic and non-antigenic MHC-II epitopes represented 65% and 35% of all predicted epitopes. 147 MHC-I antigenic epitopes were identified in FamX proteins, representing 48% of the total. That these epitopes were confined to each particular FamX clades suggests that the ability to elicit a T-cell response may vary among FamX members and should be considered in antigen selection.

The MHC-II epitope prediction was analysed using HLA alleles as previously stated (Farrell *et al*, 2016) since there is no software able to make predictions for other species besides human or mouse. The main challenge in making MHC-II epitope predictions is that the binding cleft opens at both ends in contrast to the MHC-I, complicating the prediction since the peptides that binds to the MHC-II molecule can protrude out of the core (Bordner, 2010; Jørgensen *et al*, 2010). All families presented possibly antigenic and promiscuous epitopes but they were not identified in all proteins. In a way similar to MHC-I predictions, FamX was the family with the greatest number of predicted and overlapping epitopes.

While the number of predicted linear B-cell epitopes was lower than the total number of epitopes predicted for MHC-I and MHC-II, and most of the B-cell epitopes were overlapping and predicted by one method only, the results suggest that diverse TvCSP can be bound to IgG antibodies. In a recent study, Guedes, Rodrigues *et al*, (2018) characterized B-cell epitopes using different *T. vivax* isolates from Africa and South America (Guedes *et al*, 2018). Linear B-cell epitopes described in this study were identified based on transcriptome data and tools similar to those used in this chapter resulting in four predicted epitopes, present in three FamX proteins;

TvY486_0019690 (2 epitopes), TvY486_0037990 and TvY486_0900440 (one peptide each).

Linear B-cell epitopes found in proteins from the different families suggest that specific regions of the antigens have the ability to bind specific antibodies. It should be noted that these epitopes were only linear and did not consider non-linear or discontinuous epitopes, which can occur where the amino acid chain folds in such a way to bring non-contiguous residues together (Ponomarenko and Van Regenmortel, 2009). Experimental validations of these epitopes would be necessary to confirm their possible antigenicity.

2.5. CONCLUSION

This chapter analysed the predicted protein structures of *T. vivax* cell- surface proteins from three metacyclic-form and 12 bloodstream-form protein families. It confirms that all families have a predicted cell-surface position based on bioinformatic analysis. Specific gene families have been shown not to recombine and to display low levels of amino acid polymorphism across a panel of diverse clinical isolates. This, combined with abundant, predicted immune epitopes across most families, suggests that TvCSP could include authentic vaccine antigens. In particular, a novel, family of *T. vivax*-specific transmembrane proteins ('FamX') is described consisting of 44 proteins divided in 14 different robust clades based on phylogenetic estimation. FamX has the highest number of T and B-cell predicted epitopes of all TvCSP families suggesting that most of the proteins presented immunogenic sites for MHC as well as antibody binding. This potential immunogenicity is explored further in Chapter 3.

CHAPTER 3

Identification of linear B-cell epitopes in TvCSP families using immunogenicity assays on natural infections

3.1. INTRODUCTION

The identification of potential vaccine candidates among TvCSP genes that can plausibly stimulate the host immune response represents a novel approach *T. vivax* vaccine design. The accessibility and immunogenicity of these antigens, i.e. their ability to elicit an immune response in the host (Murphy, 2012), is determined by their recognition by specific antibodies. Antibodies recognize and interact with certain targets on the antigen known as epitopes, and the robustness of antibody binding depends on immunogenicity (Mahanty *et al*, 2015). Indeed, immunogenicity of the antigen is crucial to resolution of infection, as it is related to both immune memory and adaptive immunity. In the context of vaccine development and antigen discovery, there are three main advantages that an antigen with high immunogenicity presents: 1) there is a higher affinity with the interaction epitope/specific antibody, 2) a reduced amount of the antigen is necessary to stimulate the immune response and 3) the intensity of the response is more robust in peripheral cells (Mahanty *et al*, 2015).

Immunogenic antigens should ideally elicit both humoral and cellular responses. That is, they should bear epitopes recognized by T-cells, as well as B-cells, two mediators of adaptive immunity that recognize specific epitopes with different properties (Abbas *et al*, 2014). B-cells can effectively recognize soluble and exposed antigens by B-cell receptors (BCR) that bind the membrane-bound antibodies, while T-cells recognize an antigen by their T-cell receptor (TCR) displayed on the APCs (Sanchez-Trincado *et al*, 2017).

B-cell epitopes can be further divided into two groups. Linear or continuous epitopes are fragments of the antigen with linear stretches of residues in the protein sequence. The second type are known as discontinuous or conformational epitopes, and these refer to surface residues distant in the protein sequence that are brought together by folding of the chain (Van Regenmortel, 2009). The latter corresponds to almost the majority of the epitopes found in proteins, but are less identified due to the difficulty and limitations compared to continuous epitopes. Linear B-cell epitopes are usually 15-20 aa long, easily recognized by the specific antibodies. In the case of discontinuous epitopes, the length can vary between 20-400 aa (Potocnakova *et al*, 2016). The antibody-antigen interaction has to be specific with accessible B-cell epitopes to be recognized by specific antibodies. In other words, the epitopes have to be exposed on the surface and abundantly expressed to generate a strong response. Since continuous epitopes are linear, their position relies on the protein primary sequence, folding and mobility of the region (Westwood and Hay, 2001). However, once the protein is fully folded, the binding sites of antibodies can change and discontinuous epitopes are easily recognized.

Linear B-cell epitopes have been widely used in many applications such as diagnostics, immune monitoring and vaccine development. The identification of these epitopes within a protein sequence can be achieved by different methods such as functional assays, including site-specific mutation of the antigen, 3D-structural crystallography of antigen-antibody complexes, and peptide microarrays that screen antibody binding interactions. The latter method, peptide microarrays, are a means for B-cell epitope discovery based on the Pepscan approach first described by Frank (1992), in which the ability of an antibody of interest is tested to bind against a panel of different peptides from certain antigens. The major advantage of this approach is that the desired antibodies can bind to several peptides of an antigen covering the entire protein (Ahmad *et al*, 2016). Peptide microarrays are usually printed on a solid surface like glass or plastic chip and their principle is very similar to an ELISA protocol. In an assay, the chip that can contain thousands of peptides can be probed with serum from infected or non-infected individuals to then bound by a fluorescein-tagged secondary antibody and detected with a fluorescence scanner.

Protein microarrays have been used to identify epitopes in various pathogens including viruses, bacteria (Gaseitsiwe *et al*, 2008; Valentini *et al*, 2017; Weber *et al*, 2017) and parasites. For example, peptides arrays were applied to determine allergens in the ectoparasites *Dermatophagoides farinae* (Cui *et al*, 2016). In the case of endoparasites, arrays have been used to analyse the antibody response after a malaria season to *Plasmodium falciparum* (Crompton *et al*, 2010) and for a malaria vaccine development (Loeffler *et al*, 2016). This approach has been also applied in trypanosome genomes for different purposes such as discovering new antigens for *Trypanosoma cruzi* (de Oliveira Mendes *et al*, 2013; Reis-Cunha *et al*, 2014; Carmona *et al*, 2015). Despite the fact that this approach has been carried out to analyse different immunological aspects including antigen discovery, it has not been used with any antigens of African trypanosomes. This chapter applies a peptide microarray approach to linear B-cell epitope discovery among the diverse TvCSP gene families characterised in Chapter 2.

The *T. vivax* genome encodes a large number of proteins that can be either secreted or localized in the membrane with extracellular regions. The latter are of great importance to understanding parasite interactions with the host immune system. The use of recombinant proteins (proteins encoded by recombinant DNA cloned into an expression system) allows this interaction to be studied, raising the possibility of identifying candidates that can confer protective immunity (Nascimento and Leite, 2012). However, the detection of extracellular protein interactions has been a great challenges due to their biochemical complexity (post-translational modifications) and weak interactions (Bushell *et al*, 2008; Sanderson, 2008). To overcome this issue, the high-throughput screening process called AVEXIS (Avidity-based Extracellular Interaction Screen) was developed allowing extracellular interactions with high confidence. AVEXIS assay uses mammalian cells as expression system ensuring the addition of all post-translational modifications and appropriate folding compared to other expression systems (Khan, 2013; Hunter *et al*, 2019). With AVEXIS, secreted or cell-surface proteins (type I, II and GPI-linked) are expressed recombinantly with their entire ectodomain regions allowing for authentic extracellular interactions in downstream experiments and assays (Kerr and Wright, 2012).

The expression of recombinant proteins and their application as vaccine candidates offers several advantages compared to live or DNA vaccines in terms of safety (Nascimento and Leite, 2012). The successful expression of TvCSP with a mammalian expression system based on the most immunogenic antigens from the peptide microarrays outcome can be later used to elucidate their role during infection and potential protective immunity.

This chapter aims to:

1. Screen serum samples from livestock naturally and experimentally infected with trypanosomes from across Africa and South America to identify samples positive for *T. vivax*.
2. Design a peptide array layout of *T. vivax*-specific cell-surface proteins and assay seropositive samples to identify immunogenic proteins.
3. Identify linear B-cell epitopes in significantly immunogenic proteins based on the peptide microarray assay.
4. Express recombinant forms of significantly immunogenic proteins using a mammalian protein expression system.

3.2. MATERIALS AND METHODS

3.2.1. Sera screening

Sera from naturally and experimentally infected livestock potentially positive for *T. vivax* were screened with a novel rapid diagnostic test called 'Very-Diag' (Ceva-Africa). Very-Diag is a lateral flow immunoassay for bovine sera and whole blood that can simultaneously detect antibodies against *T. congolense* and *T. vivax* in a qualitative way, based on the TcoCB1 and TvGM6 antigens respectively (Boulangé *et al*, 2017). Sera from Cameroon (n=121) came from natural infections from Gudali, Djafun and Aku breeds (n=95) that were collected in the northern regions of Ngaoundere and Touboro over a period of 15 days in the year 2016. These samples were previously screened for trypanosomes by microscopy and the results are shown in Table 3.2A. In addition, 26 naturally infected cattle from markets across Adamawa Plateau were sent to IRAD Regional Centre of Wakwa, Adamawa Region, Cameroon (7.264979, 13.547603) and received presumptive treatment with diaminazine aceturate for trypanosomes without diagnosis. Animals in this study were not screened for trypanosomes and were used for drug and vaccine trials for onchocerciasis. Sera from these animals were collected by Dr. Germanus, 2012.

Serum from Kenya (n=24) was collected from naturally infected cows in Western province over four weeks in September 2016. Kenyan sera were previously diagnosed for *T. vivax* by microscopy and PCR from where 18 were showed positive results (Table 2A). Serum from Malawi (n=40) was collected in December 2017 from cows at slaughter that were raised in an endemic area (Chikhwawa state) but were not confirmed as infected/recovered (Table 3.2A). Serum from Brazil came from sheep and calves experimentally infected with a Brazilian clinical strain (Table 3.2B). Brazilian samples were donated by Prof. M.M.G. Teixeira, Federal University of Sao Paulo and have been previously diagnosed for *T. vivax* (See below).

Brazilian samples were filter paper elutions (FTA, Micro Card, Whatman) on which sera were collected. Briefly, the elutions were obtained by cutting a piece of

1.0cmx1.0cm filter paper, which was washed with 500µl Phosphate Buffered Saline (PBS) and incubated for 48 hours at 4°C. The samples were centrifuged for 10min x 1500g at room temperature (RT) and the supernatant was used in the test. The Brazilian samples were previously tested by parasitemia and PCR using species-specific TviCaTL primers (work done at the Federal University of Sao Paulo). The samples came from 1) naturally infected cattle at chronic phase diagnosed negative for parasitemia but positive by PCR (n=11); 2) a single pool of 13 samples from experimentally infected sheep with 1×10^5 trypomastigotes TviCa strain diagnosed positive for both previous tests (n=1). The last samples were from experimentally infected calves with 1×10^5 trypomastigotes TvLins strain being positive for parasitemia only. Two calf samples were used individually on the test while the other was a pool of 6 samples from 3 different calves collected at different inoculation times.

The procedure was performed using cassettes sent by Ceva-Africa and according to the manufacturer's instructions by adding a drop of sample into the specimen well (S) of the cassette followed by a drop of dilution buffer and incubated for 10 min. Results were read using the control line to validate the test.

A.

Origin	N	Date	Host	Gender		Sample description	Diagnosis		
				M	F		Tb	Tc	Tv
Cameroon ^a	121	06/2016	Cattle	2	94	Individual	10	2	0
Kenya ^b	24	09/2016	Cattle			Individual	0	0	18
Malawi ^c	40			-	-	Pool (n=30)	0	0	0
		12/2017	Cattle			Individual (n=10)	0	0	0
Brazil	15	-	Cattle (11)			Individual	0	0	11
		04/2013 ^d	Sheep (1)	1	0	Pool	0	0	1
		03/2013 ^e	Calf (3)	3	0	Pool	0	0	3
Total	200						10	2	32

B.

Host	N	Days post infection (dpi)	Phase	Strain	Geographic origin	PCR
Sheep 1	8	2, 7, 10, 11, 12, 13, 18,19	Acute	TviCa	Catolé do Rocha/PB	+
Sheep 2	5	2, 7, 11, 13,18	Acute	TviCa	Catolé do Rocha/PB	+
Calf 1	3	38, 44, 65	Chronic	TvLins	Sao Paulo	-
Calf 2	1	56	Chronic	TvLins	Sao Paulo	-
Calf 3	2	38, 47	Chronic	TvLins	Sao Paulo	-

Table 3.1. A. Relation of samples used for the peptide microarray immunoassay. ^aSamples donated by Dr B. Makepeace (University of Liverpool). ^bSamples collected by Dr S. Silva-Pereira (University of Liverpool). ^cSamples donated by Dr S. Nkhoma (MLW Clinical Programme). All infections were natural except for two experimental infections conducted in Brazil (^{a/b}). Strain is unknown except for experimental infections: ^dTviCa, ^eTvLins. Tb: *T. brucei*, Tc: *T. congolense*, Tv: *T. vivax*. **B.** Descriptive summary of samples from Brazilian experimentally infected animals applied to the peptide microarray. All samples collected from two sheep experimentally infected with TviCa strain and three calves experimentally infected with TvLins were used as pools to be applied as primary sample in the peptide immunoassay. PB: Paraíba state. Samples donated by Prof. M.M.G. Teixeira, Federal University of São Paulo.

3.2.2. Design and production of TvCSP peptide microarray

A selection of *T. vivax* peptides were chosen to be included in the peptide microarrays. The peptides were selected based on a previous, first generation peptide microarray, which contained 67 different TvCSP sequences. The criteria to select and include the proteins in the first generation peptide array was based on taking representatives for all TvCSP families in addition to single-copy antigens with predicted cell-surface location. Based on this, members from all TvCSP families were included except from Fam34 as they showed no significant peptide abundance data as previously described (Jackson *et al*, 2015).

The production of the peptide microarrays was performed by the company PEPperPRINT (Heidelberg, Germany). The proteins sequences were divided into 15 amino acid peptides with a peptide-peptide overlap of 14 amino acids. The resulting microarray contained 37,335 unique peptides printed in duplicate (74,670 peptide spots) in addition to Polio (KEVPALTAVETGAT, 26 spots) and HA (YPYDVPDYAG 40 spots) control peptides. The first generation array was analysed using a pool of sera from Kenyan naturally infected cattle (n=18) previously diagnosed as positive by microscopy, and confirmed using the Very-Diag test as stated above. In addition, one

bovine seronegative serum for *T. vivax* was used as negative control. After the immunoprofiling, the chips were read using the microarray scanner LI-COR Odyssey Imaging System; scanning offset 0.65 mm, resolution 21 μm , scanning intensities of 7/7 (red = 700 nm/green = 800 nm).

The output from the analysis of the first generation array gave a list of peptides sorted by decreasing differential intensities. From this analysis, the 600 peptides with the highest fluorescence intensity values were included in the design of the second generation microarray. In fact, all proteins from the first generation were represented in the second generation to some extent, except the FamX antigen TvY486_0003390. Overall, 66 proteins were displayed as follows: 20 single strain antigens, 1 neo epitope (new protein not previously identified by the immune system) and 45 TvCSP antigens (Figure 3.1).

Microarray glass slides (3" x 1", 75.4 mm x 25.0 mm x 1.0 mm) were coated with polyethylene glycol (Roeder *et al*)-based graft copolymer with a thickness of 13.5nm and an additional amino acid linker (β -alanine, aspartic acid, β -alanine). The microarray was generated with 600 overlapping peptides printed in duplicate (1200 peptide spots in each array copy) of 15 amino acids long with a peptide-peptide overlap of 14 amino acids. Each slide contained five array copies and in each copy mouse monoclonal anti-FLAG(M2) (DYKDDDDKAS) Cy3 and mouse monoclonal anti-hemagglutinin (HA) from *Influenza* spp (YPYDVPDYAG) Cy5 peptides were used as controls (12 spots each control peptide) displayed on the top left and bottom right of each array.

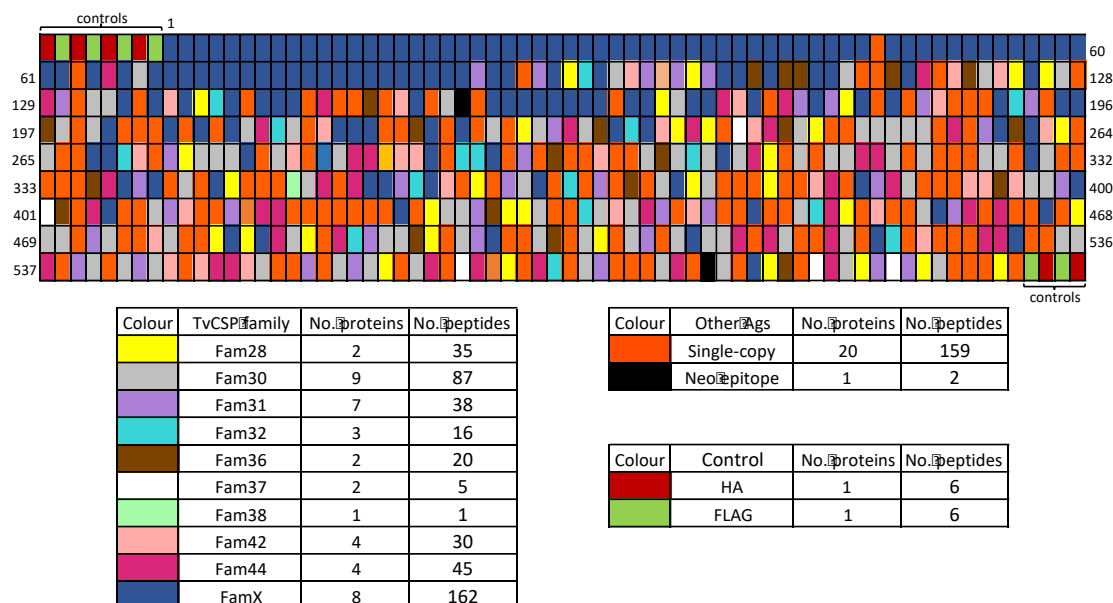


Figure 3.1. Map of a peptide microarray chip showing TvCSP families included in the design and production of the second generation based on their position. The number of peptides and proteins for each family are listed in the table below the map. The same map was used to print all chips in microarray glass slides.

3.2.3. Immunoprofiling

The list of samples used for the immunoprofiling are shown in Table 3.2. Fifty-seven seropositive *T. vivax* samples were used for the assay, of which 15 were seropositive for *T. vivax* only and 42 were a mixed infection with *T. congolense*. In addition, seventeen samples divided in three groups of samples were used as negative controls: seronegative samples for *T. vivax* from United Kingdom and Malawi (n=4 and n=6, respectively) and Kenyan seropositive samples for *T. congolense* only (single infection, n=7). The immunoassay was performed according to the PEPperCHIP Immunoassay Protocol (Heidelberg, Germany) divided in four main steps: (1) pre-staining with the conjugate, (2) incubation of sera, (3) staining with secondary antibody and (4) staining with labelled control antibodies. One slide was pre-stained with the secondary antibody to obtain local background values and to determine the possible interaction with the peptides. To achieve this, 250µl standard buffer (PBS, pH 7.4, 0.05% Tween20) was added to each array for 15 minutes and blocked with

250µl blocking buffer (standard buffer, 1% BSA) for 45 minutes. The conjugate goat-anti bovine IgG (H+L) Cy3 (Jackson ImmunoResearch Laboratories) diluted 1:4500 in staining buffer (standard buffer, 10% blocking buffer) was added to each array and incubated for 30 minutes at RT on an orbital shaker in the dark. Slides were analysed with an Agilent G2565CA Microarray Scanner (Agilent Technologies, USA) for red (670nm) and green (570nm) channels independently with 10µm resolution and the images were saved with 16-bit grayscale. The remaining slides used were not pre-stained and only the blocking step was performed to later incubate the serum samples.

Sample	Country	N	Host
Positive for <i>T. vivax</i>	Cameroon	26	Cow
	Malawi	4	Cow
	Kenya	24	Cow
	Brazil	3	Calf
		Total = 57	
Negative for <i>T.vivax</i>	United Kingdom	4	Cow
	Malawi	6	Cow
	Cameroon (positive for <i>T.congolense</i> only)	7	Cow
		Total = 17	

Table 3.2. List of samples used for the detection of immunogenic B-cell epitopes with the peptide array immunoassay. For sources, see Table 3.1.

The samples were incubated by diluting them 1:10 in staining buffer, added to each array and incubated at 4°C overnight on an orbital shaker. The interaction between *T. vivax* peptides and the primary sample antibodies were detected with the conjugate at the same dilution and conditions as the pre-staining step. The staining with labelled control antibodies was performed according to the PEPperCHIP Immunoassay Protocol and slides were analysed as previously described. The images

obtained from the scanner were used to quantify the data with a PEPSlide Analyzer software (Sicasys Software GmbH, Heidelberg, Germany) generating raw data with fluorescence intensity values.

3.2.4. Data analysis

The raw data quantified by the PEPSlide Analyzer software contains intensity values (AU) for each spot in the array. The software produced raw mean values for spots in duplicate and raw median values for the spot intensities for red and green channel independently. To achieve the background correction, local background values obtained from the pre-staining step were subtracted from the raw foreground median values for each spot. The mean for the foreground median values for spots in duplicate was calculated and three different approaches were selected to further analysed the data and compare their results in the identification of significantly immunogenic peptides (Table 3.4).

3.2.4.1. First approach – Loeffler *et al* (2016)

The identification of significant immunogenic peptides was analysed according to a previous approach specially designed for high-density peptide microarrays (Loeffler *et al*, 2016). This approach takes into account the fluorescence intensity from control antibodies to identify positive antigens within a group of arrays. The fluorescence intensity median of FLAG spots of each array was calculated to then estimate the mean of all the medians from all arrays. A normalization factor was calculated from the ratio of the median of a specific array to the mean of all FLAG medians and applied to all intensity values for each array. An inter-array normalization procedure was performed and analysed as previously described (Sundaresh *et al*, 2006; Loeffler *et al*, 2016). The data were transformed applying the Arsinh transformation previously described (Durbin *et al*, 2002; Huber *et al*, 2002) using the “vsn” package from Bioconductor (Bioconductor.org) in RStudio to stabilize the variance in the arrays and quantify differential expression between positives and negative samples. The samples were divided into two groups: positive (experimental) and negatives

(control). The standard deviation adjustment was performed using a Bayesian framework previously described (Baldi and Long, 2001). The identification of significant immunogenic peptides was analysed with a Bayes regularized unpaired two conditions t-test performed in Cyber-T (p-value <0.05) (Kayala and Baldi, 2012). An adjusted p-value < 0.05 was used to define significantly immunogenic epitopes.

3.2.4.2. Second approach – Sundaresh *et al* (2006)

Another protocol for analysing the expression profile of different antigens from peptide microarrays was previously described by Sundaresh *et al*, 2006. The data import, background correction and normalization procedures grouped the samples and standard deviation adjustment was performed in the same way as in the first approach. The main difference between these two methods is that there is no transformation factor step in this second method, and instead a comparison between each peptide signal and a true negative control signal was applied. The estimation of the true negative control signal was calculated based on the Rocke and Durbin technique in which negative control spots are absent in the array (Rocke and Durbin, 2001). After the statistical analysis, the true negative control signal estimation was compared with the signal intensities, after removing peptides with lower intensity than the control.

3.2.4.3. Third approach – limma package

Raw intensity values from the microarrays were analysed finally using the limma R package from Bioconductor (Ritchie *et al*, 2015). The data were imported from the Genepix files (.gpr) produced by the PepSlide Analyzer, selecting the “genepix” as source option and green channel intensity analysis only. The “normexp” method was selected as background correction as this is the best method to assess differential expression in microarray data when using .gpr files or similar as an output (Silver *et al*, 2008). This method takes into account one variable with normal distribution for the background noise, and another variable with exponential distribution as the background signal to model the pixel intensities based on them. The normexp is

improved by a small offset which enables the data to be shifted far from 0 giving only positive adjusted intensity values. In this case, an offset=1 was selected to stabilize the variation of log-ratios for low intensity spots.

The normalization between arrays and data transformation was achieved with the vsn method previously described. A filtering step was performed removing control peptides (HA and FLAG) from each array and the intensity values from spots in duplicate were averaged. In order to fit the lineal model, a design matrix was built to compare positive samples with the controls and the standard errors from the log-fold changes were balanced using the empirical Bayes method. Since multiple statistic tests for significant differential expression were carried out (accepted with p-value <0.05), the false discovery rate was estimated using the Benjamini and Hochberg's method (BH) for the (log₂fold-change FC >2) (Benjamini and Hochberg, 1995). The peptides were ranked based on their adjusted p-values as well as their FC generating a list with upregulated and downregulated peptides.

Analysis step	Aim	First approach Loeffler <i>et al</i> (2016)	Second approach Sundaresh <i>et al</i> (2006)	Third approach Limma
Data import	-	Mean of raw median values for spots in duplicate	Mean of raw median values for spots in duplicate	Mean raw data from genepix files
Background correction	Correct for non-specific signal generated by non-specific binding	Background subtraction	Background subtraction	Background correction with normexp
Additional step	<p><i>First approach:</i> account for serum variations</p> <p><i>Second approach:</i> account for possible contamination between adjacent peptides</p> <p><i>Third approach:</i> remove controls and average intensities for spots in duplicate</p>	Normalization factor with FLAG control spots	True negative control signal estimation	Remove controls and average of spots in duplicate
Normalization between arrays	Calibrates intensities of all chips and put them in the same scale so make them comparable	Vsn	Vsn	Vsn
Prediction of immunogenic peptides	Group positive and negative samples together.	Group arrays according to pools.	Group arrays according to pools.	Build design matrix and fit lineal model.
	Smooth standard deviation within an array.	Standard deviation adjustment.	Standard deviation adjustment.	Empirical Bayes smoothing process.
	T-test and other statistical tests comparing positives vs. negative samples.	Bayes regularised t-test	Bayes regularised t-test	Multiple statistics for differential expression.

Table 3.3. Pipeline for the identification of significant immunogenic peptides from *T. vivax* protein microarrays using Loeffler *et al* methodology (first approach), Sundaresh *et al* methodology (second approach) and limma package from Bioconductor (third approach).

3.2.5. Expression of recombinant proteins

3.2.5.1. Selection of *T. vivax* proteins and AVEXIS expression technique

Six significantly immunogenic *T. vivax* proteins ('AJ1-6', Table 3.4) were selected to be expressed recombinantly based on the peptide microarray data analysis. The expression system called AVEXIS (Avidity-Extracellular Interaction Screen) (Kerr and Wright, 2012) was used to express all AJ proteins since it is specifically intended for extracellular protein-protein interactions being able to express the entire extracellular domain of the protein as soluble recombinant proteins using mammalian cells (Sun *et al*, 2012). Protein expression (3.2.5.2-6 below) was conducted by the Cell Surface Signalling laboratory at the Wellcome Trust Institute (WTI) (Cambridge, UK).

Name	Protein ID	Family
AJ1	TvY486_0020520	FamX (clade 5)
AJ2	TvY486_0003690	FamX (clade 13)
AJ3	TvY486_0037990	FamX (clade 11)
AJ4	TvY486_0031450	Fam30
AJ5	TvY486_0004900	Fam36
AJ6	TvY486_0900440	FamX (clade 3)

Table 3.4. List of selected proteins to be recombinantly expressed by the AVEXIS technique. Four FamX members each from a different clade and one protein from Fam30 and Fam36 respectively were selected on the basis on the peptide microarray analysis as the most immunogenic proteins.

3.2.5.2. Design and construction of vector expressions

The expression vectors were amplified in *Escherichia coli* using the MultiShot Stripwell TOP10 Chemically competent cells ampicillin resistant following the manufacturer's instructions (Invitrogen, USA). To transform the competent cells, 2µl of circular plasmid was added and selective plates were used to seed 10µl cells and

culture them overnight at 37°C. Transformed *E. coli* (single colony) were grown in 50ml LB medium overnight at 37°C.

3.2.5.3. Plasmid purification

In order to purify the plasmid DNA, the PureLink HiPure Plasmid DNA Purification kit (Invitrogen, USA) was used following the manufacturer's instructions. In the final step of the maxiprep procedure, the pellet containing the purified DNA was air-dried for 10 minutes and resuspended in 500µl nuclease free water instead of TE buffer. DNA concentration was quantified by Nanodrop (Thermo Scientific, USA).

3.2.5.4. HEK293-6E cell culture and transfections

Recombinant proteins were produced by transient transfection using a HEK293-6E mammalian cell as expression system. Cell culture was performed as previously described (Kerr and Wright, 2012; Sun *et al*, 2012). Briefly, 5×10^5 cells/ml were seeded the day before transfection in 500ml Erlenmeyer flasks containing 90ml Freestyle 293 media (Life Technologies, USA) supplemented with 0.05%v/v G418 (ThermoFisher Scientific, USA) and 100µM of D-biotin (Sigma Aldrich, Germany). The cells were cultured on a shaking platform at 125rpm, 37°C, 70% humidity and 5% CO₂. All the proteins were expressed in two forms: one biotinylated and purified proteins no bio-tagged.

The transfections were performed the next day by adding 100µl (1µg/ml) plasmid DNA for purified proteins or in the presence of 10µl (1mg/ml) biotin ligase plasmid BirA (Addgene) for biotinylated forms to 5ml of pre-warmed culture media (plasmid DNA and plasmid BirA at a 10:1 ratio). Pre-warmed culture media at a final volume of 5ml containing 300µl (1mg/ml) transfection reagent polyethylenimine (Bezerra *et al*) (Longo *et al*, 2013) was combined with the first tube containing the plasmid DNA. The transfection mixture was incubated for 3 minutes at RT and added to the culture. The cells were cultured for 5 days to ensure a maximum recombinant protein yield using the same conditions as before. After this time, cultures were harvested by collecting the transfected culture and centrifuged at 3800g for 15min at 4°C. Non-bio-tagged

proteins were purified with HisTrap™ chromatography columns, a protocol previously described (Sun *et al*, 2012).

3.2.5.5. Protein normalization

A dialysis was performed using the supernatant from the previous step to remove the unconjugated D-biotin. This procedure enables AJ proteins to be used in ELISAs by eliminating the biotin that might compete with the protein for the streptavidin binding sites (Kerr and Wright, 2012). The supernatant was transferred into a 30cm snakeskin pleated dialysis tubing (MWCO=10,000, Thermo Scientific, USA) and dialyzed against PBS at 4°C overnight on a stirring plate changing the PBS every 2 hours. Finally, the sample was filtered through a 0.22µM filter and stored at 4°C. The concentration of biotinylated proteins were determined by ELISA as previously stated (Bushell *et al*, 2008; Kerr and Wright, 2012). Using Nunc streptavidin-coated plates (Thermo Scientific, USA), two-fold serial dilutions were incubated for 1h at RT. The protein activity was measured with the conjugate mouse anti-His-HRP (C-term) (Miltenyi Biotec, Germany) diluted 1:1000. The 3,3',5,5'-tetramethylbenzidine (TMB) substrate solution (Merk Millipore, USA) was added to each well and the plate was read at 650nm after 5min using a spectrophotometer.

3.2.5.6. Confirmation recombinant proteins

The successful expression and detection of AJ proteins was performed by SDS-PAGE by mixing 1µg of each protein with 15µl of sample buffer (Laemmli 2X concentrate, Sigma-Aldrich, Germany) and incubated at 95°C for 5 minutes. The mixture was loaded and separated by electrophoresis on a 12% acrylamide gel. The separated proteins were transferred from the gel onto nitrocellulose membrane by wet electroblotting and blocked with PBS pH 7.4, 4% skimmed milk (Marvel) (blocking buffer) overnight at 4°C. The membrane was washed with PBS-Tween20 0.05% and the reaction was detected using the conjugate goat anti-biotin HRP (Sigma-Aldrich, Germany) 1:2000 in blocking buffer for 2h at RT with agitation. The protein was

visualized by adding 3,3' diaminobenzidine (DAB SIGMAFAST, Sigma-Aldrich, Germany) substrate for 15min and then stopped the reaction with ddH₂O.

3.3. RESULTS

3.3.1. Serum screening

Before serum samples could be used authentically to evaluate the natural immunogenicity of TvCSP proteins, it was first necessary to confirm definitively that samples originated from animals infected with *T. vivax* using the Very-Diag test. Serological screening was first performed to 24 Kenyan serum samples previously diagnosed positive for either *T. vivax* or *T. congolense* to evaluate the reliability of the serological test. From these, 18 samples were positive for *T. vivax* by microscopy and PCR; 4 samples were positive for *T. congolense* by microscopy; and 2 samples were negative for both parasites by microscopy. The results show that of the 18 samples previously diagnosed as *T. vivax*-positive, six gave a positive result with the Very-Diag test (Figure 3.2A). Likewise, of the four *T. congolense*-positive samples, only two were positive with the test (Table 3.5). Three samples were diagnosed negative while 13 were diagnosed as mixed infections by the Very-Diag test, giving positive results for the two parasites. The latter are false positives results for *T. congolense* indicating that the specificity with Very-Diag test was less than expected.

From the naturally infected samples, 81/121 Cameroonian sera were positive for single or mixed infection while 40 were parasite-negative (Table 3.5). None of the 40 Malawian sera were positive for *T. vivax* alone. However, nine were seropositive for *T. congolense* and another seven for mixed infection. All naturally infected Brazilian cattle were negative for *T. vivax* by Very-Diag test, however three were apparently positive for *T. congolense* (Figure 3.2B). These three Brazilian samples must be false positives given that *T. congolense* is not found outside of Africa. Serum from experimentally-infected sheep in Brazil tested positive for *T. vivax*, even though the test is designed for cattle (Figure 3.2B), suggesting that the Very-Diag test can be used with other hosts besides cattle. All calf samples tested positive for mixed infections, even though they came from a pool of six sera from three animals experimentally infected with *T. vivax* Lins strain (Figure 3.2B). Moreover, two individual samples from the pool were tested individually both giving mixed infection results (Table 3.5).

Place of origin	No. samples	Host	Tv	Tc	Mixed infection	Negative
Cameroon	121	Cattle	7	55	19	40
Malawi	40	Cattle	0	9	7	24
Kenya-MP	24	Cattle	18	4	0	2
Kenya-VD	24	Cattle	6	2	13	3
Brazil	15	Cattle (n=11)	0	3	0	8
		Sheep (n=1)	1	0	0	0
		Calf (n=3)	0	0	3	0

Table 3.5. Comparison of results obtained from samples from naturally and experimentally infected livestock using Very-Diag test. Tv: *T. vivax*, Tc: *T. congolense*, Kenya-MP: samples previously diagnosed by microscopy and PCR, Kenya-VD: samples diagnosed with Very-Diag test.

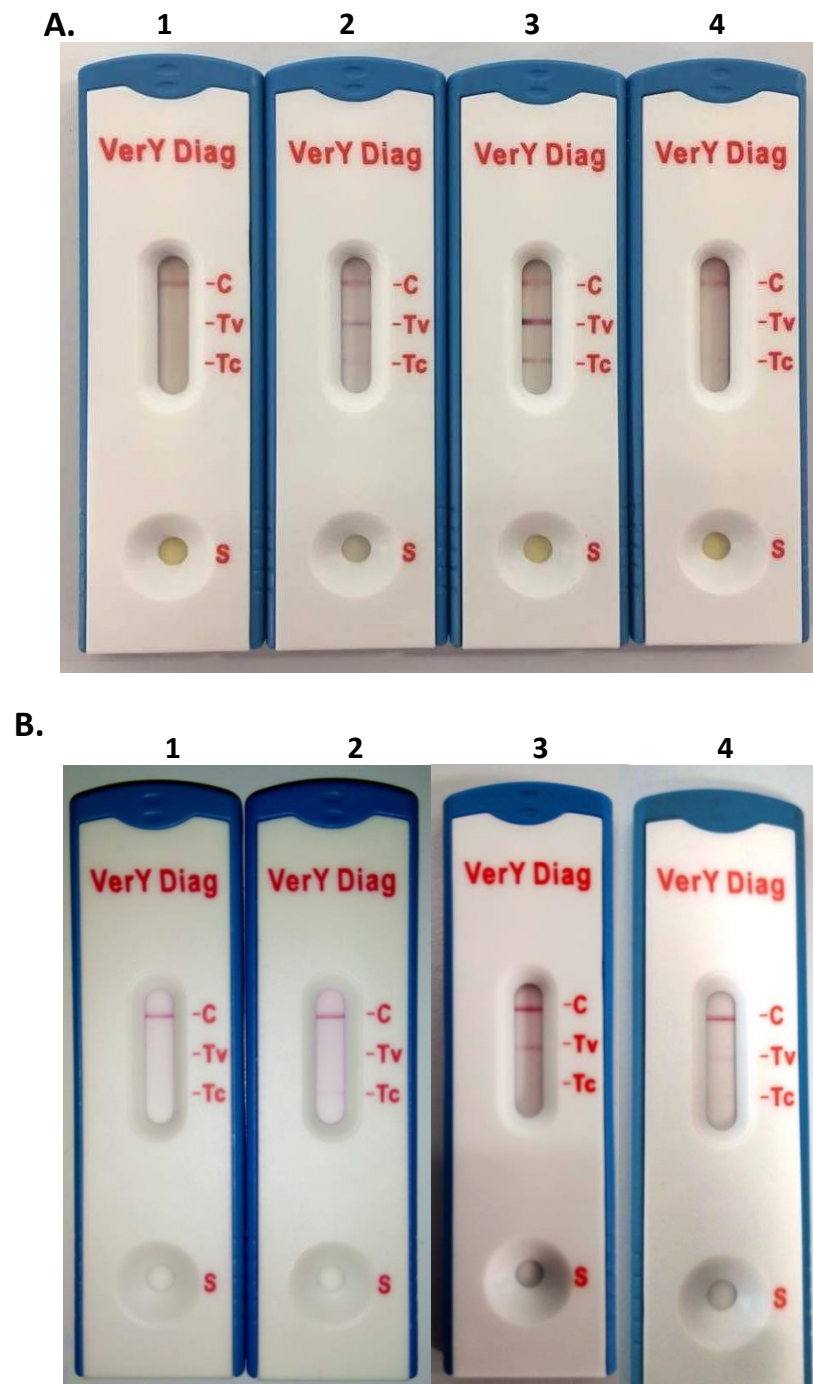


Figure 3.2. Examples of serum screening using Very-Diag tests. **A)** Example of four Very-Diag tests using Kenyan sera from naturally infected cattle previously tested by microscopy and PCR to be positive for *T. vivax*. **B)** Results of Brazilian samples applied to the Very-Diag tests using naturally and experimentally infected sera. (1) and (2) naturally infected cattle. (3) pooled sera from experimental infections in sheep and (4) pool sera from experimental infection in calves.

3.3.2. Peptide microarray analysis

3.3.2.1. Raw data

Sera confirmed to be *T. vivax*-seropositive were applied to a custom peptide microarray containing 66 TvCSP proteins, representing 10 gene families. After the application of a fluorescent, anti-bovine secondary antibody, fluorescence from each peptide spot was measured and compared to negative controls provided by naïve UK cattle. The comparison between raw fluorescent images of microarrays from positive and negative samples revealed distinct patterns. Peptide spot intensities showed a very clear and strong response in almost all positive samples regardless the country compared to negative controls (Figures 3.3-3.9). Seronegative British and Malawian samples showed almost no fluorescence with sporadic and weak binding at random positions in the array (Figure 3.7 and 3.8). *T. congolense* seropositive samples showed a minimum binding with low signal intensities (Figure 3.9). *T. vivax* positive samples produced high fluorescence intensities to certain spots, mostly at the top of the array, which indicates high antibody titres recognising the first 60 peptides (Figures 3.3-3.6). In fact, the intensity of some of these spots were as high as the anti-FLAG peptide controls, displayed at the top left and bottom right of the array.

The mean of raw median values for each country of origin was calculated and compared to examine variation by location. Although there are differences in the fluorescence intensity values (AU) between locations (Figure 3.10), it is clear that the mean signal intensity peaks showing the strongest antibody response corresponded, in all locations but not in the negative controls, to adjacent spots in the first row of the array. Peptides located in these positions derive almost entirely from FamX proteins (58 peptides), although one Fam44 peptide and another from a single-copy gene TvY486_0025790 were also among the highest mean signal intensity peaks. The Brazilian population showed the highest intensity values reaching peaks >19000 AU followed by the Cameroonian population peaks at 6000 AU. Kenyan and Malawian samples displayed intensities of 4000 AU, but with a different pattern apparently less

complex than the other positive populations. Overall, peptides located in positions other than the first and second rows on the array were very variable in intensity. The intensity pattern from the negative controls was slightly different displaying peaks at random positions with different fluorescence intensities. Moreover, some peptides presented a stronger response in the negative controls compared to seropositive samples like the peptide number 377 (₂₆₄GIDTYVEGLGEIDTL₂₇₈) from a single strain antigen and the peptide number 599 (₁₇₉TAVPDDCQVGNDTNS₁₉₃) from the Fam28 protein TvY486_0040160.

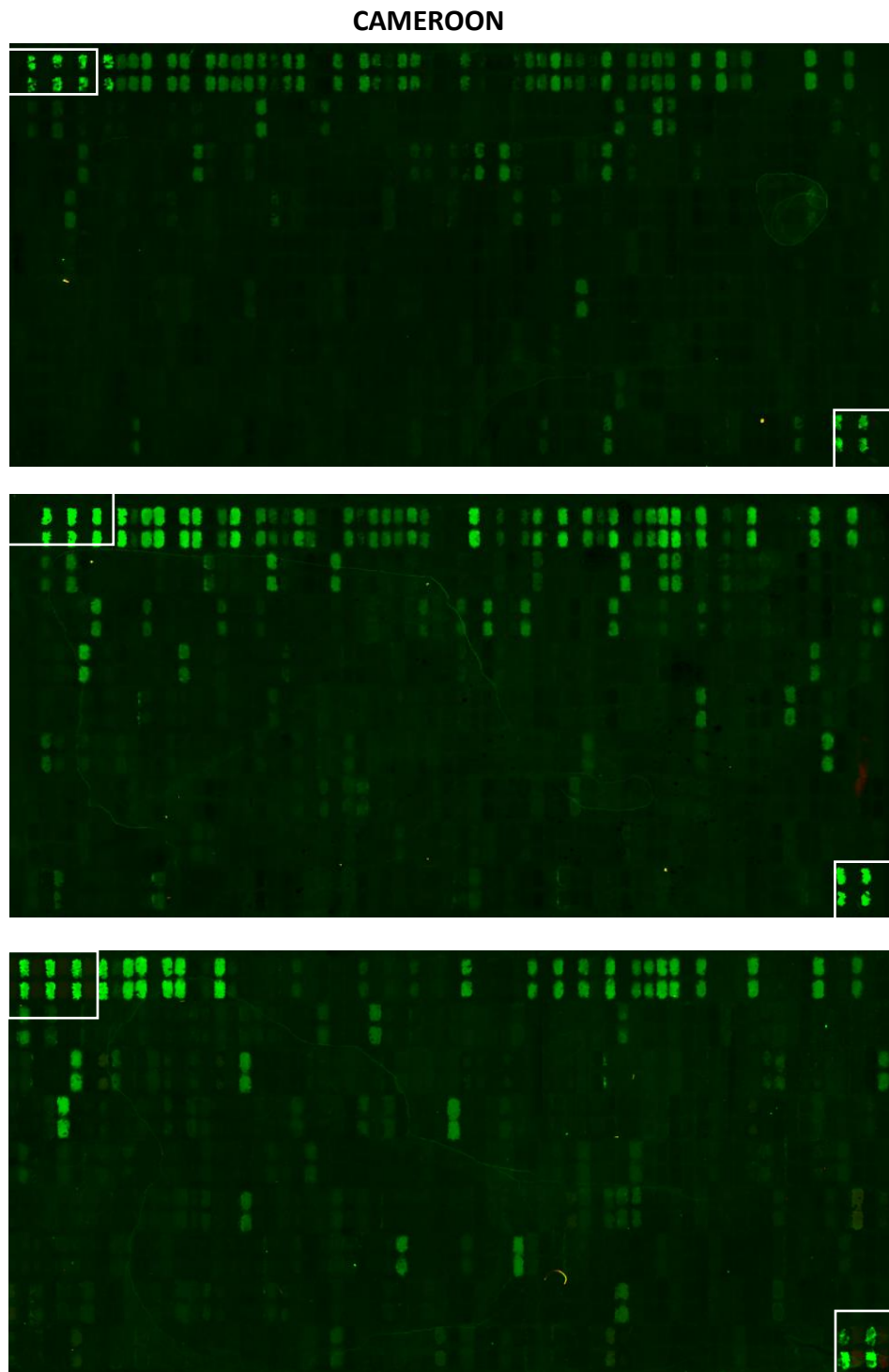


Figure 3.3. Spot intensities obtained from PEPperPRINT peptide arrays using naturally infected Cameroonian sera. Each microarray chip was incubated with an individual sample. Three panels are showed on representative of all sera. The peptide array control spots are located at the top left and bottom right of each array (highlighted in white boxes).

MALAWI

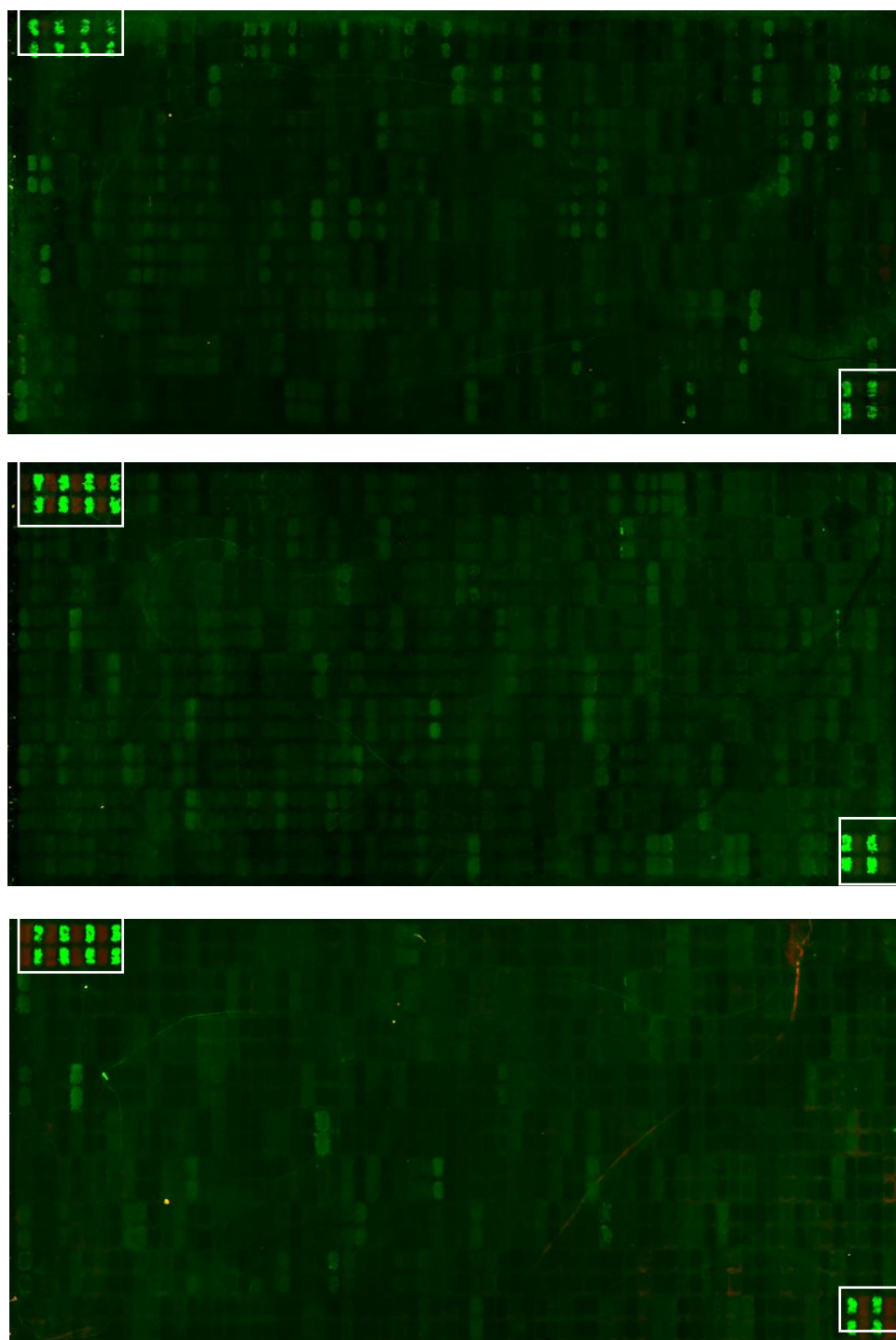


Figure 3.4. Spot intensities obtained from PEPperPRINT peptide arrays using naturally infected Malawian sera. Each microarray chip was incubated with an individual sample. Three panels are showed on representative of all sera. The peptide array control spots are located at the top left and bottom right of each array (highlighted in white boxes).

KENYA

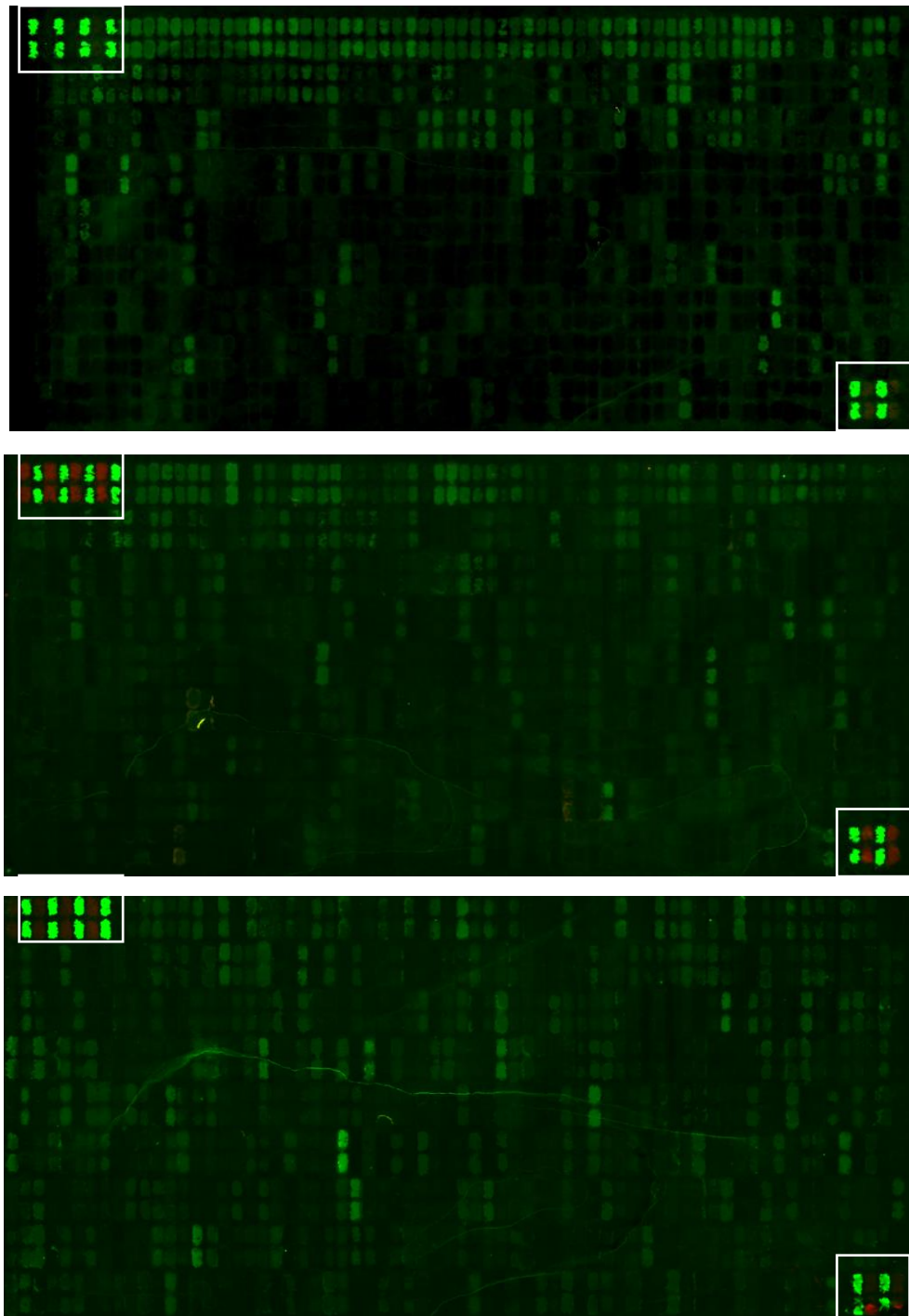


Figure 3.5. Spot intensities obtained from PEPperPRINT peptide arrays using naturally infected Kenyan sera. Each microarray chip was incubated with an individual sample. Three panels are showed on representative of all sera. The peptide array control spots are located at the top left and bottom right of each array (highlighted in white boxes).

BRAZIL

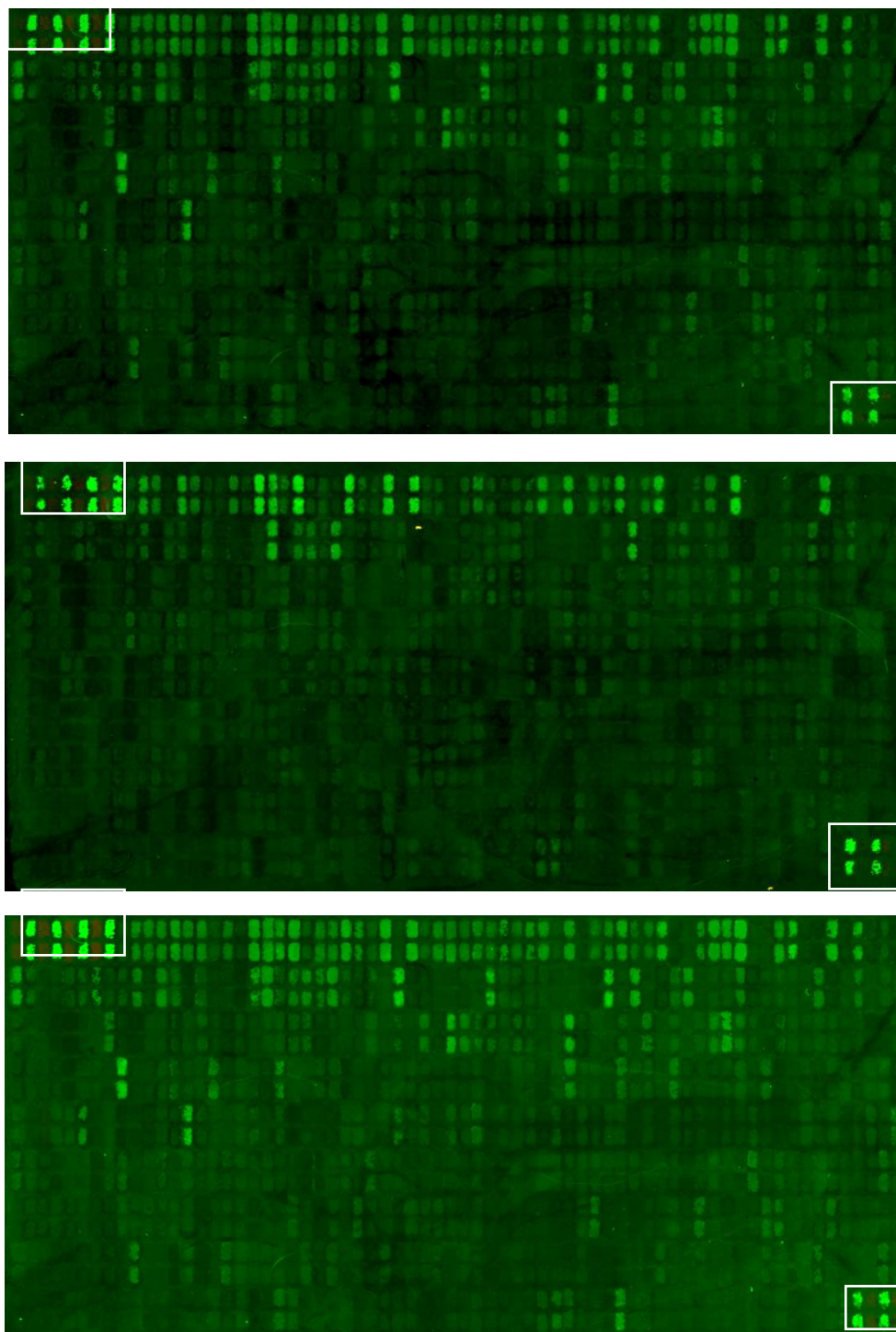


Figure 3.6. Spot intensities obtained from PEPperPRINT peptide arrays using experimentally infected samples from Brazil. Each microarray chip was incubated with an individual sample. Three panels are showed on representative of all sera. The peptide array control spots are located at the top left and bottom right of each array (highlighted in white boxes).

UNITED KINGDOM

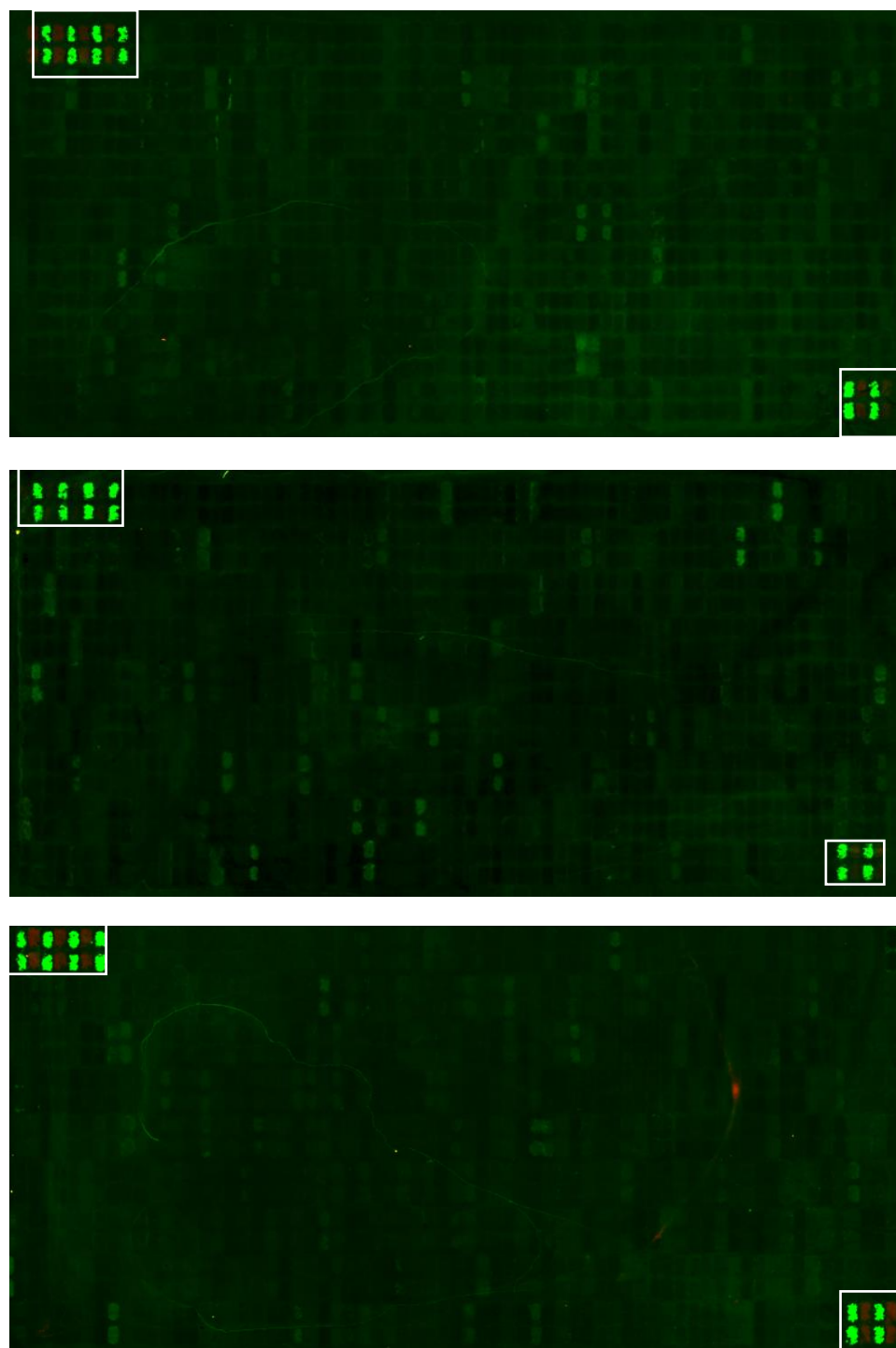


Figure 3.7. Spot intensities obtained from PEPperPRINT peptide arrays using seronegative sera from United Kingdom. Each microarray chip was incubated with an individual sample. Three panels are shown representative of all sera. The peptide array control spots are located at the top left and bottom right of each array (highlighted in white boxes).

MALAWI NEGATIVE CONTROL

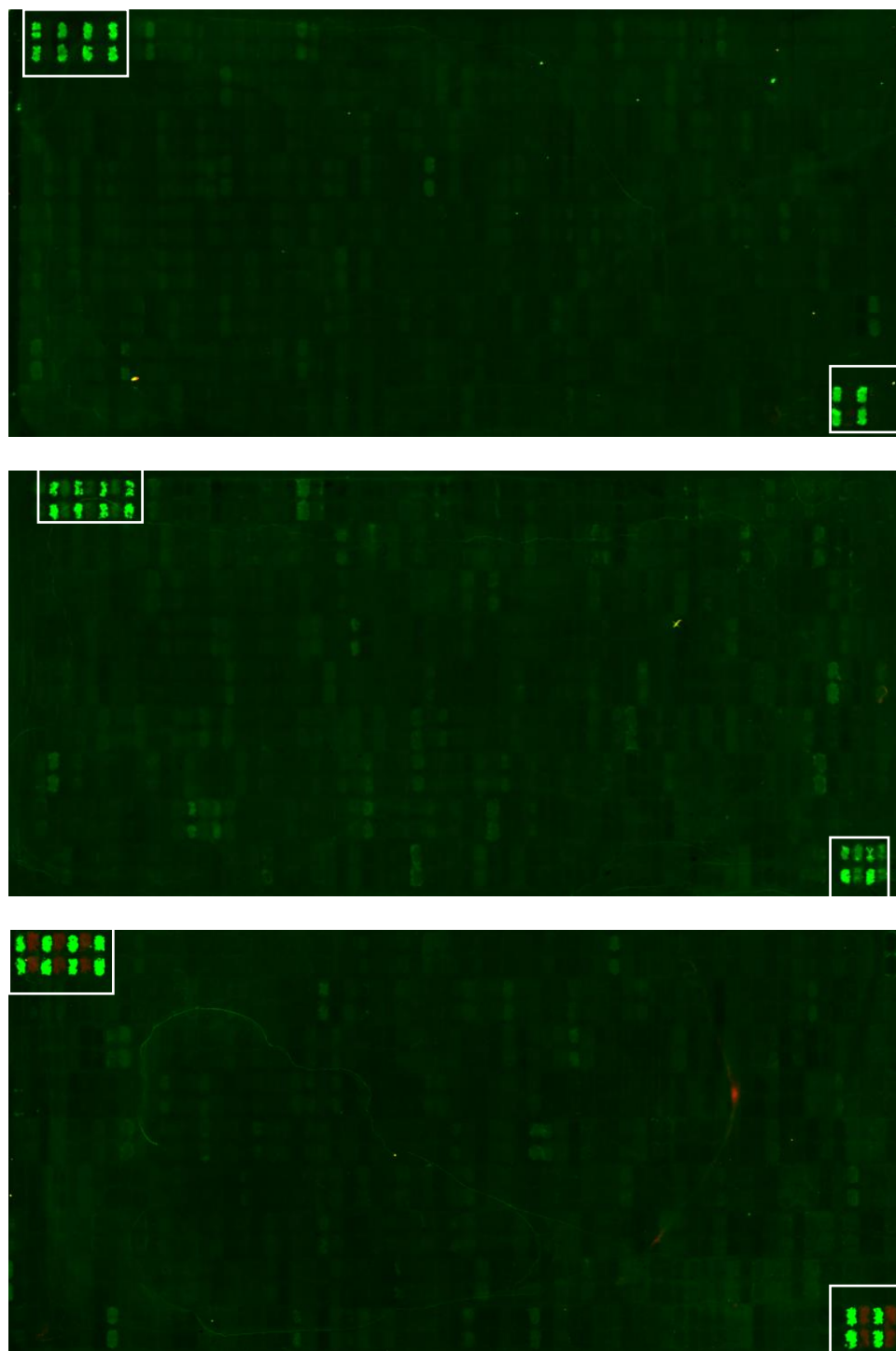


Figure 3.8. Spot intensities obtained from PEPPERPRINT peptide arrays using seronegative era from Malawi. Each microarray chip was incubated with an individual sample. Three panels are showed on representative of all sera. The peptide array control spots are located at the top left and bottom right of each array (highlighted in white boxes).

SAMPLES SEROPOSITIVE FOR *T. CONGOLENSE*

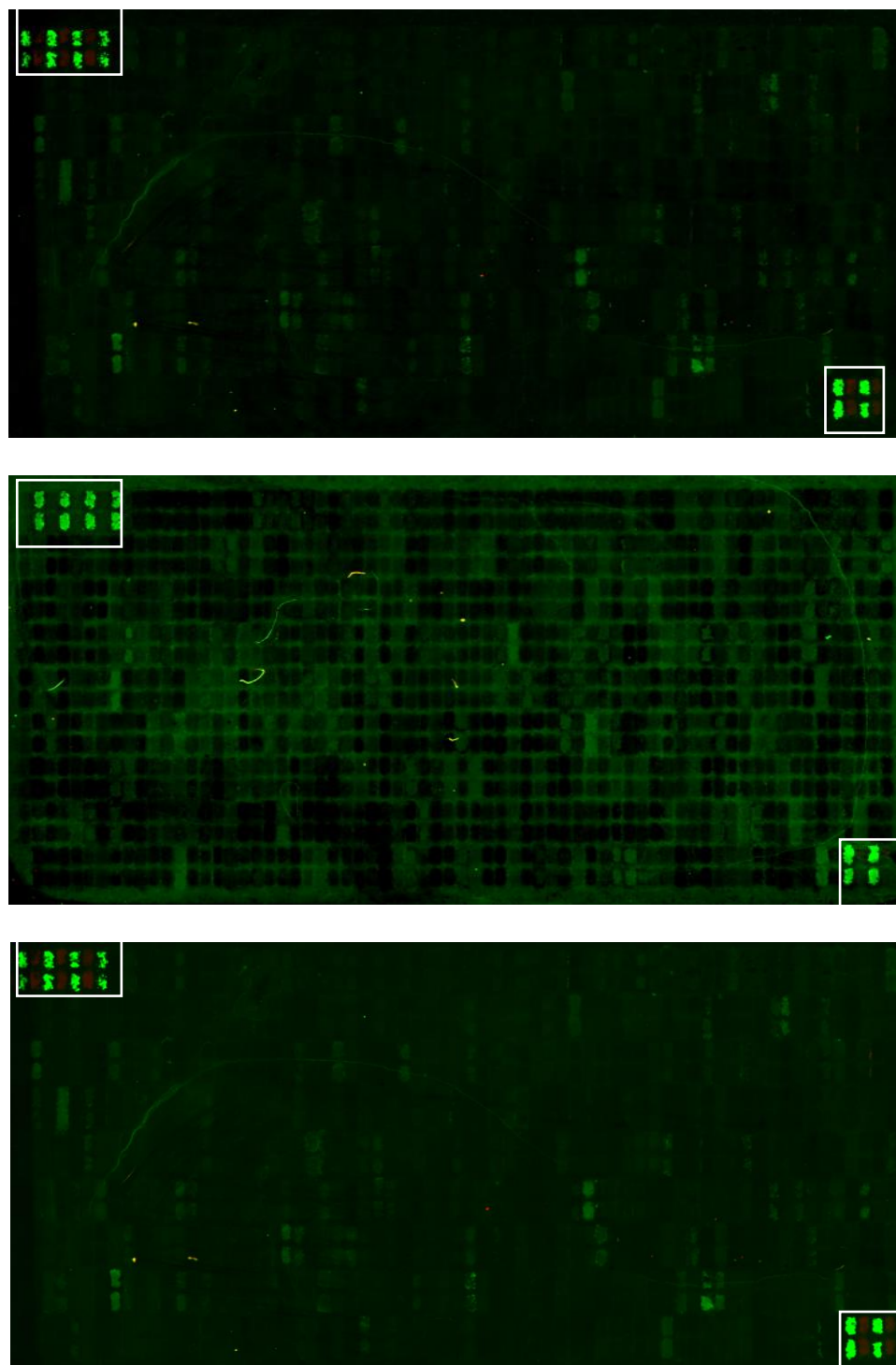
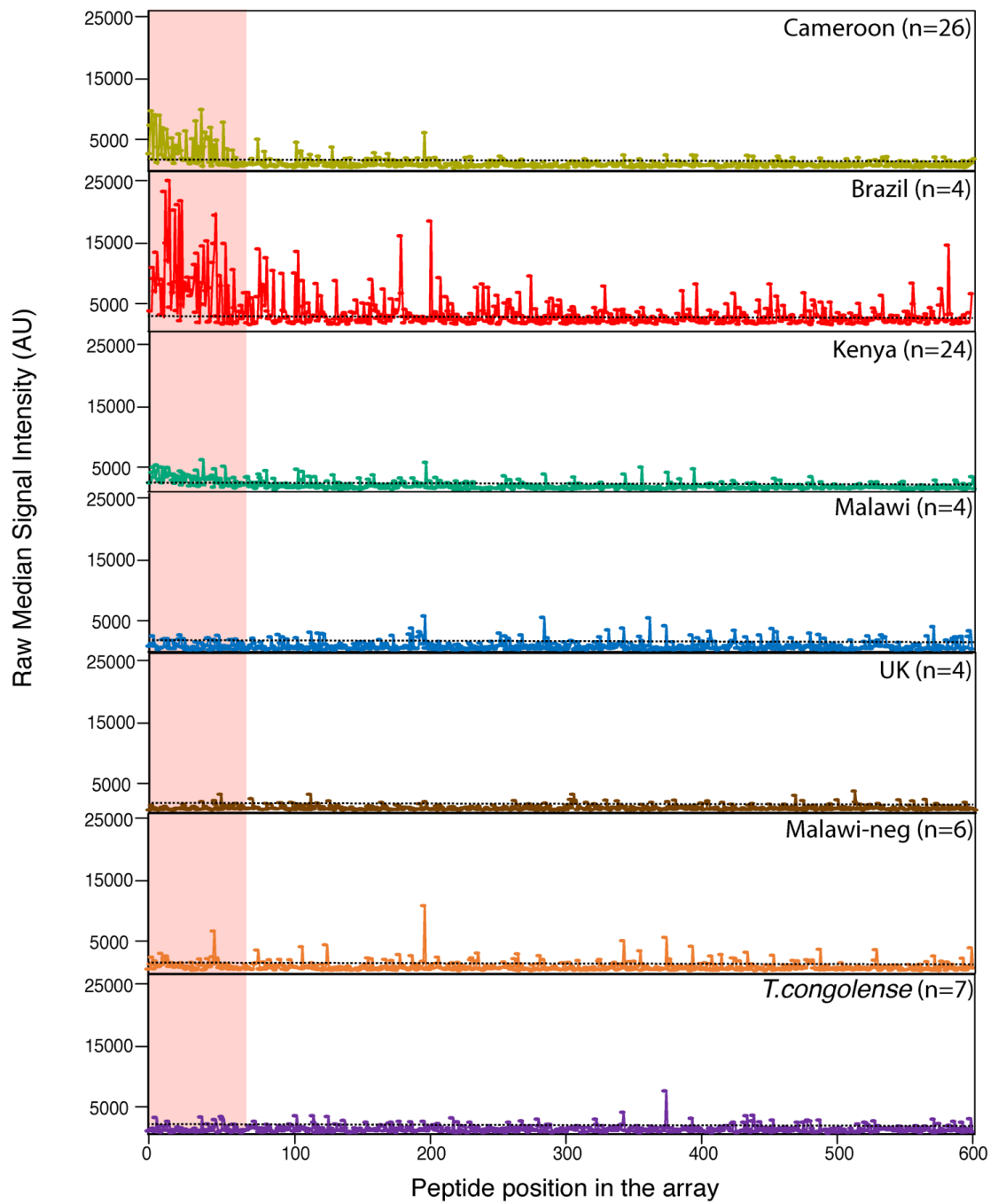


Figure 3.9. Spot intensities obtained from PEPPERPRINT peptide arrays using seropositive sera for *T. congolense* from Cameroon. Each microarray chip was incubated with an individual sample. Three panels are showed on representative of all sera. The peptide array control spots are located at the top left and bottom right of each array (highlighted in white boxes).

A.



B.

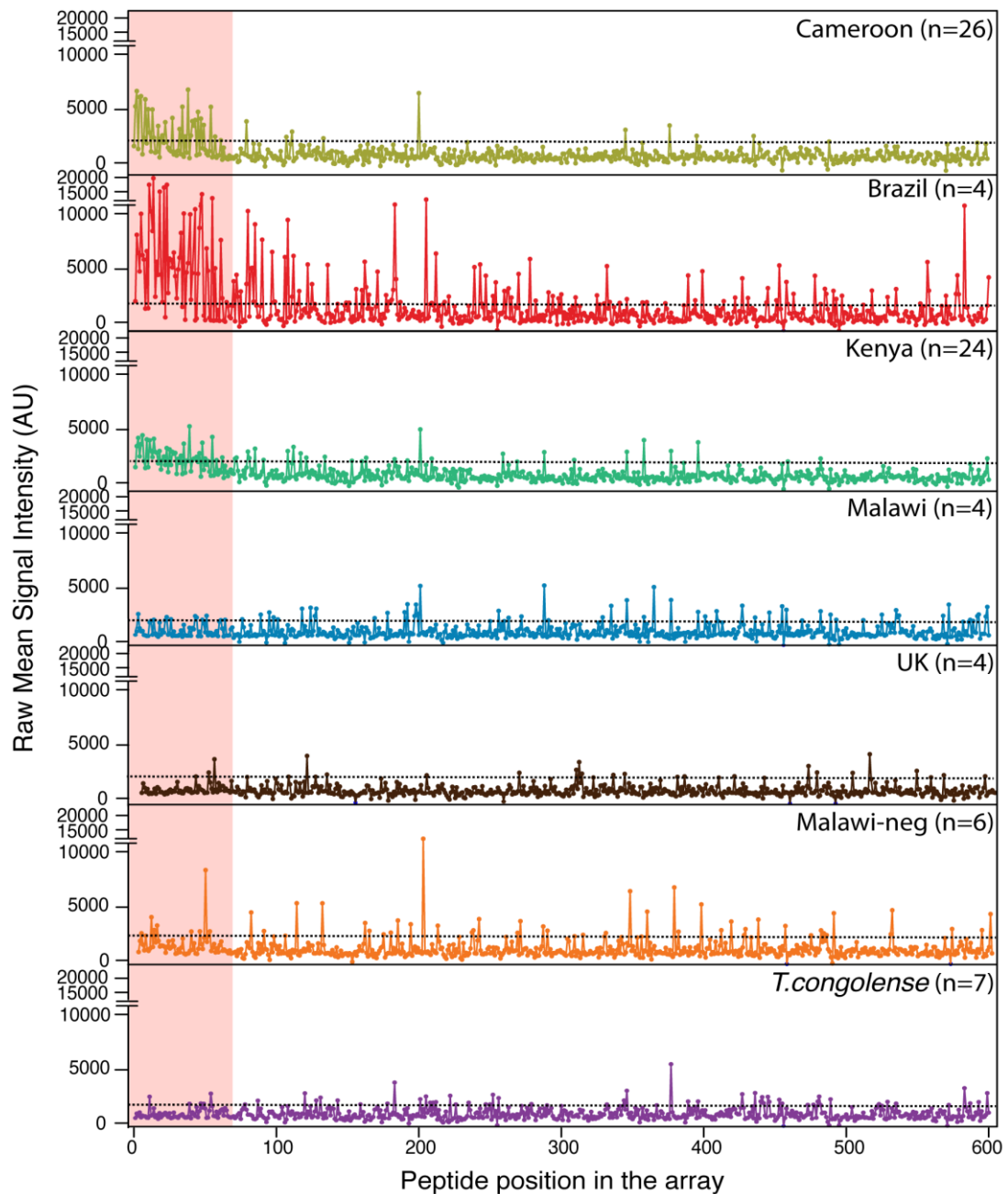


Figure 3.10 (from previous page). Scatter plot displaying the raw signal intensity (AU) of (A) all median values (first and second approach) and (B) raw mean values (third approach) for each group of samples. The IgG responses against *T. vivax* peptides are according to their position in the array. The pink area corresponds to the first 60 peptides.

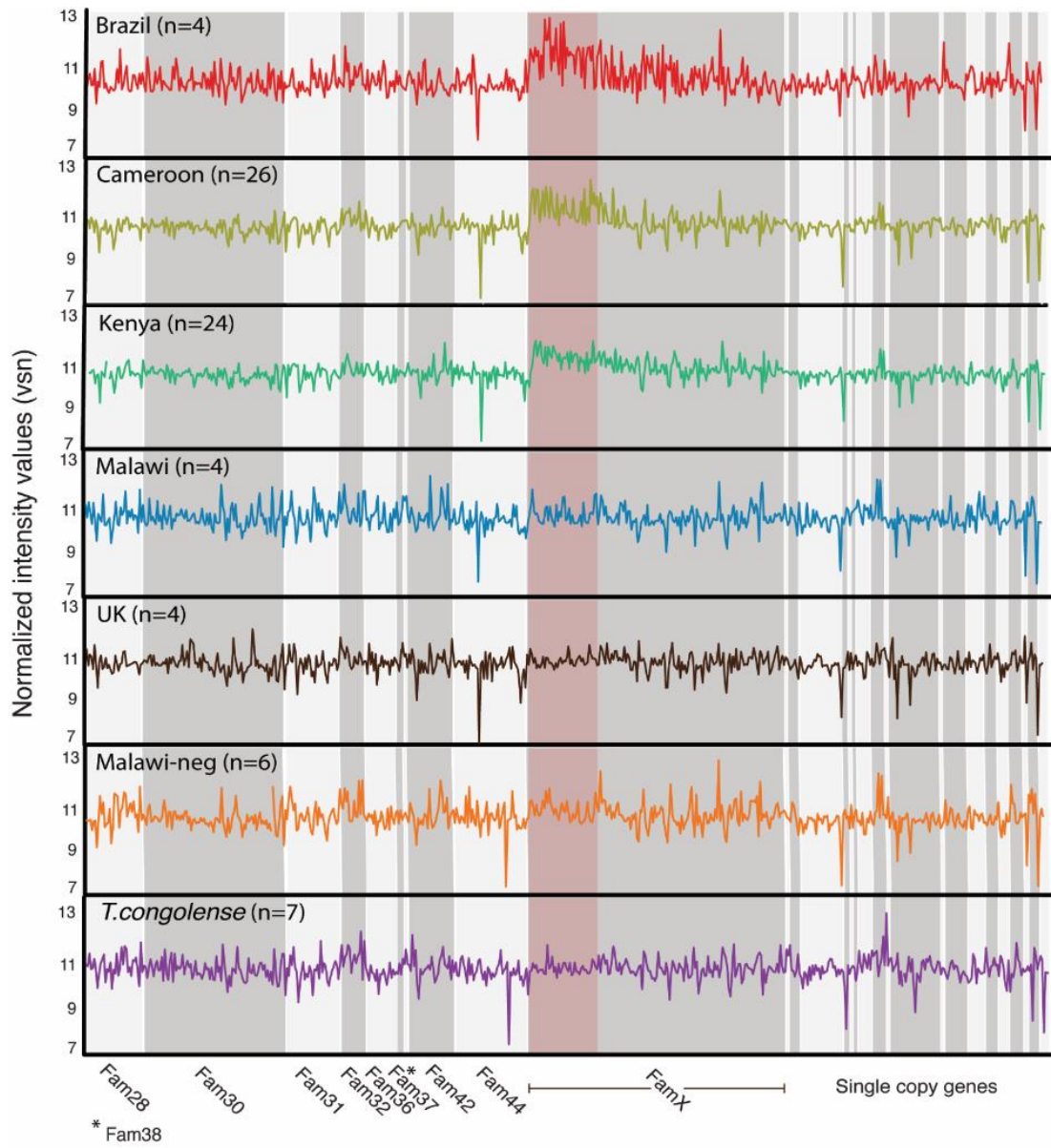
3.3.2.2. Between-array value normalization

In order to calculate the significance of antibody recognition of each peptide, it is necessary to correct raw values for variation in detection between arrays. Thus, inter-array normalization of raw intensity values was performed to achieve a constant signal to noise ratio and therefore make all the arrays comparable. No intra-array normalization was applied since the between-array normalization is the main procedure for a single-channel array analysis (Ritchie *et al*, 2015). In all approaches, normalization was carried out using the vsn package.

Raw versus normalized values for all array spots are shown in Figure 3.11, comparing the second and third normalization approaches described in Section 3.2.4. Normalized values from the first and second approaches were almost identical, since these methods differ only in data pre-processing. In the second approach, the normalized values were grouped according to locations and gene families. Normalized values ranging from 7 to 13 in intensity were the highest peaks, belonging to FamX in all positive samples. Other intensity peaks were observed in Fam32, Fam42 and some peptides from single-copy proteins.

The distribution of signal intensities normalized with limma showed a clear difference when compared with the raw data (Figure 3.11B). Before normalization, signal intensities from different array chips differed in scale and showed variation in peaks (Figure 3.10B). After normalization, such variations potentially due to manipulation and manufacture of the array chip was removed, harmonising the values between all samples and superimposing all curves. The normalized signal intensity values ranged from 4 to 13, and the highest values were again derived from FamX peptides. Indeed, regardless of the approach to data normalization, the first 60 peptides based on their position in the array (i.e. pink areas of Figure 3.11) unequivocally displayed the highest signal intensity values among *T. vivax*-positive sera, but not in negative controls.

A.



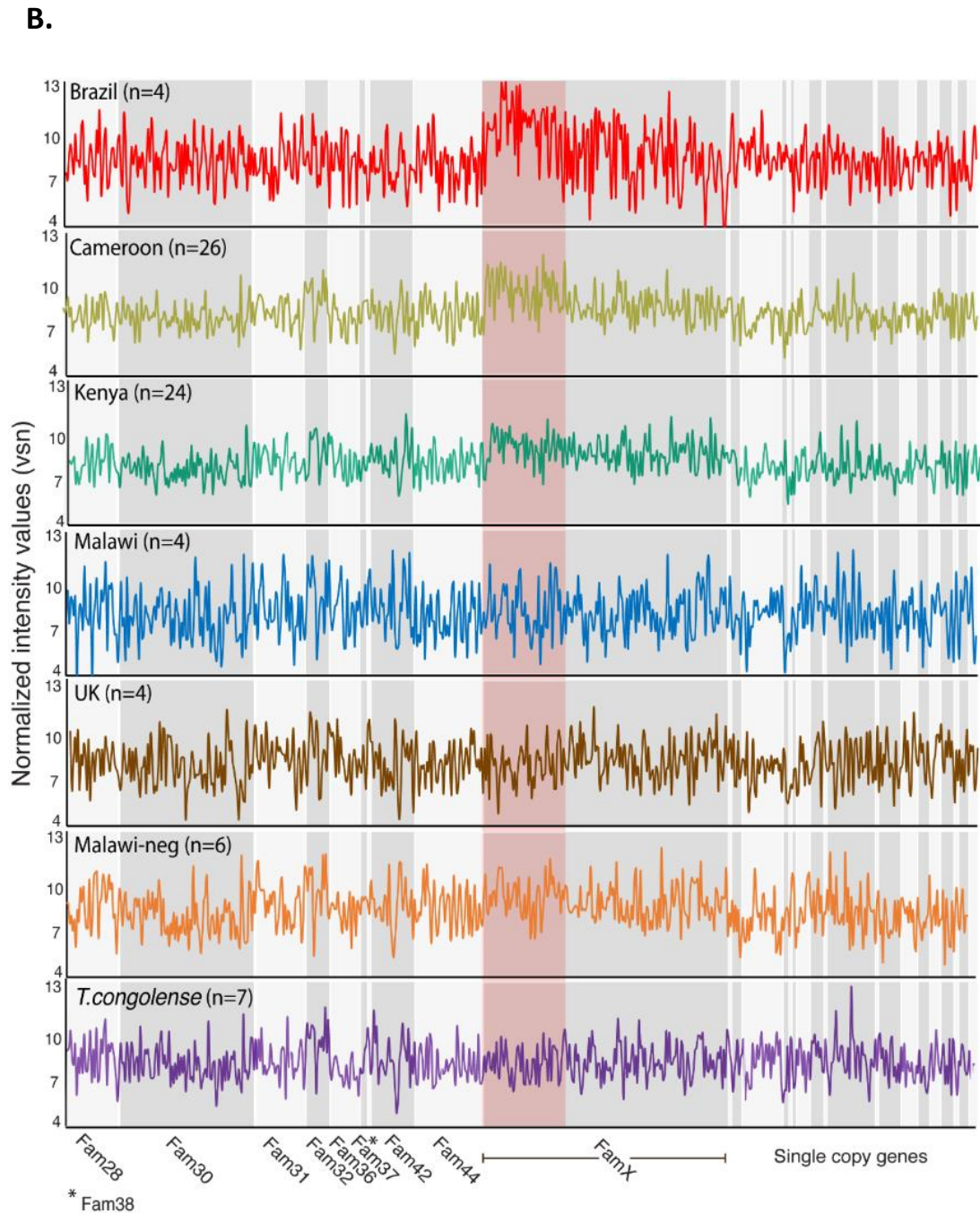


Figure 3.11 (from previous page). Scatter plot displaying normalized intensity values for all samples by location, based on the second (Acton) and third normalization approach (B.) as described in Table 3.3. The pink area corresponds to the first 60 peptides in the array.

3.3.2.3. Identification of significant immunogenic peptides

Analysis of signal intensities obtained from the *T. vivax*-positive serum samples identified 48, 31 and 36 peptide spots that had significant differences ($p < 0.05$) in fluorescence relative to negative controls, when using the first, second and third analysis method respectively. No negative controls from seronegative Malawian and British cattle showed a significant response relative to a *T. vivax*-positive samples. However, when p-values were adjusted for the false discovery rate, only the third approach using the limma package gave significant peptides. No significant peptide was identified with the first or second approach, under which all peptide spots displayed a \log_2 fold-change in intensity (i.e. *T. vivax*-positive to negative) less than two.

Of the 600 different peptide spots displayed in the microarray, 39 (6.5%) produced a significant response from *T. vivax*-positive serum relative to uninfected controls before statistical correction; five of these remained significant (1%) using the adjusted p-value and limma analysis. Of the 48 peptides found to be significant before adjustment using the first approach, 23 belong to FamX proteins, specifically TvY486_0020520 from clade 5, TvY486_0003690 from clade 7, TvY486_0039530 from clade 1, TvY486_0900440 from clade 3, TvY486_0037990 from clade 11 and TvY486_0019690 from clade 10. Besides these, 10 significant peptides belong to single-copy proteins, one each from Fam28, Fam36 and Fam44 respectively, six from Fam30, four from Fam3 and two from Fam42. All 31 significant peptides using the second approach corresponded to the same FamX proteins, with the omission of TvY486_0019690. Likewise, the significant peptides identified using limma corresponded to these same FamX proteins. The five epitopes identified by limma that remained significant after statistical adjustment all belong to FamX (Figure 3.12).

Table 3.7 shows the list of significant peptides identified by at least two different approaches. Overall, 24 epitopes were detected in at least two methods, of which 19 were identified by all three approaches (according to unadjusted p-values). Based on

these results, six proteins were identified that stimulated a robust antibody response in naturally infected livestock compared to uninfected controls. These are called AJ1-6 hereafter. These proteins are encoded by uncharacterised TvCSP genes: TvY486_0020520 (AJ1), TvY486_0003690 (AJ2), TvY486_0037990 (AJ3), TvY486_0031450 (AJ4), TvY486_0004900 (AJ5) and TvY486_0900440 (AJ6). The position of the epitopes within each protein is shown in Figure 3.13A; epitopes are located in the non-cytoplasmic domain near the TM domain in the C-terminal position. Only TvY486_0020520 displays two adjacent epitopes. The position of these epitopes was concordant with epitopes predicted in silico (Figure 3.13B).

Peptide sequence	AA range	<i>T. vivax</i> family	TvY486 ID	First approach		Second approach		Third approach	
				LogFC	P-value	LogFC	P-value	LogFC	P-value
KTGDGGDVVVSEESD	318-332	FamX	0020520	1.000	4.77E-02	1.083	2.15E-02	2.061	0.039
VSEESDSELIDLAVE	327-341	FamX	0020520	1.000	1.44E-02	1.112	3.78E-03	-	-
AVLKTGDGGDVVVSE	315-329	FamX	0020520	1.000	3.60E-02	1.085	7.56E-03	-	-
DVVVSEESDSELIDL	324-338	FamX	0020520	1.000	2.57E-02	1.078	1.62E-02	-	-
RSSADAPLEPTARDS	293-307	FamX	0020520	1.000	4.56E-02	1.051	1.37E-02	-	-
SEESDSELIDLAVEA	328-342	FamX	0020520	1.000	4.12E-03	1.118	2.31E-03	3.303	0.039
DSELIDLAVEASGQH	332-346	FamX	0020520	1.000	8.30E-03	1.070	8.89E-03	-	-
ITADDIDAEIEAVT	324-338	FamX	0003690	1.000	3.60E-02	1.113	4.94E-03	-	-
VVSEESDSELIDLAV	326-340	FamX	0020520	1.000	2.60E-02	1.100	5.50E-03	-	-
SDSELIDLAVEASGQ	331-345	FamX	0020520	1.000	2.78E-02	1.083	8.80E-03	-	-
VLKTGDGGDVVVSEE	316-330	FamX	0020520	1.000	1.20E-02	1.096	6.55E-03	2.091	0.040
ADDIDAEIEAVTGP	326-340	FamX	0003690	1.000	3.55E-02	1.092	6.75E-03	-	-
DGSDELIELALEES	353-367	FamX	0039530	1.000	3.28E-02	1.061	4.71E-02	-	-
DDIDAEIEAVTGPA	327-341	FamX	0003690	1.000	4.77E-02	1.072	2.28E-02	-	-
EESDSELIDLAVEAS	329-343	FamX	0020520	1.000	2.89E-03	1.120	1.67E-03	3.784	0.003
VTVESEDLIDLATQV	315-329	FamX	0900440	1.000	4.47E-02	1.058	2.34E-02	-	-
TADDIDAEIEAVTG	325-339	FamX	0003690	1.000	8.78E-03	1.120	1.39E-03	-	-
SSADAPLEPTARDST	294-308	FamX	0020520	1.000	2.35E-02	1.067	5.71E-03	-	-
DLMDLVDVAVGPLSDS	326-340	FamX	0037990	1.000	3.60E-02	1.047	3.71E-02	-	-
ADAPLEPTARDSTTA	296-310	FamX	0020520	1.000	4.90E-02	1.040	3.35E-02	-	-
TVSEDLIDLATQVS	316-330	FamX	0900440	-	-	1.046	3.68E-02	-	-
IDAEIEAVTGPASS	329-343	FamX	0003690	-	-	1.048	4.84E-02	2.524	0.039
KYDALSTKIGEITIS	168-182	Fam30	0031450	1.000	0.048	1.085	4.90E-02	-	-
RLESEVLNTEKKVGD	428-442	Fam36	0004900	1.000	4.47E-02	1.034	0.044	-	-

Table 3.6. List of significant peptides identified from the peptide microarray analysis using at least two approaches. Significant peptides obtained from the first and second approach are based on the unadjusted p-values while the third approach using limma shows significant peptides based on the adjusted p-values. Peptides are assigned to their corresponding amino acid sequence on the family and protein ID. FC; fold change values.

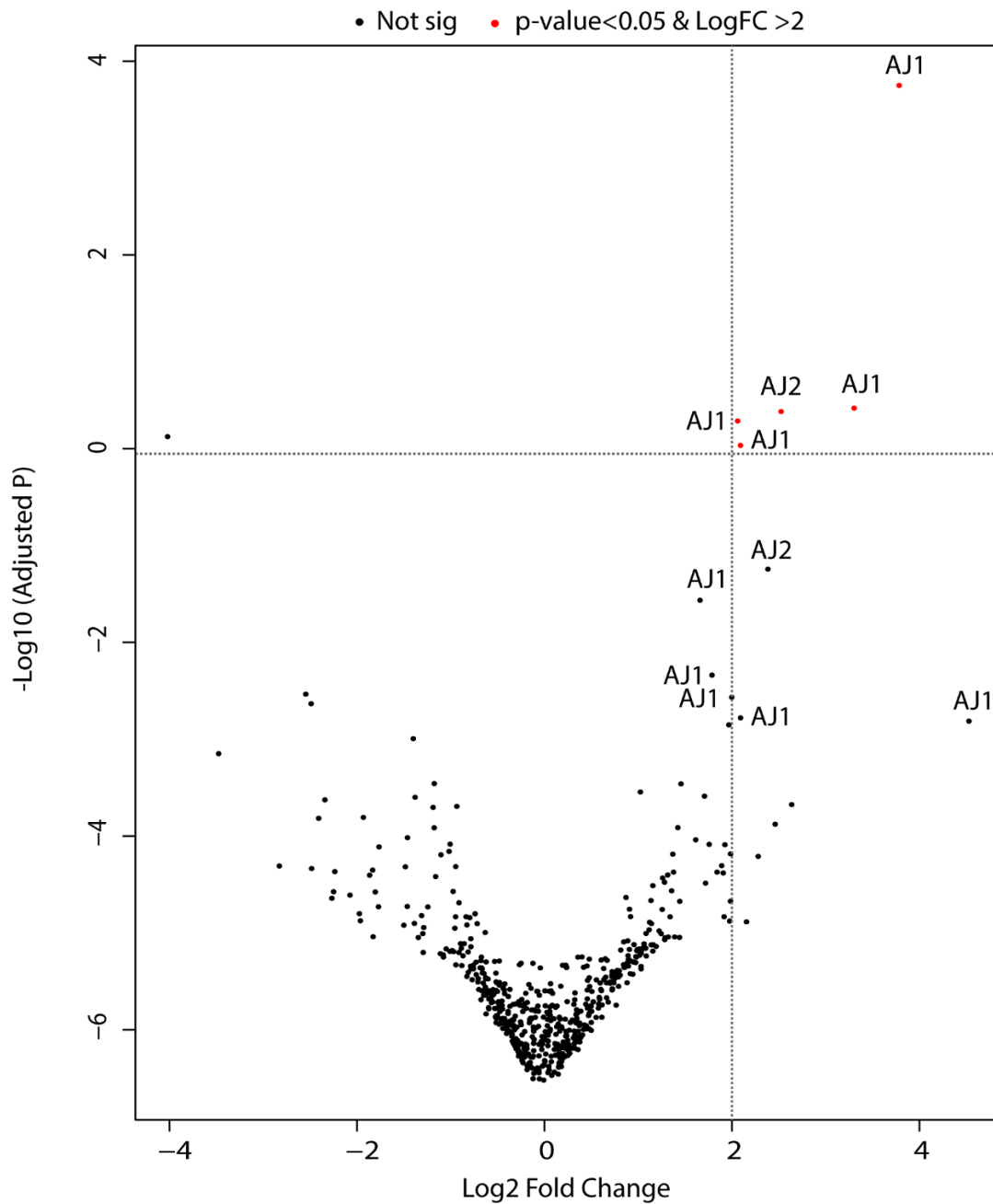


Figure 3.12. Volcano plot of limma results comparing positive samples versus controls. The data for all the peptides analysed are plotted as log₂ fold changes (X-axis) versus -log₁₀ of the adjusted p-value (Y-axis). The peptides with a significant adjusted p-value and log₂FC >2 are highlighted as red dots. The five significant peptides correspond to FamX proteins labelled as their antigen names (AJ1 and AJ2).

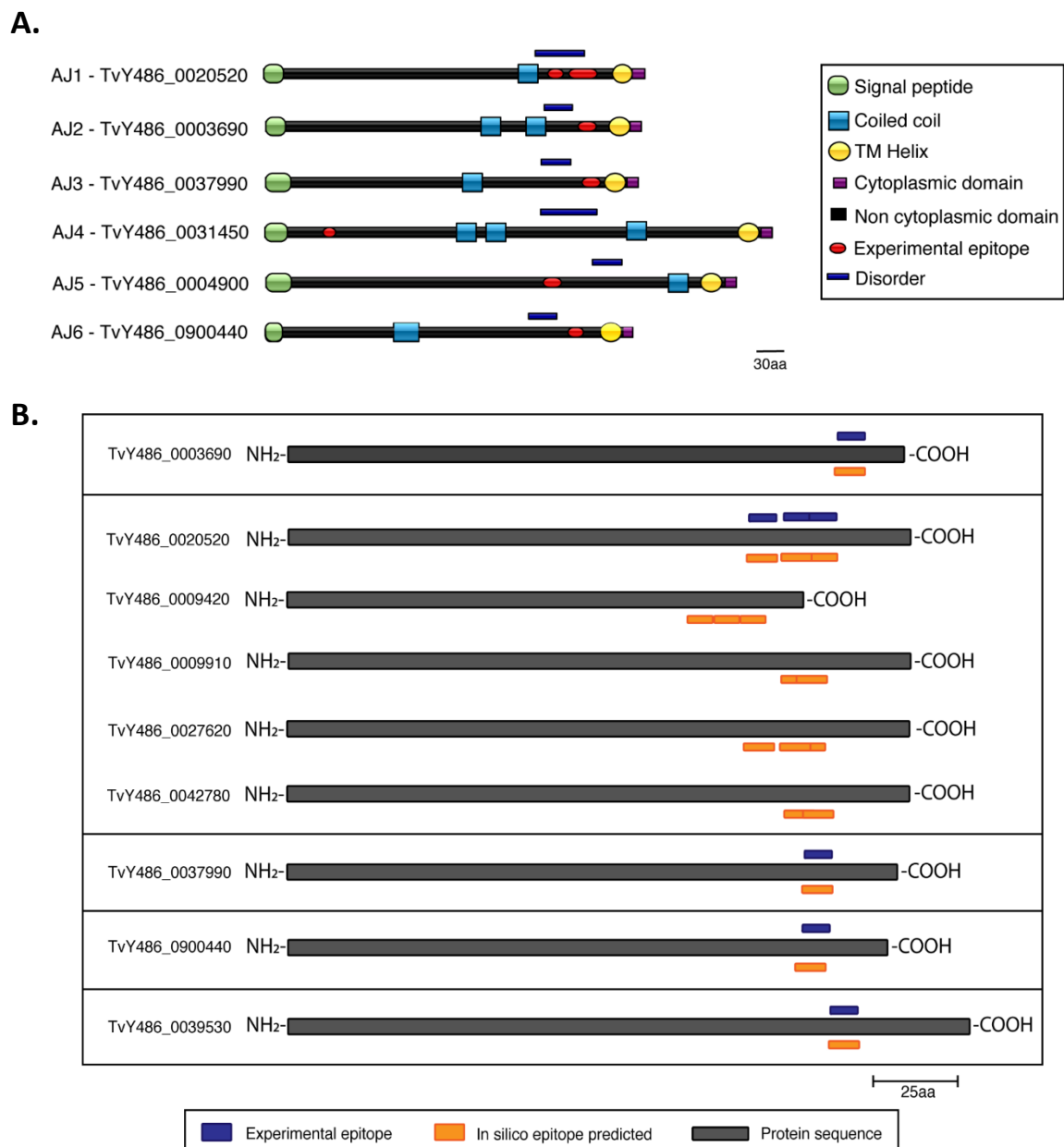


Figure 3.13. A) Location of the significant epitopes identified in the peptide microarray analysis on the protein linear structure. In silico structural description of the proteins with the different motifs expressing possibly cell-surface location is also represented. **B)** Comparison of best peptides from the peptide microarray versus the in silico predicted epitopes. Only in silico predicted epitopes located at the same position of the experimental peptides are represented.

3.3.3. Expression of recombinant proteins

The AVEXIS platform was used to express six *T. vivax* cell-specific surface proteins from FamX selected on the basis of the peptide microarray results. The entire ectodomain successfully expressed in HEK293-6E mammalian cells as soluble recombinant proteins by the Wright laboratory (WTSI). Each protein was expressed in two batches: 1) as no bio-tagged antigens purified using HisTrap chromatography columns on a ÄKTA protein purification system (GE Healthcare, USA) and 2) the second batch are normalized non-purified bio-tagged proteins allowing their interaction with streptavidin-coated ELISA plates.

Bio-tagged proteins were dialyzed after the transfection of HEK293-6E cells recovering a final volume of 50ml for AJ12, AJ3 and AJ6 respectively and 400ml for AJ1. All recombinant antigens were evaluated on their capacity to induce a protective immunity. A normalisation procedure part of AVEXIS assay was performed to identify the expression levels of each recombinant protein (Kerr and Wright, 2012). Protein concentrations were determined by indirect ELISA using streptavidin coated-plates. In the case of AJ1 protein, the results illustrate a clear difference in concentration between 1:2⁻⁸ and 1:2⁻¹² dilutions. The highest OD value obtained before the protein concentration decreases was 1.1093 for the 1:2⁻⁸ dilution therefore selecting it as optimal dilution to be used in the subsequent experiments. AJ2, AJ3 and AJ6 proteins were also normalized using eight dilutions. All these proteins showed similar expression levels having the same dilution in which they saturate the biotin binding sites. The dilution factor selected for AJ2, AJ3 and AJ6 was 1:50. Based on this results, the expression level of AJ1 was greater than any other recombinant protein expressed. Despite this difference, proteins were not concentrated to be used for further experiments.

The expression of all *T. vivax* recombinant non bio-tagged proteins were confirmed and quantified by western blot analysis and extinction coefficient calculation respectively. The blot performed under no denaturing conditions showed the

presence of a prominent band with apparent molecular weight of 50kDa for each recombinant protein (Figure 3.14). Based on the extinction coefficient calculation, the purified proteins were also abundantly expressed providing a concentration of 4.3 μ g/ml for AJ1, 5.1 μ g/ml for AJ2, 9.8 μ g/ml for AJ3 and 2.5 μ g/ml for AJ6. However, higher molecular weight bands were also observed in all antigens possibly to non-specific binding, as a result of post-translational modifications the proteins present or protein aggregation. These results confirm the abundant expression of all recombinant proteins in mammalian cells. Moreover, the western blot also indicates all proteins were successfully purified. Taken together, these findings confirmed that AJ1, AJ2, AJ3 and AJ6 were expressed as purified soluble recombinant proteins being able to be used for mice vaccination.

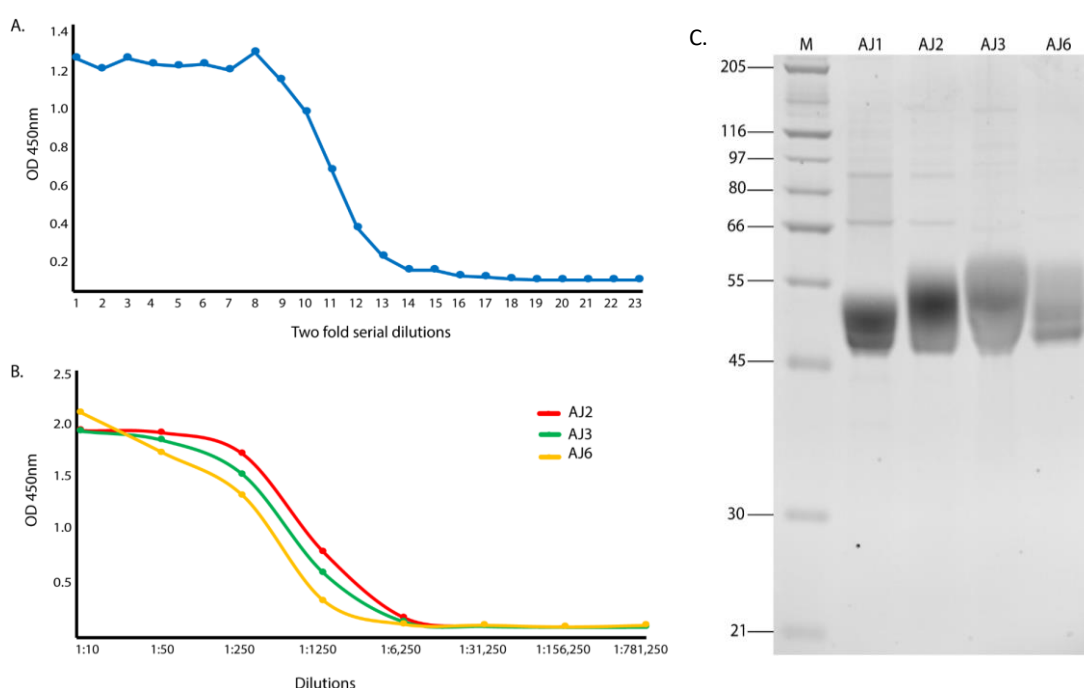


Figure 3.14. **A)** Normalization of AJ1 protein using two-fold serial dilutions. **B)** Normalization of AJ2, AJ3 and AJ6 proteins. **C)** Western blot analysis confirming protein expression. One microgram of each antigen were separated on a 12% acrylamide gel and transferred to a nitrocellulose membrane and detected using an anti-biotin secondary antibody HRP (right). M: molecular weight marker. Data prepared in the laboratory of Dr G. Wright (WTSI).

3.4. DISCUSSION

The purpose of this chapter was to evaluate the immunogenicity of a panel of TvCSP proteins, thought to be plausible components of the *T. vivax* cell-surface coat based on their *in silico* characterisation, in natural livestock infections, and so identify the most plausible antigens for vaccine development. Peptides belonging to FamX members displayed a greater response when assayed than any other TvCSP family. Indeed, of all TvCSP families, only FamX appears to reliably elicit robust antibody responses in livestock regardless of location. For this reason, FamX was analysed further, and various immunogenic epitopes were discovered.

Prior to microarray analysis, livestock sera were screened using the Very-Diag test to identify those genuinely seropositive for *T. vivax*. The test has a specificity of 95.5% and a sensitivity of 92.0% for *T. congolense* and 98.2% and 98% for *T. vivax* respectively (Boulangé *et al*, 2017). This performance is apparently superior to other diagnostic tests that can discriminate *T. vivax* infections from other African trypanosomes and related species. To date, there are several PCR tests using a variety of primers to detect *T. vivax* DNA (Masiga *et al*, 1992; Desquesnes, 1997; Desquesnes *et al*, 2001; Cox *et al*, 2005; Njiru *et al*, 2005; Hamilton *et al*, 2008; Fikru *et al*, 2014; Tran *et al*, 2014). However, in some cases these tests cannot detect very low levels of parasitemia. ELISA diagnostic techniques can detect antibodies against the parasite with a sensitivity and specificity of 97.6% and 96.9% respectively when evaluated in naturally and experimentally infected cattle (Madruga *et al*, 2006). However, despite several attempts for the identification of *T. vivax* in cattle sera with this method (Eisler *et al*, 1998), there is no specific antigen has been described yet. Furthermore, because of the low sensitivity and cross-reactivity some serological diagnostic tests may have, it is preferable to detect circulating antigens rather than antibodies since they are a real indicative of actual infection. The Very-Diag test is the first such antibody-based test for *T. vivax*.

The Very-Diag test identified 118 seropositive samples for *T. vivax* and mixed infections with *T. congolense* in Kenyan, Malawian and Cameroonian sera. In addition, the test also gave three false positives in Brazilian calf sera; they were positive for mixed infection even though the animals were experimentally infected with *T. vivax* only. This error may be due to sequence similarity between the TvGM6 antigen upon which the test is based and its homolog in *T. congolense*; the antigens contain expressed repeat units that are 49% identical at the amino acid level (Boulangé *et al*, 2017).

Since there are several published techniques with distinct procedures for microarray analysis (Robinson *et al*, 2002; Gaseitsiwe *et al*, 2008; Cui *et al*, 2016; Scholma *et al*, 2016; Weber *et al*, 2017) and no widely agreed standard, three different approaches were used to analyse the fluorescent responses of the peptide microarray to host serum. The first approach (Loeffler *et al*, 2016) provides a complete protocol that has been used successfully to identify epitopes for vaccine development. The second approach (Sundaresh *et al*, 2006) was the first publication to apply microarray techniques to analyse protein microarray data. There are only slight variations in these two approaches. Between these two methods and the third (limma package), there are three main differences: 1) the raw mean signal intensity was used instead of raw median; 2) a normexp background correction was performed instead of the normal background subtraction; and 3) the design of a matrix that allows arrays to be compared based on positive or negative samples.

Twenty-four significant responses from peptide spots were identified by at least two approaches using the raw (unadjusted) p-value of 0.05 and a $\log_{10}FC$ of >2 as thresholds, representing 8% and 5.16% of all screened epitopes using the first and second approach respectively. Of these, 13 epitopes belonged to the FamX protein TvY486_0020520 (AJ1), which had the highest number of epitopes of any TvCSP. All FamX epitopes were located near the C-terminal domain, between residues 293-367 in the protein sequence. The limma method was the only approach that gave significant peptides with $\log_2FC >2$, representing 1% of all peptides in the array, the

p-value was adjusted for false discovery. It has been demonstrated in previous studies that genes or peptides displaying a high fold-change can have a non-significant p-value nonetheless and vice versa (Jung *et al*, 2011). Peptides displaying a statistical near- or non-significance may still be taken into consideration for further analysis if they respond strongly in assays of infected serum, since they might have biological relevance for vaccine development.

Epitopes predicted by the peptide microarray were generally in agreement with in silico predictions that genuine epitopes were located near to the C-terminal domain of FamX protein sequences. The proportion of hydrophobic amino acids in these epitopes were 20%-50%, the most common residues being Alanine (A), Glutamic acid (E), Serine (S) and Threonine (T) and especially Valine (V), suggesting that these must be important for IgG binding epitopes.

The complexity of the response pattern and the relatively high number of single peptide interactions in an array can lead to unspecific binding and cross-reactivity with the peptides analysed (Katz *et al*, 2011). Comparison of seropositive versus seronegative samples as a basis for understanding humoral immunity has been used for related organisms for vaccine development, diagnosis and identification of antigenic determinants (Freitas *et al*, 2011; de Oliveira Mendes *et al*, 2013; Balouz *et al*, 2015; Loeffler *et al*, 2016). For example, microarrays were applied to *T. cruzi* infections of humans and identified significant human B-cell epitopes in 1% of the proteins analysed (Carmona *et al*, 2015). In *Plasmodium falciparum*, the antibody response before and after a malaria season recognized 491 immunogenic proteins from the 2320 used in the microarray (Crompton *et al*, 2010). The results in this chapter showed significant immunogenic epitopes representing 4% (raw p-value) and 1% (adjusted p-value) of unique and specific *T. vivax* epitopes. In this context, the results showed similar rates of global significant and non-overlapping epitopes with the *T. cruzi* study despite major differences in data normalization and analysis.

The properties of FamX proteins that make them particularly immunogenic are unclear, but will perhaps include molecular composition, protein structure, abundance and high epitope density in the case of AJ1 (Liu and Chen, 2005). The molecular weight of the protein also contributes to their immunogenicity. Overall, it is well established that small proteins (<10kDa) are poorly immunogenic and that immunogenicity tends to increase as the protein increases its size (Crumpton, 1974). The successful expression of AJ1-3 and AJ6 proteins demonstrated that all of them have a molecular weight of ~50kDa giving them the characteristics to elicit an antibody response. The determinants of an optimal immune response not only depend on the immunogenicity and nature of the antigen but also on the genetic capacity of the host to respond (Cruse and Lewis, 2010). Moreover, other factors like cell environment and the production of molecules like cytokines are also necessary for a successful activation and response. It will be vital to consider the mechanisms that FamX can trigger during an efficient immune response in considering it as a vaccine candidate.

This chapter has also showed that four immunogenic *T. vivax* proteins can be expressed in recombinant form. AJ1-3 and 6 were expressed using AVEXIS, an expression system using mammalian cells, which enables the addition of posttranslational modifications (Kerr and Wright, 2012). The latter is critical when extracellular protein-protein interactions are implicated since membrane proteins usually contains glycosylation sites as part of their structure. Moreover, the AVEXIS method is sensitive enough to detect weak membrane receptor-protein interactions, decreasing the low false-positive rate (Bushell *et al*, 2008). This is of great importance since other expression methods available are suitable for intracellular protein interactions only (Sun *et al*, 2012). The expression of AJ1-3 and AJ6 as soluble proteins occurred with high yields and reproduced their complete ectodomains. This indicates that they can be appropriately folded and, therefore, any conformational epitopes will be exposed and accessible for antibody binding (Hunter *et al*, 2019). Interestingly, AJ4 and AJ5, the only two non-FamX protein members, could not be expressed despite being predicted to be secreted proteins. Possible explanations for this

unsuccessful result could be that the proteins were expressed at very low yields that cannot be detected on a gel or that hydrophobic regions in both proteins created protein insolubility (Khan, 2013). Having expressed the extracellular regions of AJ1, AJ2, AJ3 and AJ6 entirely, their role in host pathogen interactions can now be further analysed.

3.5. CONCLUSION

Effective vaccine antigens should be recognized by specific host antibodies, elicit a robust response and confer protective immunity. The experimental identification of linear B-cell epitopes based on screening of serum from infected livestock for antibodies against TvCSP peptides has demonstrated the immunogenicity of at least six TvCSP proteins from where four were FamX members. This indicates that FamX antigens are able to stimulate a robust antibody response in naturally infected cattle. Subsequently, four FamX proteins have been successfully expressed as bio-tagged and purified recombinant proteins, facilitating an examination of their ability to protect against *T. vivax* infection, which will be analysed in the Chapter 4.

CHAPTER 4

Evaluation of the immunogenicity and protective properties of FamX recombinant antigens in a murine model

4.1. INTRODUCTION

The epitope described in Chapter 3 revealed that multiple FamX proteins contain significant linear B-cell epitopes that were immunogenic in natural infections, and which can be expressed as recombinant proteins using a mammalian expression system. The purpose of this chapter is to determine the immune response these recombinant proteins can elicit in mice and if they can confer vaccine-induced immunity to *T. vivax* infection.

The correlates of protection induced by vaccination are defined as the immune function that confers protection to a particular pathogen (Plotkin, 2010). This is important for vaccine design as it is crucial to understand the immunity induced by vaccination (Plotkin, 2001). It has been well established that antigen-specific antibodies play a key role in modulating the infection and that B-cell memory is important for prolonged protection. Nonetheless, parasitic infections are often more complex and, besides pathogen factors, host factors also are important (Plotkin, 2013). Moreover, it is well known that, while antibodies reduce the amount of circulating parasites during infections by African trypanosomes, other mechanisms such as T-cell function also play a critical role (Stijlemans *et al*, 2017).

The characterization of the immune response to a parasite infection is important to understand the biology and pathogenesis in the host. African trypanosomes are obligate extracellular parasites and once humoral responses begin they are constantly interacting with antibodies. As stated in the Chapter 1, during the innate immune response, macrophages and dendritic cells are the first line of defence against trypanosome infections (Namangala, 2012). At an early infection stage, caMφ

secrete pro-inflammatory cytokines like TNF- α , NO and IL-6 (Namangala *et al*, 2001; Baral, 2010) that contribute to the parasite control. Later, they activate the aaM ϕ that develop in a Th2 environment inhibiting the Th1 cytokines previously elicited (Namangala *et al*, 2001). This is an important hallmark of an infection with African trypanosomes and considered an important correlate of protection (Onyilagha and Uzonna, 2019). Indeed, the ability to change from a caM ϕ to an aaM ϕ enhances survival in trypanosome-infected mice (Namangala *et al*, 2000), perhaps because the pro-inflammatory cytokines produced by caM ϕ are later downregulated by anti-inflammatory cytokines produced by aaM ϕ avoiding tissue damage and survival (Onyilagha and Uzonna, 2019).

Both CD4⁺ and CD8⁺ cells help to provide protection against infection; CD4⁺ cells produce cytokines to regulate innate and adaptive immune cells contributing to resistance, whereas CD8⁺ cells have been shown to mediate protection in *T. congolense* infection in mice (Wei and Tabel, 2008). In addition, CD4⁺ cells also participate in class-switching and production of specific IgG antibodies against different antigens (Onyilagha and Uzonna, 2019). In fact, based on experimental mice infection in *T. brucei* and *T. congolense*, it has been suggested that a successful vaccine against African trypanosomes must generate Th1 cells to facilitate class-switching from IgM to IgG2a (Tabel *et al*, 2008).

Trypanosomes are able to change their morphology and structure to evade the humoral immune mechanisms, removing rapidly their VSG coat to avoiding antibody-mediated destruction. After antigen presentation, parasite-specific B lymphocytes are activated and proliferate during the first days of infection (Stijlemans *et al*, 2017). Specific antibodies bind to the parasite VSG forming immune complexes, lyse the parasite and therefore decrease parasitemia. However, antigenic variation of VSG leads to immune-evasion and prevents control of the infection (Vincendeau and Bouteille, 2006). Experimental infections with *T. brucei* in mice have demonstrated that IgG antibodies can contribute to protection by reducing circulating parasites levels (Stijlemans *et al*, 2007). In addition, experimental infections in livestock with *T. brucei* showed a correlation between trypanotolerance and the production of specific

anti-IgGs (D'leteren *et al*, 1998). Such observations suggest that B-cells and the differentiation of specific antibodies have a positive role to play in parasite control.

Mouse models have been one of the most useful tools in order to understand the pathogenesis and immunology of African trypanosomes despite biological differences with natural hosts (Antoine-Moussiaux *et al*, 2008). The characterization of African trypanosome infections, specifically for *T. brucei* and to a lesser extent for *T. congolense*, has been studied using animal models. The immune response during experimental infections in mice can be seen to depend not only on the trypanosome species but also on the parasite strain (O'Gorman *et al*, 2017) and, despite the significant progress that has been made using *T. brucei*, *in vivo* studies of *T. vivax* infection are rare. In the case of vaccine development, there have been previous attempts to induce vaccine-mediated protection using membrane antigens, again typically from *T. brucei*. Vaccination in naturally infected cattle with *T. brucei rhodesiense* using a Fp antigen produced a significant partial protection against heterologous trypanosome infection (Mkunza *et al*, 1995).

Previous chapters have identified putative cell-surface antigens specific to *T. vivax*. Given their potential surface expression, structural invariance, immunogenicity and potential no accessibility to antibodies, they may be useful vaccine candidates, and therefore, it is important to evaluate the immune response to them. Moreover, the type of immune response against each recombinant protein can be altered in the presence of different Th1 or Th2 adjuvants, and their co-administration plays a key role in the T-cell response. This chapter evaluates the immune response to each recombinant protein in the presence of three adjuvants: I) alum which induces a high antibody and Th2 immune response (Grun and Maurer, 1989), II) Montanide inducing a mixed Th1/Th2 immune response (van Doorn *et al*, 2016) and III) Quil-A which induced also a mixed Th1/Th2 response in addition to CD8⁺ T cell response (Sjölander *et al*, 2001). Quil-A is an immunostimulatory adjuvant that induces a strong and long-lasting humoral and cellular immune responses. As it is a saponin, it induces a response to T dependent and independent antigens (Singh and T O'Hagan, 2003) with a stimulation of a mixed Th1 and Th2 response (Sun *et al*, 2009). In addition to

vaccination, correlates of vaccine-induced immunity are determined for all AJ antigens.

Although, the immunobiology, host-parasite interactions and pathogenicity for African trypanosomes are based largely on *T. brucei* and *T. congolense* studies, due to well established murine models and field experiments in cattle (Morrison *et al*, 2016), this chapter exploits an experimental murine model of *T. vivax* infection established in the Wright laboratory (Sanger Institute) to characterize the immune response and protective properties of recombinant AJ proteins. These are evaluated *in vivo* using bioluminescence imaging, in which D-luciferin is injected intravenously or intraperitoneally into the animal, which then interacts with a reporter construct luciferase enzyme to produce light (Koo *et al*, 2006). This enzyme produces light emission from the animal and produces imaging contrast when the animal is placed in a dark chamber. A bioluminescent model has been successfully developed in other African trypanosomes like *T. brucei* to understand tropism (Claes *et al*, 2009), and has been established at the Sanger Institute *T. vivax* bloodstream-forms expressing *Renilla luciferase* using the transfections and cell culture methodology described in Section 3.2. The bioluminescent assays have several advantages compared to other approaches for challenge experiments: I) it has a higher signal-to-noise ratio (SNR) compared to other imaging methods (Tung *et al*, 2016), II) it has high sensitivity and specificity, III) it can track the number of parasites over a period of time (Sato *et al*, 2004) and IV) it can determine tissue tropism by pathogens within the host.

This chapter aims to:

1. Immunize BALB/c mice with each of four *T. vivax* recombinant FamX proteins (AJ1-3, 6) separately, in combination with three different adjuvants.
2. Assess the antigen-specific humoral immune response to each recombinant antigen.
3. Challenge immunized mice with *T. vivax* bloodstream-forms to evaluate the efficacy of vaccination with AJ antigens.

4. Characterise the cellular localization of the AJ proteins in bloodstream-form *T. vivax* using immuno-fluorescent microscopy.

4.2. MATERIALS AND METHODS

4.2.1. Immunization

4.2.1.1. Animals

Immunization and challenge experiments were performed at the Cell Surface Signalling laboratory of the WSI (Cambridge, UK). All animal experiments were performed in accordance with welfare regulations and with the approval of the WSI ethical committee. Forty-eight male and forty female BALB/c mice 6-8 weeks' old were maintained in a pathogen-free animal facility. Mice were housed in cages and provided with water and food *ad libitum*. The animals were acclimatized for one week and then males and females were distributed randomly in 16 and 8 groups, respectively.

4.2.1.2. Vaccine preparation

Vaccines were prepared using AJ1, AJ2, AJ3 and AJ6 proteins independently in combination with one of the three adjuvants tested to contrast different types of immune responses. The adjuvants tested were: 1) the Th2-related immune response inorganic alum (Pletinckx *et al*), 2) the Th1+Th2-related response Montanide™ W/O/W ISA 201 VG (Sappec, France) and 3) the partially purified saponin Quil-A® (Invivogen, USA) which induces Th1 as well as Th2 responses.

The vaccine formulation was prepared by combining 20µg of purified antigen with either 100µg of alum or Montanide or 15µg Quil-A respectively (Table 4.1). In the case of control groups, animals were immunized with adjuvants only using the same concentration as the vaccinated groups.

4.2.1.3. Murine immunization

The immunization schedule is represented in Figure 4.1. Male mice were randomly distributed in 16 groups (n=3). Four groups were immunized with Alum in combination with each antigen (groups AJ1-A, AJ2-A, AJ3-A, and AJ6-A) and four with each antigen co-administrated with Montanide (groups AJ1-M, AJ2-M, AJ3-M, and AJ6-M). There was a control group (n=3) for each alum or Montanide-vaccinated group. In the case of female mice, they were randomly distributed in five groups (n=8). Four of these groups were immunized with each antigen in combination with Quil-A® (groups AJ1-Q, AJ2-Q, AJ3-Q, and AJ6-Q) and one control group immunized with adjuvant only. Overall, there were 12 experimental groups (n=56) and 9 control groups (n=32).

BALB/c mice from experimental and control groups were immunized subcutaneously with 200µl volume in two injection sites (100µl/injection) at day 0 and two booster injections at day 14 and 28 respectively (Figure 4.1). Alum and Montanide-vaccinated groups were euthanized at day 42 (n=63).

4.2.2. Challenge and data acquisition

4.2.2.1. Challenge

Two weeks after the third immunization (day 42), five mice from each Quil-A vaccinated and control group were challenged intraperitoneally with 10^3 bioluminescent bloodstream trypomastigotes *T. vivax* Y486 strain generated in the WSI (Figure 4.1B). The parasites were obtained at day 7 post infection (dpi) from previous serial passages in mice. Briefly, 10µl whole blood were collected from the tail vein and diluted 1:50 with PBS+ 5% D-glucose+10% heparin. The concentration of parasites was adjusted to 10^2 parasites/200µl per mouse. The mice were infected intraperitoneally and their survival monitored daily.

4.2.2.2. In vivo imaging

Mice were injected daily from 5-8 dpi with D-luciferin (Xenogen) diluted in sterile PBS for in vivo imaging and data acquisition. Mice were injected intraperitoneally with

200 μ l luciferin solution before being anesthetized using an oxygen-filled induction chamber with 2% isoflurane. The bioluminescence was measured after 10min prior luciferin injection using the in vivo imaging system IVIS (Caliper Corp, Alameda, CA, USA). Mice were whole-body imaged in dorsal position and the signal intensity was obtained from luciferase expressed in *T. vivax*. The photon emission was captured with the Living Image software version 4.5.2 (Caliper) and the data were expressed as total photon flux (photons/second). The software generated one grey-scale reference image that was overlaid by a pseudocolor scale image indicating the intensity of the signal. For all the images generated, scales were manually set at the same values allowing comparison between them.

Group	Antigen	Adjuvant	Experimental group	Quantity		No. mice
				Antigen (μ g)	Adjuvant (μ g)	
Vaccinated	AJ1	Alum	AJ1,2,3,6-A	20	100	3
	AJ2	Montanide	AJ1,2,3,6-M	20	100	3
	AJ3	Quil-A	AJ1,2,3,6-Q	20	15	8
	AJ6	Quil-A	AJ1,2,3,6-Q	20	15	8
Control	PBS	Alum	-	-	100	3
	PBS	Montanide	-	-	100	3
	PBS	Quil-A	-	-	15	8

Table 4.1. Vaccine preparation according to the different experimental groups of mice. The vaccine formulation was prepared for each immunization dose per experimental group. Animals were immunized subcutaneously in two injection sites (100 μ l/injection) at day 0, 14 and 28 of the experiment.

4.2.2.3. Sample collection

Blood samples were taken from the tail vein of each animal and collected at day 0 (pre-immune sera), day 42 (post immune sera for alum and montanide-vaccinated mice) and day 50 (post immune sera from Quil-A-vaccinated and challenged mice). Sera were isolated from blood by centrifuging the samples for 10min x 1,500g and the supernatant was stored at -20 °C until used. Spleens were aseptically removed from the alum and Montanide-immunized animals at day 42 and from challenged mice at 8 dpi (Figure 4.1). Spleen tissue was used for *in vitro* antigen stimulation in order to quantify cytokine expression.

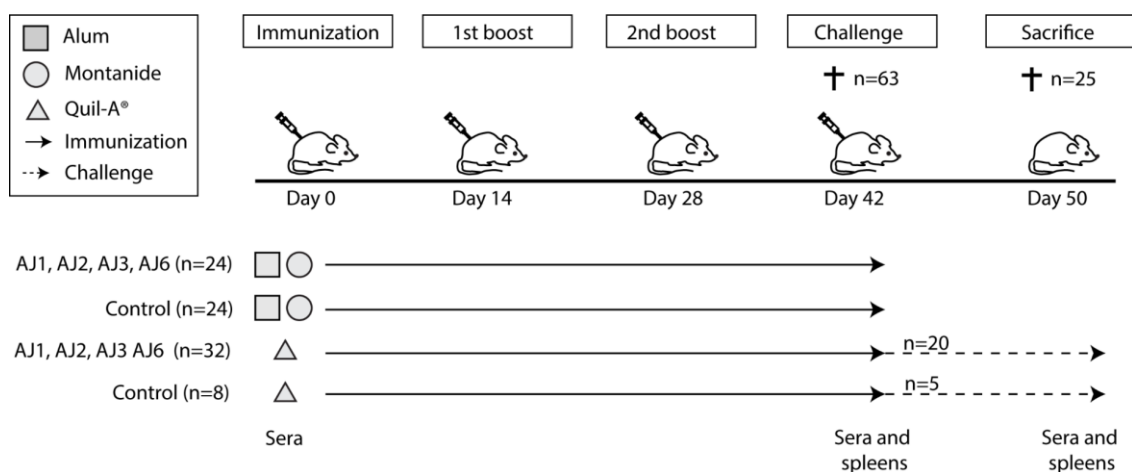


Figure 4.1. Scheme of mouse immunization protocol. BALB/c mice were immunized every two weeks with each recombinant protein in conjunction with alum, Montanide or Quil-A adjuvants while the control groups with adjuvants only. Animals were euthanized at day 42 (n=63), except 5 mice from each vaccinated and control Quil-A-based groups (n=25) which were challenged for 8 days.

4.2.3. In vitro antigen stimulation and cytokine measurement

4.2.3.1. Culture of splenocytes

Splenocytes were isolated by collecting spleens individually in tubes containing 3ml sterile PBS. The lymphocytes were separated by pouring the PBS and spleen into a 70µm cell strainer attached to a 50ml tube and pressed using a syringe plunger end. The samples were centrifuged at 800g for 3min at RT. Erythrocytes were lysed by adding 2ml ACK lysis buffer (0.15M NH₄Cl, 10mM KHCO₃, 0.1mM EDTA, pH 7.5) to the pellet and incubated for 5min. Lysis buffer was neutralized by adding 30ml of complete media (RPMI 1640 (Sigma Aldrich, Germany) supplemented with 10% heat inactivated foetal calf serum (FCS; Sigma Aldrich, Germany), 100 U/ml penicillin and 100U/ml streptomycin) and centrifuged as before. Cell viability and density was determined using a haemocytometer, diluting 10µl of the suspension with 10µl trypan blue and adjusting the concentration to 5x10⁶ cells/ml per spleen in complete media.

The cells were cultured in 48-well flat-bottom tissue culture plates (Starlab, UK) by seeding 200µl/well of each cell suspension in triplicate. Splenocytes were stimulated with 10µg/ml of each antigen diluted in complete medium for 72h at 37°C with 70% humidity and 5% CO₂. Likewise, cells were also incubated with 10µg/ml Concanavalin A (Brewer *et al*) or complete medium only as positive and negative controls, respectively. Culture supernatants were harvested after 72h of incubation and centrifuged at 2000g for 5min at RT to remove remaining cells. The supernatant was collected and stored at -20 °C until used for cytokine quantification.

4.2.3.2. Cytokine measurement

Interferon gamma (IFN- γ), tumour necrosis factor (TNF- α), interleukin-10 (IL-10) and interleukin-4 (IL-4) levels produced by spleen cells were measured by sandwich ELISA kits (ThermoFisher Scientific kit numbers 88-7314, 88-7324, 88-7105 and 88-7044 for each cytokine respectively). The measurement from unstimulated splenocytes

(incubated with medium only) was subtracted from the antigen stimulated cultures with each adjuvant treatment. The cytokine concentration was expressed as pg/ml.

4.2.4. IgG-specific antibody response in mice

To identify the presence of specific antibodies in mice sera against the recombinant proteins, a titration of IgG1 and IgG2a isotypes was performed by ELISA. This procedure was similar to the normalization step with slight modifications (Section 3.2.2.5.). 96-well streptavidin-coated plates were incubated with antigen for 1h at RT with 100µl/well of 1:250 AJ1 and 1:50 AJ2, AJ3 and AJ6 proteins respectively diluted in reagent diluent (PBS pH 7.4, 0.5% BSA). The plates were washed three times with PBS-Tween20 0.05% by immersing the plate in the buffer to fill the wells. Two-fold serial dilutions of each serum in reagent diluent were performed starting at 1:800 and 100µl/well was added to each well. The plates were incubated for 1h at RT and then washed as before. Rabbit anti-mouse IgG1 or IgG2a antibodies conjugated to HRP (Sigma-Aldrich, Germany) diluted to 1: 50,000 and 1: 25,000, respectively, were added at 100µl/well. The plates were incubated as before and after washing, 100µl/well of 3,3',5,5'-tetramethylbenzidine (TMB, Sigma-Aldrich, Germany) as substrate was incubated for 5 minutes at RT in the dark. The reaction was terminated by adding 50µl/well 0.5M HCl and the absorbance was read at 450nm using a Magellan Infinite F50 microplate reader (Tecan, Switzerland).

4.2.5. IgG-specific antibody response in cattle

The isotype profile was also analysed in samples from naturally and experimentally infected cattle (for samples, see Section 3.2.1). The ELISA was optimized using a pool of six calf samples previously evaluated in the peptide microarray assay as a positive control and a pool of UK cattle sera as negative control. For each sample displayed in Table 4.2, 100µl of two-fold serial dilutions starting from 1:25 and 1:1600 for experimental and natural infections respectively in reagent diluent were applied to the wells. The difference in dilutions was due to a normalization in protein concentration previously measured by Bradford method, intended to make sera and

paper filter elutions comparable. Bound IgG1 and IgG2 antibodies were detected by adding 100µl/well sheep anti-bovine IgG1 or IgG2 HRP (Bio-Rad, USA) at 1:5000 and 1:2500 respectively.

Sample	DPI	Infection	Geographic origin
Calf 1 – 21/03/13	44 dpi	Experimental	Sao Paulo, Brazil
Calf 1 – 11/04/13	65 dpi	Experimental	Sao Paulo, Brazil
Calf 2 – 15/03/13	56 dpi	Experimental	Sao Paulo, Brazil
Calf 2 - 02/04/13	38 dpi	Experimental	Sao Paulo, Brazil
Calf 3 – 15/03/13	38 dpi	Experimental	Sao Paulo, Brazil
Calf 3 – 24/03/13	47 dpi	Experimental	Sao Paulo, Brazil
K1, K2, K3, K4	-	Natural	Kenya
C1, C2, C3, C4	-	Natural	Cameroon
Pool NC	-	No infection	UK

Table 4.2. List of 15 samples used for the identification of IgG1 and IgG2 levels by ELISA against AJ's recombinant proteins. NC: negative control.

4.2.6. Cellular localization of AJ antigens in BSF parasites

The protocol for indirect immunofluorescence assay (IFA) was optimized to determine the cellular localization of the different antigens in bloodstream-form parasites. Different parasite fixation, blocking buffers, temperatures and conjugates were used as stated in Figure 4.2. *T. vivax* bloodstream-forms were isolated from 1ml whole blood from infected mice, by resuspending in 20ml PBS+20mM glucose (PBSG) and centrifuging at 1,500g for 10min at RT. The supernatant was collected into a new tube and centrifuged as before. The pellet containing the trypanosomes was resuspended in 50µl PBSG and centrifuged at 13,500g for 20min. The parasites were diluted in PBSG adjusting the concentration to 2.5×10^6 cells/ml and the suspension was transferred to poly-L-lysine slides for 10min to settle down. The cells were fixed

by adding 4% paraformaldehyde (PFA) in PBS directly to the suspension and incubated for 30min at RT. The slides were washed with sterile PBS, air-dried and stored at -20°C until used or blocked with blocking buffer (PBS+1%BSA) for 1h at RT. A pool of post-immune sera from mice vaccinated using Quil-A with each antigen was used as primary antibody diluted 1: 1,000 in blocking buffer and incubated overnight at 4°C. The slides were washed three times with sterile PBS 2-3min each wash and the conjugate Alexa Fluor goat anti-mouse 555 (Abcam, UK) diluted 1:500 in blocking buffer was incubated for 1h at RT. Non-bound antibodies were washed as before and mounted with one drop of Slow Fade gold antifade containing 4',6-diamidino-2-phenylindole (DAPI) (Invitrogen, USA). Images were acquired using a confocal microscope Leica TCS SP5 and fluorescence images were deconvolved with Leica Application Suite X software (Leica – Micoosystems).

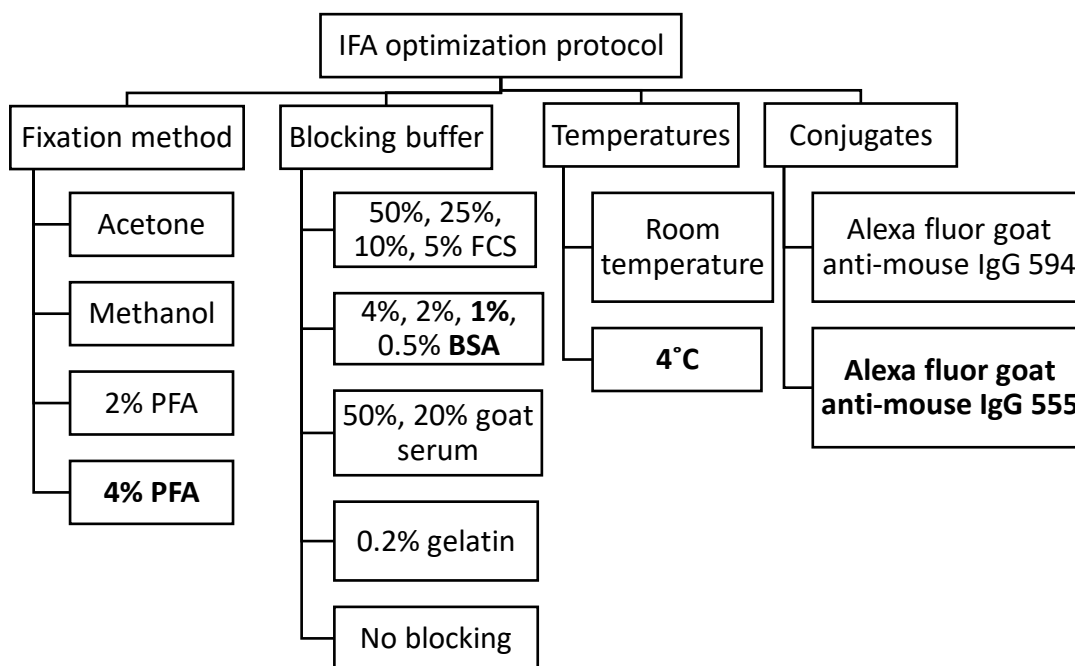


Figure 4.2. List of different fixation methods, blocking solutions, temperatures and conjugates tested for the optimization of the IFA protocol with *T. vivax* BSF. The features adopted in the optimized protocol are highlighted in bold.

To confirm the cellular localization of AJ6 antigen, a polyclonal antibody was raised in rabbits against recombinant AJ6 protein (BioServUK, Sheffield, UK). Briefly, two rabbits were vaccinated with AJ6 in combination with Freund's complete adjuvant for the first immunization and with Freund's incomplete adjuvant for two additional boosts. Animals were vaccinated every two weeks and polyclonal antibodies against AJ6 were purified from the sera obtained two weeks from the last immunization. Anti-AJ6 IgG antibodies were purified by affinity chromatography with a protein A column. The IFA protocol previously optimized was used to stain bloodstream-form cells using the purified IgG antibody and pooled pre- and post-immune sera as negative and positive controls, respectively.

4.2.7. Statistical analysis

All the mouse experiments were performed in triplicate using three or five mice per experimental group and the animals were analyzed individually. The comparison between humoral and cellular response using different adjuvants used to immunize mice was analyzed using one-way and two-way analysis of variation (ANOVA). Comparisons between pre and post challenge response was achieved with student's paired t-test. A p-value < 0.05 was considered statistically significant. Statistical analysis was performed using R 3.4.3 software.

4.3. RESULTS

4.3.1. Humoral immune response against recombinant proteins in cattle

In order to determine the precise humoral immune response against AJ proteins, IgG1 and IgG2 antigen-specific antibody titres were measured by ELISA in samples from naturally and experimentally infected cattle. Cameroonian and Kenyan seropositive samples were from naturally infected cattle while Brazilian samples were from an experimental infection with *T. vivax* (see Section 3.2.1). Brazilian samples were obtained from elutions of filter paper on which serum from the animals was collected. The results were expressed as individual curves, except where Cameroonian and Kenyan samples were expressed as mean values of the antibody titre in pooled serum.

Antigen-specific IgG1 antibodies were not detected in the negative control. Naturally infected cattle showed high specific IgG1 levels against each recombinant protein with OD values between 2.0 and 3.5 at the lowest dilution (IgG1, Figure 4.3). Kenyan and Cameroonian samples had levels of antigen-specific IgG1 significantly higher when compared to the British negative control ($p < 0.05$ in all cases). The antibody response against each recombinant protein varied by location, showing higher IgG1 levels against AJ2 and AJ3 in the Cameroonian population, versus AJ1 and AJ6 antigens in the Kenyan population. However, these differences in OD values were not significant ($p > 0.05$). For all the antigens analysed, natural infections showed a half-maximal titre (Log50%) of 2.0-2.5 corresponding to dilutions 1: 12,800 and 1: 25,600 respectively (4.1 and 4.4 Log₁₀ dilution). In addition, they showed an endpoint dilution of 1: 409,600 (5.6 Log₁₀ dilution) for AJ2 and 1: 3,276,800 (Log₁₀ dilution) for the other antigens.

Experimentally infected calves behaved differently to natural infections (Figure 4.4) exhibiting mean OD values of 0.645 ± 0.13 for AJ1, 2.14 ± 0.22 for AJ2, 2.02 ± 0.33 for AJ3 and 2.18 ± 0.22 for AJ6 (mean \pm SEM). Significant differences were found between mean values from experimental infections and the negative control in the case of AJ2,

AJ3 and AJ6 ($p < 0.05$), but not for AJ1 ($p = 0.18$). The titration curve for the last time point of each animal (A1-44 DPI, A2 56DPI and A3 47DPI) showed a significant increase of IgG1 levels compared with the first time point analysed against AJ2, AJ3 and AJ6 antigens ($p < 0.05$ in all cases). However, no differences were found between the two time points for each animal against AJ1 ($p = 0.06$, $p = 0.06$ and $p = 0.09$ for A1, A2 and A3 respectively). Curves from experimental infections showed a Log50% of 1.25 corresponding to a 1: 100 dilution (2 Log₁₀ dilution) for all antigens and an endpoint dilution of 1: 200 for AJ1, 1: 3,200 for AJ2 and AJ6 and 1: 600 for AJ3 (Table 2).

The measurement of IgG2-specific antibodies showed lower levels in both naturally and experimentally infected animals compared to the IgG1 response. Each recombinant protein showed a mean OD between 0.2 and 0.5 at the lowest dilution in naturally infected cattle (IgG2, Figure 4.3). Kenyan and Cameroonian samples showed a slight rise in IgG2 antibody levels compared with the negative control but this was not statistically different ($p > 0.05$), except when the Kenyan samples were applied to AJ6 ($p = 0.02$). Likewise, the comparison between antigens showed no significant differences ($p > 0.05$). Natural infections showed a Log50% titre of 1:3,200 for AJ1, AJ3 and AJ6 and 1: 51,200 for AJ2 with an end-point dilution of 1: 3,276,800 (Table 4.3). The titration curves for different time points of experimentally infected calf showed no difference with the amount of specific anti-IgG2 ($p > 0.05$). Indeed, all samples showed responses that are comparable with the negative control. IgG2 levels were higher in naturally infected animals compared with the experimentally infected calves but less than IgG1 levels.

These data show that both IgG1 and IgG2-specific antibodies were produced against AJ1 antigen. However, there was a higher level of IgG1-specific antibodies compared to IgG2 levels in all samples, regardless of the type of infection. These results indicate that recombinant AJ1, AJ2, AJ3 and AJ6 induce a predominantly Th2-type humoral immune response.

Antigen	IgG1- Naturally infected		IgG1-Experimentally infected	
	50% titre	End point	50% titre	Endpoint
AJ1	1:3,200	1: 3,276,800	1: 100	1: 200
AJ2	1: 51,200	1: 409,600	1: 100	1: 3,200
AJ3	1:3,200	1: 3,276,800	1: 100	1: 600
AJ6	1:3,200	1: 3,276,800	1: 100	1: 3,200

Table 4.3. 50% titre and endpoint titres of bovine IgG1 against each recombinant antigen in naturally and experimentally infected cattle.

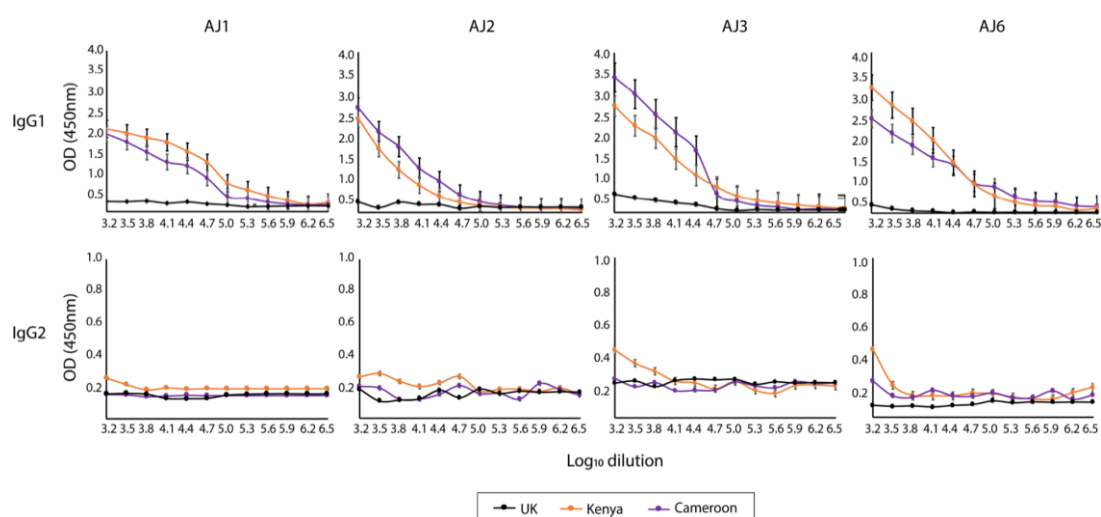


Figure 4.3. Indirect ELISA for the detection of specific antibodies against each recombinant protein in naturally infected cattle. The isotypes IgG1 and IgG2 were measured in order to determine the humoral immune response of AJ1, AJ2, AJ3 and AJ6 antigens. Each curve represents the mean \pm standard error (n=4).

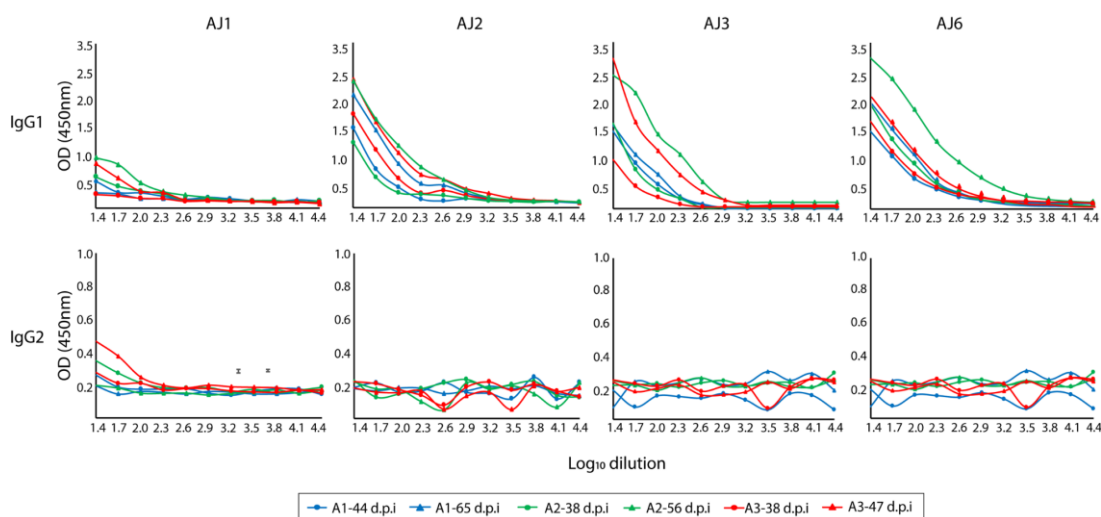


Figure 4.4. Indirect ELISA for the detection of specific antibodies against each recombinant protein in experimentally infected calves ($n = 3$; A1-3). The isotypes IgG1 and IgG2 were measured in order to determine the humoral immune response of AJ1, AJ2, AJ3 and AJ6 antigens. Each curve represents an individual sample.

4.3.2. Comparative humoral immune response against AJ antigens in mice

BALB/c mice were immunized with each individual AJ antigen in combination with alum, Montanide or Quil-A adjuvants to analyse the humoral and cellular immune response. Independently of the adjuvant or antigen, the post-immune sera showed that the proteins were able to stimulate antigen-specific antibodies leading to seroconversion. The recognition of AJ1, AJ2, AJ3 and AJ6 recombinant proteins by the immune sera indicated that antigens are immunogenic in BALB/c mice.

Comparative analysis of humoral immune responses showed similar scenarios for all antigens. Regardless of the adjuvant used, a robust IgG1-specific antibody response against each antigen was detected (Figure 4.5A-D) which was significantly greater than the respective pre-immune sera ($p < 0.001$). The comparison between adjuvants revealed that Montanide-immunized mice showed significant higher levels of IgG1 than alum and Quil-A against AJ1 ($p = 0.038$ and $p = 0.001$ respectively) and AJ2 (p

=0.038 and $p < 0.0001$ respectively). AJ1-A and AJ1-Q showed no difference in antibody levels but there was a difference between AJ2-A and AJ2-Q ($p = 0.014$). AJ3-A and AJ3-M showed higher IgG1 levels than AJ3-Q ($p = 0.01$ and $p = 0.001$ respectively), while no differences between adjuvants were observed against AJ6 ($p > 0.05$). Overall, montanide-based immunization developed the highest IgG1 antibody titres against each antigen.

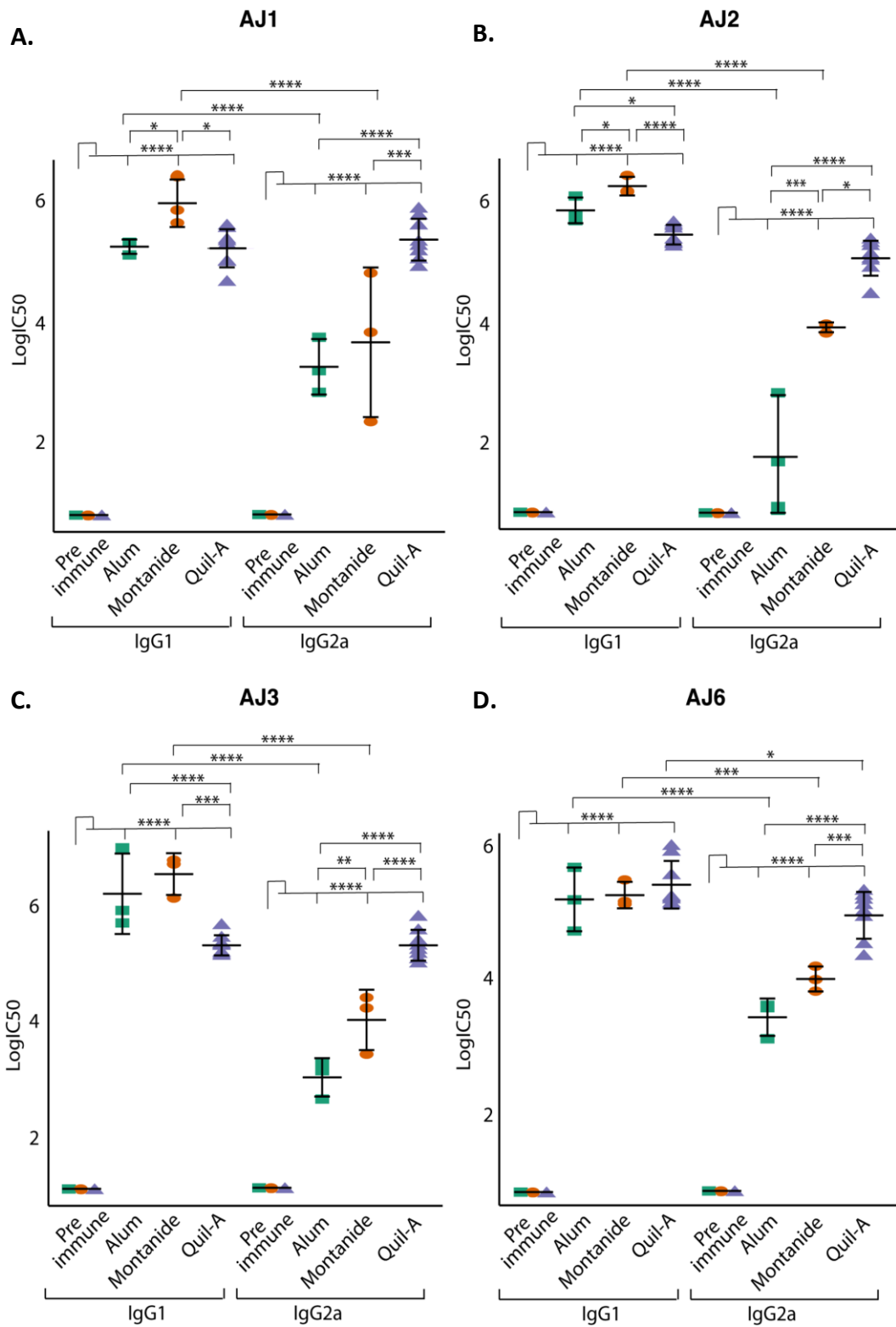
The antigens were also able to stimulate IgG2a-specific antibodies after the third protein boost (Figure 4.5A-D). As with IgG1, the antibody levels were significantly greater in post-immune sera relative to pre-immune sera regardless the adjuvant analysed ($p < 0.001$). Again, pre-immune sera were completely unresponsive to all antigens. For all antigens, the highest IgG2a titres were produced with Quil-A, followed by montanide and lastly alum. Antibody titres for were consistent across antigens, maintaining the disparities among adjuvants except for AJ2-A, the antibody titre of which was an order of magnitude lower than other applications with alum.

Mice vaccinated with alum and montanide elicited predominantly IgG1 rather than IgG2a antibodies against all the antigens, suggesting a Th2-type humoral response. In both cases, IgG1 levels were greater with two-fold better titres than IgG2a. Comparative analysis also indicated that vaccination with Quil-A did not elicit a predominant T-helper response because both IgG1 and IgG2a titres were similar for AJ1, AJ2 and AJ3. though not for AJ6, which showed higher levels of IgG1 ($p = 0.024$). These results indicate that Quil-A stimulates a mixed Th1/Th2 immune response for AJ1-3 antigens and a predominantly Th2 response against AJ6. Mice immunized with AJ6 produced IgG1-specific antibodies regardless of the different adjuvant formulations used.

The recognition of AJ1, AJ2, AJ3 and AJ6 recombinant proteins in sera from vaccinated mice was demonstrated by their interaction with antigen-specific antibodies. The seroconversion of both IgG1 and IgG2a isotype antibodies against all recombinant proteins increased upon booster immunization. The isotype profile of both antibodies in sera from vaccinated mice demonstrates that the immune

response can be biased towards a predominantly Th2 -type response in the case of alum and montanide, and a mixed Th1/Th2-type response in the case of Quil-A.

Figure 4.5 (overleaf). Titration of *T. vivax* antigens-specific IgG1 and IgG2a antibody response in BALB/c mice before and after immunization (n=3 for each group except n=8 for Quil-A pre and post vaccination). IgG1 and IgG2a specific antibody titres were measured by ELISA using two-fold serially diluted sera. Data is represented as the average of triplicates.



4.3.3. Antigen specific cellular immune response

In order to understand the type of cell-mediated immune response against AJ1, AJ2, AJ3 and AJ6 antigens, the cytokine profile of *in vitro* stimulated splenocytes was determined. In all experiments, positive and negative controls were provided by stimulation with 10 $\mu\text{g}/\text{mL}$ ConA or no stimulation (RPMI complete media only) respectively. Levels of IL-4 and IL-10 (corresponding to a Th2-type immune response) and TNF- α and IFN- γ (corresponding to a Th1 response) were measured by ELISA.

As shown in Figure 4.6, antigen-immunized mice displayed higher antigen-induced TNF- α and IFN- γ levels compared to IL-10 and IL-4. Animals immunized with AJ2, AJ3 and AJ6 proteins expressed IL-10 and IL-4 regardless of the adjuvant used (Figure 4.6A). However, immunization with AJ1 did not produce detectable values of either cytokine. All cytokine levels increased significantly after stimulation with AJ-A and AJ-M when compared to control groups stimulated with media only; the latter displayed non-detectable values ($p < 0.0001$). This indicates a specific cell-mediated immune response to each antigen. Splenocytes stimulated with 10 $\mu\text{g}/\text{mL}$ ConA mitogen (positive control) produced high levels of all cytokines, regardless of the adjuvant administered.

The results show TNF- α concentrations in the same range of 200-500pg/ml when cell stimulated with alum, Montanide or Quil-A and any recombinant protein are compared, although stimulations with montanide showed the greatest TNF- α levels, followed by alum and then Quil-A. The comparison showed no significant differences of TNF- α concentrations between antigens, independent of the adjuvant used ($p > 0.05$).

With regard to IFN- γ expression, this was at least 2.5 times greater in cells stimulated with Quil-A compared with alum and montanide in all cases (Figure 4.6B). There were significant increases when AJ1-Q and AJ1-A ($p=0.015$), AJ3-Q and AJ3-A ($p<0.0001$), AJ6-Q and AJ6-A ($p=0.016$) and AJ6-Q with AJ6-M ($p=0.002$) were compared. No significant differences were found between adjuvants in the levels of IFN- γ in

supernatants of cells stimulated with AJ2. Similar to TNF- α expression, AJ-A and AJ-M presented similar amounts of IFN- γ between 500-1000pg/ml. Stimulated splenocytes from mice immunized with each antigen showed IFN- γ concentrations similar to the positive control group stimulated with ConA.

The concentration of IL-10 in culture supernatants were highly variable, dependent on the adjuvant used (Figure 4.6C). IL-4 levels were significantly greater when antigens were co-administered with Quil-A in comparison with alum and montanide ($p < 0.001$ and $p < 0.0001$ for all cases). In fact, IL-10 expression by splenocytes from in the Quil-A vaccinated group showed the highest concentration of all cytokines analysed with an average of 5000pg/ml, while for the other adjuvants the concentrations were 2.5-5 times less. A similar scenario was observed for IL-4 expression. There was an increase in IL-4 concentration when cells were stimulated with AJ-Q compared with AJ-A, but this was non-significant. AJ3-Q stimulation produced a significant increase in IL-4 concentration compared with AJ1-Q, AJ2-Q and AJ6-Q ($p < 0.0001$ for all cases). However, besides this, IL-4 displayed the lowest expression levels of all measured cytokines and no appreciable differences were seen between adjuvants in combination with any particular antigen ($p > 0.05$).

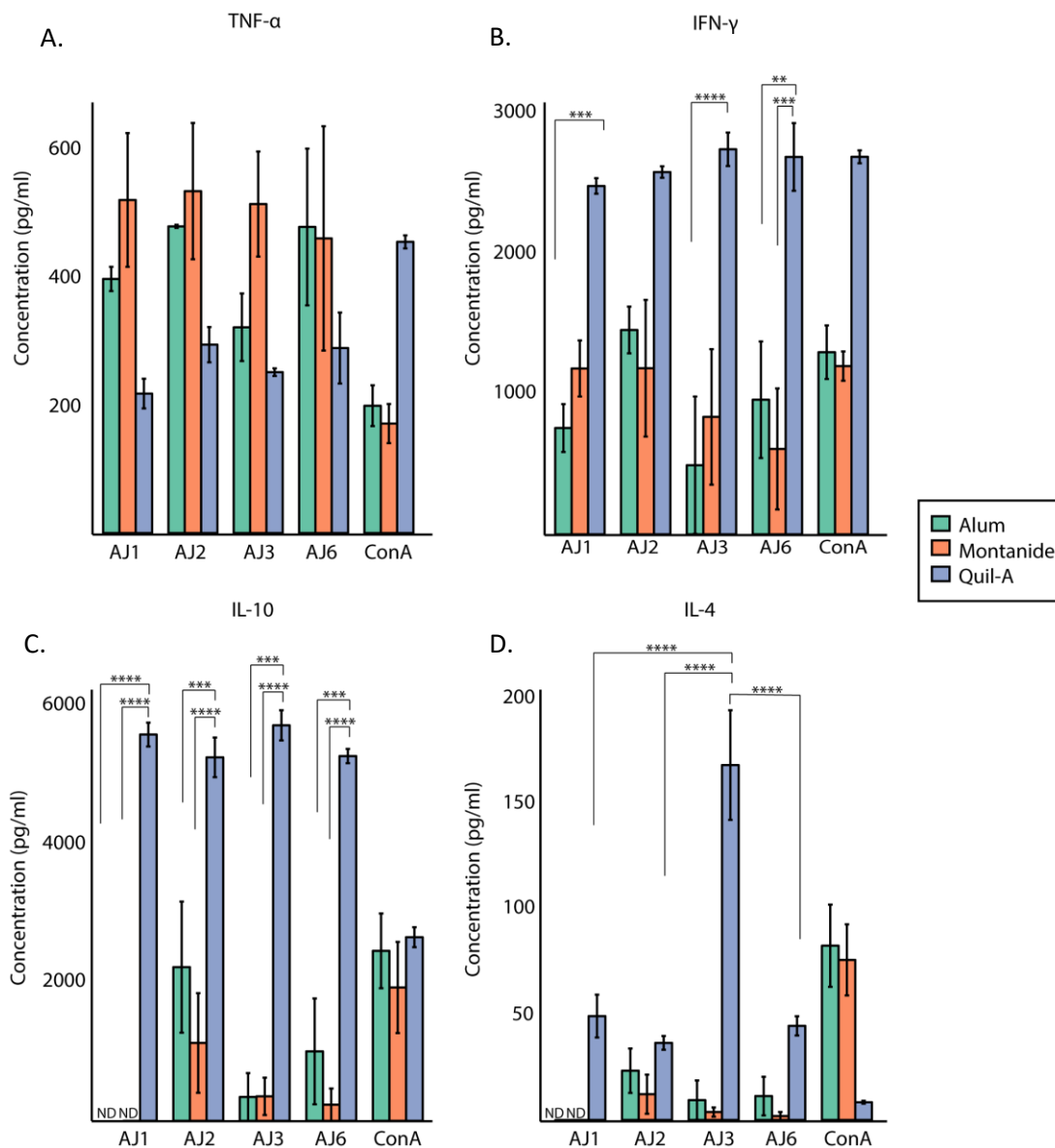


Figure 4.6. Cytokine responses in *in vitro* stimulated splenocytes from BALB/c mice vaccinated with the different panel of antigens. ND: non detectable. P-value < 0.05.

4.3.4. Protection of vaccinated mice from *T. vivax* infection

Quil-A-vaccinated mice were challenged intraperitoneally with 10^3 Y486 bioluminescent *T. vivax* bloodstream-forms to evaluate the efficacy of vaccination with AJ proteins. All mice survived to the end of the experiment (100% survival).

Parasitemia was measured daily from 5-8 dpi by bioluminescent assay (IVIS). Before the 5 dpi, the animals did not show any clinical signs and had very low levels of parasitemia. The cellular and humoral immune response induced by each antigen after challenge was also analysed as before.

Parasite bioluminescence detected in the whole body of the animals is displayed in Figure 4.7. All antigen-vaccinated and adjuvant-only mice (negative control group) had similar luciferase intensities of $1-5 \times 10^7$ p/s at 5 dpi (Figure 4.8A). One mouse from the AJ6-vaccinated group showed the lowest bioluminescence detected with almost no intensity. In comparison, bioluminescent intensities for AJ6 were significantly lower than for AJ2 and AJ3 ($p = 0.005$ and $p < 0.0001$ respectively) (Figure 4.8A). However, in all cases, bioluminescence, and therefore parasitemia, increased over the course of infection (Figure 4.8) and, by 6 dpi, the animals displayed an average luminescence of 2.8×10^8 p/s (Figure 4.8B). Comparison between antigens at this time of infection showed a significant difference in parasite luminescence between AJ1 and AJ3 ($p = 0.028$) and between AJ3 with AJ6 ($p = 0.011$). The AJ6-vaccinated group had the lowest value at 6dpi with a mean of 2.45×10^8 p/s.

At 7 dpi (Figure 4.8C), parasite luminescence was detectable not only at the site of injection but into other areas also, showing that the trypanosomes were disseminating via the bloodstream. AJ3-vaccinated mice displayed significantly higher luminescence than AJ1 ($p = 0.018$) and AJ6 ($p = 0.001$). Although non-significant, the intensity of AJ3 group (2.95×10^8 p/s) was higher even than the adjuvant-only control group (2.87×10^8 p/s) (Figure 4.8C). In all mice, the peak parasite luminescence occurred on the last day of the experiment (8 dpi). At this stage, AJ3-vaccinated mice again showed the highest parasite luminescence all the groups, still greater than unvaccinated controls, and, significantly greater than those mice vaccinated with AJ1 ($p = 0.008$) and AJ6 ($p = 0.002$).

At the end of the experiment (8 dpi, Figure 4.8D), parasite luminescence in control animals displayed no statistical difference with that of mice from any antigen-vaccinated group ($p > 0.05$). However, it is clear from Figure 4.8 and 4.9 that AJ6-

vaccinated animals displayed a clear delay in parasite proliferation, leading to a lower parasitaemia by the end of the experiment. This reduction relative to the control and other antigens approached significance ($p=0.063$) when all five replicate animals are considered. Closer inspection shows that there were large variations among AJ6-vaccinated animals in luminescence; 2/5 animals in particular displayed only modest reductions in parasitaemia (an average of 7.17×10^8 p/s on 8 dpi). If considering the other three animals only (an average of 3.38×10^8 p/s on 8 dpi), the reduction in parasitaemia is a significant difference compared to the control group ($p=0.045$). At most then, we can say that vaccination with AJ6 co-administered with Quil-A was able to delay the acute parasite infection, and significantly reduce parasitaemia, in some animals.

The change in the total luminescent flux was calculated by subtracting the antigen-vaccinated luminescence values of each animal from the control group to approximate the parasite load at each day post infection (Figure 4.9 A-D). Parasite number is clearly reduced in the AJ6 group at 8 dpi (Figure 4.9D) for 3/5 mice with a total flux reading 55.9%, 74% and 58.4% lower than the control animals, respectively. As this measurement is the same as the percentage protection, it indicates a mean protection of 62.7% for these three animals when compared with the control group at the end of the experiment.

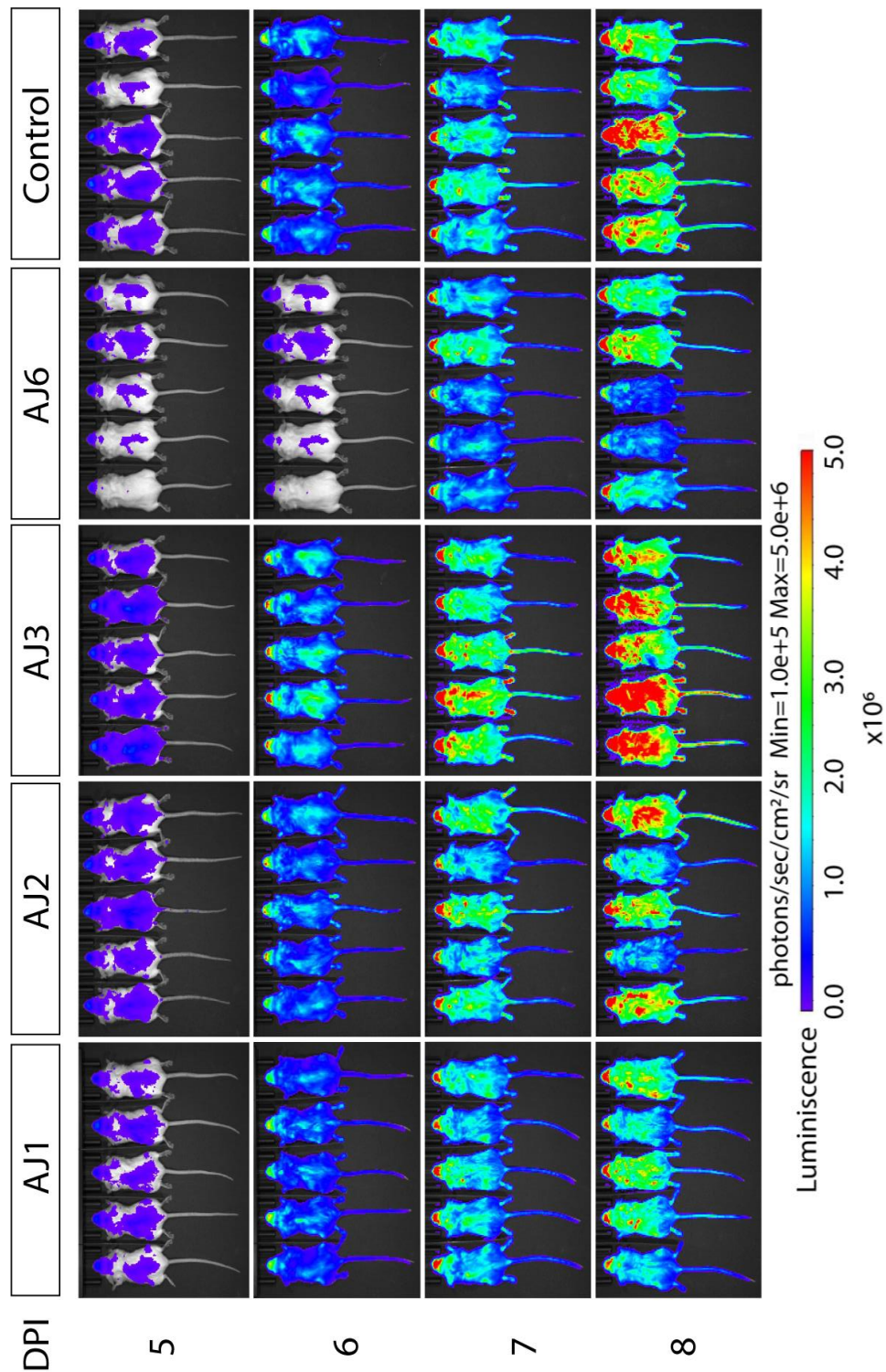


Figure 4.7. In vivo imaging of BALB/c mice immunized with each antigen co-administrated with Quil-A prior challenge with *T. vivax* (n=5/group). Daily bioluminescent images were collected from 5-8dpi. The images were standardized adjusting the scale manually. The signal intensity is represented as a pseudocolor image.

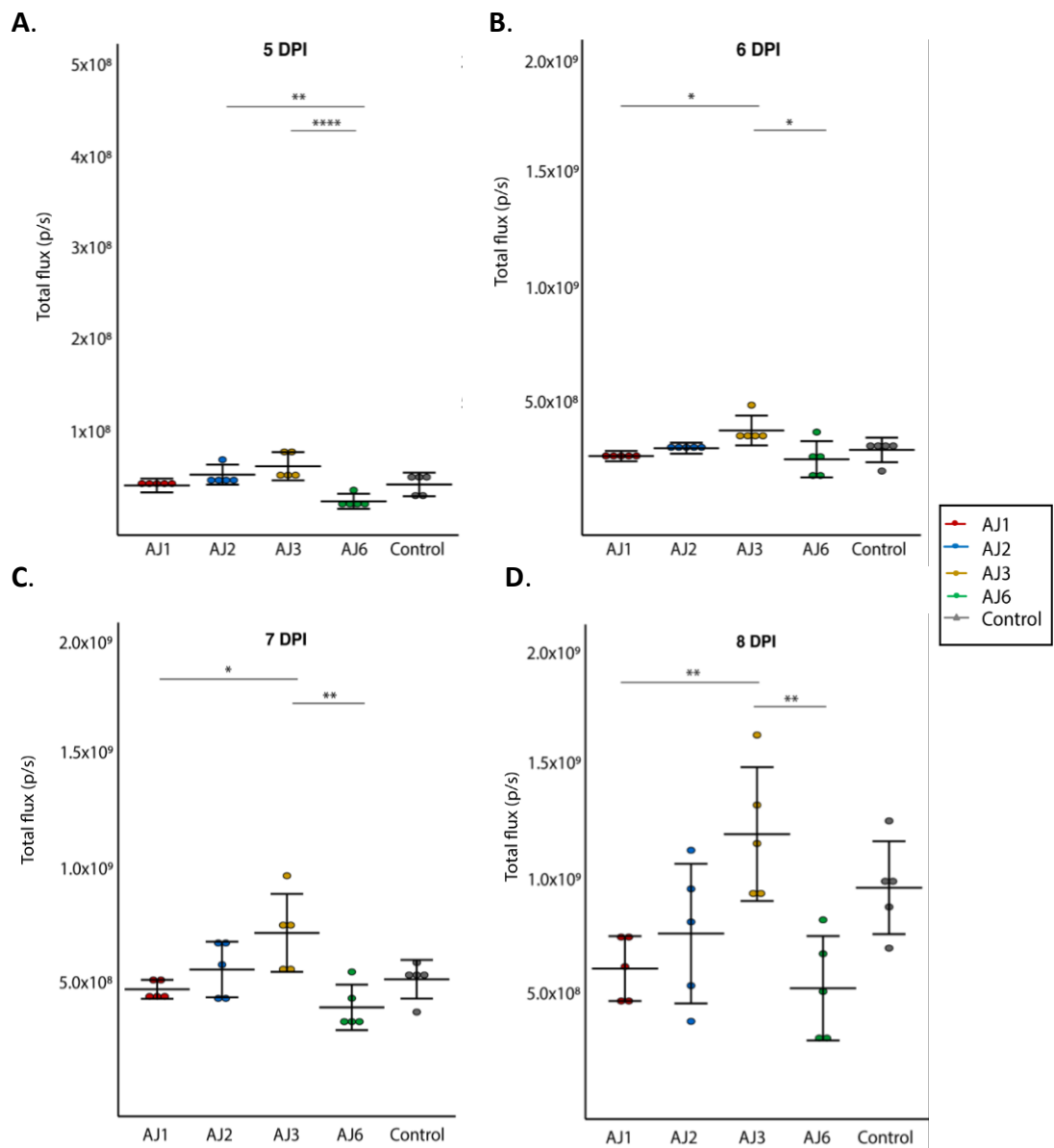


Figure 4.8. Luminescent values during the course of infection of luciferase-expressing *T. vivax* in challenged mice. The total flux (photons per second) was measured from 5-8dpi. Total flux was analysed according to each dpi (panels A, B, C, D).

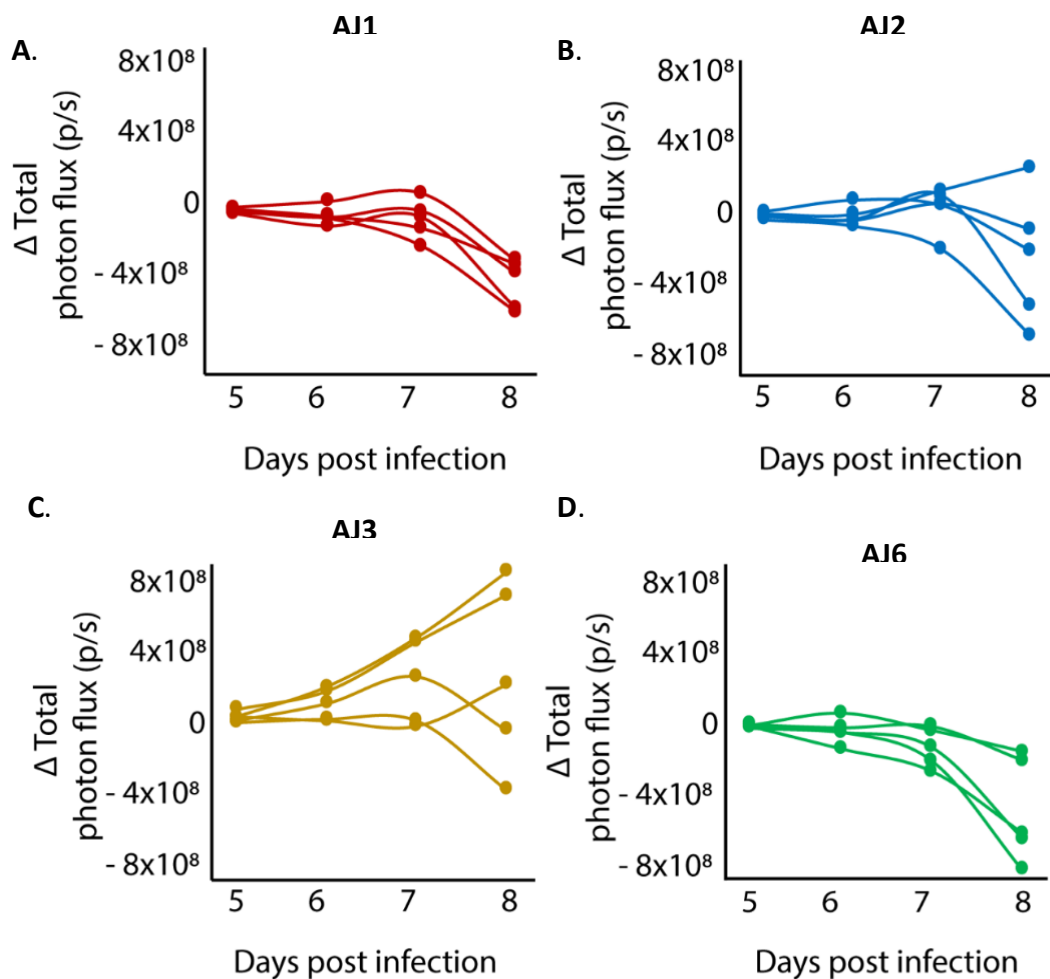


Figure 4.9. Change (Δ Total flux) in luminescence between the control group and each antigen-vaccinated group. The change in bio-luminescence was calculated as a measure of the reduction of parasite load against each antigen.

Vaccination induced antigen-specific antibodies in mice pre-challenge, but these were dominated by IgG1. Surprisingly, antigen-specific antibody levels decreased after challenge but statistically significant changes were only observed for IgG1 against AJ1 and AJ3 and IgG2a levels against AJ3 and AJ6 (Figure 4.10). The IgG1 antibody titres were significantly lower when compared pre- and post-challenge in vaccinated mice with AJ1 ($p = 0.01$) and AJ3 ($p = 0.001$). AJ2 and AJ6-vaccinated mice also displayed a decrease in IgG1 levels but these were non-significant. Immunization

also elicited high levels of IgG2a antibodies against all the antigens prior to challenge. However, after challenge a significant reduction was observed in anti-AJ3 IgG2a ($p < 0.0001$) and anti-AJ6 IgG2a ($p = 0.0004$).

Control animals immunized with Quil-A only showed no specific antibody titres against the antigens either pre-or post-challenge. The comparison of the cellular response post infection demonstrated a significant and distinguished increment of anti-AJ3 IgG1 compared to anti-AJ3 IgG2a ($p < 0.0001$) (Figure 4.10E). Likewise, anti-AJ6 IgG1 were greater than anti-AJ6 IgG2a ($p = 0.002$) (Figure 4.10E). Overall, vaccination with AJ1 and AJ2 displayed a decrease in both isotypes IgG1 and IgG2a levels but were non-significant suggesting a mixed Th1/Th2 response. Vaccination with AJ3 and AJ6 antigens developed higher levels of specific IgG1 than IgG2a suggesting a predominantly Th2 response.

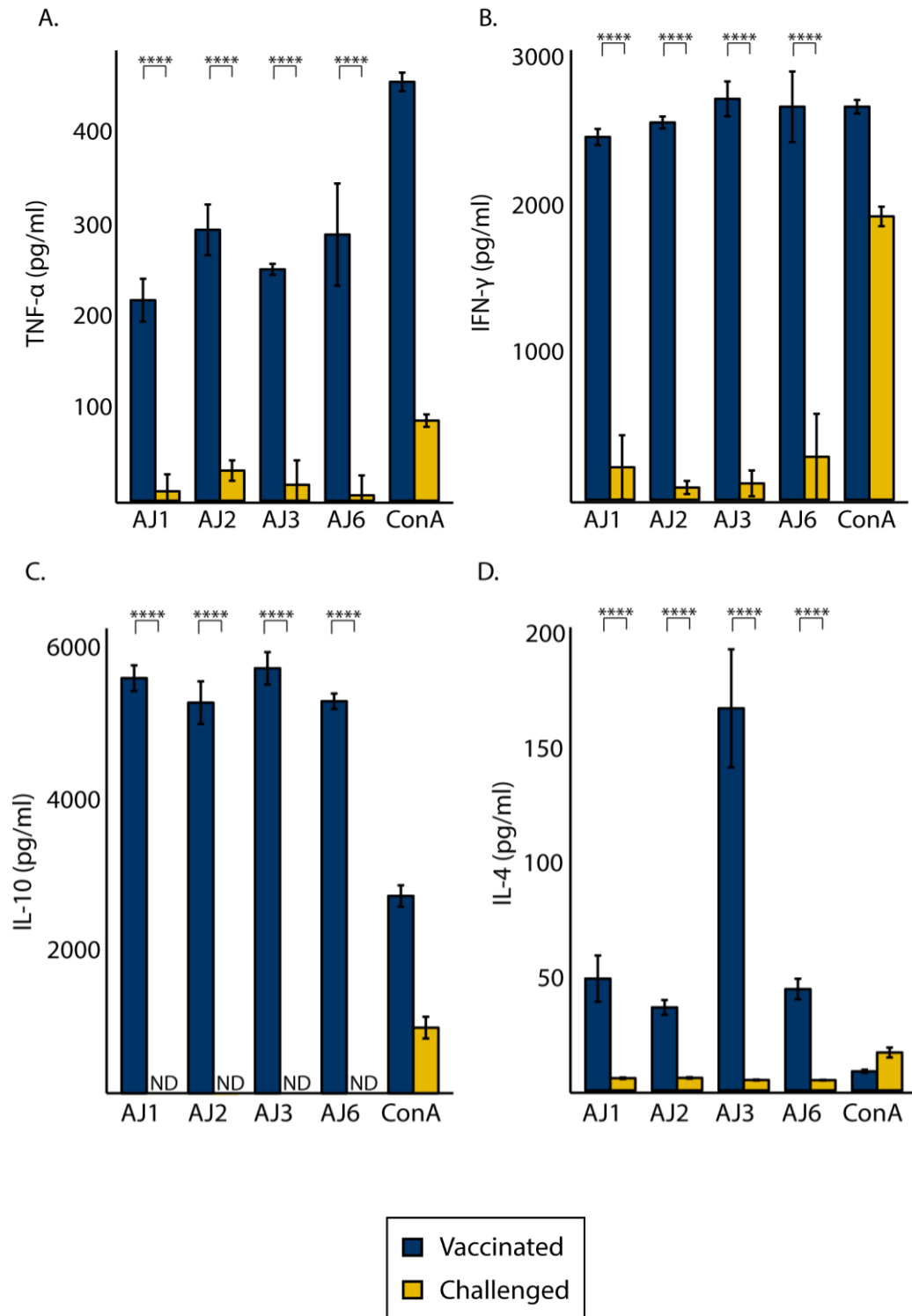
Cytokines levels after challenge were measured from five mice at random before vaccination with each antigen in conjunction with Quil-A. The response demonstrated that TNF- α and IFN- γ concentrations against each antigen were reduced significantly ($p < 0.0001$ in all cases) before and after challenge (Figure 4.10A, B). Indeed, the average TNF- α concentration for vaccinated animals pre-challenge was 300pg/ml, while this decreased by 95% post-challenge to 15pg/ml IFN- γ levels also reduced by 92.8% dropping from an average of 2500pg/ml to 180pg/ml.

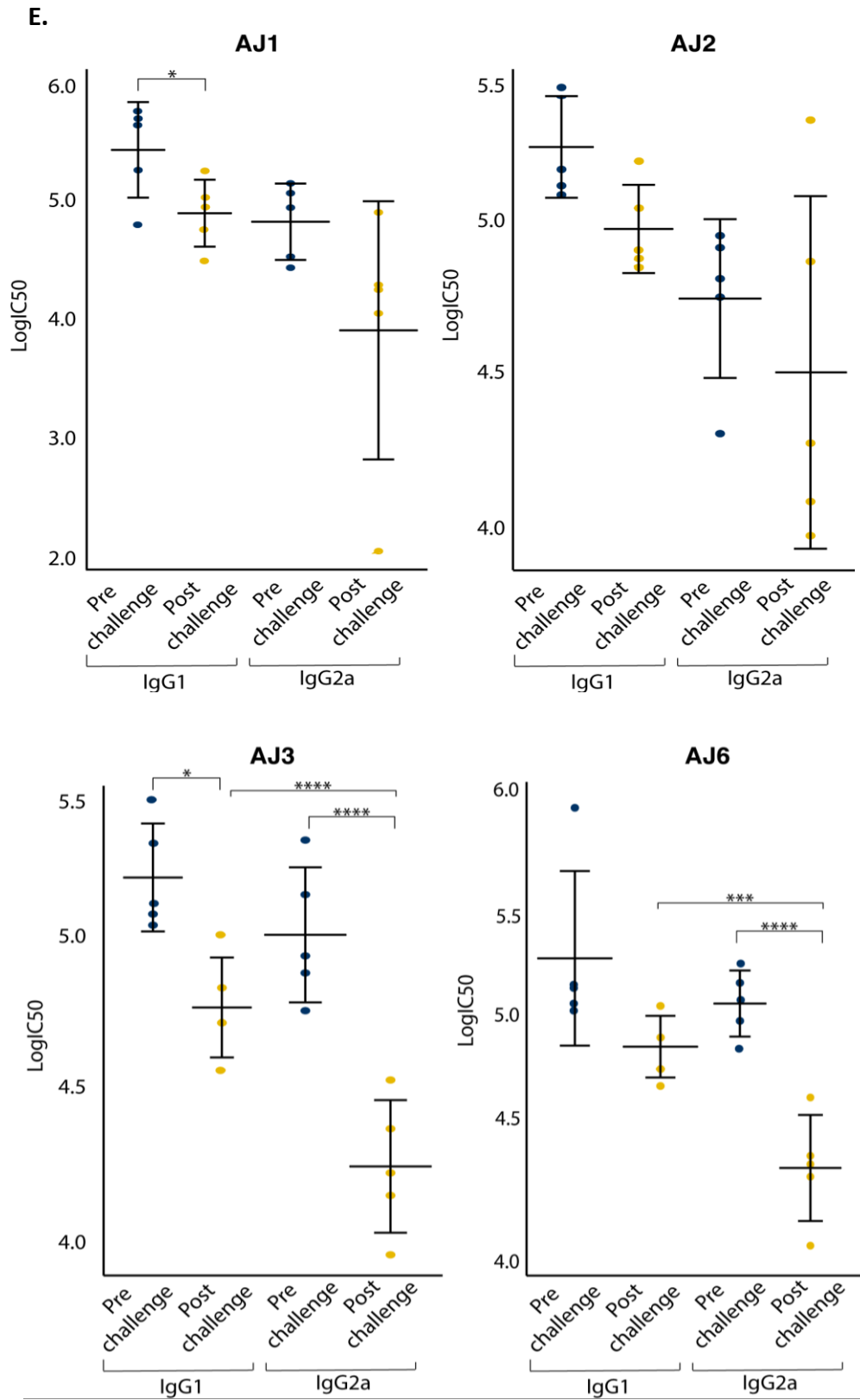
The most pronounced changes in cytokine levels after challenge were observed for IL-10 expression after 8 dpi; IL-10 concentration became non-detectable with respect to all antigens when compared with post-vaccination levels ($p < 0.001$). This could be because unstimulated cells from the adjuvant-vaccinated control group (stimulated with media only) displayed IL-10 levels as high as the challenged ones. None of the cytokines analysed were measurable in the medium-only controls, indicating that Quil-A adjuvant alone can naturally stimulate the production of certain cytokines.

IL-4 concentrations were markedly decreased after challenge, irrespective of which antigen was applied ($p < 0.0001$ for all cases). After challenge, mice displayed IL-4

levels at an average of 5pg/ml, which is comparable with ConA stimulation. For all cytokines measured, ConA in the control group were higher before challenge than after challenge (Figure 4.10E). The comparison between antigens demonstrated all AJ proteins were able to elicit similar levels for a specific cytokine. Levels of pro-inflammatory cytokines (TNF- α and IFN- γ) were higher than anti-inflammatory cytokines (IL-10 and IL-4) after 8 dpi but not statistically different ($p > 0.05$). Therefore, the results suggest that all antigens with Quil-A adjuvant were able to stimulate the cytokines analysed except IL-10, and towards a predominantly Th1-type immune response.

Figure 4.10 (overleaf). Cellular and humoral response before and after challenge with *T. vivax* in Quil-A vaccinated mice (n=8). Cytokine production by splenocytes stimulated *in vitro* (A, B, C, D) and isotype IgG profiling (E) were analyzed to determine the type of immune response elicited by each antigen. $P < 0.05$.





The immunization and challenge experiment using AJ6 co-administrated with Quil-A described in the preceding paragraphs identified a near-significant but clear reduction in parasitemia. For this reason, the experiment with AJ6 was repeated using a larger cohort of BALB/c mice ($n=15/\text{group}$) to confirm the protective effect. In this second experiment, mice were vaccinated and challenged using the same protocol and schedule as before but this time using $50\mu\text{g}$ instead of $20\mu\text{g}$ of antigen. The humoral immune response was also analysed in the second trial using the same protocol as before.

Parasite bioluminescence detected in the whole body of the animals is displayed in Figure 4.11. One mouse from the AJ6-vaccinated group was culled before 6dpi due to rectal prolapse and therefore excluded from the analysis. Luciferase intensity from AJ6-vaccinated animals was significantly lower when compared to the control group at 6 dpi ($p = 0.016$) (Figure 4.12A) with means of 1.32×10^8 and 1.71×10^8 p/s, respectively and 100% survival (Figure 4.12C). In both groups, and as in the first experiment, the luciferase intensity increased over the time of infection. At 7 dpi, both groups showed similar bioluminescence values and 100% survival. However, at 8 dpi, five animals from each group were culled due to high parasitemia (Figure 4.12B-C). Luminescence values from the surviving animals showed similar values between groups. At 9 dpi, mice from both groups displayed similar values with a mean of 1.45×10^9 and 1.60×10^9 p/s, respectively. Clearly, the parasitemia in this second experiment was higher than the first and, overall, parasitemia in AJ6-vaccinated mice was significantly reduced relative to the control group only at 6 dpi.

Cytokine levels in challenged animals culled at 8 and 9 dpi were analysed as before. There were no significant changes in TNF- α , IFN- γ and IL-10 concentrations between 8 dpi and 9 dpi (Figure 4.13A-C). There was a significant rise in IL-4 concentration (Figure 4.13D) between these days, with undetectable values at 8 dpi and an average concentration of 7.83pg/ml at 9 dpi ($p = 0.028$). The comparison between 8 dpi and 9 dpi also showed pronounced changes in IL-10 and IL-4 levels in the control group stimulated with ConA ($p = 3.40\text{E-}04$ and $p = 1.78\text{E-}04$ for IL-10 and IL-4, respectively). In all cases, cytokine concentration from splenocytes stimulated with AJ6 was lower

than the control group stimulated with ConA, except for IL-4 levels at 9 dpi (Figure 4.13D).

Cytokine concentrations at 8 dpi from the first (n=5/group) and second experiments (n=15/group) were also compared. The results showed a higher TNF- α concentration, while IFN- γ and IL-4 concentrations were lower (Figure 4.13A, C and D) in mice vaccinated with 50 μ g AJ6, although the differences were non-significant ($p > 0.05$). However, mice from the second experiment elicited higher IL-10 levels with an average of 693pg/ml compared to the undetectable values from the first experiment. Overall, the comparison of the humoral response between both challenges using AJ6 co-administrated with Quil-A showed similar cytokine expression profiles except for IL-10 concentrations which were higher in the second experiment (n=15/group).

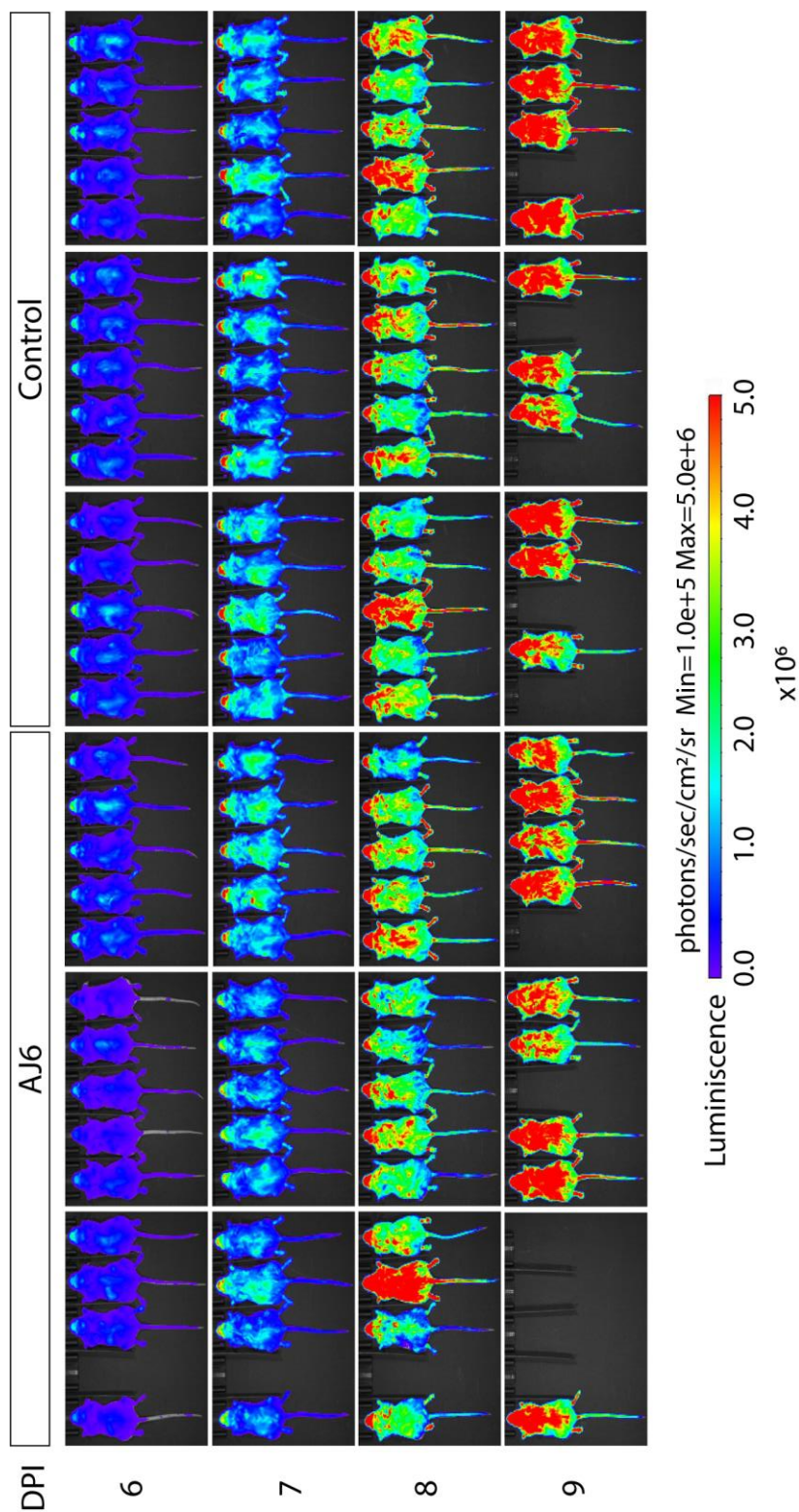


Figure 4.11. In vivo imaging of BALB/c mice immunized with AJ6+ Quil-A prior challenge with *T. vivax* (n=15/group). Daily bioluminescent images were collected from 6-9dpi. The images were standardized adjusting the scale manually. The signal intensity is represented as a pseudocolor image.

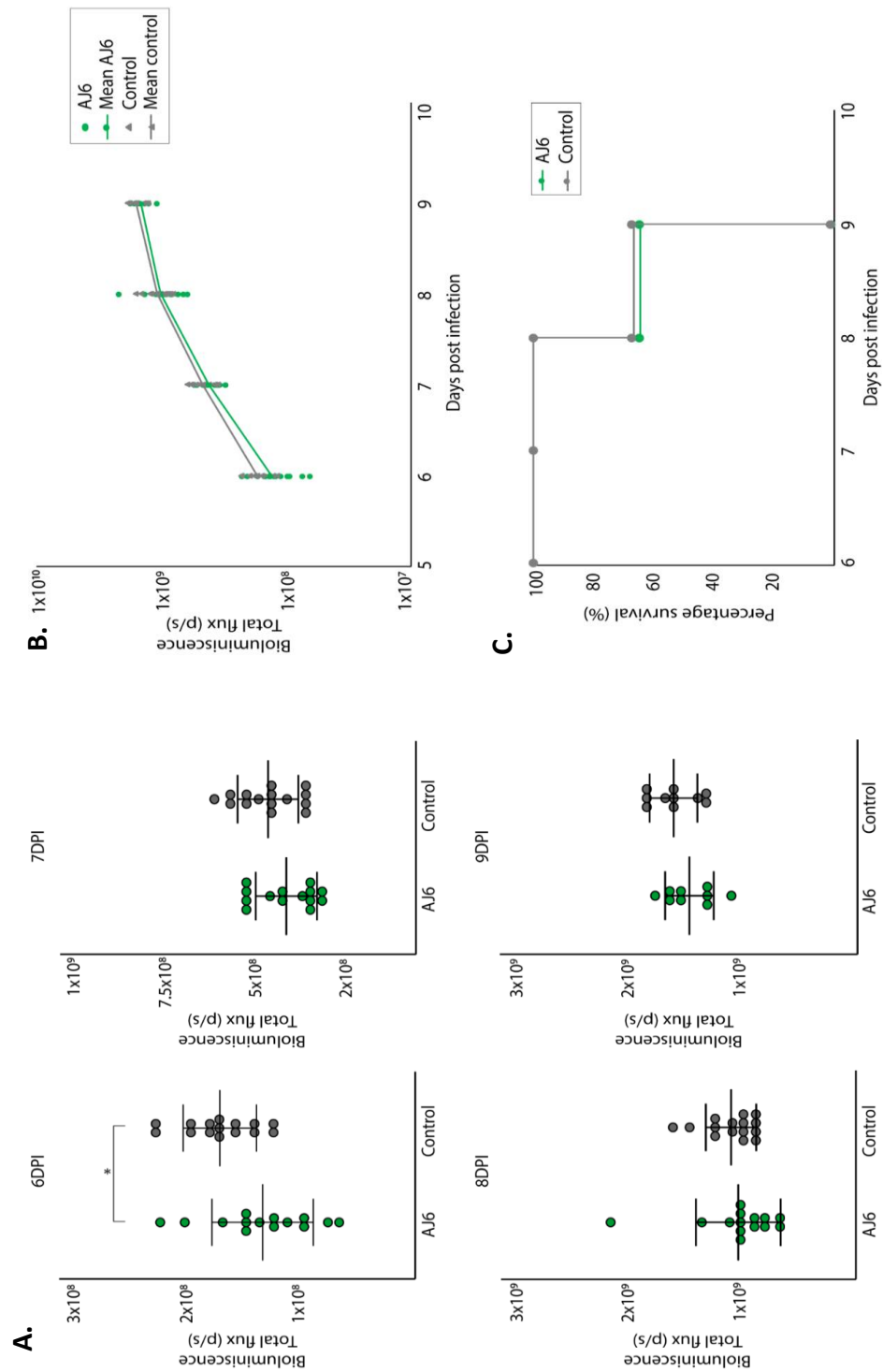


Figure 4.12. Luminescent values and survival rate during the course of infection of luciferase-expressing *T. vivax* in challenged mice vaccinated with AJ6 (n= 15/group). **A.** The total flux (p/s) was measured from 6-9dpi and analysed according to each dpi. **B.** Total flux (p/s) over time. Each curve represents the arithmetic mean of each

group. **C.** Kaplan-Meir survival curve (%) of both groups during the course of infection.

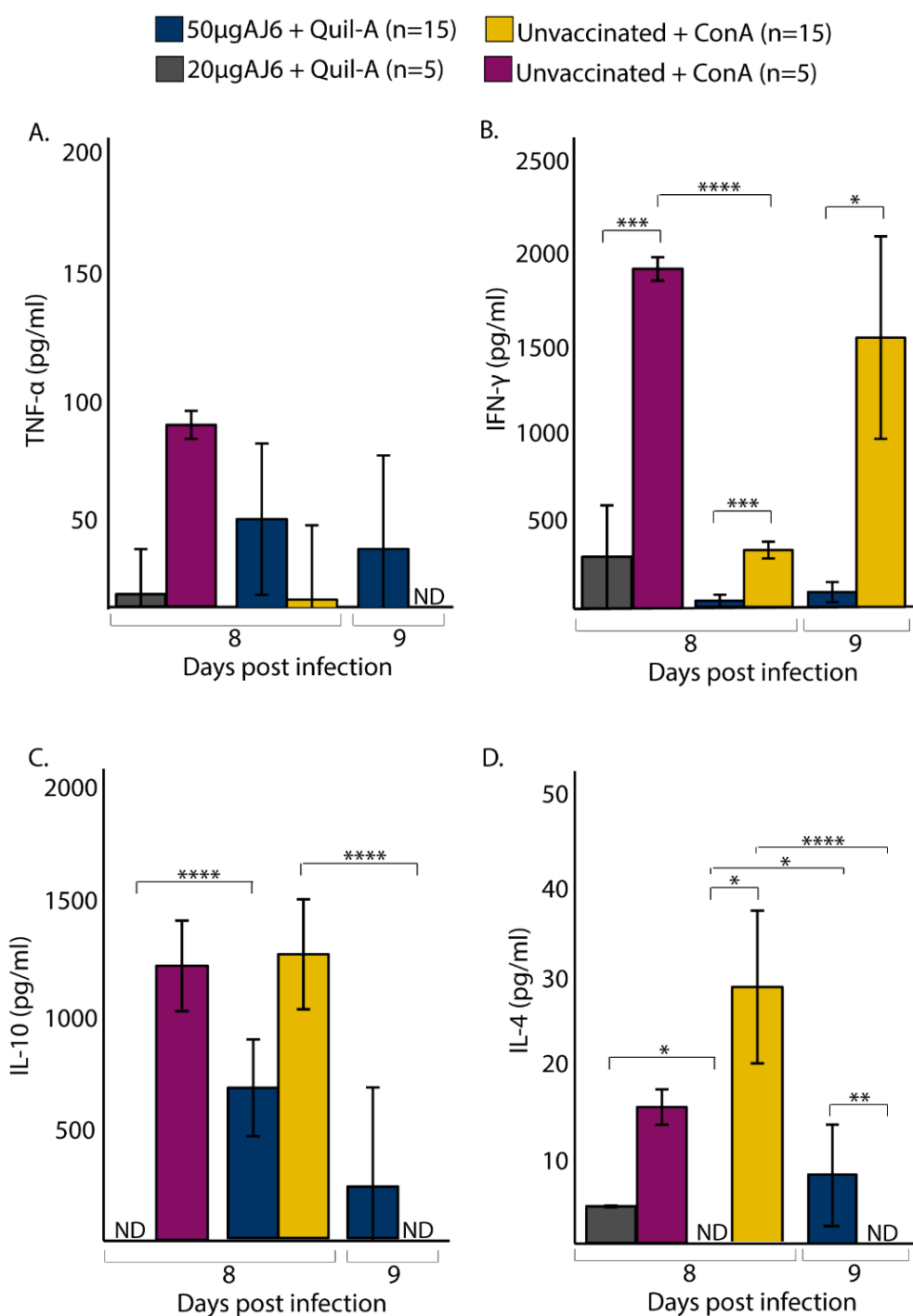


Figure 4.13. Cytokine responses in *in vitro* stimulated splenocytes after challenge with *T. vivax* in AJ6+Quil-A vaccinated mice and control group (n=15/group). **A.** TNF- α , **B.** IFN- γ , **C.** IL-10 and **D.** IL-4 cytokines were measured at 8 and 9dpi. Cytokine levels from 8dpi using 20µg (n=5) and 50µg (n=15) AJ6 were compared. ND: non detectable. P-value < 0.05.

4.3.5. Cellular localization of recombinant proteins

The subcellular localization of all AJ proteins was examined by indirect immunofluorescence analysis and confocal microscopy. The protocol was first optimized to limit background signal produced by the fixation method. After testing different fixation methods, blocking solutions, temperatures and conjugates, parasite fixation with 4%PFA gave the least background signal when incubated with blocking solution as primary antibody (blank control). In addition, using a blocking solution of 1% BSA overnight at 4°C contributed to limiting background signal intensity.

As shown in Figure 4.14, the antigens displayed differences in fluorescent intensities and cellular location. Staining with anti-AJ1 serum produced only low intensity signal from one small and unspecific location of the parasite. Staining with anti-AJ2 and anti-AJ3 sera produced similarly low intensities but in multiple locations within the cell near to the nucleus. In all three cases, the weak intensity of the staining is comparable to that of the control group, although staining is diffuse and unspecific in the control, while appears to relate to discrete cytoplasmic features otherwise. Images for anti-AJ1, AJ2 and AJ3 assays showed no fluorescence on the flagellum or in the flagellar pocket, indicating that this staining was intracellular.

The localization of AJ6 in bloodstream-form cells displayed a unique pattern compared both to the other antigens and controls. AJ6 was localized to the plasma membrane widely, both at the posterior end of the parasite near to the kinetoplast and in the flagellar pocket, and at the anterior end of the flagellum. Both locations produced approximately the same fluorescent intensity. There was no co-localisation of anti-AJ6 specific antibodies (red) and DAPI (blue) indicating that the antigen is not located in the nucleus nor in the kinetoplast. Although these patterns are typical of plasma membrane staining, the signal intensity of AJ6 fluorescence was obviously higher when compared to the control group.

Although AJ6 appears to be associated with the flagellar and cell body surfaces based on staining bloodstream-form parasites with serum from AJ6-vaccinated animals, it

remains the case that the negative control parasites, stained with pre-immune serum displayed some diffuse fluorescence. This may be due to high background noise or non-specific binding by unrelated serum factors. To confirm this, and to reproduce cell-surface localized of AJ6, a polyclonal antibody was raised in rabbits against recombinant AJ6 protein (BioServUK, Sheffield, UK).

Immunofluorescence staining of bloodstream-forms using sera from immunized rabbits demonstrated the recognition the parasite cell surface in the same way as the mouse post-immune serum (Figure 4.15). Polyclonal anti-AJ6 antibodies localized to the surface membrane with the same intensity as with the post-immune sera but with a lower background signal intensity. The stain was clearly localized to the whole parasite plasma membrane. No fluorescence was observed for the negative control using pre-immune sera, showing that purified anti-AJ6 antibodies confirm the localization of AJ6 to the whole cell-surface in *T. vivax* bloodstream forms.

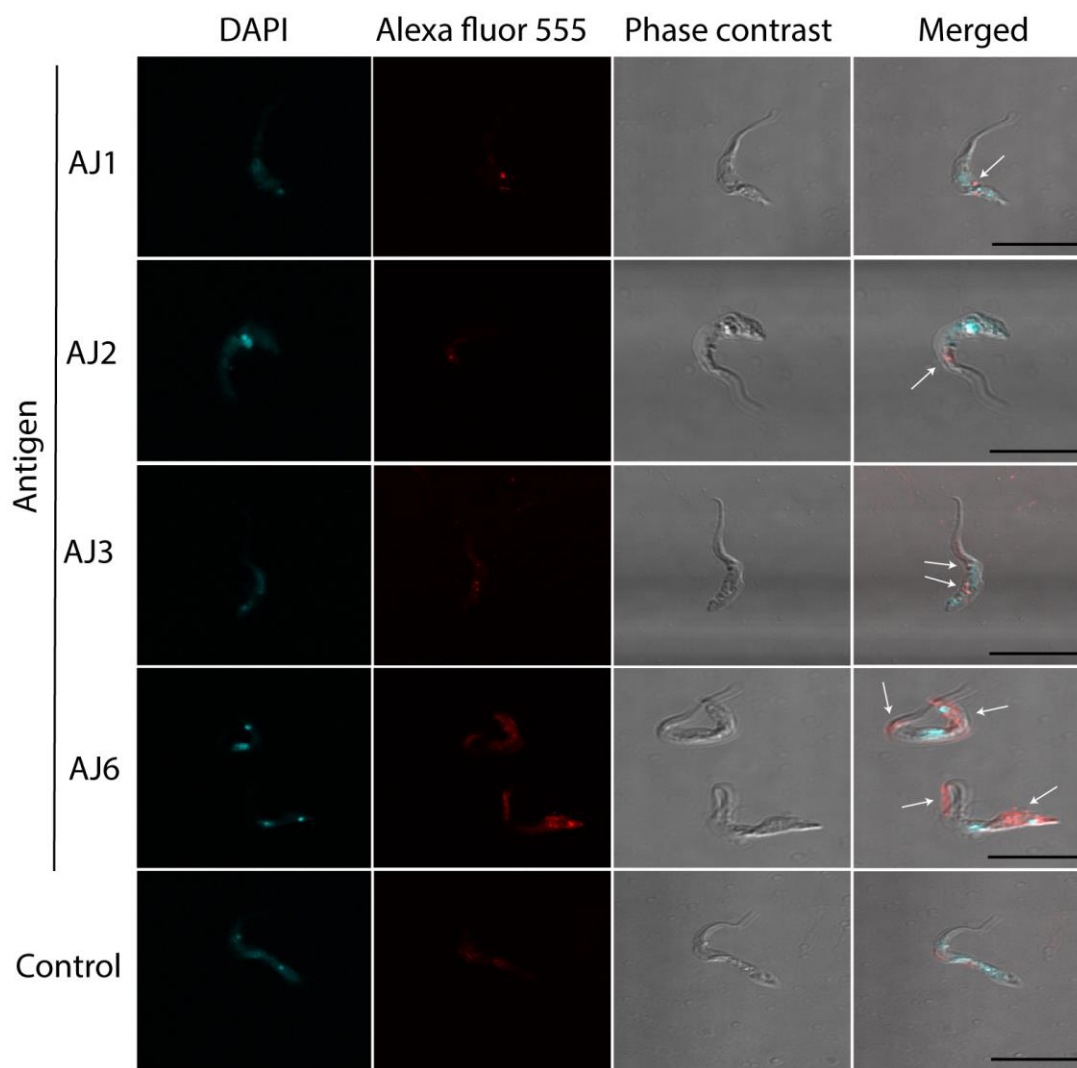


Figure 4.14. Cellular localization of AJ antigens in *T. vivax* bloodstream-forms. The immunofluorescence protocol was first optimized and images were visualized with a confocal microscope. A pool of post-immune sera was used as specific primary antibodies against each particular antigen and coupled with Alexa fluor 555 (red). Phase contrast shows *T. vivax* bloodstream-forms cells, Alexa fluor 555 shows the localization of the target proteins (indicated by arrows) and 4 ,6-diamidino-2-phenylindole (DAPI) staining shows DNA contents (nucleus and kinetoplast). Bars: 5 μ m.

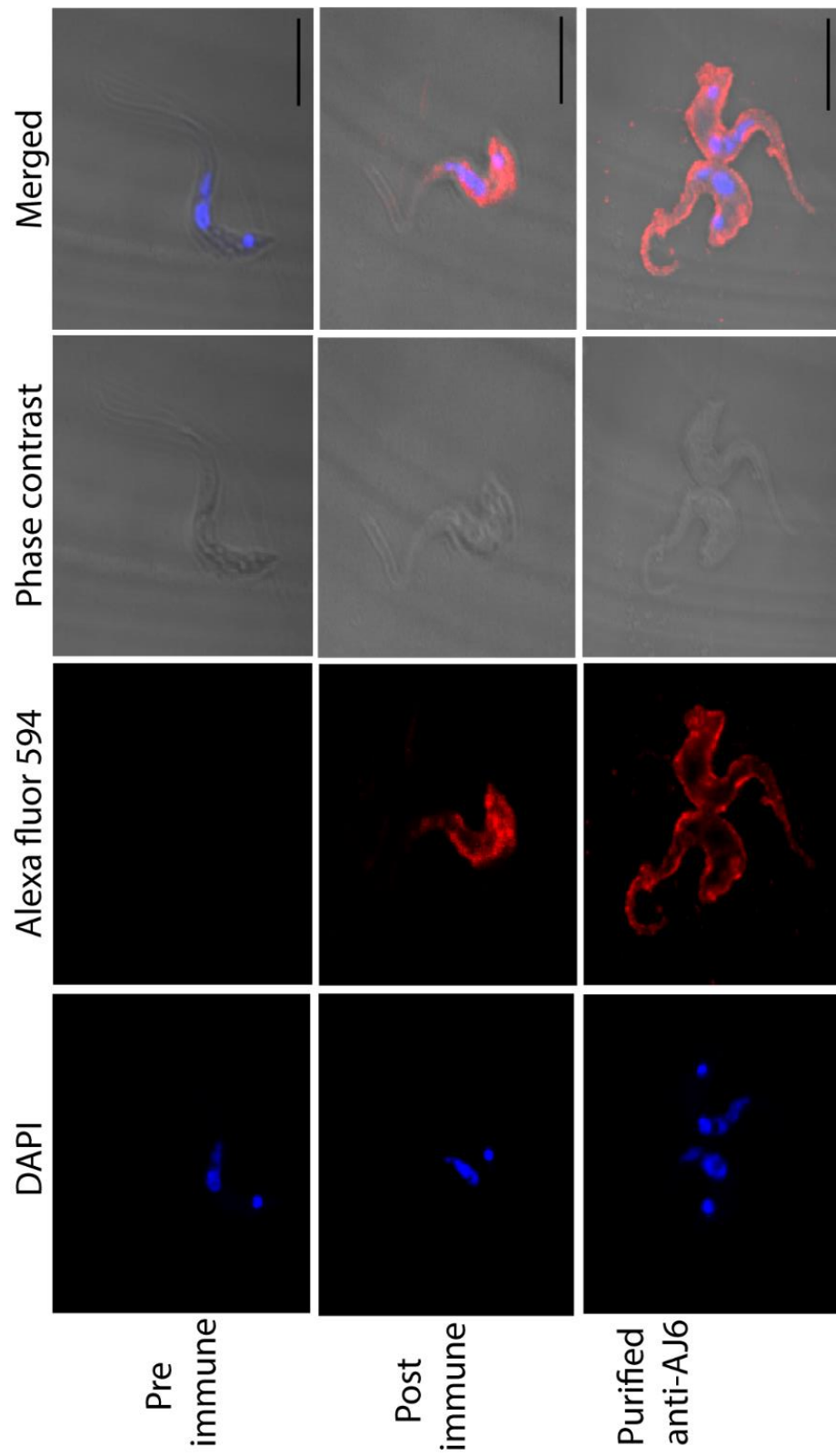


Figure 4.15 (previous page). Cellular localization of AJ6 in *T. vivax* bloodstream-forms using purified polyclonal antibodies. Purified polyclonal IgGs raised in rabbits were used as specific primary antibody to localize AJ6 and coupled with Alexa fluor 594 (red). A pool of pre- and post-immune rabbit sera were used as negative and positive controls, respectively. Phase contrast shows *T. vivax* bloodstream-forms, Alexa fluor 594 shows the localization of AJ6 and 4',6-diamidino-2-phenylindole (DAPI) staining shows DNA contents (nucleus and kinetoplast). Bars: 5µm.

4.4. DISCUSSION

This chapter has evaluated the humoral and cellular immune responses to four proteins (AJ1, AJ2, AJ3 and AJ6) in infected cattle and also when administered in a variety of adjuvants to BALB/c mice. The protective efficacy of these antigens was also tested in a mouse challenge model and mice were examined for potential correlates of protection. In addition, the subcellular localization of the four antigens was evaluated to verify if the antigens were exposed on the surface of *T. vivax* bloodstream-forms.

AJ1-3 and AJ6 bio-tagged proteins were used to determine the type of humoral response in naturally and experimentally infected cattle. The results demonstrated that all the antigens were recognized by naturally infected sera with higher titres of IgG1 than IgG2. Likewise, samples from experimentally infected animals displayed similar results but with lower titres. This may be because the samples from experimentally infected calves were eluted from filtered paper on which the sera or plasma were collected. The eluates showed high specificity against each isotype but lower titres when compared with serum samples. The same methodology of antibody elution has been used for similar purposes in other zoonotic diseases (Curry *et al*, 2011; de Oliveira *et al*, 2011), and in these there was a clear difference compared with serum results. Nonetheless, samples from naturally infected cattle showed a specific antibody response against all AJ proteins. All animals showed a strong IgG1 antibody response against the recombinant proteins indicating a Th2-type response over the course of infection in naturally and experimentally infected cattle (Spellberg and Edwards Jr, 2001; Bretscher, 2014).

Using a BALB/c mouse model, differences in the vaccine-induced humoral and cellular responses to the antigen panel when using three different adjuvants were determined. Three AJ-M mice developed mild injection site reactions, however it has been reported as a general adverse event when vaccinated with this adjuvant (van Doorn *et al*, 2016). Despite the reaction, the animals were included in the analysis.

Immunization of BALB/c mice with each antigen in any adjuvant combination resulted in seroconversion at 6 weeks after the first immunization.

Overall, AJ1, AJ2, AJ3 and AJ6 serostatus resulted in higher IgG1 than IgG2a titres in AJ-A and AJ-M vaccinated mice. Despite higher IgG2a than IgG1 levels in AJ-Q mice, only immunization with AJ6 produced a significant difference between the IgG1 and IgG2a titres. Pro- and anti-inflammatory cytokine levels were consistent with a mixed Th1-Th2 cellular response for all the antigens, including AJ6. These findings are interesting since alum stimulates a principally Th2 response, Montanide stimulates both Th1 and Th2, and Quil-A stimulates a mixed response in addition to CD8⁺ T cells (Coffman *et al*, 2010). Immunization with alum usually generates a Th2 response, promotes IL-10 production (Oleszycka *et al*, 2018) and is independent of IL-4 inhibiting a Th-1 related phenotype (Brewer *et al*, 1999). In this regard, the results suggest that the high IL-10 concentration might be inhibiting a specific Th1 response. Interestingly, the AJ1-A vaccinated group showed an absence of IL-10 but an IgG1 titre that was statistically greater than IgG2a. Likewise, the other antigens also induced greater IgG1 titres than IgG2a. In fact, this is unsurprising as susceptible mice strains like BALB/c are prone to high IgG1 antibody levels and a Th2-type response (Mosmann and Coffman, 1989). Hence, a stronger IgG1 response can be expected irrespective of the adjuvant used.

The antigen-specific cellular response indicated that each protein stimulated *in vitro* gave a strong cell-mediated immunity in splenocytes from immunized mice. Administration of alum, Montanide or Quil-A adjuvants in conjunction with a particular antigen showed differences in cytokines concentration, although the choice of antigen made no difference. There was a higher production of TNF- α and IFN- γ indicating a mixed Th1/Th2 response in all groups. It has been demonstrated that a Th1 response is important for intracellular parasites while a mixed Th1/Th2 response for extracellular pathogens (Romagnani, 1997). In fact, the latter is the most common response against most pathogens, progressing from a Th1 to a mixed Th1/Th2 mode (Bretscher, 2014). Specific antibodies reduce circulating trypanosomes during infection and Th1-type cytokines help in parasite control

(Stijlemans *et al*, 2007). In addition, polarization of naïve T-cells depends on innate immune cells, e.g. DCs, through differential production of cytokines to stimulate a Th1 or Th2 response (Spellberg and Edwards Jr, 2001). The control of parasite burden by the immune system strongly depends on the Th1-type cytokine IFN- γ production during early stages of infection in a murine model (Magez *et al*, 2006; Namangala *et al*, 2009) and in natural infections in cattle (Taylor *et al*, 1996).

IFN- γ -mediated responses occur when $\text{caM}\phi$ produce TNF- α . In this sense, the high levels of TNF- α in response to the antigens analysed here suggest that *T. vivax*-specific Th1 cells may be circulating. These findings are consistent with other studies of IFN- γ production in mice infected with *T. congolense* and *T. brucei* (Magez *et al*, 2004; Magez *et al*, 2006; Magez *et al*, 2007). TNF- α has a trypanolytic effect by binding in the FP and destroying trypanosomal lysosome-like organelles during peaks of parasitaemia (Magez *et al*, 1997; Stijlemans *et al*, 2007). Previous studies have also demonstrated high levels of TNF- α provoking a pro-inflammatory response in mice (La Greca *et al*, 2014) and cattle (Camejo *et al*, 2014) experimentally infected with *T. vivax* as well as during natural infections of cattle in Africa (Bakari *et al*, 2017).

IL-4 and IL-10 are important in downregulating the production of pro-inflammatory cytokines. Both are produced mainly during late stages of infection and are necessary to limit pathology. These results indicate that higher levels of IL-10 and IL-4 in AJ-Q group compared with AJ-A and AJ-M are both adjuvant and antigen-related. These findings are consistent with previous observations of Quil-A vaccination in murine models, in which several cytokines including IL-4, IL-10 and IFN- γ were upregulated, leading to production of cytotoxic T lymphocytes (CTL) (Sjölander *et al*, 2001). It is well established that the interaction between the antigen and the adjuvant is of high importance to an optimal response.

Given its advantages compared with the other adjuvants analysed Quil-A was selected for the experimental vaccine. First, Quil-A being an immunostimulatory complex (ISCOM) adjuvant, it provides a stronger signal stimulating DCs and $\text{M}\phi$ and interactions with APC (Sun *et al*, 2009). Second, ISCOMs promote a greater and more

prolonged antibody response. And finally, Quil-A strongly enhances CD4⁺ and CD8⁺ T-cell responses. As mentioned above, however, its overall effect is a balanced Th1 or Th2 response (Coffman *et al*, 2010). These findings are consistent with comparative adjuvant experiments in *T. cruzi* (Scott *et al*, 1984) and *T. brucei* (Lubega *et al*, 2002) demonstrating the effectiveness of Quil-A.

Using *in vivo* bioluminescent imaging during the last four days of the challenge, this chapter has shown that AJ1-3 failed to produce correlates of protection as the total flux increased over time correlating also an elevated parasite load. Conversely, three AJ6-Q mice displayed a significant 2.8-fold reduction in parasite bioluminescence (36%) at 8 dpi compared to the control group resulting in 60% partial protection of vaccine efficacy.

The antigen specific response presented in this chapter against the panel of antigens is comparable with previous experiments in other African trypanosomes. The comparison between the antibody levels before and after challenge demonstrated a slight decrease for both IgG1 and IgG2a, respectively. This results are in concordance with experimental infections with *T. congolense* in cattle (Authié *et al*, 2001), *T. vivax* in cattle (Rurangirwa *et al*, 1983) and *T. brucei* in mice (Lança *et al*, 2011) when different antigens were used to assess the potential protection against infection. A possible explanation for this event could be the reduction in number of splenic B-cells which is associated with a defect in B-cell development (Blom-Potar *et al*, 2010). Another possible explanation could be the formation of immune complex of specific antibodies with the parasite antigens making this unable to measure IgGs solely in circulation (Lindsley *et al*, 1981; Ferrante and Allison, 1983).

The cytokine profile analysed between pre- and post- challenge showed significant changes. The reduction but not absence of antigen-stimulated IFN- γ levels observed after 8 dpi could play an essential role in parasite control during early stages of infection. It is known that IFN- γ is related to resistance to African trypanosomes (Hertz *et al*, 1998) demonstrated in *T. congolense* (Guilliams *et al*, 2007) and *T. brucei* (Namangala *et al*, 2009). In addition, the antigen-stimulated TNF- α elicited by caM ϕ

due to an antigen-specific IFN- γ response might possibly be trypanolytic since these findings are in agreement with their protective role during acute AAT (Namangala *et al*, 2001). It has been shown that during a trypanosome infection, there is a switch from Th1 to Th2 response as the infection progresses (Stijlemans *et al*, 2007). This could explain the low levels of both Th2-type cytokines (IL-10 and IL-4) after stimulation with all the antigens. Similar results were obtained when antigens from related parasites such as *L. donovani* (Ghosh *et al*, 2001; Daifalla *et al*, 2015) and *T. brucei* (Ramey *et al*, 2009; Pletinckx *et al*, 2011) were used to assess the immune response in murine models using different adjuvants. Moreover, the same cytokine profile is observed in naturally infected cattle (Bakari *et al*, 2017). Taken together, the results demonstrated a Th1/Th2 response stimulated by all AJ antigens indicating that both responses coexist which would be beneficial for parasite control.

The partially protective immunity elicited by AJ6 probably implicates immunological factors other than those analysed here, since no differences in cytokine profile were observed between the partially-protected and -unprotected AJ6-Q mice. The question now arises as to whether AJ6 protection is real. A possible explanation for partial protection by AJ6 might be that the antigen can stimulate the production of nitric oxide (NO) via TNF- α , a trypanolytic factor that plays an essential role in parasite control. Indeed, it has been shown that during a *T. congolense* infection in mice, the pro-inflammatory effectors IFN- γ , TNF- α and NO are required for the control of parasitaemia and host immunity (Magez *et al*, 2007). In a *T. vivax* infection, TNF- α mediates survival in a murine model (La Greca *et al*, 2014) and NO synthesis by caM ϕ which requires TNF- α has been demonstrated to mediate the parasites clearance in *T. congolense* (Taylor, 1998) and *T. brucei* infections (Beschlin *et al*, 1998). Consequently, subsequent experiment must be carried out to answer this, possibly including other immunological parameters such as the quantification of other cytokines and molecules by flow cytometry and histology assays using the spleen in order to observe phenotypic profiles like inflammatory responses. Similar levels of partial protection were obtained using recombinant cytoskeletal proteins from *T. evansi* (Li *et al*, 2007; Li *et al*, 2009).

The IFA analysis demonstrated the cell-surface expression of AJ6 in bloodstream-forms with widespread and robust staining of the whole parasite surface, consistent with the *in silico* prediction that FamX encodes type-1 transmembrane proteins. This localization implies that AJ6 epitopes are naturally exposed on the *T. vivax* bloodstream-form surface, where they may be recognized by specific anti-AJ6 IgGs. Therefore, this, combined with its partial protective effects, means that AJ6 is a good target for vaccine development. AJ1-3, however, lacked any specific cell-surface localization, which might have two explanations: 1) AJ1-3 antigens are located inside the parasite and cell permeabilization is required to expose the proteins to cognate antibodies (White, 2013). Or 2) these antigens are surface-located but expressed in the flagellar pocket only, where they are accessible to antibodies only under certain conditions (Engstler *et al*, 2007).

Previous attempts to vaccination against *T. vivax* has been performed using whole parasites, other pathogens and surface glycoproteins without success. Invariant surface glycoproteins from *T. brucei* have been shown to confer partial protection to heterologous challenge in BALB/c mice (Lança *et al*, 2011), showing that surface proteins that do not undergo antigenic variation could have a role in conferring protective immunity as they are, in principle, exposed to the host antibodies, so long as they are present in sufficient quantities (Black and Seed, 2001). AJ6 antigen is a *T. vivax*-specific and antigenically invariant cell surface glycoprotein of bloodstream forms that is now a promising vaccine candidate.

4.5. CONCLUSION

Vaccination of BALB/c mice with all AJ antigens proved to be antigen and adjuvant-dependent. All animals seroconverted with IgG1 and IgG2a antibodies 6 weeks after the first immunization. Animals immunized with Quil-A in combination with each antigen showed higher IgG2a levels compared with alum and montanide-based immunization. The cellular response after vaccination showed higher levels of pro-inflammatory cytokines IFN- γ and TNF- α , indicating that AJ antigens elicited a mixed Th1/Th2-type response. Quil-A vaccinated mice showed significantly higher levels of

IFN- γ and IL-10 compared to the other two adjuvants. Immunization with AJ1, AJ2 and AJ3 in combination with Quil-A failed to protect mice against challenge with *T. vivax*. Immunization with AJ6 and Quil-A elicited a partially protective response with a significant decrease in the parasite burden in 3 vaccinated mice at 8dpi, indicating 60% efficacy. The AJ6 protein was localized to the entire cell surface in immunofluorescent analysis of fixed bloodstream-form cells using both post-immune serum and purified antibodies, displayed substantially greater expression than any other antigen.

CHAPTER 5

Evaluation of a FamX experimental vaccine in a caprine model

5.1. INTRODUCTION

The immune response of mice to the four AJ antigens in Chapter 4 showed that one antigen, AJ6, was able to reduce parasite burden in some animals. This result encourages us that specific FamX proteins, as the most abundant and immunogenic bloodstream-stage antigens besides VSG, might provide a means of vaccination against *T. vivax*. This chapter tests this idea directly with a vaccination and challenge study in goats using a FamX-based vaccine.

The best outcome for immunization prior to challenge is to confer sterile immunity and long-term protection (Black and Seed, 2001). Besides the encouraging outcome in AJ6-vaccinated mice, the antigen did not confer sterile immunity and only partial protection was observed in some mice. However, Dr Gavin Wright and colleagues at the WSI have observed complete, protective immunity in mice using a FamX protein closely related to AJ6, which has been called the Invariant Flagellum Antigen (IFX). IFX was discovered using a high-throughput antigen discovery approach and been successfully expressed as a recombinant protein with the AVEXIS method (Kerr and Wright, 2012). It has been previously demonstrated to induce high antibody titres with IFX+ alum administered intraperitoneally and protective immunity in BALB/c mice experimentally infected with *T. vivax* Y486 by intravenous route (Figure 5.1A). In addition, mice with IFX and alum adjuvant were fully protected for over 100 days (Figure 5.1B). These mice were entirely free of parasites and pathology. Immunogold electron microscopy analysis has localized IFX to the parasite cell-surface of parasite but, unlike AJ6, specifically to junctions between the plasma and flagellar membranes. Given its proven protective ability, IFX was selected as the antigen for a vaccination and challenge experiment in a goat model.

IFX (TvY486_0807240) is a member of FamX and therefore homologous to AJ1-3 and 6. Slightly longer than the AJ proteins, at 607 amino acids, IFX otherwise displays the same structural features typical of FamX: a signal peptide at the N-terminus, a single TMD towards the C-terminus, and a majority extracellular domain predicted to be highly glycosylated.

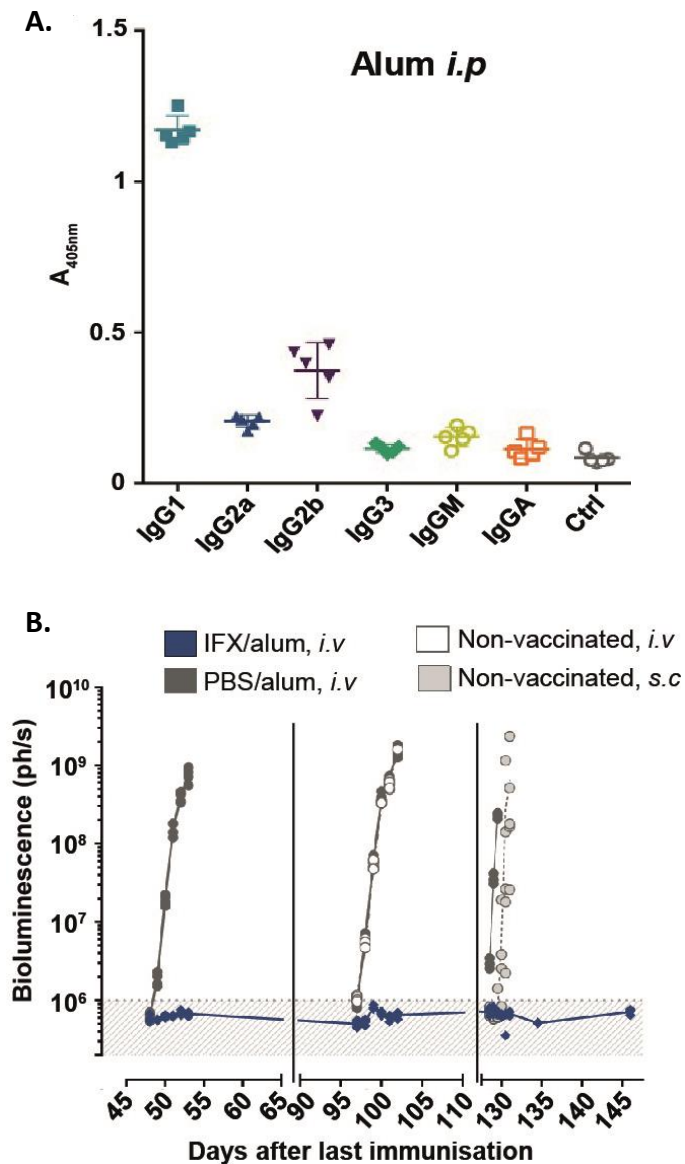


Figure 5.1. A. Antibody titration of IgG isotypes against IFX in vaccinated mice (n=15) co-administrated with alum (intraperitoneally). **B.** Long-lasting immunity against *T. vivax* infection (parasite injected intravenously) in IFX+ alum mice (n=15) compared to the control group. The protection was observed for more than 100 days after the last immunization. Data courtesy of Dr G. Wright (WSI).

This chapter evaluated the protective efficacy of IFX in Saanen goats (*Capra aegagrus hircus*) in São Paulo, Brazil, using a Brazilian *T. vivax* strain 'Miranda' (TvMi). In South America, *T. vivax* occurs in cattle, sheep, goats and wild animals. In Brazil, *T. vivax* was first reported in 1972 and animal trypanosomiasis has become an economic problem in semiarid regions in Brazil with sporadic outbreaks observed in cattle (Jones and Dávila, 2001; Cuglovici *et al*, 2010; Cadioli *et al*, 2012). In small ruminants like goats and sheep, there is a high prevalence of natural infections by *T. vivax* with 29.7% and 25.4%, respectively (Batista *et al*, 2009). In the semiarid region of Brazil, these animals are the most important livestock and can present variable signs and pathogenic features related with the parasite strain. The Miranda strain used for this challenge comes from the Miranda county in Mato Grosso do Sul, Brazil. This area is located in the Amazon state of the Pantanal, between the Brazilian, Bolivian and Paraguayan border. The strain was first studied by Paiva *et al* in Pantanal (1997) (Paiva *et al*, 2000).

The pathology and clinical signs the animals have with TvMi is unique compared to other *T. vivax* strains. TvMi strain is characterized for the lack of usual clinical signs and pathology normally described for an infection with African trypanosomes (Paiva *et al*, 2000). Animals naturally infected with TvMi are apparently healthy and mortality of these animals may be due to co-infections with other pathogens. Indeed, field studies have demonstrated that cattle infected with the strain are able to control the infection, although there is still a high frequency of outbreaks nonetheless (Martins *et al*, 2008).

The contribution of murine models to understand animal African trypanosomiasis is a valuable tool to understand pathogenesis and immunology during the infection. However, only vaccine trials in a natural host are definitive as vaccine trials in laboratory rodents might not provide an authentic host immune environment (Magez and Radwanska, 2014). There have been previous vaccine attempts against African trypanosomes using a goat model without success. For example, in 1984, Rovis *et al* demonstrated that vaccination with a purified protein of 83kDa failed to protect against *T. vivax* or *T. brucei* infection in goats and rabbits (Rovis *et al*, 1984).

As IFX confers sterile immunity in BALB/c mice, the next step is to test whether the antigen can elicit a protective response in a natural host. Hence, the potential effective immunity of IFX was analysed in a goat model after being challenged with TvMi strain.

This chapter aims to:

1. Immunize two groups of four Saanen goats with recombinant IFX protein in combination with Freund's and Quil-A adjuvants respectively.
2. Challenge vaccinated goats with *T. vivax* Miranda strain and evaluate their clinical and physical manifestations during the course of infection.
3. Determine the humoral immune response in vaccinated goats before and after the last immunisation.
4. Evaluate the immune protection against *T. vivax* challenge afforded by IFX immunization.

5.2. MATERIALS AND METHODS

5.2.1. Study ethics

The study was conducted at the Faculdade de Ciências Agrárias e Veterinárias of Universidade Estadual Paulista (UNESP) in Jaboticabal, São Paulo, Brazil. All experiments were performed under the approval of the ethical committee of UNESP and University of Liverpool AWERB. The trial was conducted under continuous veterinary supervision ensuring high standards of animal welfare.

5.2.2. Animals

Eighteen male Saanen goats (*Capra aegagrus hircus*) 8-10 months old were obtained from a non-endemic *T. vivax* area in São Paulo, Brazil. Prior to the experiment, all the animals were screened for *Eimeria sp.* and helminths by faecal egg counts per gram of faeces (OPG) and confirmed negative. They were also screened for antibodies against *T. vivax* with serology (IFI and ELISA) and Loop-Mediated Isothermal Amplification (LAMP) PCR, all tests gave negative results.

All goats were randomly distributed into two groups of vaccinated animals with IFX in combination with Freund's and Quil-A adjuvant respectively (n=4/group) and two groups of vaccinated animals with each adjuvant only (n=4/group), and additionally two goats as donor animals infected with TvMi strain from a frozen stabilate containing 3.84×10^5 parasites (the latter two animals were not used in the experiment). The animals were allocated to separate cages during the whole experiment in a fly-proof area to prevent natural infections.

5.2.3. IFX vaccination against *T. vivax*

Two weeks after acclimatization, four goats from the antigen-vaccinated group were injected subcutaneously with IFX antigen in combination with Freund's adjuvant (IFX-F group). The vaccine preparation consisted of diluting 0.12ml of 100µg IFX

recombinant protein in 2.88ml sterile PBS in conjunction with 2ml complete and incomplete Freund's adjuvant for the first and two subsequent booster injections respectively (Table 5.1). The other four goats from the antigen-vaccinated group were injected with 0.116ml of 100 μ g IFX protein diluted in 5.88ml sterile PBS with 6ml Quil-A (IFX-Q group).

Control groups comprised four goats each of which received 2ml PBS combined with 2ml Freund's adjuvant (control-F), while the four remaining goats received 6ml PBS combined with 6ml Quil-A (control-Q). For both experimental groups, the final volumes of the experimental vaccines were 4ml and 12ml for Freund's and Quil-A based, respectively.

Each vaccinated and control animal was inoculated subcutaneously with 1ml and 2ml of IFX-F and IFX-Q vaccine, respectively. Both groups were vaccinated on day 0, 14 and 28 prior challenge (Figure 5.2). All goats were monitored 4h, 24, and 48h after each immunisation performing clinical and physical examinations. Body temperature and any local adverse clinical reaction observed at injection sites were recorded.

Group	IFX (ml)	PBS (ml)	Adjuvant	Volume adjuvant (ml)	Final volume (ml)
IFX-F	0.08	1.92	Freund	2	4
Control-F	-	2	Freund	2	4
IFX-Q	0.116	5.88	Quil A	6	12
Control-Q	-	6	Quil A	6	12

Table 5.1. Vaccine formulation for antigen-vaccinated and control goats. Freund's or Quil-A adjuvant was combined with IFX antigen (IFX-F and IFX-Q) or alone (control-F and control-Q) to vaccinate goats prior challenge with *T. vivax* BSF. Volumes represent vaccine reconstitution for 4 animals per dose.

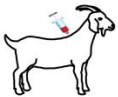




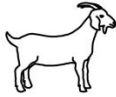
Procedure	Immunization	1st boost	2nd boost	Challenge		Euthanasia
Animals	Adjuvant			No. of parasites		
n=8	Freund			1×10 ⁴		
n=8	Quil A			1×10 ³		
						
Time	Day 0	Week 2	Week 4	Week 6	Week 7	Week 13
Samples collected	Sera			Sera	All peaks of parasitemia: sera and buffy coat	All peaks of parasitemia: sera and buffy coat
Analysis	Total IgG titration by ELISA			Total IgG titration by ELISA	Parasitemia monitored daily	Parasitemia monitored daily

Figure 5.2. Experimental design for the immunization and challenge in goats. Goats were immunized subcutaneously with IFX antigen in conjunction with Freund's adjuvant and Quil-A (n=4/group) or with the adjuvant only (n=4/group) at day 0, week 2 and week 4. Animals rested for 3 weeks and at week 7 were infected with *T. vivax* BSF for 40 days (week 8 to week 13). Sera was collected at the beginning and week 6 post immunization. Parasitaemia was recorded daily during the time of infection and sera was collected when animals showed peaks of parasitemia.

5.2.4. Collection of serum

All animals were bled to calculate their total IgG antibody titre. Sera were prepared by collecting 5ml whole blood by jugular venepuncture in an EDTA-coated tube (BD vacutainer) before the first vaccination (pre-immune serum) and 10 days after the final boost (post-immune serum). The blood was centrifuged at 13,000g for 15min collecting the serum and stored at - 20°C until use. In addition, 200µl of each sample in duplicate were transferred onto FTA Classic cards (Whatman, Cat No: WHAWB120205) and stored at RT.

5.2.5. Parasites

T. vivax Miranda strain was obtained from a frozen stock stabilate derived from sheep blood containing 64,000 parasites/ml. The strain was donated by Dr. Marta Maria Teixeira from the Department of Parasitology, São Paulo University, Brazil.

5.2.6. Challenge

The challenge of donor animals with TvMi strain was carried out one-week prior to challenge of IFX-vaccinated and control groups (36 days post-immunization). One donor animal was infected with 3.84×10^5 parasites contained in 6ml whole blood derived from the TvMi stabilate by intravenous route. The donor animal was subsequently bled every day during a week to determine the parasitaemia load by the Brenner method (Brenner, 1962).

IFX-F and control-F were challenged 43 days after the first immunisation with 10^4 trypanosomes of TvMi by intravenous route. IFX-Q and control-Q were challenged at the same time with a total of 10^3 trypanosomes of TvMi by the same administration route. The following parameters were monitored in all the animals daily: body weight (kg), temperature (C°), packed cell volume (PCV), parasitaemia and signs of any clinical manifestations.

5.2.7. Antibody titration

Total IgG antibody titres in pre- and post-immune sera were determined by ELISA as previously described (Section 4.2.4) with slight modifications. IFX-biotinylated antigen was diluted 1:2000 in PBS+0.5%BSA and incubated for 1h at RT. Nine two-fold sera dilutions were prepared starting from 1:1,000 and adding 100µl/well of each sample in triplicate. Rabbit anti-goat IgG conjugated with alkaline phosphatase (AP) (Abcam Cat No: ab6742) diluted 1:5,000 was incubated for 1h at RT. The alkaline phosphatase substrate (Sigma Aldrich, Cat No: P4744-5G) at a concentration

0.1mg/ml was diluted in ELISA buffer (10% diethanolamine, 0.5mM MgCl₂, pH 9.2 miliQ water) and added 100µl/well for 45min at RT. The plate was read at 405nm.

5.2.8. Statistical analysis

The antibody titration was performed in triplicate. All animals were analysed individually and the arithmetic mean of each group was calculated. The data are expressed as the mean \pm standard error of the mean (Ramey *et al*). The statistical significance of differences between antigen-vaccinated and control groups was calculated by Student's t-test.

5.3. RESULTS

5.3.1. Vaccine safety

Clinical and physical examinations were recorded daily during the immunization period and rectal temperature were recorded every 4, 24 and 48 hours after each vaccination. There were no severe adverse reactions observed after each vaccination with either Freund or Quil-A adjuvants, and all animals displayed normal ranges of vital parameters such as heart rate (Hr), respiratory frequency (Rf) and ruminal motility. In the case of IFX-F and control-F, all the goats displayed hyperaemia and hyperthermia and swelling of the injection site after 4 hours of each vaccination (Figure 5.3A) but without a significant increment of rectal temperature (Figure 5.3C). These local skin reactions decreased over time (at 24h and 48h respectively) after each immunization. In the case of the groups immunized with Quil-A, no systemic or local reaction was observed following vaccination (Figure 5.3B).

There was no significant difference in rectal temperature after 4, 24 and 48 hours after each vaccination with either vaccine (Figure 5.3C). However, some animals showed a slight increase of rectal temperature 24h after each vaccination. One animal from the IFX-F group (IFX-1 Freund) exhibited fever with 41.2 °C on the second vaccination. After a week following the first IFX-F immunization, mild to moderate localized pain and swelling was observed in 2/8 goats with abscess in the inoculation site. The abscess was confirmed by puncture and treatment was given daily. No abscess was observed in the control group immunized with Freund's adjuvant only.

Animals from both IFX-Q and control-Q vaccinated groups showed no significant changes in rectal temperature with absence of pain and swelling (Figure 5.3D). Physical examinations confirmed normal lymph nodes, faeces and posture without loss of body condition in all animals. Moreover, no reduction of appetite was observed during vaccination with either vaccine and the abscesses disappeared after 14 days from the first immunization. No severe systemic reactions were observed

after the second and third immunization respectively. Overall, a stronger local reaction was observed in animals immunized with IFX-F compared with IFX-Q.

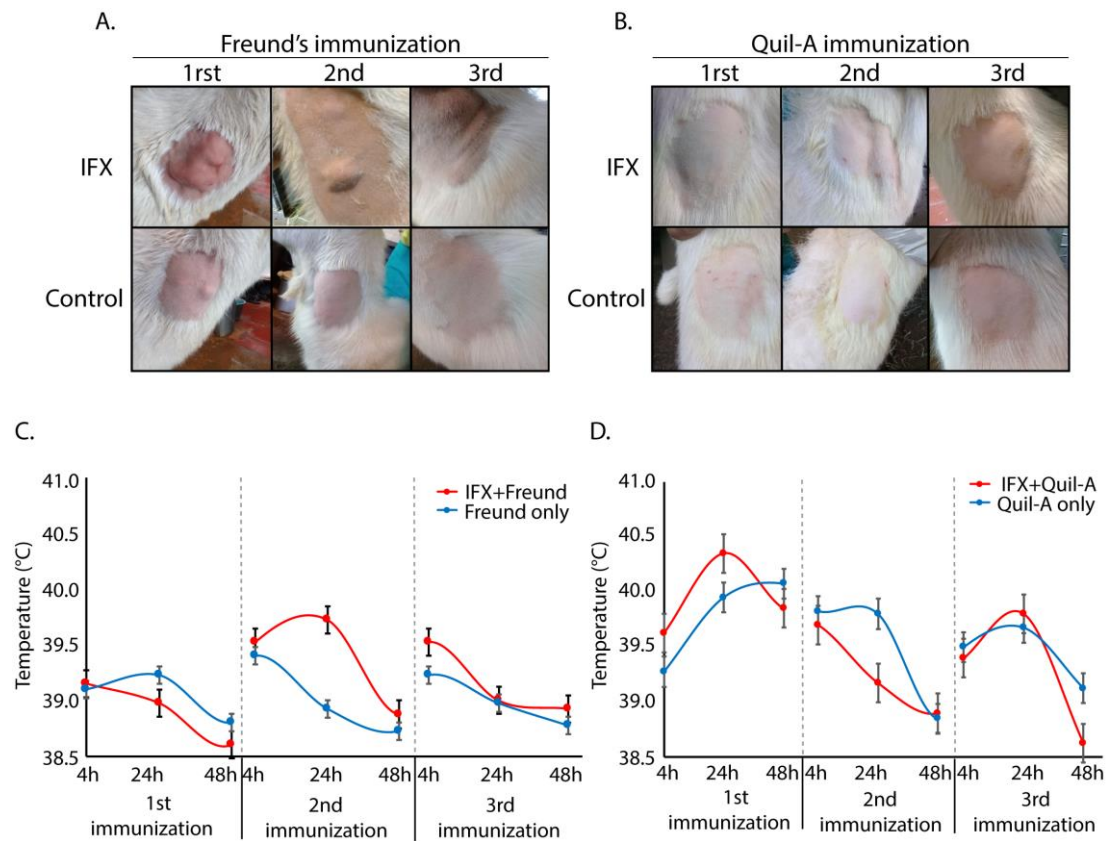


Figure 5.3. Local skin reactions at injection sites following immunization with IFX antigen in combination with Freund's (A) or Quil-A adjuvants (B). Dermal hyperaemia and increase of injection site volume was seen in some animals vaccinated with Freund+ IFX whereas no local reactions were observed on any Quil-A based vaccinated goat. Changes in body temperature at 4, 24 and 48 hours after each immunization using Freund's (C) or Quil-A (D). Each curve represents the average \pm SEM of each group (n=4).

5.3.2. Humoral immune response to an IFX + Freund's vaccine

The specific antibody response to IFX antigen was determined by measuring goat total IgG in sera from pre- and post-immunization. Absorbance values are displayed as the mean of triplicates for each goat serum in Figure 5.4. The analysis of the humoral immune response showed that the sera from IFX-F immunized goats displayed antigen-specific antibodies indicating seroconversion. All IFX-F animals showed a significantly higher specific total IgG anti-IFX antibodies at week-8 post-immunization compared to their respective samples pre immunizations ($p < 0.0001$) and control-F pre- and post-immunization ($p < 0.0001$). Moreover, goats vaccinated with Freund's adjuvant only (control group) did not produce any IFX-specific antibodies. Indeed, all pre-immunization sera showed no response, comparable with control adjuvant-only animals pre- and post-vaccination. The mean OD value for the vaccinated group post-immunization was 0.922 ± 0.04 (mean \pm SEM), for the pre-immune vaccinated group 0.044 ± 0.001 , for the control group post-immunization 0.042 and for the control group pre-immunization 0.054.

After the third boost vaccination, the IFX-specific antibody titre increased, with IFX-1 and IFX-3 goats displaying 2-fold higher titres than IFX-2 and IFX-4 animals. The difference in OD values between these two subgroups was statistically significantly ($p < 0.05$). Despite this, all vaccinated animals showed a half-maximal titre of 1: 80,000 (4.90 Log_{10} dilution) and endpoint dilution of 1: 2,560,000 (6.4 Log_{10} dilution). The seroconversion of IFX-antibodies in vaccinated goats was detected at 10 days after the last immunization (week 8). However, it may be that seroconversion is achieved in a shorter period than this.

The humoral immune response indicated that immunization of goats with IFX recombinant protein in the presence of Freund's adjuvant strongly induced specific antibodies. IFX seroconversion increased upon immunization and was detectable after 6 weeks from the first immunization.

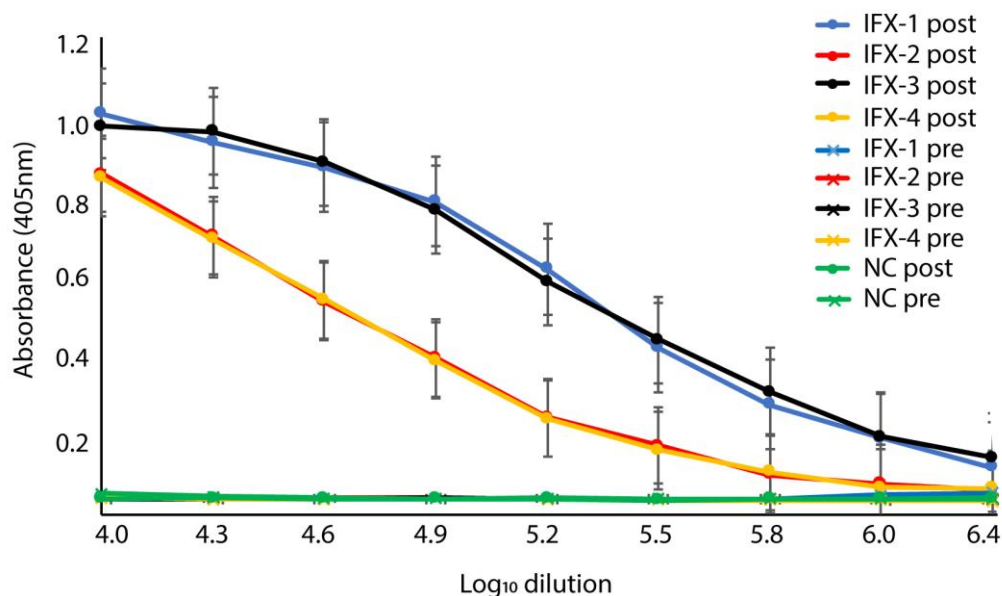


Figure 5.4. Antibody titration of *T. vivax* IFX antigen-specific antibodies produced in goats before challenge. The level of total IgG was measured by ELISA on each animal individually using two-fold serially diluted sera. The absorbance (405nm) is shown as the mean \pm SEM of triplicates for each goat serum.

5.3.3. Evaluation against homologous challenge with *T. vivax*

Vaccinated and control groups were experimentally infected with *T. vivax* bloodstream-forms to evaluate the protection properties of the IFX antigen. Ten days after the last IFX vaccination boost, all animals were infected with TvMi strain (10^4 and 10^3 bloodstream trypomastigotes for Freund and Quil-A vaccinated groups, respectively) and parasitaemia was recorded daily. *T. vivax* challenge led to acute infection in all IFX-vaccinated and control animals.

The prepatent period observed in all goats from both IFX-F and control-F groups was 6 days compared to 8 days for IFX-Q and control-Q. The first peak of parasitaemia was observed in all animals for vaccinated and control groups at 8 dpi with a mean of 4.66×10^6 and 4.83×10^6 parasites/ml for IFX-F and control-F groups respectively (Figure 5.5). Likewise, the first peak of parasitaemia observed in both groups

vaccinated with Quil-A adjuvant was at 8 dpi showing 3.33×10^6 and 2.04×10^6 parasites/ml for IFX-Q and control-Q, respectively. There were no significant differences in mean parasitaemia levels between IFX-F and control-F groups ($p = 0.89$) and between IFX-Q and control-Q groups ($p = 0.36$) during the first peak.

Goats remained infected during the course of infection and number of parasites fluctuated. Parasitaemia levels (Figure 5.5) showed no significant differences when IFX-vaccinated groups were compared with their respective controls for either vaccine ($p = 0.317$ and $p = 0.861$ for Freund and Quil-A based vaccine, respectively). Overall, goats from the antigen-vaccinated and the control groups presented similar parasitaemia patterns with peaks characteristic of an infection with African trypanosomes. Animals from the Freund-based vaccine presented approximately 6 peaks of parasitaemia (min=5, max=7 peaks respectively) throughout the experimental period. Likewise, animals from the Quil-A-based vaccine showed 7 parasitaemia peaks (min=3, max=7 peaks respectively). Regardless the adjuvant used for the vaccine, the parasitaemia peaks were observed between 8-40 dpi appearing every 3-4 days (Figure 5.5). Interestingly, one IFX-F goat showed the greatest number of peaks and also the highest number of parasites detected during the time of infection (7 parasitaemia peaks and 1.2×10^7 parasites/ml at 14 dpi-peak 3).

There was a reduction in the number of parasites after 20-22 dpi in animals immunized with either vaccine. During these non-parasitemic periods trypanosomes were undetectable in the blood and this was observed in all animals and lasted 7 days for Freund-based and 8 days for Quil-A-based vaccines before the next peak.

Besides the parasitaemia levels monitored daily, other parameters like rectal temperature, weight and PCV were observed during challenge (Figure 5.6A, B). An increase of the rectal temperature was observed at 8 dpi in all goats from IFX-F and control-F groups ($40.23 \pm 0.05^\circ\text{C}$ and $40.33 \pm 0.05^\circ\text{C}$ respectively) without significant differences between both groups ($p = 0.25$). At this same time, animals from IFX-Q and control-Q also showed a rise in rectal temperature with $40.25 \pm 0.25^\circ\text{C}$ and $40.03 \pm 0.09^\circ\text{C}$, respectively with no significant differences between them ($p = 0.42$).

At 8dpi, the PCV values were 27.5% for the IFX-F and 24.5% for the control-F displaying significant differences between groups ($p = 0.03$). However, both PCV values were within normal parameters (18-38% in goats). The comparison of PCV values between IFX-Q and control-Q showed no significant difference at 8dpi ($p = 0.55$) with a mean of 27.75% and 25.25% for each group, respectively.

The slight rise of the body temperature coincided with the first peak of parasitaemia for all animals vaccinated with Freund's. Goats showed fluctuations but no significant differences in PCV values during the course of infection displaying a mean of 22.7%, 21.8%, 23.55% and 21.7% for IFX-F, control-F, IFX-Q and control-Q, respectively ($p > 0.05$). The IFX-F group displayed fluctuations in rectal temperature (mean $39.49 \pm 0.11^\circ\text{C}$) with a rise in the last day of the experiment except for one animal (goat IFX-3). The latter animal showed no significant changes in rectal temperature or PCV despite displaying the highest number of parasites detected in blood. A similar scenario was observed in the control-F with fluctuations in temperature but under normal parameters (mean $39.59 \pm 0.10^\circ\text{C}$) with few exceptions at specific days after infection only. The IFX-Q group also showed a rise in temperature at day 30 (mean $40.25 \pm 0.33^\circ\text{C}$) and at day 40 post-challenge (mean $40.22 \pm 0.18^\circ\text{C}$).

There was a rise in rectal temperature observed in the control-F group at 40 dpi that coincided with the last peak of parasitaemia but not for the other groups. Overall, there was no significant change in the rectal temperature in *T. vivax*-infected goats with either vaccine when compared antigen-vaccinated and adjuvant-vaccinated animals (Freund: $p = 0.38$ and Quil-A: $p = 0.47$). The rise of this parameter was not directly correlated with the increase of parasites in blood except for the first peak of parasitaemia only for either vaccine.

The weight of vaccinated goats was also monitored (Figure 5.6C, D) but this showed no significant changes in the mean weight between IFX-F (30.77kg), control-F (30.25kg), IFX-Q (29.91kg) and control-Q (28.7kg) during the course of infection ($p > 0.05$). Moreover, fluctuations were observed on each animal with no significant

differences observed during the challenge ($p > 0.05$). Nonetheless, there was a significant change observed between the mean weight monitored at pre-challenge and 4 dpi for IFX-F ($25.25 \pm 1.52 \text{ kg}$ vs $30.5 \pm 0.53 \text{ kg}$ respectively, $p = 0.02$) and control-F ($24.1 \pm 0.74 \text{ kg}$ vs $29.98 \pm 0.88 \text{ kg}$, $p < 0.001$). Despite this difference, weight of all animals was within normal parameters regardless the experimental group. There were no significant differences in weight when IFX-Q and control-Q groups were compared ($p > 0.05$).

Physical examinations of the goats from all experimental groups indicated that the animals did not showed any symptomatic signs despite obvious parasitemia. All goats showed absence of diarrhoea and enlargement of lymph nodes and presented normal feed intake, rose mucus membrane with small amount of mucus secretion, Hr and Rf remain within normal parameters and the goats remained alert and apparently healthy.

All the goats immunized with either vaccine and challenged with TvMi developed acute parasitemia without any clinical manifestations and with 100% survival. The animals from all experimental groups showed high parasitemia demonstrating that subcutaneous vaccination with IFX recombinant protein in combination with Freund's or Quil-A adjuvant did not induce a protective immune response against homologous challenge.

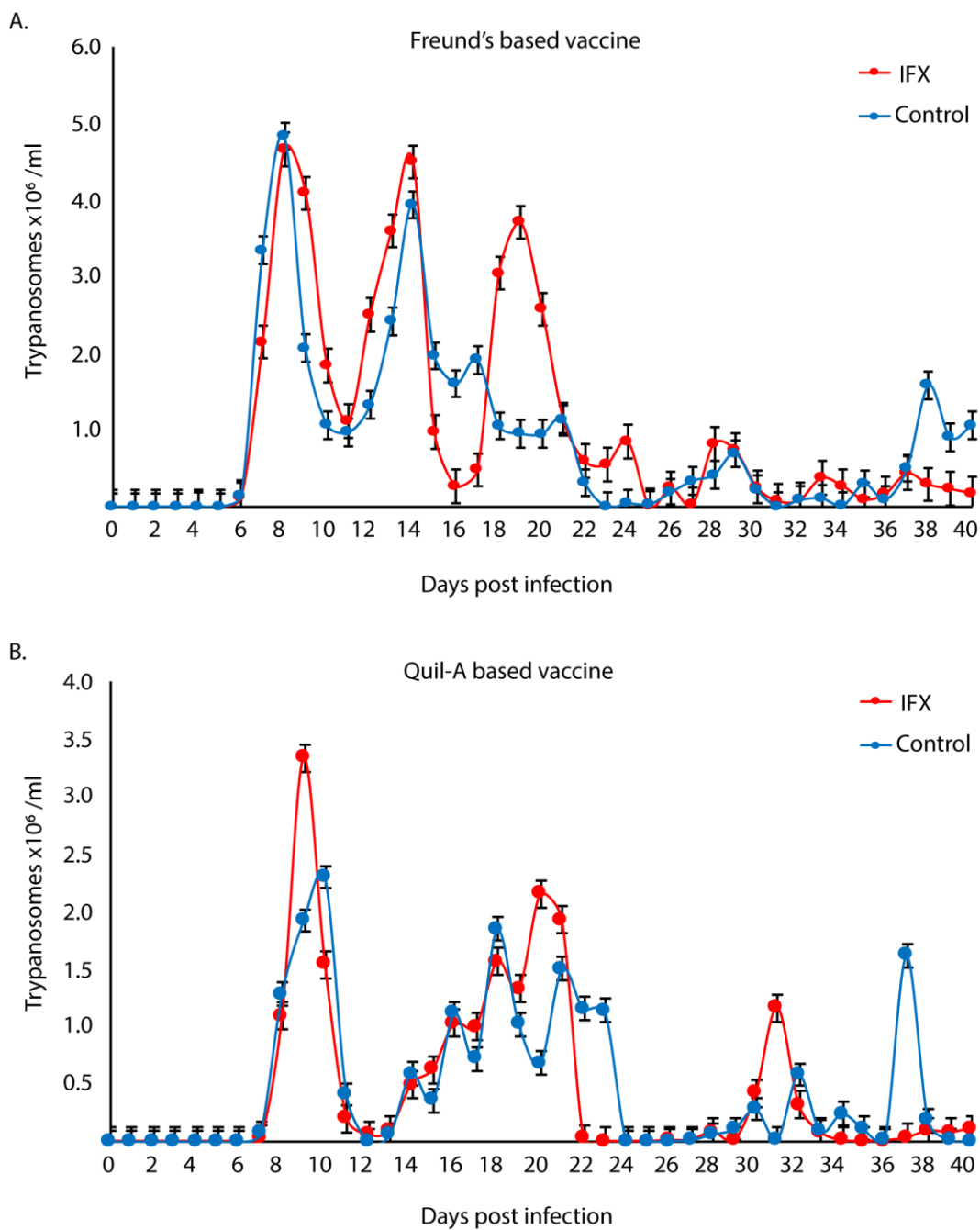


Figure 5.5. Parasitaemia levels of infected goats previously immunized with **A)** Freund's or **B)** Quil-A adjuvant during the course of infection (40 days). All animals showed peaks of parasitaemia in antigen-vaccinated and adjuvant-only groups (n=4/group). Daily parasitaemia is shown as the mean number of parasites/ml in blood for each group.

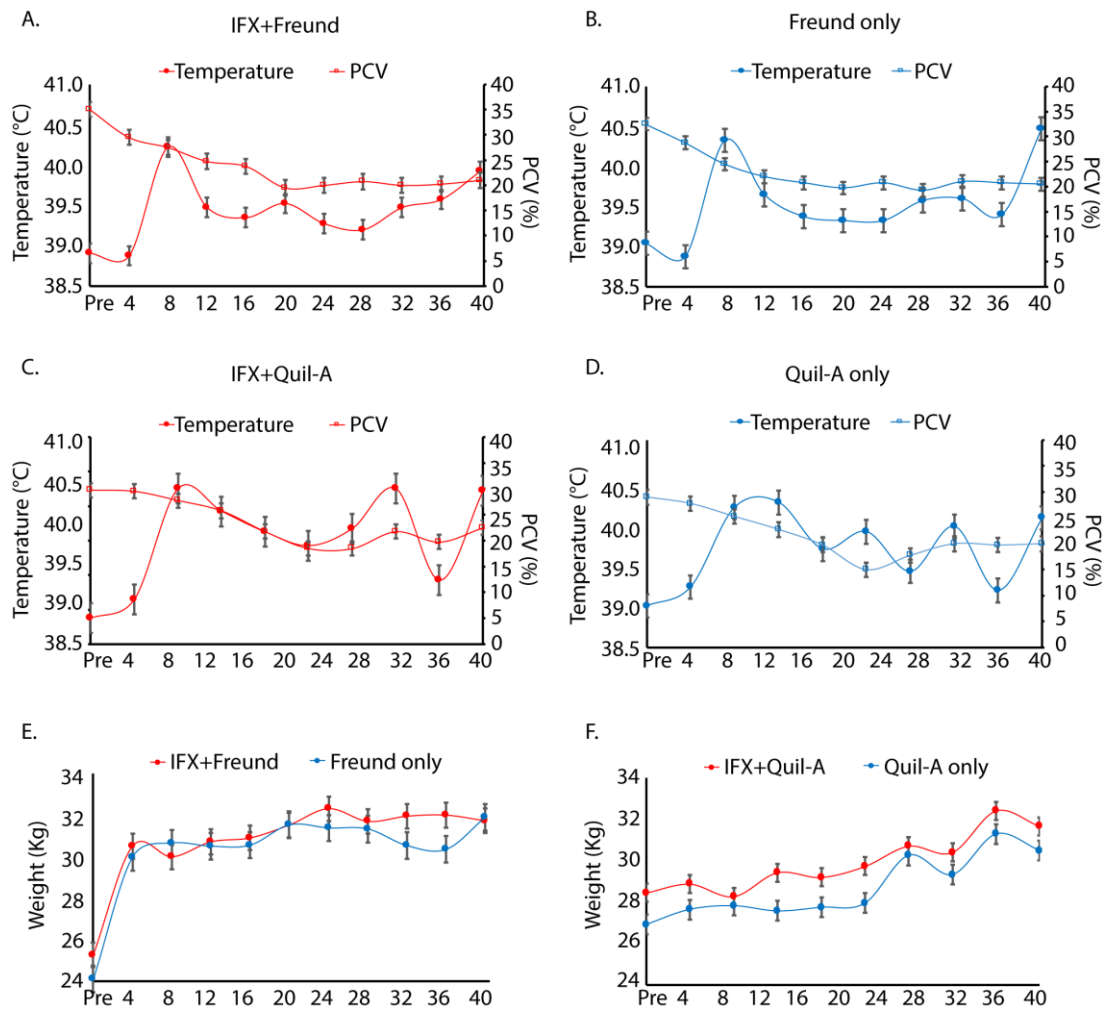


Figure 5.6. Rectal temperature and PCV values during the course of infection of goats vaccinated with IFX +Freund (A), Freund only (B), IFX +Quil-A (C) and Quil-A only (D). Weight values during the course of infection of goats immunized with IFX in combination with Freund (E) and Quil-A (F). The values are represented as mean \pm SEM of each group (n=4/group).

5.4. DISCUSSION

The aim of this chapter was to examine whether a FamX protein that protected mice from *T. vivax* infection (IFX) could also protect a natural host against *T. vivax* using a goat model. The animals were immunized with IFX co-administrated with one of two adjuvants prior to challenge. Control groups were immunized with the adjuvant only. Ultimately, goats immunized with either vaccine showed no reduction in parasitaemia during the course of infection.

The design of an effective vaccine depends on two critical parameters; the antigen that can elicit immune effectors and the selection of an adjuvant that can enhance its efficacy. The safety of the vaccine formulation is also of important concern in developing a therapeutic vaccine. In this trial, the goats were vaccinated subcutaneously with IFX antigen in the presence of Freund or Quil-A adjuvant. The comparison based on clinical and physical examinations showed a stronger local association of IFX-F vaccinated animals with hyperaemia and hyperthermia compared to the control. In contrast, no local reactions were observed in animals vaccinated with Quil-A. These findings corroborate previous animal trials that associated Freund's adjuvant formulations with lesions (Broderson, 1989) increased inflammation and toxicity are also typically observed (Broderson, 1989; Aguilar and Rodriguez, 2007). Despite these side effects, it has been demonstrated that FCA is a potent adjuvant and, due to its mycobacterial component, it enhances the stimulation of cell-mediated immunity via the activation of TLR. FIA is the alternative of FCA but lacks killed mycobacteria. FIA has been widely used in veterinary vaccines formulations against viruses and parasitic infections (Singh and T O'Hagan, 2003).

Quil-A, a saponin classified as an ISCOM, has been showed to produce less toxicity in terms of vaccine safety (Sun *et al*, 2009). Although the immunological mechanism of action is still unknown, Quil-A certainly stimulates B-cell proliferation and antibody production, potentiates the immunogenicity of the antigen and stimulates a strong T-cell response. While Quil-A is not accepted for human vaccine applications, it is the most widely adjuvant used for veterinary vaccine formulations (Sun *et al*, 2009).

Comparisons of adjuvants in vaccine experiments against *T. brucei* and *T. cruzi* demonstrated that Quil-A was the most effective (Scott *et al*, 1984; Lubega *et al*, 2002).

Goat sera were analysed for the presence of IFX-specific antibodies after immunization with the antigen co-administrated with Freund's. The results showed that IFX seroconversion was detected at week 6 from the first immunization with high IFX-specific IgG antibody titres. This is consistent with previous studies demonstrating a specific antibody production after immunization with FCA in experimental infections with *T. brucei* (Lubega *et al*, 2002). Due to the ability of Quil-A to induce strong antibody production (Sjölander *et al*, 2001), after immunizations against other parasites like against *F. hepatica* (Haçarız *et al*, 2009) and *T. congolense* (Authié *et al*, 2001), the post-immune sera of IFX-Q animals was also expected to contain specific anti-IFX IgG antibodies. It is worth noting that, due to a lack of commercially available specific conjugates targeted for goats and a poor cross-reactivity with conjugates from other species (i.e. anti-bovine antibodies), specific IgG isotypes were not measured and, instead, only total IgG was determined. Nonetheless, it would be interesting to measure IgG isotypes in order to understand the type of humoral response IFX antigen can induce. Based on the adjuvants chosen for the formulation, it might be surmised that a IFX+ Quil-A vaccine stimulates a mixed Th1/Th2 response with higher titres of both IgG1 and IgG2a antibodies (Sun *et al*, 2009), while a IFX+F vaccine produces a Th1 and Th2 immune response with a greater stimulation of IgG1 antibodies. Nonetheless, this chapter confirmed the immunogenicity of the IFX+F vaccine in goats.

Despite the promising results in a murine model, this chapter indicates that IFX antigen in combination with either Freund or Quil-A adjuvants does not provide protective immunity in challenged goats. During the challenge, weight and PCV from antigen-vaccinated and control groups remained normal with no significant differences. Moreover, no pyrexia or differences in food intake were observed even during peaks of parasitaemia. These outcomes are unlike previous studies in which African Dwarf goats were infected with *T. vivax* Y486 strain (Zwart *et al*, 1991) and

other *T. vivax* infections in different breeds of goats (van den Inch *et al*, 1976; Saror, 1980). Other reports indicate a significant decrease in body weight and PCV when goats were experimentally infected with *T. congolense* (Faye *et al*, 2005). In this chapter, the mean prepatent period was 7 dpi and the first peak of parasitaemia appeared 8 dpi for both experiments. These findings are consistent with other *T. vivax* experimental infections in natural hosts like bulls (Camejo *et al*, 2014), goats (Adeiza *et al*, 2008; Bezerra *et al*, 2018), cows (Schenk *et al*, 2001), zebu (Dagnachew *et al*, 2015) and donkeys (Rodrigues *et al*, 2015). However, there are some reports reporting a pre-patent period for experimentally infected goats of 5.3 days (Adeiza *et al*, 2008) and 4.22 days (Osman *et al*, 2008).

The fact that during the course of infection animals in both vaccinated and control groups parasitaemia was the only sign of infection, and the goats did not present any pathological features typical of trypanosomiasis suggests that this strain of *T. vivax* (TvMi) is less virulent than others used previously in similar experiments. Animals with good physical and nutritional conditions can present a favourable prognosis during *T. vivax* infection in sheep and cows (Katunguka-Rwakishaya *et al*, 1999; Paiva *et al*, 2000). Certainly, previous studies in livestock naturally infected with TvMi strain (Dávila *et al*, 2003; Martins *et al*, 2008; Cuglovici *et al*, 2010) indicate that TvMi differs from other South American strains by the absence of clinical signs, but nevertheless causes acute infection with high parasite burden.

There are several explanations for the failure to confirm IFX as a vaccine candidate against natural *T. vivax* infection. The parasite clearance in a murine model suggested that its immunogenicity is a crucial factor to elicit a robust immune response. This is of high importance since the immunogenicity refers to the ability of the antigen to provoke an immune response (Mahanty *et al*, 2015). However, the vaccine immunogenicity relies on several factors. One extrinsic factor that can contribute to the immunogenicity is the antigen dose (De Groot and Scott, 2007). In previous studies identifying vaccine candidates against *T. vivax* and *T. brucei* in a goat model, doses of 10 μ g, 20 μ g and 40 μ g (Rovis *et al*, 1984) showed no seroconversion of IgG antibodies and failure of immunoprotection. Nonetheless, other vaccine attempt in

cattle against *T. brucei* infection demonstrated that a single inoculum of 200µg of a variant-specific surface antigen (VSSA) co-administrated with an optimal adjuvant gave protection after challenge with 10^4 parasites (Wells *et al*, 1982). VSSA antigen was previously tested in mice showing protective immunity after vaccination with weekly doses of 100µg with FCA (Cross, 1975). This examples showed that the dose and antigen concentration are important for the immunogenicity. Indeed, an antigen is more immunogenic when a low concentration is needed to induce a robust response (Mahanty *et al*, 2015). Vaccination of mice with IFX gave sterile immunity using high doses of 50µg but a lack of a protective response in goats vaccinated with 100µg/dose. This suggests that dose to vaccinate goats was insufficient or that IFX is not too immunogenic as high doses are needed to observed a protective effect in mice. The latter explanation is preferred since it has been demonstrated that IFX is not immunogenic in naturally infected cattle (unpublished data).

Another important extrinsic factor that contributes the immunogenicity of the antigen is the administration route. (De Groot and Scott, 2007). IFX elicited a long-lasting immunity against *T. vivax* infection in BALB/c mice over almost 150 days after the last immunization. To achieved this, animals were immunized using alum intraperitoneally and protection was observed when challenged using intravenous and subcutaneous route. In the case of the experiments in goats, both vaccines (using Quil-A and FCA) were administrated subcutaneously and parasites administrated intravenously. This clear difference in the vaccine administration route can play an essential role in the development of a protective response. It is well known that different routes of vaccine administration can elicit a different response as in the inoculation site distinct types of antigen presenting cells (APC) can be present like specific DC subsets (Coffman *et al*, 2010; Bretscher, 2014). This means that APCs are important for the type of immune response generated and for the polarization of T naïve cells into mature Th1 or Th2 cells (Spellberg and Edwards Jr, 2001).

When testing vaccine candidates, the infection rate is important to evaluate its effectiveness. An infected tsetse fly can carry 10^4 metacyclic parasites in a single bite. In this regard, challenge trials with fewer than 10^4 parasites might bias the results

(Magez *et al*, 2010). Sterile immunity in IFX-vaccinated mice was achieved when animals were challenged with 10^2 and 10^3 parasites, while the goats were challenged with 10^4 and 10^3 parasites from a blood stabilate. Hence, the positive outcome from the murine infection might not reflect what normally happens in a natural infection with African trypanosomes due to the low infection rate used.

This chapter has demonstrated that immunized goats seroconverted for IFX antigen, with high antibody titres indicating effective polyclonal B-cell activation. These specific antibodies are a key part of an optimal immune response but clearly they are insufficient to produce a protective effect. It might be that even though high levels of total IgG anti-IFX were found after the last boost in goats, there is a weak neutralizing antibody response against IFX-specific epitopes, or that the humoral immune response is not strong enough for a long term response. In this regard, it is necessary to measure the antibody levels before and after challenge to confirm a long lasting humoral response. In other words, the level of the specific antibodies must be maintained during the infection even in the absence of circulating trypanosome antigens (Magez *et al*, 2010). The splenic B-cell depletion and as a consequence, the concentration of specific IgG antibodies after challenge might probably play a key role in why IFX failed to produce protective immunity in experimentally infected goats (Blom-Potar *et al*, 2010).

Experimental bovine trypanosomiasis with *T. vivax* demonstrated that there are differences in the serum levels of antibodies. Indeed, during the first days of an infection with *T. vivax*, there is an increase in the serum levels of IgM but it drops approximately 6 dpi. In the case of IgG isotypes, serum IgG2 was significantly lower compared to the levels in the control group (non-infected animals) but IgG1 showed no differences between both groups (Tabel *et al*, 1981). This could suggest that IgG1 antibodies could be more important than IgG2 during the infection, favouring a Th2-type response. However, it has known that a Th1 response is necessary to control parasitemia in a murine model and that the antibody response is TNF-dependant (La Greca *et al*, 2014). This has been demonstrated comparing the immune response between wild type and TNF^{-/-} mice and a possible explanation could be that TNF

affects the parasite fitness that could facilitate the parasite opsonization. The important role for parasite control and host survival has also been demonstrated in *T. brucei* and *T. congolense* infections (Magez *et al*, 1993; Magez *et al*, 1997; Iraqi *et al*, 2001; Magez *et al*, 2006). In mice, IFX produced high levels of IgG2a compared to IgG1 and, contrary to all the AJ proteins analysed in Chapter 3 and 4, were not detected by serum from naturally infected animals. However, all goats were seroconverted with total IgGs detected after the last boost. Among *T. vivax* cell-surface proteins, invariant proteins can be of variable immunogenicity only those that elicit the strongest response are considered to be immunodominant antigens. This phenomenon called a dominance hierarchy (Frank, 2002) and has a fundamental effect since the nature of the epitopes can be crucial to induce protection (Mahanty *et al*, 2015). Here, it is suggested that the goat immune system detected IFX epitopes and produced specific antibodies but other, more immunodominant proteins such as AJ6 might elicited a stronger response still.

The differences in the immune response between a mice and goats should also be taken into consideration. As stated in the Chapter 4, IFX can confer sterile immunity against *T. vivax* infection in BALB/c mice, which are prone to Th2-type responses. This means that they are likely to produce higher titres of IgG1 than of IgG2a, irrespective of the adjuvant used (Mosmann and Coffman, 1989). Moreover, as Th2 clones, they synthesize cytokines like IL-6, IL-4 and IL-5, while TNF- α levels are not detectable. However, vaccination with IFX in combination with alum and Quil-A independently showed protective responses with an increase IgG2 titres suggesting towards a Th1 immune response and probably producing high TNF- α levels. This last cytokine might be induced by IFX in mice but not necessarily in goats. In other words, a possible explanation for the negative outcome here is that the IFX vaccine did not stimulate caprine TNF- α . This explanation relies on the fact that TNF- α levels are increased during experimental infections in bulls with *T. vivax* (Camejo *et al*, 2014) and has been shown to be necessary for parasite control in C57BL/6 TNF- $^{-/-}$ mice (La Greca *et al*, 2014). As no analysis of the cytokine levels or T-cell response in response to IFX immunization was possible, it remains important compare the type of cellular response in murine and natural models.

5.5. CONCLUSION

This vaccination and challenge experiment in a goat model confirmed the seroconversion of total IgG antibodies detected 6 weeks from the first immunization when animals were vaccinated with IFX co-administrated with FCA. However, after challenge with TvMi strain all vaccinated animals, regardless of the adjuvant applied, were and developed acute infection with peaks of parasitaemia typical of *T. vivax* infection. Therefore, vaccination with IFX did not confer protective immunity in the goat contrary to the protection in acute and chronic infection in a murine model. This shows that IFX antigenicity is not sufficient to confer immunity and other immunological factors not identified must be involved in the process.

CHAPTER 6

General Discussion

African trypanosomes are obligate extracellular parasites that have developed a complex mechanism to evade the host immune response by antigenic variation. The latter provides a robust response that leads to chronic infection and has been considered the major impediment for vaccine development (Tabel *et al*, 2013). Since these proteins are exposed at the cell surface and highly immunogenic, VSGs proteins were seen as the key to producing a vaccine. However, because VSGs switch and are constantly replaced in the parasite infrapopulation, it has been well established that vaccination against these proteins will never confer sterile immunity or protection (Magez *et al*, 2010). To date, there is no vaccine for any African trypanosome and chemotherapy remains the only disease therapy. These drugs to treat trypanosomiasis, however, are toxic in treated animals and produce resistance in parasite populations.

There have been several attempts to discover antigens among non-VSG proteins, despite the common belief that the barrier produced by the highly immunogenic VSGs shield invariant proteins also located at the cell-surface. Invariant surface proteins uniformly expressed were identified to be immunogenic but conferred only partial protection (Mkunza *et al*, 1995; Lança *et al*, 2011). This may be because the mechanisms used by African trypanosomes to avoid the immune system also encompasses other strategies apart from VSGs. In fact, it seems that the parasites have developed two main protective methods to escape from the antibody-mediated process. The first is antigenic variation and the second is immunosuppression, B-cell apoptosis, inhibition of the innate immune system by adenylate cyclases and other trypanosome-derived factors (La Greca and Magez, 2011). The decrease of B-cell population in peripheral organs also needs to be taken into consideration as is one of the characteristics during an infection with *T. vivax*. This B-cell exhaustion, not compensated by new B-cells migrating from the bone marrow, decrease the population of lymphocytes during the infection. This event affects the maturation of

pro-B into pre-B precursors and not the migration of lymphocytes from the bone marrow to the periphery. Despite the origin is still unclear, B-cell depletion is another mechanism of immune evasion that lead to an inefficient parasite clearance (Blom-Potar *et al*, 2010).

In this sense, the development of an effective and protective vaccine against this disease should be focused on conserved, invariant antigens located at the cell-surface that could induce a robust protective antibody response and are constitutively expressed (Black and Seed, 2001). In addition to their cell-surface location, such antigens must be accessible to specific antibodies in order to develop a successful immune response. Thus, one of the steps in vaccine design is the discovery of species-specific antigens as potential targets. Using the reverse vaccinology approach, the methodology and analysis presented in this thesis has approached this challenge and contributed to the pursuit of an African trypanosomiasis vaccine.

In Chapter 2, bioinformatic analysis identified potential cell-surface antigens within the *T. vivax* genome from a large panel of species-specific proteins divided into families. Population genetics confirmed that some antigens were universal and displayed stable polymorphism across diverse clinical isolates. In Chapter 3, the immunogenicity of selected cell-surface antigens was assayed based on epitope mapping, revealing that one family, FamX, has the highest number of immunogenic proteins in natural *T. vivax* infections across Africa and South America. These results were concordant with in silico B-cell epitope predictions. In Chapter 4, recombinant forms of four FamX proteins used to vaccinate mice prior to parasite challenge to evaluate their potential protective role. This demonstrated seroconversion against all four 'AJ' proteins. The parasite challenge led to partial protection only when animals were vaccinated with AJ6 coadministered with Quil-A adjuvant. Moreover, AJ6 was the only antigen to be robustly located at the *T. vivax* cell-surface indicating that it was accessible host IgG antibodies. Lastly, in Chapter 5, IFX, another FamX protein, not identified in the immunogenicity assay but proven to protect mice completely, was used to coadministered to goats with Freund's adjuvant and Quil-A before challenge with a Brazilian *T. vivax* strain. While the animals showed

seroconversion to IFX with high IgG antibody titres, there was no protective immune response.

The work presented in this thesis can be extended in three ways: I) the discovery of new antigens based on B-cell epitope identification by other experimental methods or by taking into consideration proteins below the threshold from the peptide array results (described in Chapter 3), II) evaluating in more detail the immune response to the already discovered antigens (described in Chapter 4) or new antigens by immunological and molecular methods and III) applying potential vaccine candidates in a DNA vaccine rather than protein subunit vaccine.

The antigen discovery analyzed in this thesis in principle based on the linear B-cell epitope mapping can be also identified using other approaches. The peptide microarray is classified as a functional approach since it recognizes linear B-cell epitopes based on the antibody-antigen interaction. The identification of new epitopes can also be achieved using other functional experiments like nuclear magnetic resonance (NMR) spectroscopy or surface display methods (Ponomarenko and Van Regenmortel, 2009). The major advantage of NMR spectroscopy is that it can detect weak and strong interactions between the complex (Van Regenmortel, 2009) while the surface display assays based on the binding capacity between peptides displayed in a bacteriophage-surface and monoclonal antibodies although other surfaces can also be used due to the nature of the different antigens (Ahmad *et al*, 2016).

In addition to functional methods, structural approaches including X-ray crystallography recognize conformational epitopes by the structure of the antibody-antigen complex. This approach resolves the atomic interaction between antigen and antibody, and is the best technique for antigenic determinants, although it requires sophisticated machinery and crystals can be difficult to produce (Van Regenmortel, 2009). The identification of conformational rather than linear epitopes could benefit the discovery of proteins since they are the greatest percentage of epitopes found in proteins. Despite this, linear epitopes are usually identified due to their easy

recognition that can also be corroborated by *in silico* predictions. In this sense, the linear epitopes that did not pass the significance threshold in the peptide array analysis (Chapter 3) might also be taken into account for further experiments. Indeed, the discovery of AJ6 antigen was based on the raw p-value rather than the adjusted p-value from the analysis, meaning that there might be other antigens that can potentially have a protective role during a *T. vivax* infection.

The evaluation of the murine immune response presented in this thesis focused on recombinant AJ antigens and a possible polarization towards a Th1 or Th2 response when different adjuvants were coadministered. Animals vaccinated with Quil-A were then challenged to determine their potential protective effect. Moreover, the protective role of the IFX antigen was assessed in a natural host also describing the humoral immune response. Further experiments can be assess the antigens analyzed for a better understanding of the immunological processes and their role in a potential protective immunity. It has been established that both CD4⁺ and CD8⁺ T-cells are fundamental for controlling African trypanosomiasis (Onyilagha and Uzonna, 2019) and, in fact, it is suggested that future vaccines against African trypanosomes should generate T-helper cells towards a Th1 response (Tabel *et al*, 2008). However, experimental bovine infections demonstrated that during a *T. vivax* infection, there is a reduction of IgG2 antibodies suggesting that the previous assumption may work for *T. brucei* or *T. congolense* vaccines, but not necessarily for *T. vivax* (Tabel *et al*, 1981). In this regard, the T-cell response to novel antigens should also be investigated. In a murine model, T-cell proliferation assays can compare stimulated and unstimulated cells from vaccinated mice after an *in vitro* stimulation to measure cellular immunity. In addition, the T-cell response against AJ antigens and IFX could be assessed by quantifying different types of T-cell populations like regulatory T-cells (T_{regs}) by fluorescence-activated cell sorting (FACS). Analysing the cytokine profile against IFX using the same panel of cytokines and including others not evaluated in Chapter 3, e.g. IL-2 and nitric oxide, which are known to play a fundamental role during an infection with African trypanosomes (Stijlemans *et al*, 2017) should also be considered for future work.

Another approach for vaccine design is the development of a DNA vaccine rather than a protein vaccine. Typically, DNA vaccines are composed of bacterial plasmids that encode the protective antigen and are taken up by mammalian cells where proteins are expressed (Ivory and Chadee, 2004). DNA vaccines have different advantages especially in parasitic diseases such as inducing a strong long-lasting immune response, utility in the use of multivalent vaccines, use of genetic adjuvants and others. In fact, DNA vaccines has been applied against several parasitic infections like *L. amazonensis* (Campbell *et al*, 2003), *L. major* (Campos-Neto *et al*, 2002), *Plasmodium spp* (Parker *et al*, 2001; Kumar *et al*, 2002) and *Schistosoma mansoni* (Dupré *et al*, 2001). Thus, DNA vaccines might also be designed to express AJ proteins, perhaps co-administrated with a genetic adjuvant to enhance co-stimulatory molecules like cytokines and a stronger T-cell response.

This thesis has focused on species-specific antigens expressed mainly in bloodstream-forms. Yet, when a tsetse fly bites the mammalian host, it inoculates metacyclic-form parasites rather than bloodstream-forms. Therefore, antigen discovery directed towards metacyclic-stage proteins might also be a useful approach to AAT vaccine design (Magez *et al*, 2010). Specific gene families expressed mainly in *T. vivax* metacyclic-forms such as Fam27, Fam35 and Fam43 could be targeted for vaccine development if their cell-surface location is confirmed.

The design of an effective vaccine against *T. vivax* relies on a sophisticated understanding of host-parasite immune interaction. The immune evasion strategies, pathogenicity and the role of specific immunological factors involved in trypanosomiasis have been characterized largely for *T. brucei* and, to a lesser extent, *T. congolense* only (Stijlemans *et al*, 2016). This is mainly because murine and bovine models are available for both species (Morrison *et al*, 2016). Although such models bring huge advantages in terms of immunological research, it may not be sensible to extrapolate this information to *T. vivax*, assuming that it has the same mechanisms. While a murine model for *T. vivax* has been developed to overcome this problem (Blom-Potar *et al*, 2010) there is still no natural host infection model. This will be

crucial to understanding the host-parasite interactions and immuno-manipulation during a *T. vivax* infection.

Natural hosts are also crucial in validating potential vaccine candidates that have proven efficacious in laboratory rodents. In general, after the identification of potential antigens against a particular pathogen, the protective role and immune protection should be tested in small and large animals. Nonetheless, it is more convenient to do vaccine trials in rodents due to their easy handling, low cost and large sample size (Hein and Griebel, 2003). Ultimately, however, in the case of AAT, trials on its natural host like cattle, goats and sheep are essential and ensure that we understand any protective immunity properly. Moreover, vaccine trials in livestock permit a proper evaluation of vaccine safety and potential risks during vaccination, hazard of contamination, influence of chemotherapy with vaccination and potential revaccination (Pipano, 1995).

Vaccines against protozoal infections can bring enormous benefit to livestock production and also benefit humans exposed to zoonotic diseases in endemic areas (Meeusen *et al*, 2007). Veterinary protozoal vaccines have been successfully produced based on live or attenuated pathogen strains (Meeusen *et al*, 2007). However, since vaccines often require constant reapplication, commercial vaccines can be uneconomical to use and mutations in vaccine strains can lead to reversion to virulence. Recombinant vaccines are beneficial since they do not require a cold-chain for transportation as live vaccines do (Jenkins, 2001) and, although subunit vaccines are yet to produce better results against protozoal pathogens than live or attenuated vaccines, (although perhaps mitigating disease pathology), they remain the objective. Many vaccine candidates for AAT have been tested in murine and bovine models mainly but, to date, no effective vaccine exists (Stijlemans *et al*, 2017), leading some to suggest that immunosuppression may make the development of an effective vaccine impossible (Black and Mansfield, 2016).

Assuming that this is ultimately proven too pessimistic, it will be difficult to deploy a vaccine against AAT since pharmaceutical companies are unwilling to invest in

diseases that affect poorest people and cannot generate profit, despite the huge impact AAT has on agricultural production in a great part of Africa (Ilemobade, 2009). Moreover, the massive wild animal reservoir of African trypanosomes ensures constant sylvatic transmission and thus prevent controls of the disease and a successful vaccination route (Stijlemans *et al*, 2016). Drug resistance by the inappropriate use of trypanocides (Baker *et al*, 2013) contribute to treatment failure for AAT, increasing the cost burden to countries trying to combat poverty (Shaw, 2009). Overall, vaccine development for *T. vivax* may be made more plausible by the discovery of conserved, immunogenic antigens on a cell-surface that departs substantially from that understood for *T. brucei*. Nonetheless, the path to a vaccine against AAT is a long-term process, of which antigen discovery is the first step. The eradication of AAT by vaccination might be possible in the future but many challenges remain.

6.1. FINAL CONCLUSION

Using a reverse vaccinology approach, this thesis identified specific antigens of *T. vivax* as potential vaccine candidates. The *in silico* analysis of 15 TvCSP gene families resolved those that encode surface proteins with minimal polymorphism but a universal presence in parasite clinical isolates. Epitope mapping subsequently narrowed the field further by showing which TvCSP were naturally immunogenic, focusing on one protein family, FamX, which showed the greatest number of immune cell epitopes. Four FamX proteins were expressed in recombinant form and one of these ('AJ6') was then observed to induce higher levels of pro-inflammatory cytokines (IFN- γ and TNF- α) in an adjuvant-dependent manner, leading to a mixed Th1/Th2-type immune response and reduced parasite burden when used to vaccinate mice. AJ6 was also localised across the cell surface of bloodstream-form *T. vivax*. Despite protecting mice and producing robust seroconversion in immunized goats, another FamX protein (IFX) failed to provide any protection against *T. vivax* infection. In conclusion, the cell-surface of *T. vivax* bloodstream forms contain novel, non-VSG proteins with no equivalent in *T. brucei* and *T. congolense*, which present favourable

properties as surface antigens. FamX proteins, and particularly AJ6, are a promising basis for further research towards a vaccine against animal African trypanosomiasis.

References

- Abbas AK, *et al.* Cellular and molecular immunology E-book: Elsevier Health Sciences; 2014.
- Acton QA. Virus Receptors—Advances in Research and Application: 2013 Edition: ScholarlyBrief: ScholarlyEditions; 2013.
- Adam Y, *et al.* Bovine trypanosomosis in the Upper West Region of Ghana: Entomological, parasitological and serological cross-sectional surveys. *Research in veterinary science.* 2012;92(3):462-8.
- Adeiza A, *et al.* Comparative haematological changes in experimentally infected Savannah brown goats with *Trypanosoma brucei* and *Trypanosoma vivax*. *African Journal of Biotechnology.* 2008;7(13).
- Aguilár J & Rodríguez E. Vaccine adjuvants revisited. *Vaccine.* 2007;25(19):3752-62.
- Ahmad TA, *et al.* B-cell epitope mapping for the design of vaccines and effective diagnostics. *Trials in Vaccinology.* 2016;5:71-83.
- Ahmed A-Q, *et al.* Species-specificity in endoplasmic reticulum signal peptide utilization revealed by proteins from *Trypanosoma brucei* and *Leishmania*. *Biochemical Journal.* 1998;331(2):521-9.
- Antoine-Moussiaux N, *et al.* Contributions of experimental mouse models to the understanding of African trypanosomiasis. *Trends in Parasitology.* 2008;24(9):411-8.
- Authié E. Trypanosomiasis and trypanotolerance in cattle: a role for congopain? *Parasitology Today.* 1994;10(9):360-4.
- Authié E, *et al.* Immunisation of cattle with cysteine proteinases of *Trypanosoma congolense*: targetting the disease rather than the parasite. *International journal for parasitology.* 2001;31(13):1429-33.
- Bai X, *et al.* An immunoregulatory peptide from tsetse fly salivary glands of *Glossina morsitans morsitans*. *Biochimie.* 2015;118:123-8.
- Bakari SM, *et al.* Serum biochemical parameters and cytokine profiles associated with natural African trypanosome infections in cattle. *Parasites & vectors.* 2017;10(1):312.
- Baker N, *et al.* Drug resistance in African trypanosomiasis: the melarsoprol and pentamidine story. *Trends in parasitology.* 2013;29(3):110-8.
- Baldi P & Long AD. A Bayesian framework for the analysis of microarray expression data: regularized t-test and statistical inferences of gene changes. *Bioinformatics.* 2001;17(6):509-19.
- Balouz V, *et al.* Mapping antigenic motifs in the trypomastigote small surface antigen from *Trypanosoma cruzi*. *Clinical and vaccine immunology.* 2015;22(3):304-12.
- Baral TN. Immunobiology of African trypanosomes: need of alternative interventions. *BioMed Research International.* 2010;2010.
- Barrett MP, *et al.* The trypanosomiasis. *The Lancet.* 2003;362(9394):1469-80.
- Batista J, *et al.* Infection by *Trypanosoma vivax* in goats and sheep in the Brazilian semiarid region: from acute disease outbreak to chronic cryptic infection. *Veterinary parasitology.* 2009;165(1-2):131-5.

Bell JS & McCulloch R. Mismatch repair regulates homologous recombination, but has little influence on antigenic variation, in *Trypanosoma brucei*. *Journal of Biological Chemistry*. 2003;278(46):45182-8.

Benjamini Y & Hochberg Y. Controlling the false discovery rate: a practical and powerful approach to multiple testing. *Journal of the royal statistical society Series B (Methodological)*. 1995:289-300.

Berkovits BD & Mayr C. Alternative 3' UTRs act as scaffolds to regulate membrane protein localization. *Nature*. 2015;522(7556):363.

Berriman M, *et al.* The genome of the African trypanosome *Trypanosoma brucei*. *science*. 2005;309(5733):416-22.

Beschin A, *et al.* *Trypanosoma brucei* infection elicits nitric oxide-dependent and nitric oxide-independent suppressive mechanisms. *Journal of leukocyte biology*. 1998;63(4):429-39.

Bezerra NM, *et al.* Detection of *Trypanosoma vivax* DNA in semen from experimentally infected goats. *Veterinary research communications*. 2018;42(2):131-5.

Bhatia V, *et al.* Utility of the *Trypanosoma cruzi* sequence database for identification of potential vaccine candidates by *in silico* and *in vitro* screening. *Infection and immunity*. 2004;72(11):6245-54.

Black SJ & Mansfield J. Prospects for vaccination against pathogenic African trypanosomes. *Parasite immunology*. 2016;38(12):735-43.

Black SJ & Seed JR. *The African Trypanosomes*: Springer Science & Business Media; 2001.

Blom-Potar MC, *et al.* *Trypanosoma vivax* infections: pushing ahead with mouse models for the study of Nagana. II. Immunobiological dysfunctions. *PLoS neglected tropical diseases*. 2010;4(8).

Blom-Potar MC, *et al.* *Trypanosoma vivax* infections: pushing ahead with mouse models for the study of Nagana. II. Immunobiological dysfunctions. *PLoS neglected tropical diseases*. 2010;4(8):e793.

Bordner AJ. Towards universal structure-based prediction of class II MHC epitopes for diverse allotypes. *PLoS One*. 2010;5(12):e14383.

Borst P & Cross GA. Molecular basis for trypanosome antigenic variation. *Cell*. 1982;29(2):291-303.

Borst P & Fairlamb A. Surface receptors and transporters of *Trypanosoma brucei*. *Annual Reviews in Microbiology*. 1998;52(1):745-78.

Botero D, *et al.* *Parasitosis humanas*. 4th ed: Organización Mundial de la Salud; 2003.

Boulangé A, *et al.* Development of a rapid antibody test for point-of-care diagnosis of animal African trypanosomosis. *Veterinary parasitology*. 2017;233:32-8.

Brener Z. Therapeutic activity and criterion of cure on mice experimentally infected with *Trypanosoma cruzi*. *Revista do Instituto de Medicina Tropical de São Paulo*. 1962;4(6):389-96.

Bretscher P. On the mechanism determining the TH1/TH2 phenotype of an immune response, and its pertinence to strategies for the prevention, and treatment, of certain infectious diseases. *Scandinavian journal of immunology*. 2014;79(6):361-76.

Brewer JM, *et al.* Aluminium hydroxide adjuvant initiates strong antigen-specific Th2 responses in the absence of IL-4-or IL-13-mediated signaling. *The Journal of Immunology*. 1999;163(12):6448-54.

Broderson J. A retrospective review of lesions associated with the use of Freund's adjuvant. *Laboratory animal science*. 1989;39(5):400-5.

Broderson JR. A retrospective review of lesions associated with the use of Freund's adjuvant. *Laboratory Animal Science*. 1989;39(5):400-5.

Brown D & Waneck GL. Glycosyl-phosphatidylinositol-anchored membrane proteins. *Journal of the American Society of Nephrology*. 1992;3(4):895-906.

Bruce D. The croonian lectures on trypanosomes causing disease in man and domestic animals in central Africa: delivered before the royal college of physicians of London. *British Medical Journal*. 1915;2(2846):91.

Bushell KM, *et al.* Large-scale screening for novel low-affinity extracellular protein interactions. *Genome research*. 2008;18(4):622-30.

Cadioli FA, *et al.* First report of *Trypanosoma vivax* outbreak in dairy cattle in São Paulo state, Brazil. *Revista Brasileira de Parasitologia Veterinária*. 2012;21(2):118-24.

Camejo MI, *et al.* TNF-alpha in bulls experimentally infected with *Trypanosoma vivax*: A pilot study. *Veterinary immunology and immunopathology*. 2014;162(3-4):192-7.

Campbell CO, *et al.* In silico characterization of an atypical MAPK phosphatase of *Plasmodium falciparum* as a suitable target for drug discovery. *Chemical biology & drug design*. 2014;84(2):158-68.

Campbell K, *et al.* DNA immunization with the gene encoding P4 nuclease of *Leishmania amazonensis* protects mice against cutaneous leishmaniasis. *Infection and immunity*. 2003;71(11):6270-8.

Campos-Neto A, *et al.* Vaccination with plasmid DNA encoding TSA/LmST11 leishmanial fusion proteins confers protection against *Leishmania major* infection in susceptible BALB/c mice. *Infection and immunity*. 2002;70(6):2828-36.

Carmona SJ, *et al.* Towards high-throughput immunomics for infectious diseases: use of next-generation peptide microarrays for rapid discovery and mapping of antigenic determinants. *Molecular & Cellular Proteomics*. 2015;14(7):1871-84.

Chenet SM, *et al.* Genetic diversity and population structure of genes encoding vaccine candidate antigens of *Plasmodium vivax*. *Malaria journal*. 2012;11(1):68.

Claes F, *et al.* Bioluminescent imaging of *Trypanosoma brucei* shows preferential testis dissemination which may hamper drug efficacy in sleeping sickness. *PLoS neglected tropical diseases*. 2009;3(7):e486.

Clarkson M. Trypanosomiasis of domesticated animals of South America. *Transactions of the Royal Society of Tropical Medicine and Hygiene*. 1976;70(2):125-6.

Clements JE, *et al.* Antigenic variation in lentiviral diseases. *Annual review of immunology*. 1988;6(1):139-59.

Coffman RL, *et al.* Vaccine adjuvants: putting innate immunity to work. *Immunity*. 2010;33(4):492-503.

Connor R. The diagnosis, treatment and prevention of animal trypanosomiasis under field conditions. FAO (Food and Agriculture Organization of the United Nations) Animal Production and Health Paper. 1992;100.

Connor R. The impact of nagana. Onderstepoort Journal of Veterinary Research. 1994;61:379-83.

Cortez A, *et al.* The taxonomic and phylogenetic relationships of *Trypanosoma vivax* from South America and Africa. Parasitology. 2006;133(2):159-69.

Coustou V, *et al.* Sialidases play a key role in infection and anaemia in *Trypanosoma congolense* animal trypanosomiasis. Cellular microbiology. 2012;14(3):431-45.

Cox A, *et al.* A PCR based assay for detection and differentiation of African trypanosome species in blood. Experimental parasitology. 2005;111(1):24-9.

Crompton PD, *et al.* A prospective analysis of the Ab response to *Plasmodium falciparum* before and after a malaria season by protein microarray. Proceedings of the National Academy of Sciences. 2010;107(15):6958-63.

Cross G. Identification, purification and properties of clone-specific glycoprotein antigens constituting the surface coat of *Trypanosoma brucei*. Parasitology. 1975;71(3):393-417.

Crumpton MJ. Protein antigens: the molecular bases of antigenicity and immunogenicity. The antigens: Elsevier; 1974. p. 1-78.

Cruse JM & Lewis RE. Atlas of immunology: CRC Press; 2010.

Cuglovici D, *et al.* Epidemiologic aspects of an outbreak of *Trypanosomavivax* in a dairy cattle herd in Minas Gerais state, Brazil. Veterinary parasitology. 2010;169(3-4):320-6.

Cui Y, *et al.* Sequential epitopes of *Dermatophagoides farinae* allergens identified using peptide microarray-based immunoassay. IUBMB life. 2016;68(10):792-8.

Curry PS, *et al.* Filter-paper blood samples for ELISA detection of *Brucella* antibodies in caribou. Journal of Wildlife Diseases. 2011;47(1):12-20.

D'leteren G, *et al.* Trypanotolerance, an option for sustainable livestock production in areas at risk from trypanosomosis. OIE Revue Scientifique et Technique. 1998;17(1):154-75.

da Silva AS, *et al.* First report of *Trypanosoma vivax* in bovines in the State of Rio Grande do Sul, Brazil/Primeiro registro de *Trypanosoma vivax* em bovinos no Estado do Rio Grande do Sul, Brasil. Ciência Rural. 2009;39(8):2550-5.

Da Silva AS, *et al.* Horses naturally infected by *Trypanosoma vivax* in southern Brazil. Parasitology research. 2011;108(1):23-30.

Dagnachew S & Bezie M. Review on *Trypanosoma vivax*. Afr J Basic Appl Sci. 2015;7(1):41-64.

Dagnachew S, *et al.* Comparative clinico-pathological observations in young Zebu (*Bos indicus*) cattle experimentally infected with *Trypanosoma vivax* isolates from tsetse infested and non-tsetse areas of Northwest Ethiopia. BMC veterinary research. 2015;11(1):307.

Daifalla NS, *et al.* Differential immune response against recombinant *Leishmania donovani* peroxidase 1 and peroxidase 2 proteins in BALB/c mice. Journal of immunology research. 2015;2015.

Darji A, *et al.* Inhibition of T-cell responsiveness during experimental infections with *Trypanosoma brucei*: active involvement of endogenous gamma interferon. *Infection and Immunity*. 1993;61(7):3098-102.

Dávila A, *et al.* Using PCR for unraveling the cryptic epizootiology of livestock trypanosomosis in the Pantanal, Brazil. *Veterinary parasitology*. 2003;117(1-2):1-13.

De Groot AS, *et al.* T cell epitope identification for bovine vaccines: an epitope mapping method for BoLA A-11. *International journal for parasitology*. 2003;33(5):641-53.

De Groot AS & Scott DW. Immunogenicity of protein therapeutics. *Trends in immunology*. 2007;28(11):482-90.

de Oliveira AP, *et al.* Blood or serum collected on filter paper for detection of antibodies to bovine herpesvirus type 1 (BoHV-1). *Acta Scientiae Veterinariae*. 2011;39(1).

de Oliveira Mendes TA, *et al.* Identification of strain-specific B-cell epitopes in *Trypanosoma cruzi* using genome-scale epitope prediction and high-throughput immunoscreening with peptide arrays. *PLoS neglected tropical diseases*. 2013;7(10):e2524.

Delafosse A, *et al.* Epidemiology of *Trypanosoma vivax* infection in cattle in the tse-tse free area of Lake Chad. *Preventive veterinary medicine*. 2006;74(2-3):108-19.

Delespaux V, *et al.* Molecular tools for the rapid detection of drug resistance in animal trypanosomes. *Trends in parasitology*. 2008;24(5):236-42.

Desai DV & Kulkarni-Kale U. T-cell epitope prediction methods: an overview. *Immunoinformatics*. 2014:333-64.

Desquesnes M. Evaluation of a simple PCR technique for the diagnosis of *Trypanosoma vivax* infection in the serum of cattle in comparison to parasitological techniques and antigen–enzyme-linked immuno sorbent assay. *Acta tropica*. 1997;65(3):139-48.

Desquesnes M. Livestock trypanosomoses and their vectors in Latin America: OIE (World Organisation for Animal Health); 2004.

Desquesnes M & Davila A. Applications of PCR-based tools for detection and identification of animal trypanosomes: a review and perspectives. *Veterinary parasitology*. 2002;109(3):213-31.

Desquesnes M & Dia ML. *Trypanosoma vivax*: mechanical transmission in cattle by one of the most common African tabanids, *Atylotus agrestis*. *Experimental parasitology*. 2003;103(1-2):35-43.

Desquesnes M, *et al.* Detection and identification of *Trypanosoma* of African livestock through a single PCR based on internal transcribed spacer 1 of rDNA. *International journal for parasitology*. 2001;31(5):610-4.

Donati C & Rappuoli R. Reverse vaccinology in the 21st century: improvements over the original design. *Annals of the New York Academy of Sciences*. 2013;1285(1):115-32.

Donelson JE, *et al.* Multiple mechanisms of immune evasion by African trypanosomes. *Molecular and biochemical parasitology*. 1998;91(1):51-66.

Doytchinova IA & Flower DR. VaxiJen: a server for prediction of protective antigens, tumour antigens and subunit vaccines. *BMC bioinformatics*. 2007;8(1):4.

Dupré Lc, *et al.* Immunostimulatory effect of IL-18-encoding plasmid in DNA vaccination against murine *Schistosoma mansoni* infection. *Vaccine*. 2001;19(11-12):1373-80.

Durbin BP, *et al.* A variance-stabilizing transformation for gene-expression microarray data. *Bioinformatics*. 2002;18(suppl_1):S105-S10.

Duxbury R, *et al.* Trypanosoma congolense: immunization of mice, dogs, and cattle with gamma-irradiated parasites. *Experimental parasitology*. 1972;32(3):527-33.

e Silva RdF, *et al.* Combination of in silico methods in the search for potential CD4+ and CD8+ T cell epitopes in the proteome of *Leishmania braziliensis*. *Frontiers in immunology*. 2016;7.

Eickhoff CS, *et al.* An immunoinformatic approach for identification of *Trypanosoma cruzi* HLA-A2-restricted CD8+ T cell epitopes. *Human vaccines & immunotherapeutics*. 2015;11(9):2322-8.

Eisenhaber B, *et al.* Prediction of potential GPI-modification sites in proprotein sequences. *Journal of molecular biology*. 1999;292(3):741-58.

Eisler MC, *et al.* Sensitivity and specificity of antigen-capture ELISAs for diagnosis of *Trypanosoma congolense* and *Trypanosoma vivax* infections in cattle. *Veterinary parasitology*. 1998;79(3):187-201.

EL-Manzalawy Y, *et al.* Predicting linear B-cell epitopes using string kernels. *Journal of molecular recognition*. 2008;21(4):243-55.

Engstler M, *et al.* Hydrodynamic flow-mediated protein sorting on the cell surface of trypanosomes. *Cell*. 2007;131(3):505-15.

Eshetu E & Begejo B. The current situation and diagnostic approach of Nagana in Africa: A review. *Journal of Natural Sciences Research*. 2015;5(17):117-25.

Farrell D, *et al.* Integrated computational prediction and experimental validation identifies promiscuous T cell epitopes in the proteome of *Mycobacterium bovis*. *Microbial genomics*. 2016;2(8).

Faye D, *et al.* Influence of an experimental *Trypanosoma congolense* infection and plane of nutrition on milk production and some biochemical parameters in West African Dwarf goats. *Acta tropica*. 2005;93(3):247-57.

Ferguson M, *et al.* Glycosyl-phosphatidylinositol moiety that anchors *Trypanosoma brucei* variant surface glycoprotein to the membrane. *Science*. 1988;239(4841):753-9.

Ferguson MA. The structure, biosynthesis and functions of glycosylphosphatidylinositol anchors, and the contributions of trypanosome research. *J Cell Sci*. 1999;112(17):2799-809.

Ferguson MA, *et al.* Glycosylphosphatidylinositol anchors. 2009.

Ferrante A & Allison A. Alternative pathway activation of complement by African trypanosomes lacking a glycoprotein coat. *Parasite immunology*. 1983;5(5):491-8.

Fidelis Junior OL, *et al.* Evaluation of clinical signs, parasitemia, hematologic and biochemical changes in cattle experimentally infected with *Trypanosoma vivax*. *Revista Brasileira de Parasitologia Veterinária*. 2016;25(1):69-81.

Field MC & Carrington M. The trypanosome flagellar pocket. *Nature Reviews Microbiology*. 2009;7(11):775-86.

- Fikru R, *et al.* A proline racemase based PCR for identification of *Trypanosoma vivax* in cattle blood. *PLoS one*. 2014;9(1):e84819.
- Finelle P. African animal trypanosomiasis. IV. Economic problems. *World animal review*. 1974.
- Fleming JR, *et al.* Proteomic selection of immunodiagnostic antigens for *Trypanosoma congolense*. *PLoS neglected tropical diseases*. 2014;8(6).
- Fleming JR, *et al.* Proteomic identification of immunodiagnostic antigens for *Trypanosoma vivax* infections in cattle and generation of a proof-of-concept lateral flow test diagnostic device. *PLoS neglected tropical diseases*. 2016;10(9):e0004977.
- Frank SA. *Immunology and evolution of infectious disease*: Princeton University Press; 2002.
- Freitas LM, *et al.* Genomic analyses, gene expression and antigenic profile of the trans-sialidase superfamily of *Trypanosoma cruzi* reveal an undetected level of complexity. *PLoS One*. 2011;6(10):e25914.
- Garcia H, *et al.* The detection and PCR-based characterization of the parasites causing trypanosomiasis in water-buffalo herds in Venezuela. *Annals of Tropical Medicine & Parasitology*. 2005;99(4):359-70.
- Gardiner P. Recent studies of the biology of *Trypanosoma vivax*. *Advances in Parasitology*. 1989;28:229-317.
- Gardiner PR, *et al.* Characterization of a small variable surface glycoprotein from *Trypanosoma vivax*. *Molecular and biochemical parasitology*. 1996;82(1):1-11.
- Gaseitsiwe S, *et al.* Pattern recognition in pulmonary tuberculosis defined by high content peptide microarray chip analysis representing 61 proteins from *M. tuberculosis*. *PLoS one*. 2008;3(12):e3840.
- Geerts S, *et al.* African bovine trypanosomiasis: the problem of drug resistance. *Trends in parasitology*. 2001;17(1):25-8.
- Geysen D, *et al.* PCR-RFLP using *Ssu-rDNA* amplification as an easy method for species-specific diagnosis of *Trypanosoma* species in cattle. *Veterinary Parasitology*. 2003;110(3-4):171-80.
- Ghosh A, *et al.* Immunization with A2 protein results in a mixed Th1/Th2 and a humoral response which protects mice against *Leishmania donovani* infections. *Vaccine*. 2001;20(1-2):59-66.
- Greif G, *et al.* Transcriptome analysis of the bloodstream stage from the parasite *Trypanosoma vivax*. *BMC genomics*. 2013;14(1):149.
- Grun JL & Maurer PH. Different T helper cell subsets elicited in mice utilizing two different adjuvant vehicles: the role of endogenous interleukin 1 in proliferative responses. *Cellular immunology*. 1989;121(1):134-45.
- Guedes RLM, *et al.* A comparative in silico linear B-cell epitope prediction and characterization for South American and African *Trypanosoma vivax* strains. *Genomics*. 2018.
- Guerfali F, *et al.* An in silico immunological approach for prediction of CD8+ T cell epitopes of *Leishmania major* proteins in susceptible BALB/c and resistant C57BL/6 murine models of infection. *Infection, Genetics and Evolution*. 2009;9(3):344-50.
- Guilliams M, *et al.* Experimental expansion of the regulatory T cell population increases resistance to African trypanosomiasis. *The Journal of infectious diseases*. 2008;198(5):781-91.

Guilliams M, *et al.* African trypanosomiasis: naturally occurring regulatory T cells favor trypanotolerance by limiting pathology associated with sustained type 1 inflammation. *The Journal of Immunology*. 2007;179(5):2748-57.

Gupta S, *et al.* In silico characterization of Plasmodium falciparum purinergic receptor: a novel chemotherapeutic target. *Systems and synthetic biology*. 2015;9(1):11-6.

Guy AJ, *et al.* Structural patterns of selection and diversity for Plasmodium vivax antigens DBP and AMA1. *Malaria journal*. 2018;17(1):183.

Haçarız O, *et al.* The effect of Quil A adjuvant on the course of experimental Fasciola hepatica infection in sheep. *Vaccine*. 2009;27(1):45-50.

Hamilton P, *et al.* A novel, high-throughput technique for species identification reveals a new species of tsetse-transmitted trypanosome related to the Trypanosoma brucei subgenus, Trypanozoon. *Infection, Genetics and Evolution*. 2008;8(1):26-33.

Hegde NR, *et al.* The use of databases, data mining and immunoinformatics in vaccinology: where are we? Expert opinion on drug discovery. 2018;13(2):117-30.

Hein WR & Griebel PJ. A road less travelled: large animal models in immunological research. *Nature Reviews Immunology*. 2003;3(1):79-84.

Heinzel FP, *et al.* Production of interferon gamma, interleukin 2, interleukin 4, and interleukin 10 by CD4+ lymphocytes in vivo during healing and progressive murine leishmaniasis. *Proceedings of the National Academy of Sciences*. 1991;88(16):7011-5.

Hertz CJ, *et al.* Resistance to the African trypanosomes is IFN- γ dependent. *The Journal of Immunology*. 1998;161(12):6775-83.

Hoare CA. Morphological and Taxonomic Studies on Mammalian Trypanosomes. V. The Diagnostic Value of the Kineto-plast. *Transactions of the Royal Society of Tropical Medicine and Hygiene*. 1938;32(3).

Hoare CA. The trypanosomes of mammals. A zoological monograph. *The trypanosomes of mammals A zoological monograph*. 1972.

Holmes P. Tsetse-transmitted trypanosomes—their biology, disease impact and control. *Journal of invertebrate pathology*. 2013;112:S11-S4.

Hoof Lv, *et al.* Quelques observations sur les trypanosomes des grands mammifères au Congo Belge. *Acta trop*. 1948;5:327.

Horn D. Antigenic variation in African trypanosomes. *Molecular and biochemical parasitology*. 2014;195(2):123-9.

Hornby HE. Animal trypanosomiasis in Eastern Africa, 1949. *Animal trypanosomiasis in Eastern Africa, 1949*. 1952.

Huber W, *et al.* Variance stabilization applied to microarray data calibration and to the quantification of differential expression. *Bioinformatics*. 2002;18(suppl_1):S96-S104.

Hunter M, *et al.* Optimization of Protein Expression in Mammalian Cells. *Current protocols in protein science*. 2019;95(1):e77.

Huson DH. SplitsTree: analyzing and visualizing evolutionary data. *Bioinformatics (Oxford, England)*. 1998;14(1):68-73.

Ilemobade A. Tsetse and trypanosomiasis in Africa: the challenges, the opportunities. *Onderstepoort Journal of Veterinary Research*. 2009;76(1):35-40.

- Iraqi F, *et al.* Susceptibility of tumour necrosis factor- α genetically deficient mice to *Trypanosoma congolense* infection. *Parasite immunology*. 2001;23(8):445-51.
- Ivory C & Chadee K. DNA vaccines: designing strategies against parasitic infections. *Genetic vaccines and therapy*. 2004;2(1):17.
- Jackson AP, *et al.* A cell-surface phylome for African trypanosomes. *PLoS Negl Trop Dis*. 2013;7(3):e2121.
- Jackson AP, *et al.* Antigenic diversity is generated by distinct evolutionary mechanisms in African trypanosome species. *Proceedings of the National Academy of Sciences*. 2012;109(9):3416-21.
- Jackson AP, *et al.* Global gene expression profiling through the complete life cycle of *Trypanosoma vivax*. *PLoS Negl Trop Dis*. 2015;9(8):e0003975.
- Jenkins MC. Advances and prospects for subunit vaccines against protozoa of veterinary importance. *Veterinary Parasitology*. 2001;101(3-4):291-310.
- Jespersen MC, *et al.* BepiPred-2.0: improving sequence-based B-cell epitope prediction using conformational epitopes. *Nucleic Acids Research*. 2017.
- Johnson CM. Bovine Trypanosomiasis in Panama¹. *The American Journal of Tropical Medicine and Hygiene*. 1941;1(2):289-97.
- Jones TW & Dávila AM. *Trypanosoma vivax*—out of Africa. *TRENDS in Parasitology*. 2001;17(2):99-101.
- Jordan A. Trypanosome infection rates in *Glossina morsitans morsitans* Newst. in Northern Nigeria. *Bulletin of Entomological Research*. 1964;55(2):219-31.
- Jordan A. Tsetse-flies (glossinidae). *Medical insects and arachnids*: Springer; 1993. p. 333-88.
- Jørgensen KW, *et al.* Structural properties of MHC class II ligands, implications for the prediction of MHC class II epitopes. *PloS one*. 2010;5(12):e15877.
- Jung K, *et al.* Reporting FDR analogous confidence intervals for the log fold change of differentially expressed genes. *BMC bioinformatics*. 2011;12(1):288.
- Katunguka-Rwakishaya E, *et al.* The influence of energy intake on some blood biochemical parameters in Scottish Blackface sheep infected with *Trypanosoma congolense*. *Veterinary parasitology*. 1999;84(1-2):1-11.
- Katz C, *et al.* Studying protein–protein interactions using peptide arrays. *Chemical Society Reviews*. 2011;40(5):2131-45.
- Kaur J, *et al.* In silico screening, structure-activity relationship, and biologic evaluation of selective pteridine reductase inhibitors targeting visceral leishmaniasis. *Antimicrobial agents and chemotherapy*. 2011;55(2):659-66.
- Kaushik A, *et al.* In silico characterization and molecular dynamics simulation of Pfcyc-1, a cyclin homolog of *Plasmodium falciparum*. *Journal of Biomolecular Structure and Dynamics*. 2014;32(10):1624-33.
- Kayala MA & Baldi P. Cyber-T web server: differential analysis of high-throughput data. *Nucleic acids research*. 2012;40(W1):W553-W9.
- Kelley LA, *et al.* The Phyre2 web portal for protein modeling, prediction and analysis. *Nature protocols*. 2015;10(6):845-58.
- Kerr JS & Wright GJ. Avidity-based extracellular interaction screening (AVEXIS) for the scalable detection of low-affinity extracellular receptor-ligand interactions. *Journal of visualized experiments: JoVE*. 2012(61).

Khademvatan S, *et al.* In silico and in vitro comparative activity of novel experimental derivatives against *Leishmania major* and *Leishmania infantum* promastigotes. *Experimental parasitology*. 2013;135(2):208-16.

Khan KH. Gene expression in mammalian cells and its applications. *Advanced pharmaceutical bulletin*. 2013;3(2):257.

Kinabo L. Pharmacology of existing drugs for animal trypanosomiasis. *Acta tropica*. 1993;54(3-4):169-83.

Koo V, *et al.* Non-invasive in vivo imaging in small animal research. *Analytical Cellular Pathology*. 2006;28(4):127-39.

Krafsur E. Tsetse flies: genetics, evolution, and role as vectors. *Infection, Genetics and Evolution*. 2009;9(1):124-41.

Kramer S, *et al.* Genome-wide in silico screen for CCCH-type zinc finger proteins of *Trypanosoma brucei*, *Trypanosoma cruzi* and *Leishmania major*. *BMC genomics*. 2010;11(1):283.

Krinsky WL. Tsetse flies (Glossinidae). *Medical and veterinary entomology*: Elsevier; 2019. p. 369-82.

Kumar S, *et al.* MEGA7: Molecular Evolutionary Genetics Analysis version 7.0 for bigger datasets. *Molecular biology and evolution*. 2016;33(7):1870-4.

Kumar S, *et al.* A DNA vaccine encoding the 42 kDa C-terminus of merozoite surface protein 1 of *Plasmodium falciparum* induces antibody, interferon- γ and cytotoxic T cell responses in rhesus monkeys: immuno-stimulatory effects of granulocyte macrophage-colony stimulating factor. *Immunology letters*. 2002;81(1):13-24.

Kuzoe F & Schofield C. Strategic review of traps and targets for tsetse and african trypanosomiasis control. *Strategic review of traps and targets for tsetse and African trypanosomiasis control*. 2004.

La Greca F, *et al.* Antibody-mediated control of *Trypanosoma vivax* infection fails in the absence of tumour necrosis factor. *Parasite immunology*. 2014;36(6):271-6.

La Greca F & Magez S. Vaccination against trypanosomiasis: can it be done or is the trypanosome truly the ultimate immune destroyer and escape artist? *Human vaccines*. 2011;7(11):1225-33.

Lança ASC, *et al.* *Trypanosoma brucei*: immunisation with plasmid DNA encoding invariant surface glycoprotein gene is able to induce partial protection in experimental African trypanosomiasis. *Experimental parasitology*. 2011;127(1):18-24.

Leger M & Vienne M. Epizootie à trypanosomes chez les bovidés de la Guyane Française. *Bull Soc Pathol Exot*. 1919;12:258-66.

Leppert BJ, *et al.* The soluble variant surface glycoprotein of African trypanosomes is recognized by a macrophage scavenger receptor and induces $\text{I}\kappa\text{B}\alpha$ degradation independently of TRAF6-mediated TLR signaling. *The Journal of Immunology*. 2007;179(1):548-56.

Lew-Tabor A & Valle MR. A review of reverse vaccinology approaches for the development of vaccines against ticks and tick borne diseases. *Ticks and tick-borne diseases*. 2016;7(4):573-85.

Li H & Durbin R. Fast and accurate long-read alignment with Burrows–Wheeler transform. *Bioinformatics*. 2010;26(5):589-95.

Li H, *et al.* The sequence alignment/map format and SAMtools. *Bioinformatics*. 2009;25(16):2078-9.

Li S-Q, *et al.* Immunization with recombinant actin from *Trypanosoma evansi* induces protective immunity against *T. evansi*, *T. equiperdum* and *T. b. brucei* infection. *Parasitology research*. 2009;104(2):429-35.

Li SQ, *et al.* Immunization with recombinant beta-tubulin from *Trypanosoma evansi* induced protection against *T. evansi*, *T. equiperdum* and *T. b. brucei* infection in mice. *Parasite Immunology*. 2007;29(4):191-9.

Lima CR, *et al.* In silico structural characterization of protein targets for drug development against *Trypanosoma cruzi*. *JOURNAL OF MOLECULAR MODELING*. 2016;22(10).

Lindsley H, *et al.* Detection and composition of immune complexes in experimental African trypanosomiasis. *Infection and immunity*. 1981;33(2):407-14.

Liu W & Chen YH. High epitope density in a single protein molecule significantly enhances antigenicity as well as immunogenicity: a novel strategy for modern vaccine development and a preliminary investigation about B cell discrimination of monomeric proteins. *European journal of immunology*. 2005;35(2):505-14.

Loeffler FF, *et al.* High-Density Peptide Arrays for Malaria Vaccine Development. *Vaccine Design: Methods and Protocols: Volume 1: Vaccines for Human Diseases*. 2016:569-82.

Longo PA, *et al.* Transient mammalian cell transfection with polyethylenimine (PEI). *Methods in enzymology*. 529: Elsevier; 2013. p. 227-40.

Lubega GW, *et al.* Immunization with a tubulin-rich preparation from *Trypanosoma brucei* confers broad protection against African trypanosomiasis. *Experimental parasitology*. 2002;102(1):9-22.

Luckins A. Methods for diagnosis of trypanosomiasis in livestock. *World animal review*. 1992;70(71):15-20.

Luckins AG, *et al.* Non-tsetse-transmitted animal trypanosomiasis. The trypanosomiasis. 2004:269-81.

Madruga CR, *et al.* The development of an enzyme-linked immunosorbent assay for *Trypanosoma vivax* antibodies and its use in epidemiological surveys. *Memórias do Instituto Oswaldo Cruz*. 2006;101(7):801-7.

Magetz S, *et al.* Current status of vaccination against African trypanosomiasis. *Parasitology*. 2010;137(14):2017-27.

Magetz S, *et al.* Specific uptake of tumor necrosis factor- α is involved in growth control of *Trypanosoma brucei*. *The Journal of cell biology*. 1997;137(3):715-27.

Magetz S, *et al.* Murine tumour necrosis factor plays a protective role during the initial phase of the experimental infection with *Trypanosoma brucei brucei*. *Parasite immunology*. 1993;15(11):635-41.

Magetz S & Radwanska M. Adaptive immunity and trypanosomiasis-driven B-cell destruction. *Trypanosomes and Trypanosomiasis: Springer*; 2014. p. 115-38.

Magetz S, *et al.* Tumor necrosis factor (TNF) receptor-1 (TNFp55) signal transduction and macrophage-derived soluble TNF are crucial for nitric oxide-mediated *Trypanosoma congolense* parasite killing. *Journal of Infectious Diseases*. 2007;196(6):954-62.

- Magez S, *et al.* Interferon- γ and nitric oxide in combination with antibodies are key protective host immune factors during *Trypanosoma congolense* Tc13 infections. *The Journal of infectious diseases*. 2006;193(11):1575-83.
- Magez S, *et al.* P75 tumor necrosis factor–receptor shedding occurs as a protective host response during African trypanosomiasis. *The Journal of infectious diseases*. 2004;189(3):527-39.
- Mahanty S, *et al.* Immunogenicity of infectious pathogens and vaccine antigens. *BMC immunology*. 2015;16(1):31.
- Mamabolo M, *et al.* Natural infection of cattle and tsetse flies in South Africa with two genotypic groups of *Trypanosoma congolense*. *Parasitology*. 2009;136(4):425-31.
- Mansfield JM, *et al.* Bridging innate and adaptive immunity in African trypanosomiasis. *Trypanosomes and Trypanosomiasis*: Springer; 2014. p. 89-114.
- Martins CF, *et al.* *Trypanosoma vivax* infection dynamics in a cattle herd maintained in a transition area between Pantanal lowlands and highlands of Mato Grosso do Sul, Brazil. *Pesquisa Veterinária Brasileira*. 2008;28(1):51-6.
- Masiga DK, *et al.* Sensitive detection of trypanosomes in tsetse flies by DNA amplification. *International journal for parasitology*. 1992;22(7):909-18.
- Matthews KR. The developmental cell biology of *Trypanosoma brucei*. *Journal of cell science*. 2005;118(2):283-90.
- Matthews KR & Gull K. Evidence for an interplay between cell cycle progression and the initiation of differentiation between life cycle forms of African trypanosomes. *The Journal of cell biology*. 1994;125(5):1147-56.
- Mayr C. Evolution and biological roles of alternative 3' UTRs. *Trends in cell biology*. 2016;26(3):227-37.
- Mazumder B, *et al.* Translational control by the 3'-UTR: the ends specify the means. *Trends in biochemical sciences*. 2003;28(2):91-8.
- McKenna A, *et al.* The Genome Analysis Toolkit: a MapReduce framework for analyzing next-generation DNA sequencing data. *Genome research*. 2010;20(9):1297-303.
- Meeusen EN, *et al.* Current status of veterinary vaccines. *Clinical microbiology reviews*. 2007;20(3):489-510.
- Mkunza F, *et al.* Partial protection against natural trypanosomiasis after vaccination with a flagellar pocket antigen from *Trypanosoma brucei rhodesiense*. *Vaccine*. 1995;13(2):151-4.
- Morrison LJ, *et al.* Animal African Trypanosomiasis: Time to Increase Focus on Clinically Relevant Parasite and Host Species. *Trends in parasitology*. 2016.
- Morrison WI, *et al.* Protective immunity and specificity of antibody responses elicited in cattle by irradiated *Trypanosoma brucei*. *Parasite Immunology*. 1982;4(6):395-407.
- Mosmann TR & Coffman R. TH1 and TH2 cells: different patterns of lymphokine secretion lead to different functional properties. *Annual review of immunology*. 1989;7(1):145-73.
- Murphy KP, Travers; Mark, Walport; Charles, Janeway *Immunobiology* Garland Science. New York. 2012:136-7.
- Murray M. Livestock productivity and trypanotolerance: network training manual: ILRI (aka ILCA and ILRAD); 1983.

- Murray M, *et al.* Diagnosis of African trypanosomiasis in the bovine. *Diagnosis of African trypanosomiasis in the bovine.* 1979;73(1):120-1.
- Mwongela G, *et al.* Acute *Trypanosoma vivax* infection in dairy cattle in coast province, Kenya. *Tropical Animal Health and Production.* 1981;13(1):63-9.
- Naessens J. Bovine trypanotolerance: a natural ability to prevent severe anaemia and haemophagocytic syndrome? *International Journal for Parasitology.* 2006;36(5):521-8.
- Nakayasu ES, *et al.* Improved proteomic approach for the discovery of potential vaccine targets in *Trypanosoma cruzi*. *Journal of proteome research.* 2011;11(1):237-46.
- Namangala B. Contribution of innate immune responses towards resistance to African trypanosome infections. *Scandinavian journal of immunology.* 2012;75(1):5-15.
- Namangala B. How the African trypanosomes evade host immune killing. *Parasite immunology.* 2011;33(8):430-7.
- Namangala B, *et al.* Both type-I and type-II responses contribute to murine trypanotolerance. *Journal of Veterinary Medical Science.* 2009;71(3):313-8.
- Namangala B, *et al.* Quantitative differences in immune responses in mouse strains that differ in their susceptibility to *Trypanosoma brucei brucei* infection. *Journal of Veterinary Medical Science.* 2009;71(7):951-6.
- Namangala B, *et al.* Attenuation of *Trypanosoma brucei* is associated with reduced immunosuppression and concomitant production of Th2 lymphokines. *The Journal of infectious diseases.* 2000;181(3):1110-20.
- Namangala B, *et al.* Alternative versus classical macrophage activation during experimental African trypanosomiasis. *Journal of Leukocyte Biology.* 2001;69(3):387-96.
- Namangala B & Odongo S. *Animal African trypanosomiasis in sub-Saharan Africa and beyond African borders. Trypanosomes and trypanosomiasis: Springer; 2014. p. 239-60.*
- Nanda Kumar Y, *et al.* Computational screening and characterization of putative vaccine candidates of *Plasmodium vivax*. *Journal of Biomolecular Structure and Dynamics.* 2016;34(8):1736-50.
- Nascimento I & Leite L. Recombinant vaccines and the development of new vaccine strategies. *Brazilian journal of medical and biological research.* 2012;45(12):1102-11.
- Nei M. *Molecular evolutionary genetics: Columbia university press; 1987.*
- Nelson CW, *et al.* SNPGenie: estimating evolutionary parameters to detect natural selection using pooled next-generation sequencing data. *Bioinformatics.* 2015;31(22):3709-11.
- Nguyen T-T, *et al.* Application of crude and recombinant ELISAs and immunochromatographic test for serodiagnosis of animal trypanosomiasis in the Umkhanyakude district of KwaZulu-Natal province, South Africa. *Journal of Veterinary Medical Science.* 2015;77(2):217-20.
- Njiru Z, *et al.* The use of ITS1 rDNA PCR in detecting pathogenic African trypanosomes. *Parasitology Research.* 2005;95(3):186-92.

Nosjean O, *et al.* Mammalian GPI proteins: sorting, membrane residence and functions. *Biochimica et Biophysica Acta (BBA)-Reviews on Biomembranes*. 1997;1331(2):153-86.

O'Gorman GM, *et al.* Cytokine mRNA profiling of peripheral blood mononuclear cells (PBMC) from trypanotolerant and trypanosusceptible cattle infected with *Trypanosoma congolense*. *Physiological Genomics*. 2017.

Ochola LI, *et al.* Allele frequency-based and polymorphism-versus-divergence indices of balancing selection in a new filtered set of polymorphic genes in *Plasmodium falciparum*. *Molecular biology and evolution*. 2010;27(10):2344-51.

Oleszycka E, *et al.* The vaccine adjuvant alum promotes IL-10 production that suppresses Th1 responses. *European journal of immunology*. 2018;48(4):705-15.

Oliveira J, *et al.* First report of *Trypanosoma vivax* infection in dairy cattle from Costa Rica. *Veterinary parasitology*. 2009;163(1-2):136-9.

Onyilagha C & Uzonna JE. Host Immune Responses and Immune Evasion Strategies in African trypanosomiasis. *Frontiers in Immunology*. 2019;10:2738.

Ooi C-P, *et al.* The cyclical development of *Trypanosoma vivax* in the tsetse fly involves an asymmetric division. *Frontiers in cellular and infection microbiology*. 2016;6:115.

Opperdoes FR & Szikora J-P. In silico prediction of the glycosomal enzymes of *Leishmania major* and trypanosomes. *Molecular and biochemical parasitology*. 2006;147(2):193-206.

Osman N, *et al.* Susceptibility of Sudanese Nubian goats, Nilotic dwarf goats and Garag ewes to experimental infection with a mechanically transmitted *Trypanosoma vivax* stock. *Pakistan journal of biological sciences: PJBs*. 2008;11(3):472-5.

Osório ALAR, *et al.* *Trypanosoma (Duttonella) vivax*: its biology, epidemiology, pathogenesis, and introduction in the New World-a review. *Memórias do Instituto Oswaldo Cruz*. 2008;103(1):1-13.

Overath P, *et al.* Invariant surface proteins in bloodstream forms of *Trypanosoma brucei*. *Parasitology Today*. 1994;10(2):53-8.

Pacheco MA, *et al.* A comparative study of the genetic diversity of the 42 kDa fragment of the merozoite surface protein 1 in *Plasmodium falciparum* and *P. vivax*. *Infection, Genetics and Evolution*. 2007;7(2):180-7.

Paiva F, *et al.* *Trypanosoma vivax* em bovinos no Pantanal do Estado do Mato Grosso do Sul, Brasil: I.-Acompanhamento clínico, laboratorial e anatomopatológico de rebanhos infectados. *Rev Bras Parasitol Vet*. 2000;9(2):135-41.

Parker S, *et al.* Safety of a GM-CSF adjuvant-plasmid DNA malaria vaccine. *Gene therapy*. 2001;8(13):1011-23.

Patel P, *et al.* Genetic diversity and antibody responses against *Plasmodium falciparum* vaccine candidate genes from Chhattisgarh, Central India: implication for vaccine development. *PloS one*. 2017;12(8):e0182674.

Pattaradilokrat S, *et al.* Genetic diversity of the merozoite surface protein-3 gene in *Plasmodium falciparum* populations in Thailand. *Malaria journal*. 2016;15(1):517.

Paulick MG & Bertozzi CR. The glycosylphosphatidylinositol anchor: a complex membrane-anchoring structure for proteins. *Biochemistry*. 2008;47(27):6991-7000.

Pejaver V, *et al.* The structural and functional signatures of proteins that undergo multiple events of post-translational modification. *Protein Science*. 2014;23(8):1077-93.

Pereira SS, *et al.* Variant antigen repertoires in *Trypanosoma congolense* populations and experimental infections can be profiled from deep sequence data using universal protein motifs. *Genome research*. 2018;28(9):1383-94.

Pereira SS, *et al.* Variant antigen diversity in *Trypanosoma vivax* is not driven by recombination. *BioRxiv*. 2019:733998.

Perry BD. Towards a healthier planet: Veterinary epidemiology research at the International Laboratory for Research on Animal Diseases (ILRAD) and the International Livestock Research Institute (ILRI), 1987–2014. 2015.

Pfeifer B, *et al.* PopGenome: an efficient Swiss army knife for population genomic analyses in R. *Molecular biology and evolution*. 2014;31(7):1929-36.

Pierleoni A, *et al.* PredGPI: a GPI-anchor predictor. *BMC bioinformatics*. 2008;9(1):392.

Pillay D, *et al.* *Trypanosoma vivax* GM6 antigen: a candidate antigen for diagnosis of African animal trypanosomiasis in cattle. *PloS one*. 2013;8(10):e78565.

Pinger J, *et al.* Variant surface glycoprotein density defines an immune evasion threshold for African trypanosomes undergoing antigenic variation. *Nature Communications*. 2017;8(1):828.

Pipano E. Live vaccine against hemoparasitic disease in livestock. *Veterinary parasitology*. 1995;57(1-3):213-31.

Pletinckx K, *et al.* Similar inflammatory DC maturation signatures induced by TNF or *Trypanosoma brucei* antigens instruct default Th2-cell responses. *European journal of immunology*. 2011;41(12):3479-94.

Plotkin SA. Complex correlates of protection after vaccination. *Clinical infectious diseases*. 2013;56(10):1458-65.

Plotkin SA. Correlates of protection induced by vaccination. *Clin Vaccine Immunol*. 2010;17(7):1055-65.

Plotkin SA. Immunologic correlates of protection induced by vaccination. *The Pediatric infectious disease journal*. 2001;20(1):63-75.

Pollock J. Training Manual for Tsetse Control Personnel: Tsetse Biology, Systematics and Distribution; Techniques: Fao; 1982.

Ponomarenko JV & Van Regenmortel MH. B cell epitope prediction. *Structural bioinformatics*. 2009:849-79.

Potocnakova L, *et al.* An introduction to B-cell epitope mapping and in silico epitope prediction. *Journal of immunology research*. 2016;2016.

Quevillon E, *et al.* InterProScan: protein domains identifier. *Nucleic acids research*. 2005;33(suppl_2):W116-W20.

Quevillon E, *et al.* InterProScan: protein domains identifier. *Nucleic acids research*. 2005;33(suppl 2):W116-W20.

Quispe P, *et al.* Prevalencia de *Trypanosoma vivax* en bovinos de cuatro distritos de la provincia de Coronel Portillo, Ucayali. *Revista de Investigaciones Veterinarias del Perú*. 2003;14(2):161-5.

Radwanska M, *et al.* Trypanosomiasis-induced B cell apoptosis results in loss of protective anti-parasite antibody responses and abolishment of vaccine-induced memory responses. *PLoS pathogens*. 2008;4(5).

Radwanska M, *et al.* Antibodies raised against the flagellar pocket fraction of *Trypanosoma brucei* preferentially recognize HSP60 in cDNA expression library. *Parasite immunology*. 2000;22(12):639-50.

Radwanska M, *et al.* Salivarian Trypanosomosis: A review of parasites involved, their global distribution and their interaction with the innate and adaptive mammalian host immune system. *Frontiers in immunology*. 2018;9:2253.

Ramey K, *et al.* Immunolocalization and challenge studies using a recombinant *Vibrio cholerae* ghost expressing *Trypanosoma brucei* Ca²⁺ ATPase (TBCA2) antigen. *The American journal of tropical medicine and hygiene*. 2009;81(3):407-15.

Rappuoli R. Reverse vaccinology. *Current opinion in microbiology*. 2000;3(5):445-50.

Reis-Cunha JL, *et al.* Genome-wide screening and identification of new *Trypanosoma cruzi* antigens with potential application for chronic Chagas disease diagnosis. *PloS one*. 2014;9(9):e106304.

Resch AM, *et al.* Evolution of alternative and constitutive regions of mammalian 5'UTRs. *BMC genomics*. 2009;10(1):162.

Ribeiro JM & Francischetti IM. Role of arthropod saliva in blood feeding: sialome and post-sialome perspectives. *Annual review of entomology*. 2003;48(1):73-88.

Ritchie ME, *et al.* limma powers differential expression analyses for RNA-sequencing and microarray studies. *Nucleic acids research*. 2015;43(7):e47-e.

Robinson WH, *et al.* Autoantigen microarrays for multiplex characterization of autoantibody responses. *Nature medicine*. 2002;8(3):295-301.

Rocke DM & Durbin B. A model for measurement error for gene expression arrays. *Journal of computational biology*. 2001;8(6):557-69.

Rodrigues CM, *et al.* Field and experimental symptomless infections support wandering donkeys as healthy carriers of *Trypanosoma vivax* in the Brazilian Semiarid, a region of outbreaks of high mortality in cattle and sheep. *Parasites & vectors*. 2015;8(1):564.

Rodrigues CM, *et al.* New insights from Gorongosa National Park and Niassa National Reserve of Mozambique increasing the genetic diversity of *Trypanosoma vivax* and *Trypanosoma vivax*-like in tsetse flies, wild ungulates and livestock from East Africa. *Parasites & vectors*. 2017;10(1):337.

Roeder P, *et al.* Acute *Trypanosoma vivax* infection of ethiopian cattle in the apparent absence of tsetse. *Tropical Animal Health and Production*. 1984;16(3):141-7.

Romagnani S. The th1/th2 paradigm. *Immunology today*. 1997;18(6):263-6.

Rost B, *et al.* The predictprotein server. *Nucleic acids research*. 2004;32(suppl_2):W321-W6.

Roubaud E & Provost A. Sensibilité du lapin au trypanosome des ruminants des Antilles T. viennei, souche américaine de T. cazalboui (vivax). *Bull Soc Path Exot*. 1939;32(5):6.

Rovis L, *et al.* Failure of trypanosomal membrane antigens to induce protection against tsetse-transmitted *Trypanosoma vivax* or *T. brucei* in goats and rabbits. *Acta tropica*. 1984;41(3):227-36.

Rurangirwa F, *et al.* The effect of *Trypanosoma congolense* and *T vivax* infections on the antibody response of cattle to live rinderpest virus vaccine. 1980.

- Rurangirwa F, *et al.* Immune depression in bovine trypanosomiasis: effects of acute and chronic *Trypanosoma congolense* and chronic *Trypanosoma vivax* infections on antibody response to *Brucella abortus* vaccine. *Parasite immunology*. 1983;5(3):267-76.
- Saha S & Raghava G. Prediction of continuous B-cell epitopes in an antigen using recurrent neural network. *Proteins: Structure, Function, and Bioinformatics*. 2006;65(1):40-8.
- Sanchez-Trincado JL, *et al.* Fundamentals and methods for T-and B-cell epitope prediction. *Journal of immunology research*. 2017;2017.
- Sanderson CM. A new way to explore the world of extracellular protein interactions. *Genome research*. 2008;18(4):517-20.
- Saror D. Observations on the course and pathology of *Trypanosoma vivax* in Red Sokoto goats. *Research in Veterinary Science*. 1980;28(1):36-8.
- Sato A, *et al.* In vivo bioluminescence imaging. *Comparative medicine*. 2004;54(6):631-4.
- Savage AF, *et al.* Transcript expression analysis of putative *Trypanosoma brucei* GPI-anchored surface proteins during development in the tsetse and mammalian hosts. *PLoS neglected tropical diseases*. 2012;6(6):e1708.
- Schenk MA, *et al.* Avaliação clínico-laboratorial de bovinos Nelore infectados experimentalmente com *Trypanosoma vivax*. *Pesq Vet Bras*. 2001;21(4):157-61.
- Scholma J, *et al.* Improved intra-array and interarray normalization of peptide microarray phosphorylation for phosphoproteome and kinome profiling by rational selection of relevant spots. *Scientific reports*. 2016;6:26695.
- Schwede A, *et al.* How does the VSG coat of bloodstream form African trypanosomes interact with external proteins? *PLoS pathogens*. 2015;11(12):e1005259.
- Scott M, *et al.* Adjuvant requirements for protective immunization of mice using a *Trypanosoma cruzi* 90K cell surface glycoprotein. *International Archives of Allergy and Immunology*. 1984;74(4):373-7.
- Seed JR & Black SJ. A proposed density-dependent model of long slender to short stumpy transformation in the African trypanosomes. *The Journal of parasitology*. 1997;656-62.
- Seidl A, *et al.* Estimated financial impact of *Trypanosoma vivax* on the Brazilian Pantanal and Bolivian lowlands. *Memórias do Instituto Oswaldo Cruz*. 1999;94(2):269-72.
- Sendashonga CN & Black S. Humoral responses against *Trypanosoma brucei* variable surface antigen are induced by degenerating parasites. *Parasite immunology*. 1982;4(4):245-57.
- Sette A & Rappuoli R. Reverse vaccinology: developing vaccines in the era of genomics. *Immunity*. 2010;33(4):530-41.
- Seyed N, *et al.* In silico analysis of six known *Leishmania* major antigens and in vitro evaluation of specific epitopes eliciting HLA-A2 restricted CD8 T cell response. *PLoS neglected tropical diseases*. 2011;5(9):e1295.
- Sharma AK, *et al.* Structural characterization of the C-terminal coiled-coil domains of wild-type and kidney disease-associated mutants of apolipoprotein L1. *The FEBS journal*. 2016;283(10):1846-62.

Shaw A. Assessing the economics of animal trypanosomosis in Africa-history and current perspectives. *Onderstepoort Journal of Veterinary Research*. 2009;76(1):27-32.

Shimogawa MM, *et al.* Cell surface proteomics provides insight into stage-specific remodeling of the host-parasite interface in *Trypanosoma brucei*. *Molecular & cellular proteomics*. 2015;14(7):1977-88.

Sileghem M, *et al.* Active suppression of interleukin 2 secretion in mice infected with *Trypanosoma brucei* AnTat 1.1. *E. Parasite immunology*. 1986;8(6):641-9.

Silva MRG, *et al.* Cloning, characterization and subcellular localization of a *Trypanosoma cruzi* argonaute protein defining a new subfamily distinctive of trypanosomatids. *Gene*. 2010;466(1):26-35.

Silva MS, *et al.* Trans-sialidase from *Trypanosoma brucei* as a potential target for DNA vaccine development against African trypanosomiasis. *Parasitology research*. 2009;105(5):1223.

Silva R, *et al.* Outbreaks of trypanosomosis due to *Trypanosoma vivax* in cattle in Bolivia. *Veterinary parasitology*. 1998;76(1-2):153-7.

Silva RAMS, *et al.* Outbreak of trypanosomiasis due to *Trypanosoma vivax* (Ziemann, 1905) in bovines of the Pantanal, Brazil. *Memórias do Instituto Oswaldo Cruz*. 1996;91(5):561-2.

Silver JD, *et al.* Microarray background correction: maximum likelihood estimation for the normal-exponential convolution. *Biostatistics*. 2008;10(2):352-63.

Singh M & T O'Hagan D. Recent advances in veterinary vaccine adjuvants. *International journal for parasitology*. 2003;33(5-6):469-78.

Sjölander A, *et al.* Immune responses to ISCOM[®] formulations in animal and primate models. *Vaccine*. 2001;19(17-19):2661-5.

Soria-Guerra RE, *et al.* An overview of bioinformatics tools for epitope prediction: implications on vaccine development. *Journal of biomedical informatics*. 2015;53:405-14.

Sow A, *et al.* Field detection of resistance to isometamidium chloride and diminazene aceturate in *Trypanosoma vivax* from the region of the Boucle du Mouhoun in Burkina Faso. *Veterinary parasitology*. 2012;187(1-2):105-11.

Spellberg B & Edwards Jr JE. Type 1/Type 2 immunity in infectious diseases. *Clinical Infectious Diseases*. 2001;32(1):76-102.

Spickler AR. *Emerging and exotic diseases of animals*. 4th ed: CFSPH Iowa State University; 2010.

Squire F. Seasonal variation in the incidence of *Trypanosoma vivax* in *Glossina palpalis* (R.-D.). *Bulletin of Entomological Research*. 1951;42(2):371-4.

Stephen LE. *Trypanosomiasis: a veterinary perspective*. Wheaton, London. 1986:1-551.

Stevenson P, *et al.* Rinderpest vaccination and the incidence and development of trypanosomosis in cattle. *Tropical animal health and production*. 1999;31(2):65-73.

Steverding D. The history of African trypanosomiasis. *Parasites & vectors*. 2008;1(1):3.

Steverding D, *et al.* Transferrin-binding protein complex is the receptor for transferrin uptake in *Trypanosoma brucei*. *The Journal of Cell Biology*. 1995;131(5):1173-82.

Stijlemans B, *et al.* Immune evasion strategies of *Trypanosoma brucei* within the mammalian host: progression to pathogenicity. *Frontiers in Immunology*. 2016;7:233.

Stijlemans B, *et al.* African trypanosomiasis: from immune escape and immunopathology to immune intervention. *Veterinary parasitology*. 2007;148(1):3-13.

Stijlemans B, *et al.* African Trypanosomes Undermine Humoral Responses and Vaccine Development: Link with Inflammatory Responses? *Frontiers in immunology*. 2017;8:582.

Stijlemans B, *et al.* The central role of macrophages in trypanosomiasis-associated anemia: rationale for therapeutical approaches. *Endocrine, Metabolic & Immune Disorders-Drug Targets (Formerly Current Drug Targets-Immune, Endocrine & Metabolic Disorders)*. 2010;10(1):71-82.

Subramanian S. The effects of sample size on population genomic analyses—implications for the tests of neutrality. *BMC genomics*. 2016;17(1):123.

Sun H-X, *et al.* ISCOMs and ISCOMATRIX™. *Vaccine*. 2009;27(33):4388-401.

Sun Y, *et al.* A benchmarked protein microarray-based platform for the identification of novel low-affinity extracellular protein interactions. *Analytical biochemistry*. 2012;424(1):45-53.

Sundaresh S, *et al.* Identification of humoral immune responses in protein microarrays using DNA microarray data analysis techniques. *Bioinformatics*. 2006;22(14):1760-6.

Swain SL. T-Cell Subsets: Who does the polarizing? *Current Biology*. 1995;5(8):849-51.

Tabel H, *et al.* Experimental bovine trypanosomiasis (*Trypanosoma vivax* and *T. congolense*). III. Serum levels of immunoglobulins, heterophile antibodies, and antibodies to *T. vivax*. *Tropenmedizin und Parasitologie*. 1981;32(3):149-53.

Tabel H, *et al.* Immunosuppression: cause for failures of vaccines against African trypanosomiasis. *PLoS neglected tropical diseases*. 2013;7(3):e2090.

Tabel H, *et al.* T cells and immunopathogenesis of experimental African trypanosomiasis. *Immunological reviews*. 2008;225(1):128-39.

Tafur T, *et al.* Prevalencia de *Trypanosoma vivax* en bovinos de selva alta en la provincia de Chachapoyas, Amazonas. *Revista de Investigaciones Veterinarias del Perú*. 2002;13(2):94-7.

Tajima F. DNA polymorphism in a subdivided population: the expected number of segregating sites in the two-subpopulation model. *Genetics*. 1989;123(1):229-40.

Tajima F. Statistical method for testing the neutral mutation hypothesis by DNA polymorphism. *Genetics*. 1989;123(3):585-95.

Takala SL, *et al.* Extreme polymorphism in a vaccine antigen and risk of clinical malaria: implications for vaccine development. *Science translational medicine*. 2009;1(2):2ra5-2ra5.

- Tamura K & Nei M. Estimation of the number of nucleotide substitutions in the control region of mitochondrial DNA in humans and chimpanzees. *Molecular biology and evolution*. 1993;10(3):512-26.
- Taylor K & Authié EM-L. 18 Pathogenesis of Animal Trypanosomiasis. the Trypanosomiasis. 2004:331.
- Taylor K, *et al.* Nitric oxide synthesis is depressed in *Bos indicus* cattle infected with *Trypanosoma congolense* and *Trypanosoma vivax* and does not mediate T-cell suppression. *Infection and immunity*. 1996;64(10):4115-22.
- Taylor KA. Immune responses of cattle to African trypanosomes: protective or pathogenic? *International journal for parasitology*. 1998;28(2):219-40.
- Taylor KA, *et al.* *Trypanosoma congolense*: B-lymphocyte responses differ between trypanotolerant and trypanosusceptible cattle. *Experimental parasitology*. 1996;83(1):106-16.
- Taylor KA & Mertens B. Immune response of cattle infected with African trypanosomes. *Memórias do Instituto Oswaldo Cruz*. 1999;94(2):239-44.
- Taylor M. Coop RL. Wall, RL. *Veterinary parasitology* 4th ed West Sussex (UK): John Wiley & Sons. 2016:7-200.
- Telleria EL, *et al.* Insights into the trypanosome-host interactions revealed through transcriptomic analysis of parasitized tsetse fly salivary glands. *PLoS neglected tropical diseases*. 2014;8(4):e2649.
- Tran T, *et al.* Development and evaluation of an ITS1 “Touchdown” PCR for assessment of drug efficacy against animal African trypanosomosis. *Veterinary parasitology*. 2014;202(3):164-70.
- Tung JK, *et al.* Bioluminescence imaging in live cells and animals. *Neurophotonics*. 2016;3(2):025001.
- Uilenberg G & Boyt W. A field guide for the diagnosis, treatment and prevention of African animal trypanosomosis: Food & Agriculture Org.; 1998.
- Valentini D, *et al.* Peptide microarray-based characterization of antibody responses to host proteins after bacille Calmette–Guérin vaccination. *International Journal of Infectious Diseases*. 2017;56:140-54.
- van den Inch T, *et al.* The pathology and pathogenesis of *Trypanosoma vivax* infection in the goat. *Research in Veterinary Science*. 1976;21(3):264-70.
- van Doorn E, *et al.* Safety and tolerability evaluation of the use of Montanide ISA™ 51 as vaccine adjuvant: a systematic review. *Human vaccines & immunotherapeutics*. 2016;12(1):159-69.
- Van Meirvenne N, *et al.* Antigenic variation in syringe passaged populations of *Trypanosoma (Trypanozoon) brucei*. 1. Rationalization of the experimental approach. *Ann Soc Belg Med Trop*. 1975;55:1-23.
- Van Meirvenne N, *et al.* Antigenic variation in syringe passaged populations of *Trypanosoma (Trypanozoon) brucei*. II. Comparative studies on two antigenic-type collections. *Ann Soc Belg Med Trop*. 1975;55(1):25-30.
- Van Regenmortel MH. What is a B-cell epitope? *Epitope Mapping Protocols: Second Edition*. 2009:3-20.
- Vanhollebeke B, *et al.* A haptoglobin-hemoglobin receptor conveys innate immunity to *Trypanosoma brucei* in humans. *Science*. 2008;320(5876):677-81.

- Velez-Ramirez D, *et al.* BRF1, a subunit of RNA polymerase III transcription factor TFIIIB, is essential for cell growth of *Trypanosoma brucei*. *Parasitology*. 2015;142(13):1563-73.
- Vincendeau P & Bouteille B. Immunology and immunopathology of African trypanosomiasis. *Anais da Academia Brasileira de Ciências*. 2006;78(4):645-65.
- Vita R, *et al.* The immune epitope database (IEDB) 3.0. *Nucleic acids research*. 2014;43(D1):D405-D12.
- Weber CA, *et al.* T cell epitope: friend or foe? Immunogenicity of biologics in context. *Advanced drug delivery reviews*. 2009;61(11):965-76.
- Weber LK, *et al.* Antibody fingerprints in lyme disease deciphered with high density peptide arrays. *Engineering in Life Sciences*. 2017.
- Weber LK, *et al.* Single amino acid fingerprinting of the human antibody repertoire with high density peptide arrays. *Journal of Immunological Methods*. 2017;443:45-54.
- Weedall GD & Conway DJ. Detecting signatures of balancing selection to identify targets of anti-parasite immunity. *Trends in parasitology*. 2010;26(7):363-9.
- Wei G & Tabel H. Regulatory T cells prevent control of experimental African trypanosomiasis. *The Journal of Immunology*. 2008;180(4):2514-21.
- Wells P, *et al.* Immunization of cattle with a variant-specific surface antigen of *Trypanosoma brucei*: influence of different adjuvants. *Infection and immunity*. 1982;36(1):1-10.
- Westwood OM & Hay FC. *Epitope mapping: a practical approach*: Oxford University Press, USA; 2001.
- White SH. *Membrane protein structure: experimental approaches*: Springer; 2013.
- Whitelaw D, *et al.* Extravascular foci of *Trypanosoma vivax* in goats: the central nervous system and aqueous humor of the eye as potential sources of relapse infections after chemotherapy. *Parasitology*. 1988;97(1):51-61.
- Wiederschain GY. *Essentials of glycobiology*. *Biochemistry (Moscow)*. 2009;74(9):1056-.
- Williams D, *et al.* The role of anti-variable surface glycoprotein antibody responses in bovine trypanotolerance. *Parasite Immunology*. 1996;18(4):209-18.
- Woo PT. The haematocrit centrifuge for the detection of trypanosomes in blood. *Canadian Journal of Zoology*. 1969;47(5):921-3.
- Yahya MFZR, *et al.* Investigation on Nuclear Transport of *Trypanosoma brucei*: An in silico Approach. *Bioinformatics: InTech*; 2012.
- Yaro M, *et al.* Combatting African Animal Trypanosomiasis (AAT) in livestock: The potential role of trypanotolerance. *Veterinary Parasitology*. 2016;225:43-52.
- Zhang L, *et al.* TEPITOPEpan: extending TEPITOPE for peptide binding prediction covering over 700 HLA-DR molecules. *PLoS One*. 2012;7(2):e30483.
- Zwart D, *et al.* Effect of *Trypanosoma vivax* infection on body temperature, feed intake, and metabolic rate of West African dwarf goats. *Journal of Animal Science*. 1991;69(9):3780-8.